MEASURING MITOCHONDRIAL DNA DAMAGE IN *CAENORHABDITIS ELEGANS*, IMPLICATIONS FOR AGEING AND HEALTHSPAN

NG LI FANG

NATIONAL UNIVERSITY OF SINGAPORE

2014

MEASURING MITOCHONDRIAL DNA DAMAGE IN *CAENORHABDITIS ELEGANS*, IMPLICATIONS FOR AGEING AND HEALTHSPAN

NG LI FANG

(B. Sc., NATIONAL UNIVERSITY OF SINGAPORE)

A THESIS SUBMITTED

FOR THE DEGREE OF DOCTOR OF PHILOSOPHY

DEPARTMENT OF BIOCHEMISTRY

NATIONAL UNIVERSITY OF SINGAPORE

2014

Declaration

I hereby declare that this thesis is my original work and it has been written by me in its entirety.

I have duly acknowledged all the sources of information which have been used in the thesis.

This thesis has also not been submitted for any degree in any University previously.

_____

NG LI FANG

10th November 2014

Acknowledgements

Pursuing this PhD degree has been a life- and mind-changing experience for me. My journey towards the completion of this degree would not have been possible without the extraordinary people who have guided and supported me along the way.

It is a true pleasure to thank all those people who made this thesis possible and an enjoyable experience for me.

My sincere thanks to my main supervisor, Professor Barry Halliwell for his trust in me and for giving me the chance to participate in his research project for my PhD study. His invaluable guidance and advice as well as patience were vital for the success of my PhD study. I am really grateful for his encouraging and constructive feedbacks.

I would also like to express my deepest gratitude to my Co-supervisor, Dr. Jan Gruber for his constant guidance, advice, support and patient mentorship. Thank you for the inspiration, encouragement and enthusiasm you have given me during the course of my studies. I thank you for your intellectual discussions, thought-provoking questions and constructive criticisms in my lab works and also in the writing of journal papers and thesis. Your enthusiasm for science and research is contagious, thank you for showing me the excitement of science and research!

Special thanks to my thesis advisory committee members, Professor Frank Watt and Professor Sit Kim Ping for their supports, helpful insights and suggestions for the progression of my research.

I would like to extend my gratitude to all the past and present members of the lab including (alphabetical order) Emelyne Teo, Irwin Cheah, Long Lee Hua, Ranjan Manickaratnam, Sebastian Schaffer, Sherry Huang, Terry Yew, Vanessa Lam, Wong Yee Ting, Wu Yilian and Yee Zhuang Li for their discussions, supports and also providing a friendly and productive environment to work with.

I am forever thankful to my beloved parents, and my siblings, Chean, Hoong, Yang and Theng. My family has always been my strongest support through the hurdles along the way. Their unwavering love, encouragement and patient are incalculably valuable to my success.

Last but not least, to my husband, Kang Hao, I thank you for your unconditional love, understanding, help, encouragement and honest criticisms. Thank you for being my study buddy and hanging in there with me. I can never thank you enough for your all support now and forever!

Journal Publications and Conference attended

Journal publications:

Published:

1. **Ng, L. F**.; Gruber, J.; Cheah, I. K.; Goo, C. K.; Cheong, W. F.; Shui, G.; Sit, K. P.; Wenk, M. R.; Halliwell, B. The mitochondria-targeted antioxidant MitoQ extends lifespan and improves healthspan of a transgenic Caenorhabditis elegans model of Alzheimer disease. *Free radical biology & medicine* **71:**390-401; 2014.

2. Gruber, J.; Chen, C.; Fong, S.; **Ng, L. F**.; Teo, J. W.; Halliwell, B. Caenorhabditis elegans, what we can and cannot learn from ageing worms? *Antioxidants & redox signaling*; 2014.

3. Tam, Z. Y.; Gruber, J.; **Ng, L. F**.; Halliwell, B.; Gunawan, R. Effects of lithium on age-related decline in mitochondrial turnover and function in caenorhabditis elegans. *Journals of Gerontology - Series A Biological Sciences and Medical Sciences* **69:**810-820; 2014.

4. Yan, Y.; **Ng, L. F**.; Ng, L. T.; Choi, K. B.; Gruber, J.; Bettiol, A. A.; Thakor, N. V. A continuous-flow C. elegans sorting system with integrated optical fiber detection and laminar flow switching. *Lab on a chip* **14***:*4000-4006; 2014.

5. Qabazard, B.; Li, L.; Gruber, J.; Peh, M. T.; **Ng, L. F**.; Kumar, S. D.; Rose, P.; Tan, C. H.; Dymock, B. W.; Wei, F.; Swain, S. C.; Halliwell, B.; Stürzenbaum, S. R.; Moore, P. K. Hydrogen sulfide is an endogenous regulator of aging in *caenorhabditis elegans*. *Antioxidants and Redox Signaling* **20**:2621-2630; 2014.

6. Cheah, I. K.; Ong, R. L. S.; Gruber, J.; Yew, T. S. K.; **Ng, L. F**.; Chen, C. B.; Halliwell, B. Knockout of a putative ergothioneine transporter in Caenorhabditis elegans decreases lifespan and increases susceptibility to oxidative damage. *Free radical research* **47:**1036-1045; 2013.

7. Ranjan, M., Gruber, J., **Ng, L.F.,** Halliwell, B. Repression of the mitochondrial peroxiredoxin antioxidant system does not shorten life span but causes reduced fitness in *Caenorhabditis elegans* , *Free Radical Biology and Medicine* **63** , pp. 381-389.2013.

8. Suresh, K P, J. Gruber, **L F NG**, B Halliwell and R. Gunawan, "Maximizing signal-to-noise ratio in the random mutation capture assay."*Nucleic Acids Res*. 2012 Mar;**40**(5):e35. Epub 2011 Dec 17.

9. Schaffer, S., Gruber, J., **Ng, L.F.**, Fong, S., Wong, Y.T., Tang, S.Y., Halliwell, B. The effect of dichloroacetate on health- and lifespan in *C.elegans*. *Biogerontology*. **12**:195-209; 2011.

10. Gruber, J., **Ng, L.F.,** Fong, S., Wong, Y.T., Koh, S.A., Ce-belle,C., Shui,G., Cheong, W.F., Marcus.R.W.,Schaffer, S., ,Halliwell,B., Mitochondrial changes in ageing *Caenorhabditis elegans* - what do we learn from superoxide dismutase knockouts? *PLoS One*. 2011;**6**(5):e19444. Epub 2011 May 18.

11. Pun, P.B.L.*, Gruber, J.*, Tang, S.Y., Schaffer, S., Ong, R.L.S., Fong, S., **Ng, L.F**., Cheah, I., Halliwell, B., Ageing in nematodes: Do antioxidants extend lifespan in *Caenorhabditis elegans*?, *Biogerontology*, **11** (1), pp. 17-30, 2010.

12. Gruber, J. Poovathingal, S. K., Schaffer, S, **Ng, L.F.**, Gunawan R., Halliwell, B. *Caenorhabditis elegans* lifespan studies: The challenge of maintaining synchronous cohorts, *Rejuvenation Research*,**13** (2-3), pp. 347-349, 2010.

13. Gruber, J., **Ng, L.F**., Poovathingal, S.K., Halliwell, B. Deceptively simple but simply deceptive - *Caenorhabditis elegans* lifespan studies: Considerations for aging and antioxidant effect, *FEBS Letters* , **583** (21), pp. 3377-3387, 2009.

14. Parthasarathy, K., **Ng, L.**, Lin, X., Ding, X.L., Pervushin, K., Gong, X., Torres, J. Structural Flexibility of the Pentameric SARS Coronavirus Envelope Protein Ion Channel, *Biophysical Journal*, **95** (2008), L39-41L

15. Gan, S.W., **Ng, L**., Lin, X., Gong, X., Torres, J. Structure and ion channel activity of the human respiratory syncytial virus (hRSV) small hydrophobic protein transmembrane domain, *Protein Science*, **17** (2008), 813-820.

16. Torres, J., Maheswari, U., Parthasarathy, K., **Ng, L**., Ding, X.L., Gong, X. Conductance and amantadine binding of a pore formed by a lysine-flanked transmembrane domain of SARS coronavirus envelope protein, *Protein Science*, **16** (2007), 2065-2071.

In preparation:

1. **Li Fang Ng**, Jan Gruber, Fong, Sheng, Barry Halliwell, DNA damage in nucleus and mitochondria of *C. elegans* - effect of age, radiation and antioxidants.

2. Yee Ting Wong[1], Koh Soon Ann Sean[2], Jan Gruber[1], **Li Fang Ng[1]**, Elizabeth Armstrong[3], Penney Trevor Bruce[2], and Barry Halliwell[1] , Nootropic drug, Piracetam extends life span and improves motility, learning and memory in aging *Caenorhabditis elegans.*

Conference attended:

1. Conference poster presented at 17th Biennial Meeting of Society for Free Radical Research International (SFRRI 2014), 23rd -26th March 2014.

   Li Fang Ng, Jan Gruber, Sheng Fong & Barry Halliwell. Sequence specific quantitative real-time PCR as a useful assay to determine mitochondrial DNA damage in *Caenorhabditis elegans.*

Table of Contents

Summary

The mitochondrial free radical theory of ageing (mFRTA) proposes that loss of mitochondrial DNA (mtDNA) integrity as result of damage by endogenous reactive oxygen species (ROS) is a major cause of age-dependent mitochondrial degeneration. I have developed a sensitive S-XL-qRT-PCR DNA damage assay that can measure DNA damage in *Caenorhabditis elegans* (*C. elegans*), particularly mtDNA. I found that mtDNA damage in *C,elegans* is usually low, in the order of less than one lesion per molecule of mtDNA. This low level of mtDNA damage is probably not sufficient to interfere significantly with mitochondrial function to play a part in reducing the lifespan of the nematodes. Pharmacological interventions using a mitochondrial targeted antioxidant, MitoQ do not alter the mtDNA damage of a transgenic *C. elegans* model of Alzheimer disease despite an increase in the lifespan and healthspan of the nematodes. In fact, I found that the protective effect in lifespan and healthspan may be caused by highly specific protective effects on the ETC and mitochondrial membrane. This further supports the idea that mtDNA damage is not a determinant of ageing.

List of Tables

List of Figures

List of Abbreviations and Keywords

6-4 PPs	-	6-4 photoproducts
8OHdG	-	8-hydroxy-2' –deoxyguanosine
8-OxoG	-	8-oxo-7,8-dihydroguanine
Acetyl-coA	-	Acetyl coenzyme A
AD	-	Alzheimer disease
ADP	-	Adenosine diphosphate
APP	-	Amyloid precursor protein
ATP	-	Adenosine triphosphate
C. elegans	-	Caenorhabditis elegans
COX	-	Cytochrome *c* oxidase
CPDs	-	Cyclobutane pyrimidine dimers
CSE	-	Cystathionine γ lyase
Ct	-	Threshold cycle
CuZnSOD	-	Copper Zinc SOD
DCFDA	-	2, 7-dichlorofluorescein diacetate
dTPP	-	Decyltriphenylphosphonium
ESCODD	-	European Standards Committee for Oxidative DNA Damage
$FADH_2$	-	Flavin adenine dinucleotide
Fpg	-	Formamidopyrimidine DNA glycosylase
FRTA	-	Free-radical theory of ageing
γ-radiation	-	Gamma radiation
GC-MS	-	Gas chromatography–mass spectrometry
GPx	-	Gluthathione peroxidase
GSH	-	Gluthathione
HNE	-	4-hydroxy-2-nonenal
HPLC-ECD detection	-	High-performance liquid chromatography-electrochemical
LC- MS	-	Liquid chromatography/mass spectrometry

LC-MS/ MS - Liquid chromatography/tandem mass spectrometry

mFRTA - Mitochondrial free radical theory of ageing

MitoQ - MitoQ (mitoquinone mesylate: [10-(4, 5-dimethoxy-2-methyl-3, 6-dioxo-1, 4- cycloheexadienlyl) Decyltri-phenylphosphonium methanesulfonate])

MnSOD - Manganese SOD

MPST/3-MST - 3-mercaptopyruvate transferase

mtDNA - Mitochondrial DNA

NADH - Nicotinamide adenine dinucleotide

$NO^{\cdot}$ - Nitric oxide

$NO_2 \cdot$ - Nitrogen dioxide

$^1O_2$ - Singlet oxygen

$O_2^{\cdot}$ - Superoxide anion

OCl^- - Hypochlorite

$OH \cdot$ - Hydroxyl radical

OH^- - Hydroxyl ions

$ONOO^-$ - Peroxynitrite

PCC - Protein carbonyl content

Prdx - Peroxiredoxins

qPCR - Quantitative PCR

qRT-PCR - Quantitative real time PCR

RT-PCR - Real Time PCR

ROS - Reactive oxygen species

SOD - Superoxide dismutase

S-PCR - Short-PCR

S-XL-qRT-PCR - Short and extra-long-qRT-PCR

TCA - Tricarboxylic acid cycle

Trx - Thioredoxin

UV - Ultraviolet

UVA - Ultraviolet A

UVB	-	Ultraviolet B
UVC	-	Ultraviolet C
XL-PCR	-	Extra long-PCR

1. Introduction

1.1. The demography of ageing populations

The world population is rapidly ageing. Population ageing is defined as a process that changes the global age distribution of the population toward older ages, increasing the proportion of the elderly in the total population. Since the beginning of recorded history, the number of children under the age of 5 has always outnumbered people aged 65 and above. However, this situation will be reversed for the first time in human history, by the year 2050, when the elderly population is projected to exceed the young. A direct consequence of the ongoing dramatic decline in birth rates, coupled with increases in life expectancy, population ageing will continue to accelerate over the next few decades. In the year 1950, the total population of people aged 65 and older was approximately 131 million, representing only 5% of the global population. In a report published by the World Health Organization (WHO), the number of people aged 65 and above is projected to increase from 524 million to almost 1.5 billion between the years 2010 and 2050 [1]. In most countries, the oldest group among the elderly population, constituting people aged 80 and above, is growing faster than any other age group. The proportion of this age group at the total global population is projected to increase from 1 % in the year 1950 to 4 % by the year 2050. Although this age group still constitutes only a small proportion of the total population, the rapid growth of this age group has important implication to society, related to demand for long term care. Generally, the rapid increase in the number of people aged 65 and above will have profound impact on global economic, social and political conditions [1] as they have different needs and productive capacities [2] than those people from the younger age group.

Over the last half of 20th century, the total fertility rate (the average number of children that would be born to a woman over her lifetime) has fallen drastically, from 5.0 to 2.7 children per woman. The global fertility rate has significantly declined, but differing patterns of fertility behavior in different countries have caused the decline to be varied widely. In the more developed countries, such as Europe, Japan and Singapore, the fertility rate has fallen well

below the replacement level of 2.1 [3, 4]. As for the developing countries, the drop in the fertility rate started later compared to developed countries but proceed faster. The total fertility rate dropped by 60 % between the year 1950 and the year 2005 in developing countries [5]. According to a report by Sarah Harper published in the year 2005, Asia and Latin America are also experiencing a steady fall in fertility rate with birthrate as low as 1.4 in Hong Kong, 1.5 in Singapore, 1.8 in Korea, 2.1 in Chile and 2.3 in Brazil [3]. The decline in the fertility rate is still ongoing, for instance, Singapore's total fertility rate in the year 2012 had fallen to below 1.2 children per woman [6].

Under current mortality conditions of 7.99 deaths per 1000 person each year for all age groups in the world population, more people are expected to survive to old age. About 75 % of newborns will live to age 60 and about 30 % will survive till age 80. Overall, the global life expectancy, which is defined as the average number of years a new born is expected to live, has improved with the global increased of life expectancy at birth by almost 20 years from the year 1950 to 2005 [5]. Life expectancy is an indicator of the condition of life and health status of a population. The higher the life expectancy, the better the condition of a country [2, 7]. While life expectancy rate is improved in almost every country, the improvement in the life expectancy at birth in the developing countries over the last half-century is still higher (23.1 years) than developed countries (9.4 years). However, this steady increase in life expectancy still favors developed countries as individual born in developed countries are expected to outlive individuals in less developed countries by almost 12 years according to current mortality conditions [5]. Thus, with the increase in life expectancy, about 88 % of newborns are expected to survive till age 60 and more than half to age 80 by the year 2050 [5]. According to a WHO report in the year 2011, Singapore has the fourth-best life expectancy in the world. People living in Singapore have average life expectancy of 82 years, ranking Singapore after Japan, Switzerland and Australia. Improvement in the average life expectancy can be considered one of the society's greatest achievements and is due to medical advances, better nutrition, health-

care, education and economic development. However, together with lower birth rate, the resulting population ageing poses new challenge.

1.1.1. The challenge of global ageing

The shift in the distribution of global age structure poses social, political and economic challenges to individuals, families and societies. Population ageing is likely to burden health systems because age is the single biggest risk factor for many diseases including cancer, diabetes, cardiovascular disease, stroke and neurodegenerative diseases [8]. For instance, Alzheimer disease (AD) is a progressive, age-related neurodegenerative disease and is the most common form of dementia [9, 10]. AD is an increasingly serious public health challenge, especially in countries with large ageing populations. Currently, the total number of people with AD is estimated to be 34 million people worldwide and this figure is expected to triple over the next 40 years [10].

One of the major concerns that is often mentioned is the rise of health care cost as populations age. For example, in the United States, healthcare cost grew faster than the economy as a whole from the year 1980 to the year 2004 [11]. The healthcare expenses for the whole US populations increased from USD$255 billion in the year 1980 to USD$1.9 trillion in the year 2004 [11]. The costs of caring and managing elderly suffering from health problems or disabilities will continue to increase with the growing numbers of aged-people. For instance, the prevalence of AD is very low at younger ages and high in elderly people. In the year 2010, less than 3 % of people aged 65 to 69 suffer from dementia worldwide, but almost 30 % of elderly aged 85 and above suffered from some form of dementia [12]. The cost of care for AD is daunting. In the 2010 World Alzheimer report, the annual global cost of caregiving for dementia was estimated to exceed USD$600 billion in the year 2010 [12, 13]. In the United States, approximately 5.4 million Americans are suffering from AD and the cost of caring for AD patients in this alone is estimated to exceed USD$200 billion annually. If no disease-modifying therapies are developed, this cost is projected to increase to USD$1.2 trillion in the year 2050 [14].

In addition to cost, the demographic transformation to ageing population will tend to lower labour force participation, thus affect the economic growth [2]. Traditionally, people in the working ages of 15 to 64 are expected to provide support to those in the dependent ages of 15 and below or 65 and above. This is known as potential support ratio, which is an indicator of productive working-age people for every older person in the population. The global potential support ratio is projected to drop drastically, by more than 50 % over the next 50 years. By the year 2050, the global potential support ratio is expected to decline to 4.1 from the numerical value of 9.1 in the year 2000, with the highest percentage decrease in the developing countries [5]. For instance, a report released by National Population and Talent Division of Singapore stated that due to low fertility rate of only 1.2 in Singapore, the potential support ratio in Singapore dropped drastically from 13.5 in the year 1970 to 4.8 today. In another 15 years, this ratio is expected to drop more than 50 % to 2.1 [15]. The widespread decrease of the potential support ratio increases the economic burden of working individuals in order to maintain stable flow of benefits and supports to the elderly population.

Population ageing is a powerful and transforming demographic force. With the increasing number of people entering older ages combined with steady improvement in human life expectancy, the understanding of the mechanism underlying ageing and age-related diseases is becoming more important as the need to develop interventions that can delay ageing, improve lifespan and healthspan. Thus ageing research is needed to elucidate the nature of ageing and age-related changes in humans as well as diseases and conditions associated with growing old. This effort is important to find ways of preventing or ameliorating such age-related diseases with the aim of promoting healthy and active years late in life.

1.2. Ageing

Ageing is a time-related progressive accumulation of detrimental changes that are associated with increasing susceptibility to disease and death [16].

The American gerontologist, Bernard Strehler [17] suggested four criteria to define age-related changes (ageing) which includes [17, 18]:

1. Ageing is a universal phenomenon that all individuals share. It is associated with natural age-dependent changes that must occur in different degrees in all individuals of a species.

2. Ageing is an intrinsic process which means the causes of normal age-related changes must be endogenous and must not depend on extrinsic factors. This is a criterion suggested to distinguish universal ageing and intrinsic ageing as certain age-related changes may be universal but a consequence of a modifiable, environmental effect on living systems. For instance, genetic damage due to cosmic radiation is universal but not intrinsic damage to the system.

3. Ageing must be progressive, usually considered as a process rather than sudden event. This process is a gradual age changes occur with time throughout the lifespan of an organism and the age-related changes start to occur in individuals even when they were young.

4. Ageing is the accumulation of various deleterious process which affects the functions of cells, tissues, organs and ultimately the organisms. This is because most age dependent deleterious effects, particularly the decline in functional capacity is reflected in an increased in mortality rate. However, not all age-related changes are deleterious, some age-correlated changes like development process and adaptive process that results in improvement of an organism's survival capacity are not consider ageing, these are part of developmental process rather that ageing.

In general, ageing is associated with a decline in efficiency of physiological processes which include biological function on molecular, cellular and tissue level [19]. These physiological processes reduce the efficiency of body metabolism, resulting in the disruption of body functional processes and ultimately death. Characteristic signs of ageing in human include a

gradual decline in height and weight due to loss of muscle and bone mass, a lower metabolic rate, a decline in memory, vision, as well as an increase in the susceptibility to disease.

1.3. Theories of Ageing

Almost every important discovery of molecular biology has stimulated the development of different theories of ageing [20]. The study of the ultimate causes of ageing and the mechanisms by which we age has generated more than 300 scientific theories of ageing and the number continues to grow [21]. However, these different theories of ageing are not mutually exclusive, but they may overlap at some level and may in fact be complementary to other theories [20, 22]. Theories of ageing can be classified into evolutionary theories of ageing and causality/molecular theories of ageing [23]. Evolutionary theories of ageing try to address how ageing evolves and why ageing occurs whereas causality/molecular theories of ageing explain how ageing and death occur on a molecular level [23, 24].

1.3.1. Evolutionary theories of ageing

The evolution of ageing theories aim to understand why ageing evolves and why different biological species age at different rates [25]. The evolutionary theories of ageing describe ageing through the interaction of two important processes; natural selection and mutation [26]. In a given environment, every trait can be classified into neutral, beneficial or detrimental according to its fitness value. This value describes the ability of an individual to survive and reproduce. Over several generations, genes that improve organism's survival due to forces of extrinsic mortality (e.g. starvation, environmental variations, predation and disease) and genes that enhance reproductive capacity are selected for [27-29]. For instance, genes that are able to enhance rapid development and reproduction are selected for in organisms living in environments with high extrinsic mortality; whereas for organisms living in environments with low extrinsic mortality, genes that increase the longevity and reproductive fitness are favored [22]. Therefore, these genes become dominant within the population. Supporting this theory is the study by Austad conducted in the year 1993 where he compared the lifespan of opossums living in environments subject to predators or free of predators. Consistent with the

evolutionary theory of ageing, the protected opossums aged more slowly and thus had a longer life expectancy [22, 30].

Evolutionary explanations of aging are classified into [20, 26]: (a) mutation accumulation theory, (b) antagonistic pleiotropy theory and (c) disposable soma theory.

1.3.1.1. Mutation accumulation theory

The mutation accumulation theory of ageing is based on Medawar's insight (1952) that the decline in the force of selection means that there is no mechanism to prevent the accumulation of late-acting mutations that are not deleterious to reproductive success in the population [20, 31]. This theory emphasizes that these detrimental, late-acting mutations are not selected against by natural selection at young age, hence, these genes would accumulate and lead to pathology and death at old age [20, 26, 32]. For example, a mutant gene that kills young people will be strongly selected against and have little chance to reproduce, therefore being eliminated from the population. This can be explained using the example of a rare, fatal genetic disease, progeria. Patients with progeria, particularly young children develop symptoms of premature ageing. They only live for about 12 years, consequently, they have no chance to reproduce and to pass their mutant genes to next generations [33]. In contrast, patients with Huntington's disease (an inherited neurodegenerative genetic disorder that causes damage to brain cells leading to cognitive decline and dementia) usually develop physical symptoms of this disease between 30 to 40 years of age. People carrying the mutation for this late-onset disease can therefore reproduce before the illness occurs, thereby allowing the mutation to escape natural selection and pass the gene to their next generations [34].

Although both Progeria and Huntington's are considered relatively rare genetic disorders, Progeria is an extremely rare genetic disease with an incidence rate of about 1 in every 8 million people worldwide [35]. By contrast, the gene for Huntington's disease appears more frequently than Progeria at approximately 1 in 20,000 people worldwide [36, 37]. Overall, the mutation accumulation theory of ageing suggests that, since there is little force of selection on late acting

genes through possible accumulation with late acting detrimental effects, a very large number of genes might be distributed through the genome contributing to disease and ageing [25, 26].

1.3.1.2. Antagonistic pleiotropy theory of ageing

Pleiotropy is a situation in which a single gene influences multiple phenotypic traits. Antagonistic pleiotropy describes a situation in which the expression of one pleiotropic gene provides both beneficial and detrimental effects to the organisms. In the year 1957, George Williams further developed Medawar's theory by considering pleiotropic genes and suggested the antagonistic pleiotropy theory of ageing. This theory proposes that organismal age because of combined effect of many genes that offer beneficial effects early in life but have adverse (antagonistic) pleiotropic effects in late life. [38]. The antagonistic pleiotropy theory assumes that natural selection favored pleiotropic genes that have beneficial effects on reproduction or physical fitness early in life and that these genes will therefore be selected for, regardless of the various accompanying detrimental side effects in later life [24]. Support for the antagonistic pleitropy theory of ageing has been found in the experiment on natural populations of *Poecilia reticulata* guppies [39]. In one study, guppies derived from more dangerous environments with high extrinsic mortality rate were introduced into an environment with low extrinsic mortality rate. The pattern of senescence of these two groups of guppies was compared. The introduced guppies still had higher reproduction capacity and experienced senescence earlier than those from natural low extrinsic mortality rate environments. This early onset of senescence may involve the immune system and this may be part of the trade-offs to have significance detrimental impact on fitness and lifespan. There is, however, a second study that does not support the classical antagonistic pleitropy theory of ageing. In this study, guppies from more dangerous environments with high extrinsic mortality rate have lower rate of ageing and do not experience senescence earlier than those from natural low extrinsic mortality rate environments but this population of guppies experienced a more rapid deterioration in physical performance (eg. Swimming performance) [40].

1.3.1.3.Disposable Soma theory of ageing

Proposed by Thomas Kirkwood in the year 1977 [41], the disposable soma theory of ageing can be considered as an extension of the antagonistic pleitropy theory of ageing, suggesting the relationship between reproduction and lifespan. The key idea is that organisms have to ration resources between maintenance of the soma and reproduction [41, 42]. Kirkwood states that all living organisms have limited energy resources [38] and that ageing might be due to progressive accumulation of unrepaired damage over time, resulting from the trade-off between the metabolic cost of reproduction and body maintenance. When resources are limited, evolutionary forces tend to allocate resources to reproduction and thus there are fewer resources for somatic maintenance (in other words longevity). This is a successful strategy because the chance of an organism dying young in the wild is high and it is not sensible to invest resources in maintenance to result in organisms' survival much beyond their essential lifespans, which is the natural lifespan of a species [43]. Resources allocation is important because the germ line (reproductive cells) must be maintained throughout the generations, whereas the soma serves only a single generation [25]. Supporting evidence for this antagonistic pleitropy theory including the disposable soma theory of ageing comes from studies in both *Drosophila* and *C.elegans* where longevity often inversely correlates with reproductive capacity [44, 45].

Overall, evolution acts to maximise reproductive fitness and selects for a longevity that is beneficial to reproductive success for continuation of generations. Therefore, evolutionary theories of ageing try to address the observation that ageing is a phenomena that takes place in protected environment in which the survival of an organism beyond its essential lifespan is possible and likely [46].

It is important to note that evolutionary theories of ageing explain why ageing occurs (how particular traits that affect ageing might accumulate in the population) while mechanistic theories which will be discussed later, explaining how ageing occurs (molecular mechanism underlying the process of ageing). These two types of ageing theories are complementary in the explanation of the normal ageing process.

1.3.2. Damage-accumulation theories of ageing

Numerous molecular or mechanistic theories of ageing have been proposed. As early as the year 1900s, Max Rubner found that large animals tend to live longer than small animals and that those small animals had higher metabolic rates [47, 48]. Based on his observations, he suggested a relationship between metabolic rate, body size and longevity. Later in the year 1928, Raymond Pearl further expanded on this inverse relationship between metabolism and lifespan, formulating the rate of living hypothesis of ageing [49]. He observed that *Drosophila* cultured at different temperatures have different metabolic rates and thus have different lifespans. Based on this observation, he proposed metabolism causes ageing and therefore metabolic rate determines ageing rate (Figure 1.1). This implies that the higher the metabolic rate (energy consumption), the faster the biochemical processes underlying life and thus the faster an organism ages. In other words, animals are born with finite lifetime metabolic capacity [47, 50]. Over time, evidence to support this living theory became less convincing. For example, the rate of living theory does not explain why birds and bats live longer than mice although they have relatively high metabolic rates [43]. Furthermore, regular exercise, which increases the metabolic rate, does not result in higher mortality in mammals [51, 52]. Also not in agreement with this theory are some caloric restriction studies in rodents, suggesting that limited calorie intake can increase lifespan without reducing metabolic rate as compared to control animals [53]. These are only some examples which make clear that energy metabolism alone could not explain lifespan [54]. While the rate-of living theory is no longer accepted nowadays, it directed ageing research to focus on oxygen metabolism [43, 55, 56] as oxygen is the main requirement during aerobic metabolism. The free-radical theory of ageing (FRTA), which will be discussed in the next section, was later developed by Denham Harman in the year 1956 [57]. The FRTA provided a link between metabolism and ageing [47, 58] and is a possible explanation that might account for the observations of Max Rubner and Raymond Pearl.

The FRTA is one of the more popular and well-studied ageing theories today. It proposes that ageing results from the progressive accumulation of free radical-mediated damage, causing random deleterious damage to macromolecules *in vivo* and that this damage is ultimately the cause of age-dependent diseases and death [8, 57, 59]. Biological macromolecules such as, proteins, lipids and nucleic acids are susceptible to free radicals attack, and the extent of free radical-mediated damage is dependent on genetic and environmental factors [57, 60]. Harman

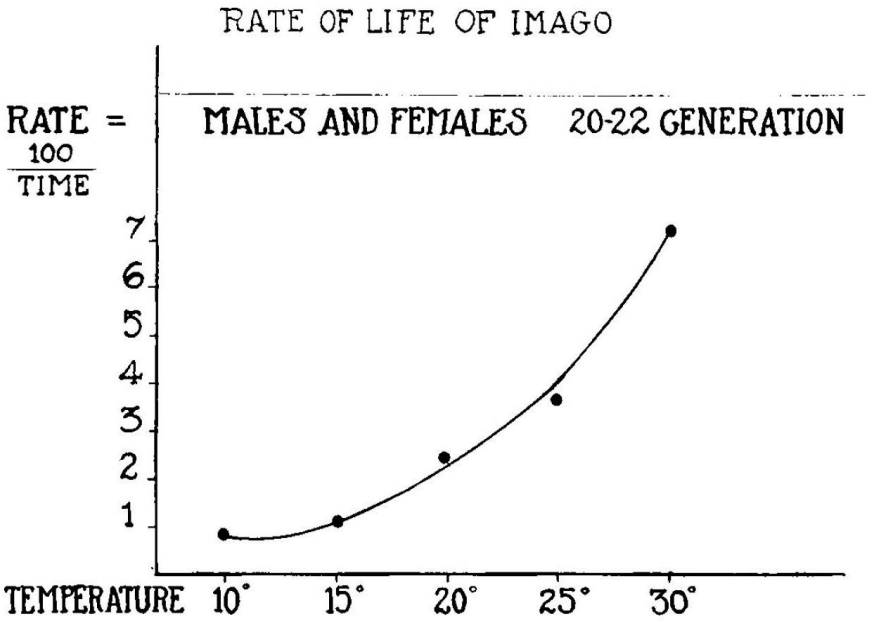

Adapted from J. Loeb and J. H. Northrop, 1917

Figure 1.1. The effect of temperature on the metabolic rate of *Drosophila*. Animals cultured at higher temperature have higher metabolic rate. The faster the energy consumption, the faster the biochemical process thus the animals age faster.

postulated his theory based on the observations that irradiation generates free radicals and that high reactivity free radicals are also produced in living systems under normal conditions. These observations are supported from the study using paramagnetic resonance absorption method which demonstrated the discovery of unpaired electrons (free radicals) in biological system [61]. The FRTA suggests that the amount of free radicals increases with high metabolic rate [57] and free radicals matter to ageing. In support of this theory, increased molecular damage

with advancing age was indeed found in various laboratory animal models including *C.elegans*, flies and mice [57, 62-65]. Harman's FRTA did not gain much attention initially. However, his theory started to gain support and acceptance when McCord and Fridovich discovered SOD enzymes that degrade superoxide in the year 1969 [66].

Harman initially suggested free radicals production during normal metabolism without specifying their source, later in the year 1972, he refined the FRTA by proposing that mitochondria may be the source and target of free radical reactions [67, 68]. This version of the FRTA is commonly known as mitochondrial free radical theory of ageing (mFRTA) [69]. The mFRTA postulates accumulation of partially unrepaired mitochondrial damage produced as by-products during normal metabolism as the driving force of the ageing process [67, 69, 70]. Harman's mFRTA received further support when Britton Chance observed the generation of hydrogen peroxide (H_2O_2) in isolated mitochondria in the year 1973 [71], which provides evidence about the role of free radicals in living systems.

The mFTRA is based on several concepts [72-77]:

(a) Mitochondrial reactive oxygen species (ROS) increase with age

(b) Mitochondrial ROS-scavenging enzymes' activity decreases with age

(c) mtDNA mutation accumulates with age

(d) mtDNA mutation impairs mitochondrial ETC function, further elevates mitochondrial ROS production, thereby facilitates mutation accumulation and increases macromolecules damaged.

Over the years, there was a great deal of experimental evidence that has accumulated to support as well as challenge aspects of the mFRTA. For instance, mitochondria of old animals are indeed less efficient than the young animals which might be attributed to increased mitochondrial ROS generation in older animals. Old animals also generally have higher markers of oxidative damage with increased protein, lipid and nucleic acid oxidation [62, 75-

77]. There is evidence for age-associated accumulation of mitochondrial mutation such as point mutation and deletion. For example, Corral-Debrinski *et al.* showed increased mitochondrial deletions with advanced age in different regions of human brain [78]. Furthermore, the mtDNA of old rhesus monkey also accumulates high levels of deletions in skeletal muscles. Some experimental data that support this theory come from studies of lifespan in different species, such as nematodes, flies and mice [62, 79-87]. These studies demonstrated that longer-lived species typically have lower mitochondrial ROS production thus lower oxidative damage to macromolecules. However, this is not always the case and some studies have failed to support the mFRTA. *C.elegans* lacking mitochondrial SOD (MnSOD) did not experience reduced lifespan or increased accumulation of oxidative damage [62, 63, 88]. Similarly, the longest living rodent, the naked-mole rat, is able to live longer with extended health span compared to normal mice, even though it accumulates high level oxidative damage at young age [89].

1.4. Reactive Oxygen Species

A free radical is an atom, molecule or ion that contains one or more unpaired electrons [8]. Free radicals can have positive, negative or neutral charge. Free radicals can be formed by either donating or accepting one electron from a non-radical species, forming radical cation (equation 1) or radical anion (equation 2) respectively [8]. In addition to these two chemical processes, formation of free radicals may also involve a process known as homolytic bond fission. This process involves the breaking of a covalent bond and one electron from the covalent bond remains on each atom after the homolytic cleavage (equation 3). The dissociation of the covalent bond requires a significant amount of energy such as energy provided by heat, ultraviolet light or ionizing radiation [8]. Generally, free radicals are short-lived, unstable and have high tendency to react with other molecules.

Equation 1 : $A - e^{-} \longrightarrow A^{\cdot +}$

Equation 2: $B + e^{-} \longrightarrow B^{\cdot -}$

Equation 3: $A : B \longrightarrow A^{\cdot} + B^{\cdot}$

Reactive oxygen species (ROS) are chemically reactive molecules (including free radicals) that contain at least one atom of oxygen. All oxygen radicals are ROS but not all ROS are oxygen radicals [8]. Some of the examples of oxygen radicals are superoxide anion ($O_2^{\cdot -}$) and hydroxyl radical ($OH^{\cdot}$). In contrast, examples of non-radical derivatives of oxygen which are also considered as ROS are hydrogen peroxide (H_2O_2), peroxynitrite ($ONOO^-$) and hypochlorite (OCl^-) [8, 90].

ROS can be generated in living systems by either exogenous or endogenous sources. Exogenous ROS sources includes ultraviolet (UV), ionizing radiation, chemical pollutants and some medications. Endogenous ROS are generated intracellularly through multiple mechanisms, the major process being oxidative phosphorylation.

The process of ROS production and detoxification is generally tightly regulated, ROS can be beneficial and detrimental to living systems depending on nature, locations and concentrations of the ROS. There is a large body of evidence that demonstrate the use of free radicals in various physiological functions that benefit the living systems [91], such as in the cellular signaling functions and defense against infectious agents [92]. ROS, maintained at proper (low or moderate) cellular concentration can be beneficial to living systems, including physiological roles in cell signaling as second messenger molecules [93]. However, excessive ROS production or deficiency of antioxidant enzymes, is known to be harmful to the living systems. ROS at high concentration can be detrimental to cell structures, damage biological macromolecules including proteins, lipids and nucleic acids and therefore disrupt cellular function [91, 92]. Nitric oxide ($NO^{\cdot}$), a gaseous free radical and signaling molecules, is an example of ROS that is both beneficial and detrimental. $NO^{\cdot}$ plays an important role in biological processes, particularly in blood vessel homeostasis to inhibit vascular smooth muscle growth [94, 95]. $NO^{\cdot}$ also plays a role in cell signaling, it acts as secondary messenger in neurons and macrophages [93]. In contrast to the useful functions, excess $NO^{\cdot}$ can contribute to cell injury [93].

A disturbance in the balance between ROS production and detoxification in biological systems is termed oxidative stress. Oxidative stress has been implicated in the development of several human diseases including some neurodegenerative diseases, cancer and cardiovascular disease.

1.5. Mitochondria

ROS are metabolic by-products which are constantly generated as part of normal aerobic life and mitochondria are known to be the main producer of ROS in animals [96, 97]. Mitochondria are often called "cellular power plants" because they play a prominent role in producing the majority of adenosine triphosphate (ATP) via oxidative phosphorylation [98]. In addition to energy generation, mitochondria are also involved in apoptosis [99], ion homeostasis [100], and other biochemical metabolic pathways include calcium signaling [101] and steroid synthesis [102].

Mitochondria are highly organized structures, bound by two phospholipid bilayers, the inner and outer membrane, leading to the formation of two compartments, the matrix and the intermembrane space (Figure 1.2) [103]. These inner and outer membranes are quite distinct in appearance and function, with different enzymes and reactions confined to different membranes and compartments [104]. The outer mitochondrial membrane encloses the entire organelle and contains porins, which are the integral proteins that form channels to allow ions and large molecules through the outer mitochondrial membrane [105]. Unlike the outer mitochondrial membrane, the inner mitochondrial membrane does not contain porins and therefore is impermeable to ions and most metabolites. However, there are numerous specific transporters in the inner mitochondrial membrane that facilitate metabolic communication with other cell compartments. Mitochondria are also highly mobile organelles. They form dynamic networks that continuously undergo fusion and fission events [103, 106]. Mitochondrial fusion and fission are important for modulating cellular redox status, maintaining mtDNA integrity, mitochondrial networks and function [107]. In addition, mitochondrial fusion and fission events also play important roles in several disease-related processes such as apoptosis and mitophagy [106, 108] . For instance, studies have shown that Alzheimer disease (AD) patients have

imbalance in the expression of mitochondrial fusion and fission proteins resulting in mitochondrial fragmentation [109, 110].

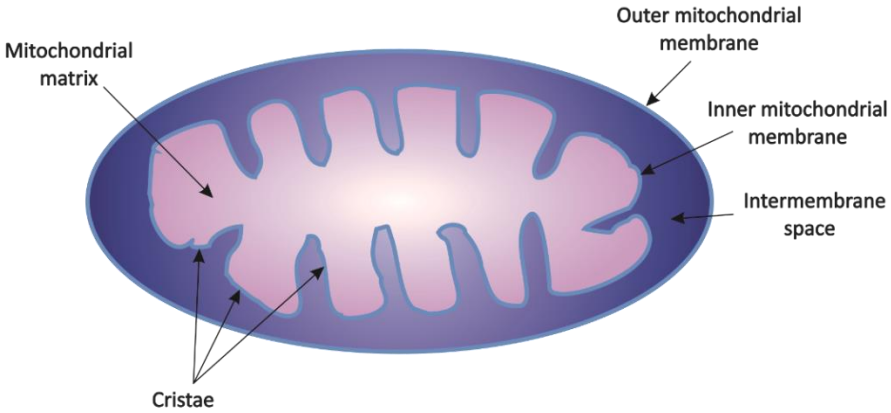

Figure 1.2. Structure of a mitochondrion. Mitochondria are membrane bound organelles that are surrounded by two membranes, the outer and inner mitochondrial membrane. In electro micrograph, the mitochondrion is oval in shape and has an average size ranging from 0.5 to 1.0 μm. The number of mitochondria per cell varies widely, depending on the metabolic requirements of the cell.

Cellular respiration takes place in three stages: glycolysis, tricarboxylic acid (TCA) cycle and oxidative phosphorylation (Figure 1.3). Nutrients such as glucose can be broken down into pyruvate during glycolysis in the cytoplasm. Pyruvate is transported to the mitochondria where it is converted into acetyl coenzyme A (acetyl-CoA). Subsequently, acetyl-CoA enters the TCA cycle and is further oxidized to carbon dioxide, this process produces nicotinamide adenine dinucleotide (NADH) and flavin adenine dinucleotide ($FADH_2$). NADH and $FADH_2$ are energy-rich molecules that act as a source of electrons for the oxidative phosphorylation (Figure 1.4).

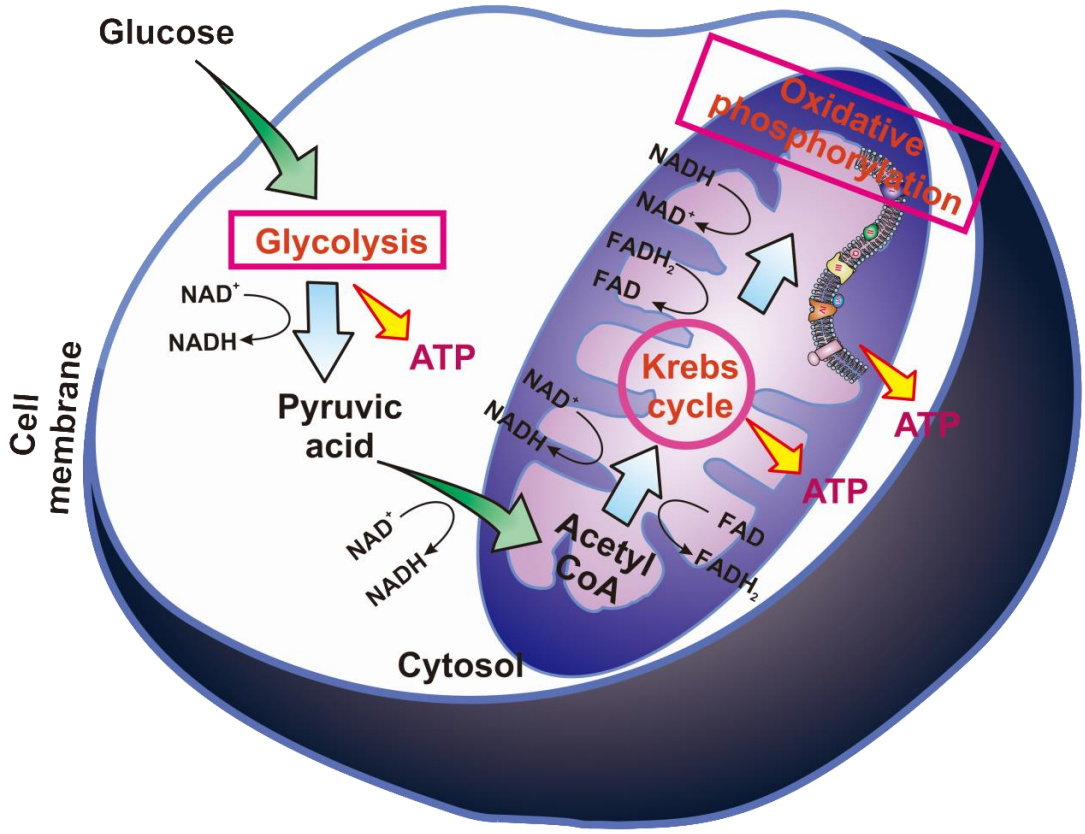

Figure 1.3. An overview of cellular respiration. Cellular respiration is carried out in three stages: glycolysis, TCA cycle and oxidative phosphorylation. The first stage in cellular respiration is the biochemical process called glycolysis, occurring in cytoplasm. Glycolysis converts glucose to pyruvate, generates ATP and NADH. Pyruvate generated during glycolysis is then transported to mitochondria and converted to acetyl-CoA. The second biochemical pathway is known as TCA cycle, where the acetyl-CoA enters TCA cycle, converts into CO_2, generating ATP, NADH and $FADH_2$. TCA cycle occurs at the matrix of the mitochondria. The third stage of the cellular respiration is the oxidative phosphorylation, takes place in inner mitochondrial membrane. Oxidative phosphorylation is the metabolic pathway in which ATP is formed as a result of electrons transfer from NADH and $FADH_2$.

Oxidative phosphorylation is the metabolic process by which respiratory enzymes in the mitochondrial inner membrane use energy released by the oxidation of nutrients to generate ATP. The prominent role of mitochondria in ATP production is due to the presence of five distinct insoluble integral membrane protein complexes which are embedded in the inner mitochondrial membrane (Figure 1.4). These mitochondrial respiratory chain complexes are the main enzymatic machinery of the oxidative phosphorylation [111].

The ETC complexes are:

1. Complex I: NADH dehydrogenase or NADH- ubiquinone oxidoreductase, is the first enzyme of the respiratory chain. It catalyzes NADH oxidation by transferring electrons from NADH to ubiquinone (a lipid-soluble carrier). NADH is oxidized by reducing flavin mononucleotide to $FMNH_2$. Electrons are then transferred from $FMNH_2$ to Fe-S cluster to ubiquinone. During the transfer of the electrons, protons are transported across the inner mitochondrial membrane, contributing to the proton-motive force.

2. Complex II: succinate dehydrogenase or succinate ubiquinone oxidoreductase. Additional electrons are transferred from complex II to ubiquinone. The electrons transfer originates from complex II by oxidation of succinate to fumarate while passing electrons on to FAD which then is reduced to $FADH_2$. $FADH_2$ then passes its electrons to Fe-S clusters and then to ubiquinone. Unlike complex I, no proton-motive force is generated.

3. Complex III: cytochrome c reductase, bc1 complex or ubiquinone-cytochrome *c* oxidoreductase. Complex III catalyzes the reduction of cytochrome c by transferring electrons that were accepted from complex I and II from ubiquinone to cytochrome c (a water-soluble electron carrier). During this process, proton motive force is generated.

4. Complex IV: cytochrome *c* oxidase (COX) or reduced cytochrome c: oxygen oxidoreductase. Complex IV is the terminal enzyme of the respiratory chain. In complex IV, electrons were transferred from cytochrome c to complex IV and were then transferred to molecular oxygen one at a time to produce water molecules.

5. Complex V: ATP synthase or proton-translocating ATP synthase. Complex V is responsible for ATP production from ADP and inorganic phosphate, driven by the transmembrane electrochemical proton potential difference generated by the transfer of electrons.

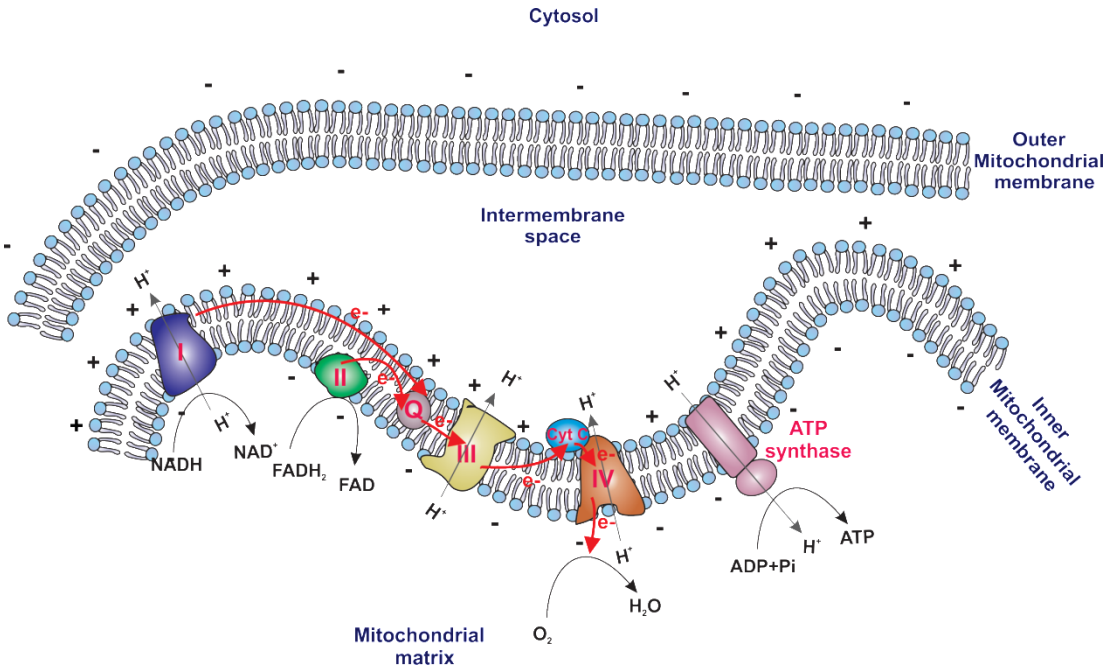

Figure 1.4. A schematic of mitochondrial ETC complexes. Oxidative phosphorylation is the last step of cellular respiration and depends on electron transfer on ETC complexes. The mitochondrial ETC complexes consists of five complexes, namely complex I to IV.

In general, electrons enter the ETC via complex I and II respectively [98]. In a stepwise pattern, the electrons from both complex I and II are then carried by the electron carriers, ubiquinone or coenzyme-Q to complex III. The electrons are then transferred from complex III to cytochrome *c*, located within the intermembrane space. In complex IV, electrons from the cytochrome *c* are transferred to oxygen, the terminal electron acceptor where oxygen is reduced and water formed as the product.

The flow of electrons by the ETC complexes results in a net efflux of protons through complex I, III and IV from the mitochondrial matrix into the mitochondrial inter-membrane space creating an electrochemical proton gradient. This electrochemical proton gradient is used to drive ATP synthesis from adenosine diphosphate (ADP) and inorganic phosphate through the

enzymatic activity of ATP synthase. Since the mitochondrial inner membrane is impermeable to ions, the protons can only reenter the matrix through special proton channel protein, complex V [112]. The PMF drives the passage of protons back into the mitochondrial matrix through complex V, thus driving the synthesis of ATP from ADP and phosphate.

1.5.1. Mitochondria as a cellular source of ROS production

ROS can be generated at numerous sites within the cell with mitochondria being the major cellular source of ROS [113]. A main factor that controls mitochondrial ROS production is the redox state of the mitochondrial ETC [114]. During the final reaction of oxidative phosphorylation, the final electron acceptor, oxygen, is reduced to water (Equation 4). However some electrons from the ETC can leak to oxygen prematurely, causing electron reduction of molecular oxygen to generate superoxide (Equation 5), which is a charged, relatively unstable intermediate [96]. Superoxide is the precursor of most ROS and a mediator in oxidative chain reactions in ETC [8, 58, 74, 115]. ROS are mainly generated in this way within ETC complex I and III [116, 117]. Complex I produces the most superoxide radicals compared to other complexes in the mitochondrial ETC and that superoxide produced is being released to the matrix side of the Inner mitochondrial membrane (Figure 4) [118-120]. There is evidence that there are two distinct superoxide production sites from complex I, (i) the flavin from flavin mononucleotide moiety and (ii) $QH^{\cdot}$ in the ubiquinone binding site [115, 121]. Whereas, complex III releases superoxide to both the mitochondrial matrix and intermembrane space (Figure 4) [122] . Rich and Bonner first suggested that Q_o semiquinone which is situated next to intermembrane space is the site of superoxide production in complex III [115, 121, 123-125] .

Superoxide is the first radical produced in mitochondria. It is generally membrane impermeable and is converted to hydrogen peroxide (H_2O_2) (Equation 6) by metal dependent enzyme superoxide dismutase (SOD) (manganese SOD (MnSOD) in the mitochondrial matrix or Copper Zinc SOD (CuZnSOD) in all cell compartments except the mitochondrial matrix [121, 126]. Unlike superoxide, the uncharged H_2O_2 is a compound of relatively poor reactivity, more

stable than superoxide and can diffuse through the mitochondrial membranes. H_2O_2 is, in turn, broken down into water [121] (Equation 7) by glutathione peroxidase (GPx), peroxiredoxins (Prdx), glutathione (GSH) and thioredoxin-2 (Trx) in the mitochondrial matrix or is removed by catalase in the cytosol and peroxisomes [127]. However, in the presence of transition metals such as iron, H_2O_2 can undergo Fenton reaction and generate the extremely reactive hydroxyl radical ($OH^{\cdot}$) (Equation 8). There are two other important radical species, nitric oxide ($NO^{\cdot}$) and peroxynitrite ($ONOO^-$). Superoxide can react with $NO^{\cdot}$ to generate $ONOO^-$ which is subsequently converted to other reactive radicals includes nitrogen dioxide ($NO_2^{\cdot}$) and $OH^{\cdot}$ [58].

Equation 4: $O_2 + 4H^+ + 4e^- \rightarrow 2H_2O$

Equation 5: $O_2 + e^- \rightarrow O_2^{\bullet -}$

Equation 6: $O_2^{\bullet -} + e^- + 2H^+ \rightarrow H_2O_2$

Equation 7: $2H_2O_2 \rightarrow 2H_2O + O_2$

Equation 8: $H_2O_2 + Fe^{2+} \rightarrow HO\bullet + OH^- + Fe^{3+}$

ROS can damage lipids, proteins and nucleic acids. Furthermore, the products of oxidation of these macromolecules can cause secondary damage to proteins which causes proteins to degrade and lose their catalytic function [128]. The significance of ROS production in mitochondria is demonstrated in the studies using MnSOD knockout mice and flies where failing to remove the mitochondrial ROS reduces the lifespan of the mice [129, 130]. Unlike MnSOD knockout mice and flies, MnSOD deletion in nematodes did not altered lifespan or increase oxidative damage [62, 63, 88]. However, there is evidence that knocking out MnSOD in nematodes inhibited the mitochondrial ETC [62, 63] which is thought to be a compensatory mechanism. Nevertheless, mitochondrial-generated ROS can be considered as a major source of cellular damage.

1.5.2. Mitochondria as target of ROS

As the main site of oxidative phosphorylation, mitochondria are exposed to relatively high concentration of ROS and may therefore susceptible to ROS-mediated damage [96, 124]. Although H_2O_2 can diffuse through the mitochondrial membrane, other ROS such as $O_2^{\bullet -}$ are not membrane permeable, and probably react with macromolecules inside the mitochondria. ROS produced outside mitochondria by other cellular sources may also be targeted to mitochondria [124, 131], thus causing additional mitochondrial damage. Such cellular locations include the endoplasmic reticulum [132], cytosol [133], peroxisome [134], plasma membrane [135] and extracellular space [136]. ROS can react with and are able to cause damage to a wide range of biomolecules such as lipids, proteins and nucleic acids.

1.5.2.1. Oxidative damage to mitochondrial lipids

Mitochondrial lipid peroxidation refers to ROS attack on mitochondrial lipid, particularly on free lipids or lipids in the mitochondrial membrane [58]. Lipid peroxidation might be particularly harmful to mitochondria because mitochondria contain cardiolipin as a major and important component of mitochondrial inner membrane. Cardiolipin is exclusively found in the inner mitochondrial membrane [137, 138] and is vulnerable to peroxidation because of its high degree of polyunsaturated fatty acids [137]. Lipid peroxidation generates lipid radicals, which can further react with oxygen or other lipids forming lipid peroxidation products such as 4-hydroxy-2-nonenal (HNE) and malondialdehyde [58, 139]. Lipid peroxidation therefore can progress in a chain reaction and these lipid peroxidation products can subsequently cause cellular damage by reacting with other lipids, proteins and nucleic acids. Peroxidation of lipids can also alter membrane fluidity and permeability, thus directly affecting the ETC function [140, 141]. The product of oxidized lipids, HNE can induce mitochondrial uncoupling proteins, causing protons leak across mitochondrial membrane [142].

1.5.2.2. Oxidative damage to mitochondrial proteins

Proteins can also be damaged by oxidative conditions either by direct oxidation of amino acids in the protein sequence or as a secondary consequence of lipid peroxidation, for example, HNE

can introduce carbonyl groups to the protein [76, 124, 143]. Mitochondrial proteins are highly susceptible to oxidative damage such as carbonylation and nitration [144]. Mitochondrial protein oxidation may modify amino acid residues, altering mitochondrial ETC metabolic enzymes functions including ATP synthase, pyruvate decarboxylase complex activity, NADH dehydrogenase and aconitase activity [139, 144-146]. Consistent with a role of ROS in ageing, increased oxidized proteins in human [147, 148], mice [149] and *C. elegans* [62, 150] show a positive correlation with age. This is consistent with the notion that accumulation of oxidized protein may play a part in ageing.

1.5.2.3. Oxidative damage to mitochondrial DNA (mtDNA)

DNA damage appears ubiquitous in biological systems and is often proposed to be a main mechanism of ageing [151]. DNA damage is important because other macromolecules such as proteins and RNA can be replaced if damaged thus blocking the progressive accumulation of damage of these macromolecules over a lifetime [152]. Genetic defects in DNA are particularly harmful to organisms as they may lead to mutation, modify gene expression and replication, and in the case of mtDNA cause impairment of mitochondrial function, eventually leading to metabolic dysfunction and degenerative diseases including neurodegeneration [153-156].

1.5.3. Mitochondrial genome

Mitochondria are of particular interest because they are the only organelles in animals that have their own genetic information (DNA) [127]. MtDNA was discovered in the year 1963 by Margit M. K. Nass and Sylvan Nass using electron microscopy [157]. Besides having their own genome, mitochondria also have their own ribosomes and transfer ribonucleic acids (tRNA), independent of the nucleus. MtDNA molecules are typically 13 to 18 kb in length [112, 154, 158, 159]. For instance, *C. elegans* mitochondrial genome is 13,794 nucleotides in length, encoding 12 polypeptides of the mitochondrial respiratory chain complexes, 2 ribosomal RNAs (12S rRNA and 16S rRNA) as structural part of mitochondrial ribosomes and 22 transfer RNA essential for mitochondrial translation [160, 161]. They have a closed circular double stranded DNA structure, organized into DNA-protein structures known as nucleoids. These nucleoids

reside within the mitochondrial matrix and attach to the mitochondrial inner membrane [158, 159]. Despite having their own DNA, about 98% of the mitochondrial proteins are nuclear encoded, synthesized in the cytosol and translocated into the mitochondria by mitochondria-import peptides [103]. The number of mitochondria as well as the mtDNA content in each cell varies, depending on the type of cell and the metabolic activities of the tissues [158, 162]. For instance, muscle tissue has relatively high number of mitochondria due to its high energy requirements [163]. In *C. elegans*, mtDNA content varies with developmental stage. Adult *C. elegans* have much higher mtDNA content than both embryos and larvae because during development mitochondrial copy number increases significantly and oocytes also contain 24,000 copies of mtDNA [160, 161]. However, we have found that the mtDNA copy number declines as the nematodes age [62].

1.5.4. mtDNA damage induced by ROS

MtDNA is under constant attack by ROS and is exposed to oxidative damage leading to genetic defects. Not all ROS can damage DNA and different ROS cause various types of mutagenic or lethal lesions to DNA [8]. Examples of the main types of DNA damage including alkylation damage, hydrolytic damage, formation of adducts, DNA stand breaks and oxidation damage, especially 8-hydroxy-2' -deoxyguanosine (8OHdG) [152].

1.5.4.1. Alkylation damage

DNA alkylation damage occurs when an alkylating agent such as Methyl methanesulfonate and 10-decarbamoyl mitomycin C, covalently modifies DNA by transferring an alkyl group to a DNA base. Alkylating agents are therefore mutagenic and cytotoxic. There are two types of alkylating agents: exogenous and endogenous. Exogenous agents such as anticancer compounds and endogenous agents for instance S-adenosylmethionine are alkyl donors that can cause DNA lesions at DNA heterocyclic bases or the DNA backbone [164, 165].

1.5.4.2. Hydrolytic damage

The covalent structure of DNA, in particular the glycosidic bond that holds the nucleobases to the sugar phosphate backbone is relatively unstable and is subjected to spontaneous hydrolytic

damage by water molecules [166, 167]. Hydrolysis of glycosidic bond results in the loss of purine or pyrimidine bases forming abasic (apurinic or apyrimidic respectively) sites[168]. The process of breaking the chemical bond connecting the purine base (adenine or guanine) from the deoxyribose phosphate backbone leaving an apurinic, site is known as depurination while the loss of pyrimidine base (cytosine and thymine) from DNA forming apyrimidic site is known as depyrimidination. Depurination and depyrimidination are potentially lethal to the cells as unrepaired abasic sites can inhibit transcription.

1.5.4.3. Formation of bulky adducts

DNA adducts are altered forms of DNA that occur when DNA is covalently bonded to carcinogenic chemicals from endogenous or exogenous sources [168]. In humans, DNA adducts are caused by natural hormone including estrogen or other endogenous sources such as malondialdehyde or HNE which are naturally occurring products of lipid peroxidation [169, 170]. Covalent binding of exogenous sources to DNA molecule includes acetaldehyde /tobacco smoke and cisplatin/chemotherapy drugs, which can form DNA adducts thus damaging the DNA [171].

1.5.4.4. DNA stand breaks

DNA strand breaks refer to single- or double-strand DNA cleavage in DNA double helix. Single-strand breaks occur when both the nucleotide base and deoxyribose backbone are lost from DNA structure. Such DNA strand breaks can arise either directly from the attack by ROS or indirectly during the process of repair of other DNA lesions [172]. In contrast, double-strand breaks form when the phosphate backbones of both complementary DNA strands are cleaved simultaneously. They can be formed as a consequence of the unrepaired DNA structure during the formation of single-strand breaks. DNA strand breaks can also be caused by exogenous factors such as exposure to irradiation [173]. DNA double-strand breaks are proposed to be one of the most toxic lesions in DNA. A single double-strand break can be sufficient to kill a cell and cause genomic instability [174].

1.5.4.5. Formation of pyrimidine dimers

Pyrimidine dimers are molecular lesions that are characterized by the covalent cross-linkages of two neighbouring pyrimidine residues within a strand of DNA [175]. UV radiation induces the formation of two types of photoproducts, namely cyclobutane pyrimidine dimers (CPDs) and 6-4 photoproducts (6-4 PPs) [175, 176]. 6-4 PPs are less common but more mutagenic than CPDs. Both lesions can distort the DNA structure, disrupt polymerases and thereby impeding transcription and replication.

1.5.4.6. Oxidation of bases

The continuously generation of ROS as by-products of normal metabolism is one cause of DNA oxidation and could be one of the leading contributors to DNA damage under normal conditions. DNA oxidation can occur at either sugar units, phosphates and nucleobases [177, 178]. Oxidative DNA damage to sugar units generates carbon-centered sugar radicals that further react with oxygen and cause the DNA to lose nucleobases or formation of DNA strand breaks [178]. ROS attack can also occur at both purine or pyrimidine. For instance, oxidative damage of DNA bases at guanine residue [179] can lead to the formation of 8-oxo-7,8-dihydroguanine (8-OxoG). Cyclopurine and cyclopyrimidine are formed when both sugar and base of DNA are attacked by ROS, this is mainly caused by ionizing radiation or cancer drugs [180, 181].

Oxidised DNA loses genetic integrity, which can directly or indirectly inhibit normal biological functions. Oxidative damage to DNA is associated with ageing [62] and age-dependent diseases such as AD [182, 183] and Parkinson's diseases [184].

1.6. Ways to cause DNA damage

1.6.1. Damage by endogenous ROS

Many types of ROS are produced *in vivo* during normal metabolism. Of the ROS, the highly reactive OH• is considered the main contributor to ROS-mediated damage and can easily react with DNA to generate oxidized bases and abasic sites. OH• can also indirectly generate other DNA damage products include DNA–DNA intra-strand adducts, DNA strand breaks and DNA–protein cross-links [185].

1.6.2. Damage from gamma radiation

Gamma (γ) radiation refers to short wavelength and high frequency electromagnetic radiation that has high energy and high penetrating power. γ radiation is harmful to living systems as it can readily penetrate most materials. Examples of γ emitters include iodine-131, cesium-137 and cobalt-60. γ radiation has been shown to cause mtDNA damage. Exposure to γ generates ROS with OH• being the major and most damaging product [186, 187]. γ radiation creates a variety of DNA damage including generation of single- and double- strand breaks, abasic sites, oxidized bases and DNA-proteins crosslinks [188-190]. These DNA lesions can cause chromosomal abbreviations, deletions and mutation, which ultimately leads to genome instability and cell death [190].

1.6.3. Damage from Ultraviolet light

Ultraviolet (UV) light is part of the electromagnetic radiation that has shorter wavelength and higher frequency than visible light, thus it is more energetic and damaging. UV light is emitted by the sun or specialized lights such as mercury lamps and to some degree by fluorescent lights. Based on the amount of energy and wavelength, UV light can be divided into subtypes, of which the most common are ultraviolet A (UVA), ultraviolet B (UVB) and ultraviolet C (UVC). The shorter the wavelength, the more harmful UV light is to living systems [191]. UVA has a longer wavelength (320-400nm) and lower penetrating power. UVA hardly has enough energy to cause DNA damage directly [175]. However, UVB, which is in the middle range of UV wavelength (280-320nm), carries more energy and is able to cause DNA lesions directly. UVC (200-280nm) is blocked by the ozone layer and cannot penetrate through the atmosphere [192]. However, UVC is the most energetic and most harmful UV light. UV radiation can cause the formation of CPDs predominantly and 6-4 PPs to a lesser extent [193, 194]. Indirectly, exposure to UV irradiation can also stimulate intracellular production of ROS, therefore generating more DNA damage including 8-OxoG, strand breaks, DNA-protein crosslinks [191, 195, 196].

1.6.4. Damage by ROS generating chemicals : paraquat and Juglone

Both paraquat and juglone are commonly used ROS generating chemicals that are thought to be reduced upon entering the cells and therefore produce more ROS from oxygen [63, 197, 198]. Their main molecular mechanism of toxicity as an electron acceptor is based on redox cycling and intracellular oxidative stress generation. Paraquat is a widely used herbicide [198]. Several studies have reported paraquat toxicity oxidative stress, modifying DNA bases (increase in 8-OxoG formation) and forming DNA strand breaks [198]. Juglone is a natural toxic compound that can be found in one type of plant known as Black Walnut [199]. It is being used as dye and is also under study as anti-cancer compound [200]. The generation of ROS by both paraquat and juglone can trigger DNA damage and act as potential inhibitors of ETC [198, 201].

1.7. Age-related mtDNA damage and mitochondrial diseases

The mFRTA proposed that accumulation of mitochondrial damage is the cause of ageing. However, there are many types of macromolecular damage and there is no consensus regarding which type of damage, if any, plays the central causal role in driving ageing. I will discuss the mtDNA damage in greater detail as this is the focus of my research. There is a large body of evidence suggesting that cellular DNA is constantly exposed to endogenous and exogenous DNA-damaging agents, and accumulation of genetic damage has long been suggested to cause ageing and mitochondrial diseases [152, 202-204]. The relevance of mtDNA to ageing has been suggested by Miquel *et al.* where they proposed that free radical attack on mtDNA and the inner mitochondrial membrane plays a key role in cellular senescence [67]. Numerous studies have since demonstrated accumulation of mtDNA damage in an age-dependent manner, for example in human brain tissue [205], skeletal muscle [206] and cardiac muscle [207]. In addition, oxidative mtDNA lesions were also observed to accumulate in rat and mice [208, 209], *Drosophila* [210] and *C.elegans* [62]. Some animal models with accelerated mtDNA damage accumulation showed premature ageing phenotypes or shorter lifespan. Mice overexpressing catalase targeted to mitochondria have less oxidative damage to mtDNA and longer lifespan

[211]. These animal studies support the idea that DNA damage or DNA damage consequences are involved in ageing [212]. However, in the case of *C. elegans*, knocking out mitochondrial SOD or even *sod-2* and *sod-3* double knock out mutant, devoid of all mitochondrial SOD activity, does not result in the expected lifespan shortening, despite increases in oxidised protein [62, 63, 88, 213, 214]. However, to date, no mtDNA damage data was reported in these MnSOD mutant nematodes. In another example, deletion of *C. elegans* peroxisomal catalase shortens the lifespan yet the animals surprisingly experience lower oxidative damage to protein [215]. Animal studies have thus produced conflicting results. Further insight into the importance of oxidative damage; particularly mtDNA damage is needed in order to test if mtDNA damage is a determinant of ageing.

Accumulation of mtDNA damage has also been suggested to contribute to the development and progression of several diseases such as Alzheimer disease [216, 217], Parkinson's disease [218], diabetes [219], cancer [220] and Huntington's disease [221]. AD, is the most common age-dependent neurodegenerative disease [10, 222]. The "Amyloid hypothesis" states that accumulation of Aβ is integral to AD pathogenesis. It is believed that the presence of Aβ plays a key role in the synaptic damage and neuronal loss that characterises AD [223, 224]. Oxidative stress is closely associated with Aβ accumulation and is believed to play a crucial role in AD pathogenesis [90, 225-227]. In 1994, Butterfield *et al.* showed that Aβ peptides can initiate neuronal lipid peroxidation [227, 228]. AD patients also suffer from increased levels of lipid peroxidation [229], increased formation of advanced glycation end products [230], elevated protein nitration [231] and increased levels of oxidative DNA damage markers [205].

Apart from directly promoting oxidative damage, there is evidence that Aβ targets the mitochondria, causing impairment of ETC complexes, resulting in elevation of ROS production [232, 233]. Interestingly, several studies have reported that Aβ is actively imported into mitochondria through cellular trafficking systems [232]. Manczak and co-workers showed that Aβ readily penetrates the mitochondria and localises to mitoplasts [233], where the ETC complexes reside. This localisation is in line with the finding that Aβ inhibits, in particular complex IV of the ETC [234, 235]. Indeed, early signs of AD include decreased respiratory

chain enzyme activity and reduced mitochondrial membrane potential [236, 237]. In addition, Aβ may contribute even further to mitochondrial dysfunction through disruption of mitochondrial fusion and fission processes, leading to mitochondrial fragmentation [109]. Again, several studies have demonstrated the accumulation of mtDNA damage to be associated with age-related mitochondrial diseases [226, 238], therefore, accurate measurement of mtDNA damage level is important in the study of ageing.

1.8. Measurement of Oxidative DNA damage

Over the years, several techniques have been developed to measure oxidative damage to DNA in purified DNA, cultured cells and tissues. Common techniques include [239-241]:

a) Analytical methods such as high-performance liquid chromatography-electrochemical detection (HPLC-ECD), gas chromatography–mass spectrometry (GC-MS), liquid chromatography/tandem mass spectrometry (LC-MS/ MS) and liquid chromatography/mass spectrometry (LC- MS)

b) Immunology methods

c) Fluorescence-based approaches such as Comet assay and Pico green double-stranded DNA assay

d) Radiolabelled probe such as ^{32}P-postlabeling assay

e) Quantitative PCR-based technique

In general, each technique has specific advantages and limitations. The analytical methods such as HPLC and GCMS are specific to the type of oxidized DNA products that can be detected and they may also provide structural information of the DNA adducts. However, one limitation of these approaches is that they typically require relatively large amount of starting material [242].

Another example, the comet assay, is a sensitive assay that can measure a wide range of DNA damage products [243]. However, due to the small size of mtDNA molecules, this assay cannot measure DNA damage in mtDNA.

The radiolabelled probe assay is well known for its high sensitivity. DNA damage determination can be carried out by administering a radiolabelled compound to laboratory animals and measuring the isotopes ratio. This assay can detect a broad range of DNA adducts and requires only a small amount of DNA sample [241, 244].

Lastly, the quantitative PCR based methods are highly sensitive and gene-specific assay that can be simultaneously used to measure DNA damage in both mitochondria and nuclei. There are various PCR-based assays that have been used to study the oxidative DNA damage including single-strand ligation PCR strand-specific QPCR, and ligation-mediated PCR [245]. I have successfully developed a novel sequence specific DNA damage method based on the PCR based techniques. I will discuss this method in greater detail in chapter 3.

1.8.1. Purpose of developing a sequence-specific DNA damage assay

The purpose of developing sequence-specific DNA damage assay to detect damaged DNA in *C. elegans* is because

i. *C. elegans* are relatively small in size. Therefore, it is difficult to use HPLC method that requires relatively large quantities of starting material [242].
ii. Only 1 % of the DNA in *C. elegans* consists of mtDNA. Some assay such as the comet assay cannot be used to detect DNA damage in mitochondria as mtDNA molecules are too small to be detected and will diffuse away even before electrophoresis starts [246]. Physicochemical methods are not suitable for mitochondrial ageing in *C. elegans* as extraction of large enough mtDNA is a challenge and also the difficulties in purification of mtDNA from total DNA.

1.8.2. PCR-based assays

The PCR–based assays have been widely used to detect and measure DNA damage and repair, such as gene-specific quantitative PCR (qPCR) [245], long qPCR [241], ligation- mediated PCR [247], Fpg-qRT-PCR [248], radiolabelled-qPCR [249] and strand-specific qPCR [250]. However, some of these methods cannot detect the amplification and the DNA molecules in real time. Furthermore, many of these methods are semi-quantitative and only give relative comparison of DNA damage level. Although some of the assays can be used quantitatively, careful calibration and standardization is required. Moreover, some of these PCR techniques required multiple post-PCR processing steps such as quantifying PCR products using PicoGreen fluorescent dye [251], using alkaline elution and measurement of DNA fractions by fluorometry [245]. Furthermore, PCR products can also be quantified by radiolabelling the PCR products and quantification of DNA by gel densitometry [249] or using PCR methods to quantify mitochondrial copy number [241] of the PCR products. However,multiple pre- or post- PCR processing steps are time consuming and tend to reduce signal to background noise ratio as multiple processing steps increase the sources of variation that collectively contribute to the increased in noise signal. Therefore, careful optimization of these multi-step procedures needed to ensure a reliable experimental data.

1.8.3. Sequence-specific quantitative real time PCR (qRT-PCR)

Many PCR based DNA damage assays amplify short DNA target. I have compared several variations of sequence-specific qRT-PCR based DNA damage assays and optimised a qRT-PCR based DNA damage assay using amplification of short and long DNA targets to quantify DNA damage in *C. elegans* which I will discuss in greater detail in chapter 3.

1.9. Animal models of ageing research

Over the years, scientific advances have provided foundations to generate useful animal models to study the ageing process. Various animals have been used to study ageing in the laboratory, ranging from birds, mice, flies and worms [252]. The use of animals in ageing research allows us to address those conserved (public) mechanisms that apply throughout the animal kingdom

[253]. In addition, this approach is the only way to address aspects of human ageing (for practical and ethical reasons) that are difficult to study directly in human beings. For instance, longitudinal investigations of ageing usually require monitoring of a group of individuals from birth till death. Such ageing research in human beings will take many years, but in worms it only takes less than a month. Moreover, laboratory animals allow us to clone many genetically identical animals and subject these animals to controlled conditions [252, 254]. However, laboratory animals are different from human in many ways. The relevance of laboratory animals to the understanding of ageing in human depends on whether the specific functions and biological systems studied are appropriate models for human ageing. Some common (public) ageing mechanisms might be involved in animals across different phyla although some mechanisms are species-specific (private) [255, 256]. Studying ageing in animals from different phyla provides insight into how the common mechanisms, such as public ageing mechanisms are and in any can be translated into an understanding of human ageing [253, 255]. In my projects, I used *C. elegans* as the model of my research studies for investigating the role of DNA damage in ageing.

1.9.1. *C. elegans* as a model organism for ageing research

C. elegans is a small (about 1 mm in length and 80 μm in width) and transparent nematode that feeds on bacteria and lives in temperate soil environments. Most *C. elegans* exist as hermaphrodites and only a small percentage occur as male *C. elegans*. Hermaphrodite *C. elegans* cannot cross-fertilize. One of the advantages of *C. elegans* in ageing research is their short lifespan (mean lifespan of 20 days when cultured at 20 ℃), developing rapidly (from egg to adult in about 2.5 days) and reproducing through self-fertilization of hermaphrodites producing about 300 cloned offspring [257]. Moreover, maintaining *C. elegans* in the laboratory is relatively easy and inexpensive, which further facilitates large scale production, genetic manipulation and experimental treatments of nematodes in short period of times. *C. elegans* has a number of features that make it an attractive model for ageing research. It is a multicellular organism that goes through complex developmental processes; therefore, it may

resemble more complicated organisms in fundamental ways. Hermaphrodite *C. elegans* contains a constant 959 somatic cells while male *C. elegans* comprises 1031 somatic cells. It has 302 neuronal cells that make it one of the simplest organisms with a nervous system [258]. The *C. elegans* genome carries homologs of about 60-80% of human genes [259], making it an attractive organism for modeling human ageing and human diseases [257]. *age-1* is the first lifespan-extending gene ever identified and was first found in *C. elegans* [260]. The identification of such single gene mutations that can extend lifespan dramatically has shed light on fundamental questions relative to ageing. The identification of a single gene mutation, for instance, makes it clear that ageing rate is not a consequence of the combination of a large number of independent biochemical mechanisms controlled by many genes, as often thought previously [252].

Many human disease genes have orthologs in the genome of *C. elegans*. Coupled with the availability of complete sequences of both genomes, this facilitates investigation of human genetic and age-related diseases, including those genes associated with Alzheimer disease [261], Parkinson's disease [262] and Huntington disease [263]. For instance, *C. elegans* has been widely used as the model organism to study AD. One of the pathological hallmarks of AD is the accumulation of beta-amyloid (Aβ) peptide that is formed by sequential cleavage of large amyloid precursor protein (APP) [264]. It is believed that Aβ plays a key role in the synaptic damage and neuronal loss that characterises AD [223, 224]. *C. elegans* has *apl-1*, a single gene that is related to human APP. Interestingly, overexpression or loss of function of this *apl-1* gene has deleterious effect on the nematode [265], although *C. elegans* does not contain β-secretase that cleaves APP and produce Aβ peptides [266]. In addition, transgenic *C.elegans* models of AD, overexpressing human Aβ have also been engineered and model the pathological processes of AD [261].

1.10. Pharmacological interventions to modulate DNA damage

One of the proposed public mechanisms of ageing is the mitochondrial deterioration caused by accumulation of ROS-mediated mitochondrial damage [8, 57, 69]. Therefore, there is a

considerable interest to develop mitochondrial pharmacological intervention strategies to reduce mitochondrial oxidative damage. The main approach is to target compounds to mitochondria, in the hope that this may increase lifespan, improve healthspan, decrease mitochondrial damage and prevent or delay age-dependent deterioration in mitochondrial function and onset of mitochondrial diseases. Targeting compound to mitochondria is facilitated by large mitochondrial membrane potential and mitochondrial protein import machinery, which can be used to deliver compounds to mitochondria [267].

1.10.1. Mitochondria-targeted antioxidants, MitoQ

Small molecules such as vitamin E, vitamin C and ubiquinone have limited therapeutic success as mitochondrial therapies, probably because these compounds are widely distributed within the body with only a small percentage of these small molecules are taken up by mitochondria [267-270]. However, compound can be targeted specifically to mitochondria. For example, the mitochondria-targeted antioxidant, MitoQ (mitoquinone mesylate: [10-(4, 5-dimethoxy-2-methyl-3, 6-dioxo-1, 4-cycloheexadienlyl) Decyltri-phenylphosphonium methanesulfonate]) [271]. MitoQ is a mitochondria-targeted ubiquinol, produced by covalently attaching a ubiquinone moiety to the lipophilic decyltriphenylphosphonium (dTPP) cation through a 10-carbon aliphatic carbon chain (Figure 1.5) [271]. MitoQ selectively absorbs and concentrates several hundred-fold in the mitochondrial matrix due to the large mitochondrial membrane potential [271-274]. The ubiquinone moiety of MitoQ is then inserted into the lipid bilayer of the mitochondrial matrix and rapidly reduced by complex II to ubiquinol, which acts as the active antioxidant. This ubiquinol moiety is continuously recycled to the active antioxidant by the respiratory chain [271, 275]. MitoQ has been specifically designed with the aim of protecting the mitochondrial membrane against lipid peroxidation [276]. MitoQ is one of the best characterised mitochondria-targeted antioxidants and even has been reported to prevent cognitive decline and early neuropathology in one study using a transgenic mouse model of AD [272]. Exploration of the effects of MitoQ on ROS production and ROS-mediated damage in nematodes may provide insight into possible further pharmacological interventions to

potentially alleviate a range of disease states, many of which are associated with age-dependent mitochondrial decline.

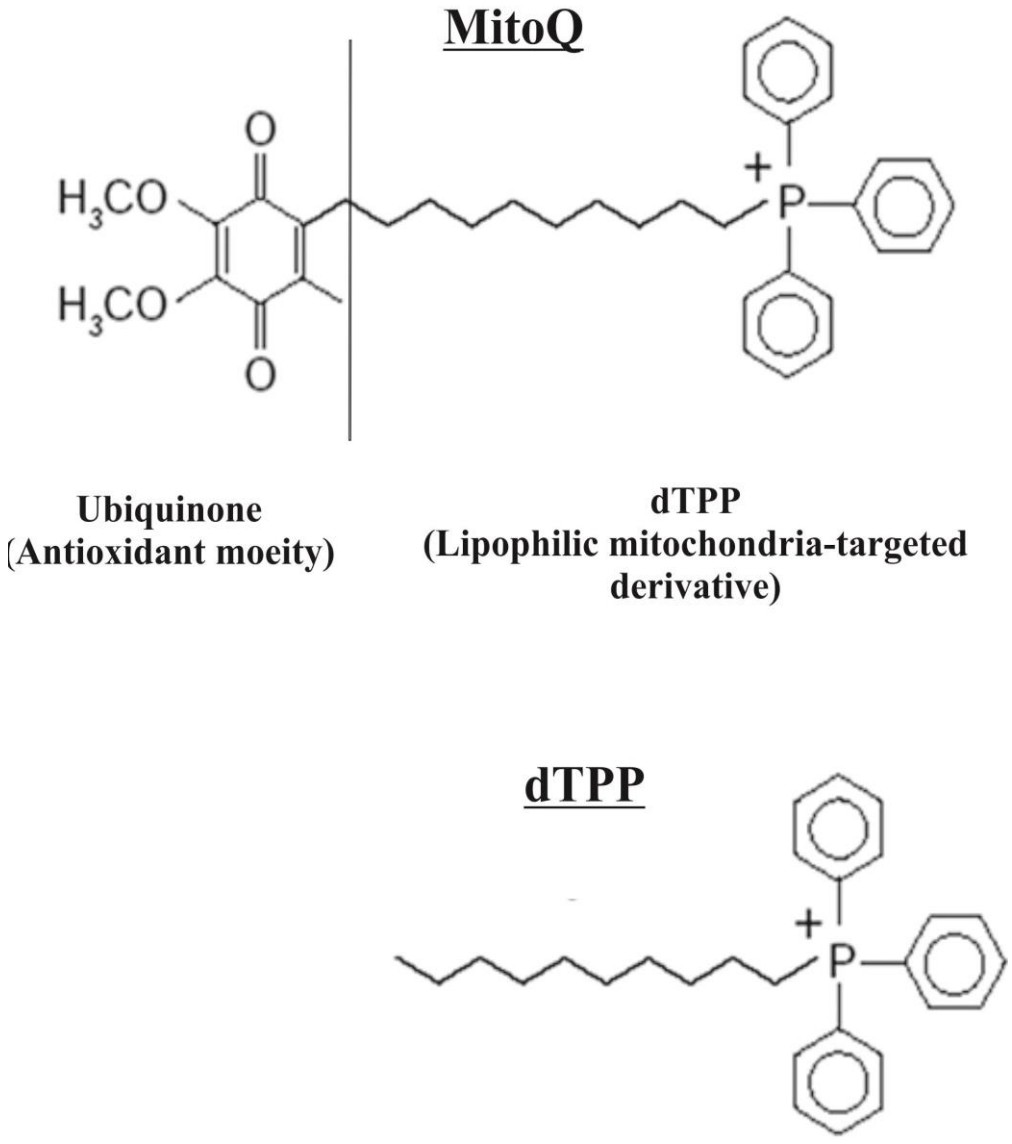

Adapted from Mitchell *et al*., 2011[277]

Figure 1.5. The chemical structure of MitoQ (top) and dTPP (bottom). MitoQ has two main complenents, the ubiquinone derivative that is responsible for the antioxidant capability of mitoQ and the lipophilic mitochondria targeted derivative.

1.11. Hypothesis and objectives

It is often suggested that the accumulation of free-radical mediated oxidative damage to macromolecules, particularly to mtDNA, might be the major cause of ageing. Therefore, I hypothesized that if mtDNA damage is related to ageing, then long-lived species or strains should suffer from less mtDNA damage than short-lived species or stains. To test this hypothesis, I decided to quantify the levels of mtDNA damage in various strains of *C. elegans*.

However, to date, there is no mtDNA damage assay that can reliably measure the level of damaged mtDNA in *C. elegans*. I therefore, developed, tested and optimized a DNA damage assay that can measure damaged DNA in mitochondria of *C. elegans*. With the new method, I further investigated and elucidated the role of mtDNA in ageing of *C. elegans*. Based on the above hypothesis, genetic, physical or pharmacological interventions were also performed, testing interventions that might modify oxidative damage to mtDNA and thus should modulate lifespan and healthspan.

2. Materials and Methods

2.1. *C. elegans* strains used and general maintenance of the nematodes

In this study, the Bristol N2 (wild type), JK1107 (*glp-1*), CL2006 (*unc-54/Aβ1-42*), GA480 (*sod-2/sod-3*), OK2040 (*mpst-1*) and TK22 (*mev-1*) of *C. elegans* strains were used. All strains (unless otherwise stated) were maintained and cultivated at 20 ℃ in appropriate incubators on nematode growth medium (NGM) agar plates seeded with *Escherichia coli (E. coli)* strain OP50-1 which is a Streptomycin resistant strain of OP50. The JK1107 (*glp-1*) strain is a temperature sensitive mutant that is fertile at 17 ˚C but sterile at 25.5 ˚C, therefore, this strain were maintained at 17 ℃ and cultivated at 25.5 ℃ on NGM agar plates to prevent progeny. All nematode strains as well as the *E. coli* strain used in this study were obtained from the *Caenorhabditis* Genetics Centre (University of Minnesota, Minneapolis, MN).

2.2. Preparation of bacterial food source (*Escherichia coli* (*E. coli*) OP50-1 strain)

Using sterile technique, single colonies of *E. coli* OP50-1 were picked from steak plate agar supplemented with Luria-Bertani (LB) agar (5 g Bacto-tryptone, 2.5 g Bacto-yeast, 2.5 g NaCl, 7.5 g agar and 500 ml of MiliQ water, pH 7.5, sterilized by autoclaving) into 5 ml of LB broth (10 g Bacto-tryptone, 5 g Bacto-yeast, 5 g NaCl and 1 L MiliQ water, pH to 7.0, sterilized by autoclaving) supplemented with the 5 µl filter sterilized 200 mg/ml streptomycin and grown overnight at 37 ℃ at 220 rpm to generate a starter culture. The starter culture was transferred into 1 L LB broth supplemented with 10 ml filter sterilized 200 mg/ml streptomycin and grown overnight at 37 ℃ at 220 rpm. The E. coli were harvested by centrifugation at 5000 g for 10 min at 4 ℃. The *E. coli* pellets were then re-suspended using sterile M9 buffer (3 g KH_2PO_4, 6 g Na_2HPO_4, 5 g NaCl, 1 ml 1 M $MgSO_4$ and I L MiliQ water, sterilized by autoclaving) and concentrated to 10^{10} cells/ml (at 600 nm, the concentration of bacterial cells at OD_{600} = 1 is 5 x 10^8 cells/ml). The concentrated *E. coli* solution is then aliquoted, stored at -80 ℃ freezer and can be used to seed the NGM agar plates.

2.3. Preparation of NGM petri plates

Preparation of NGM agar plates was as previously described in [278, 279] and has to be done aseptically in a laminar flow cabinet after sterilizing the NGM agar mix. Briefly, NGM was prepared by mixing 1.5 g NaCl, 8.5 g Bacto agar, 1.25 g peptone and 487.5 ml MiliQ water in a 500 ml duran bottle. The agar was then autoclaved to melt it and to sterilize it. After autoclaving, the agar was cooled to 55 ℃ in a pre-heated water bath, after which, 500 µl filter sterilized 1M $CaCl_2$, 500 µl filter sterilized 1M $MgSO_4$, 500 µl filter sterilized 5 mg/ml cholesterol (dissolved in ethanol), 500 µl filter sterilized 200 mg/ml streptomycin, and 12.5 ml filter sterilized 1M KPO_4 were added and then mixed by swirling. Using sterile procedures, the NGM mix solution was dispensed into petri plates using disposable serological pipettes and left to solidify. A constant amount of agar was dispensed into each petri plate to reduce the need for refocusing the microscope when viewing the worms from one plate to another plate [278, 279]. NGM agar plates were then seeded with appropriate volume of *E. coli* OP50-1 liquid culture depending on the intended used, the bacterial lawns were then left to dry and store at 4 ° C for up to one month.

2.4. Maintaining age-synchronized animals

For all experiments, synchronous culture of worms were obtained by hypochlorite treatment of gravid nematodes to collect the eggs as described in [278]. I used small scale and large scale worm synchronization methods for the egg preparation.

To prepare small amount of synchronous worms, small scale egg preparation method was used. Briefly, the worms on a 94 mm petri plate were washed off the plate with sterile M9 buffer. The liquid was collected and 1 ml of liquid was aliquoted into 1.5 ml micro-centrifuge tube. Household bleach (5 % solution of sodium hypochlorite) and 5 N NaOH were prepared in ratio of 2:1. 430 µl of the freshly prepared bleach and NaOH mix solution was then added into each micro-centrifuge tube. The micro-centrifuge tubes containing worms and eggs were vortexed for 20 s every 2 min for a total of 10min. The sample was checked under the microscope. The incubation in the bleach and NaOH mix can be terminated once all the worms are lysed and the

incubation time cannot be more than 10 min. The sample was then subjected to centrifugation at 1500 g for 1 min to pellet the released eggs. The egg pellet was washed with 1 ml M9 buffer. The washing step was repeated for 3 times. Lastly, the eggs were allowed to hatch and grow on NGM plates without any addition of treatment compounds unless otherwise stated.

To prepare large amount of worms, large scale hypochlorite treatment of gravid nematodes protocol was used. Briefly, worms were washed off the plates with M9 buffer, the liquid was collected in 15 ml of centrifuge tube and M9 buffer was added to top up the volume to 7ml. 2 ml of Household bleach (5% solution of sodium hypochlorite) and 1 ml of 5 N NaOH was added to the nematodes solution and incubated for up to 10 min at room temperature. The mixture was vortexed for 20 s every 2 min. Once all the nematodes were lysed after checking under the microscope, the mixture was centrifuged at 2500 g for 1 min at room temperature. The pellet containing eggs was washed with 10 ml of M9 buffer and the washing step was repeated three times. Lastly, the pellet was re-suspended in 500 µl to 1 ml of M9 buffer and eggs were transferred to clean NGM plates seeded with bacterial lawn. The eggs were allowed to hatch and grow on NGM plates until further analysis.

2.5. Preparation and treatment of nematodes with compounds

2.5.1. MitoQ and dTPP

Stock solutions of MitoQ and dTPP were prepared by dissolving in deionized water and filtered-sterilized before adding into NGM agar or *E.coli* OP50-1 to the desired final concentrations of 0.1, 1 and 5 µM. Synchronized young adults of transgenic CL 2006 animals (Day 4 post-hatching) were transferred and cultured on NGM plates with and without addition of treatment compounds till harvesting.

2.6. DNA damage induced by gamma and ultraviolet radiation

2.6.1. Gamma irradiation of worms

Worms on NGM plates with food were irradiated in Cobalt-60 gamma-ray irradiator with total doses of 20 and 40 kRad. Worms were immediately (within an hour) collected and used for the appropriate assays after exposing the animals to the desired gamma radiation doses.

2.6.2. UV irradiation of worms

Worms were washed off the plates and washed three times with M9 buffer to remove excess bacteria. Worm pellets without bacteria were transferred to fresh NGM agar plates without food and were evenly spread across the plates to prevent overlapping of worms. CL-1000 ultraviolet crosslinker with an emission peak at 254 nm was used to irradiate the nematodes. Worms on NGM agar plates without the plates cover were exposed to 400 J/m^2 UVC source. Immediately after UVC exposure, worms were washed off the plates and immediately (within an hour) collected for the appropriate assays.

2.7. Comet assay

C. elegans embryonic cells were prepared from eggs isolated from young gravid adults as described in [280-282]. Briefly, large quantities of gravid adult worms were used and worms were lysed using 5 ml egg isolation solution consisting of 1 ml fresh Chlorox, 0.25 ml 10 N NaOH, and 3.75 ml sterile MilliQ water. The lysis reactions were stopped when 80 % of the worms were lysed by adding the egg buffer (118 mM NaCl, 48 mM KCl, 2 mM $CaCl_2$, 2mM $MgCl_2$, 25 mM Hepes, pH 7.3, 340 mOsm). The eggs were pelleted by centrifugation at 350 g for 5 min, supernatant were discarded and fresh egg buffer was added. The washing steps were repeated for three times. The egg pellet was separated from worms' debris by flotation on a sucrose cushion consisting 2 ml of sterile egg buffer and 2 ml of 60 % sucrose. The suspension was centrifuged at 350 g for 3 min. Eggs were then transferred to a sterile 15 ml centrifuge tube and washed three times with sterile egg buffer to remove the sucrose.

To prepare the dissociated embryonic cells, 100 µl of 1 U/ml Chitinase in egg buffer were added to the egg pellet. The resuspended egg pellet was incubated at room temperature with gentle rocking for 20 to 80 min until about 80 % of the egg shells were digested. The egg shell digestion reaction was stopped by adding 800 µl of L-15 cell culture medium without phenol red (containing 10% (v/v) heat-inactivated fetal bovine serum, 50 U/ml penicillin and 50 mg/ml streptomycin). The digested eggs were centrifuged at 900 g for 3 min at 4 ℃, supernatant was discarded and 800 µl of fresh L-15 cell culture medium was added. Gentle repeated pipetting at the side of the Eppendorf tube was done to dissociate the embryonic cells until single cell suspension was obtained. The dissociated cell suspension was centrifuged at 900 g for 3 min at 4 ℃ and the pellet was resuspended in 500 µ of fresh L-15 cell culture medium. The cell suspension was then filtered using an 18 gauge needle to remove the hatched larvae. The cells were then centrifuged at 900 g for 3 min at 4 ℃ and resuspended in appropriate volume of L-15 cell culture medium depending on the cells density. The cell suspension was plated onto four-well Lab-Tek II - CC2 chamber slide (Nunc, Thermo Fisher Scientific Inc) and kept in a humidified incubator at 22 ℃ overnight for cell differentiation.

After 24 hours, the degree of DNA damage was determined using the alkaline comet assay according to [282, 283]. Microscope slides were precoated with a layer of 1 % normal melting temperature agarose and air-dried at room temperature. The agarose precoated microscope slides were then stored with desiccant. 100 µl of 0.5 % low melting point agarose were added onto the center of the precoated microscope slide. Immediately, microscope slides with the cultured embryonic cells were left to cool. The microscope slide with cells was slipped out and cells were left in agarose. 1.2 ml of 1 % low melting point agarose was added on top of the first layer of agarose. The microscope slides were allowed to solidify for 2 min on an ice-cooled tray. After the agarose has gelled, the microscope slides were immersed in a covered container containing ice-cold alkaline lysing solution (1.2 M NaCl, 100 mM EDTA, 0.1 % sodium dodecyl sulfate (SDS), 0.26 M NaOH, pH > 13) for at least one hour or overnight at 4 ℃ in the dark. After lysis, the microscope slides were removed from lysing solution and were place in a

horizontal gel electrophoresis chamber filled with electrophoretic buffer (300 mM of NaOH and 1 mM of EDTA, pH>13) for one hour at room temperature. Electrophoresis was conducted at 25 V and 300 mA for 10 min in a chamber cooled on ice. Following electrophoresis at 4 ℃, the slides were rinsed twice with neutralization solution (400 mM Tris, pH 7.5) and dried at room temperature. Prior to scoring, the slides were then stained with 300 µl of 10000 x diluted SYBR Green I (Molecular Probes, Invitrogen Inc) and placed at 4 ℃ until slides analysis. To observe the comets, the microscope slides were examined using confocal fluorescence microscope (LSM 510 Carl Zeiss, Jena, Germany). At least 300 randomly selected cells were analyzed and the extent of DNA migration was determined using image analysis software, CometScore (TriTek Corp, USA).

2.8. mtDNA copy number

MtDNA copy number as was quantified as previously described in [161, 284]. Briefly, individual worms were picked from the stock plate into PCR tubes containing 50 µl of ice-cold worm lysis buffer (50 mM KCl, 2.5 mM $MgCl_2$, 10 mM Tris-HCl, 0.01 % Gelatin, 0.45 % Tween-20, 0.45 % Nonidet P-40, 100 µg/ml freshly added Proteinase K). The worms were subjected to three times of freeze-thaw cycles at -80 ℃. The worms were then incubated at 60 ℃ for 1 hour and followed by 10 min incubation at 95 ℃ to inactivate the Proteinase K. Samples were stored at -80 ℃ until further analysis.

mtDNA copy number of individual nematodes was determined by quantitative real-time PCR (qRT-PCR) amplifying a 71 bp region of the mitochondrial genome using the worm lysate as the source of DNA template and the mtDNA (short fragment) primers and probe (F1: 5'- GAG CGT CAT TTA TTG GGA AGA AGA-3' (nucleotides 1838-1861 mtDNA); R1:5'- TGT GCT AAT CCC ATA AAT GTA ACC TT-3' (nucleotides 1883-1908 mtDNA) and P1:5'- FAM-AAA ATC GTC TAG GGC CCA C-3'(nucleotides 1863-1881 mtDNA)). The probe was labeled with a specific reporter (FAM-labeled) and has non-fluorescent quencher (MGB Probes) (Applied Biosystems). This assay was performed using a reference sample of known copy

number (quantified by serial dilution generating actual rather than relative copy numbers). A serial of ten-fold dilutions of the worm lysate of the reference sample were used.

qRT-PCR amplification was performed in 20 µl reactions containing 1 µl of worm extract, 10 µl of 10X TaqMan Universal PCR Master Mix (Applied Biosystems), 0.18 µl of 100 µM each primers, 1 µl of 20 µM probe and 7.64 µl of nuclease free water. PCR was carried out in StepOne Plus™ Real-Time PCR System, under the following cycling conditions: 2 min at 50 ° C, 10 min at 95 ℃, 50 cycles of 15 s at 95 ℃ and 60 s at 60 ℃. Fluorescence intensity data were collected at the annealing stage (60 ℃). At least three non-template-controls were included with each experiment. The copy number of the samples was determined by comparing the amplification Ct value of the samples to the Ct value of the reference sample with known copy number.

2.9. Mitochondrial DNA extraction for qRT-PCR

mtDNA was extracted as previously described in [150] with several modifications. To isolate mtDNA, relatively large batches (about 5,000 to 10,000) of nematodes were used. Briefly, worms were washed off the plates with ice-cold S-basal buffer (100.1 mM NaCl, 5.7 mM K_2HPO_4, 44.1 mM KH_2PO_4, 0.01 mM cholesterol) for three-times. The worms were then washed twice with ice-cold isolation buffer (210 mM mannitol, 70 mM sucrose, 0.1 mM EDTA, 5 mM Tris-HCl, pH 7.4). Animals were collected and homogenized in isolation buffer using a Teflon-glass homogenizer. Debris and nuclei were removed from the homogenate by differential centrifugation at 600 g for 10 min at 4 ℃. The pellet was discarded and supernatant containing mitochondria was further centrifuged at 7200 g for 10 min at 4 ℃ to obtain mitochondrial pellet. The pellet was resuspended in Tris-EDTA buffer (50 mM Tris-HCl, 0.1 mM EDTA, pH 7.4). DNA from crude mitochondria was purified using Prepman Ultra Sample Preparation Reagent (Applied Biosystems), according to the manufacturer's protocol.

2.10. Amplification factor determination

Amplification factor was determined for each primer sets used for mtDNA damage assay. Ten-fold serial dilutions of mtDNA extract ranging from no dilution to 10^6 X dilutions were used to construct the standard curve for amplification factor determination.

For short PCR fragments (up to 300 bp), the qRT-PCR was performed using FAM-labelled dye in StepOne Plus™ Real-Time PCR system. The qRT-PCR amplification was performed in a 25 µl reaction similar to the reactions set up and PCR cycling conditions for S-qRT-PCR that mentioned below.

For long PCR fragments, the qRT-PCR was performed using SYBR Green I nucleic acid gel stain dye in StepOne Plus™ Real-Time PCR system. The qRT-PCR amplification was performed in a 25 µl reaction similar to the reactions set up and PCR cycling conditions for S-qRT-PCR that mentioned below.

The difference in the ΔCt was used to construct the standard curve which was used for determination of amplification factor for the respective primers set used.

2.11. Formamidopyrimidine DNA glycosylase (Fpg) Fpg-qRT-PCR assay

Following mtDNA extraction and purification, mtDNA was diluted five-fold with nuclease free water. For Fpg digest and undigested sample, 20 µl of diluted mtDNA was digested with 0.5 µl of 8 U/µl Fpg enzyme (New England Biolabs), incubated in 4 µl of 10 X NE buffer 1, 0.4 µl of 1 mg/ml bovine serum albumin (BSA, New England Biolabs) in a total volume of 40 µl. A mock (omitting enzyme) digest sample, same volume (20 µl) of diluted mtDNA was incubated with 4 µl of 10 X NE buffer 1 and 0.4 µl of 1 mg/ml BSA without the addition of Fpg enzyme in a total volume of 40 µl reaction. The Fpg digest and mock digest sample with the exception of undigested sample, were incubated at 37 ˚C for 2 h, followed by "boosting" with additional 4 µl of 1.2 U/µl Fpg enzyme in 1X NE Buffer 1 for another 2 h at 37 ˚C. For mock digest sample, 4 µl of 1 X NE buffer 1 was added during the "boosting" instead of Fpg enzyme. Undigested mtDNA sample was incubated at 4 ˚C throughout. Fpg enzyme was then heat

inactivated at 60 ˚C for 10 min. This was carried out in parallel for each sample. All samples were then cooled at 4 ℃ for 5 minutes and immediately used for qRT-PCR or stored at –20 ˚C until further analysis.

qRT-PCR reaction was performed on ABI StepOne Plus™ Real-Time PCR System in MicroAmp optical 96-well reaction plates. The qRT-PCR was conducted using double strand DNA binding dye (SYBR Green I nucleic acid gel stain, Life Technologies, Thermofisher Scientific Inc). qRT-PCR amplification was performed in 25 µl reactions containing : 4.1 µl of nuclease-free water (Promega, Fitchburg, Wisconsin, USA), 7.5 µl of 3.3 X XL Buffer II, 2 µl of GeneAmp 10 mM dNTP Blend , 1 µl of 10 µM each primer (1st BASE, Singapore), 0.4 µl of 25 mM $Mg(OAc)_2$ Solution, 2.5 µl of 1 mg/ml BSA (New England Biolabs), 4 µl of 0.25 U/µl rTth XL DNA polymerase , 0.5 µl of 10 X SYBR Green I nucleic acid gel stain and 2 µl sample (fpg ,mock digest or undigested mtDNA) or nuclease-free water for Non-template-control.

The qRT-PCR was assessed in a 6.3 kbp region of the mitochondrial genome with primer sequences based on [285]. Long fragment primers: forward primer: (5'-3') TCG CTT TTA TTA CTC TAT ATG AGC G (nucleotides 1818-1842 mtDNA) whereas, reverse primer: (5'-3') TCA GTT ACC AAA ACC ACC GAT T (nucleotides 8111-8090 mtDNA). The qRT-PCR cycling profile was an initial denaturation at 94 ℃ for 2 min, followed by 60 cycles at 93 ℃ for 10 s, 62 ℃ for 10 min, and 68 ℃ for 30 s, ending with a final extension at 68 ℃ for 30 min. Fluorescence intensity data were collected at the annealing stage (60 ℃). At least three well replicates were performed for the qRT-PCR amplification.

2.12. Sequence-specific mitochondrial DNA damage (S-XL-qRT-PCR)

Following mtDNA extraction and purification, mtDNA of one of the samples (reference sample) was used to quantify the mtDNA copy number using the mtDNA copy number quantification method as mentioned above.

After determining the mtDNA copy number of the reference sample, mtDNA damage was assesed using two independent qRT-PCRs: S-qRT-PCR and XL-qRT-PCR, which were performed on the same day.

For S-qRT-PCR, PCR reaction was performed on ABI StepOne Plus™ Real-Time PCR System in MicroAmp optical 96-well reaction plates. The qRT-PCR was conducted using short fragment primers and FAM-labelled Taqman probe as mentioned above in a 71 bp mitochondrial region. qRT-PCR amplification was performed in 25 µl reactions containing: 9.79 µl of nuclease-free water (Promega, Fitchburg, Wisconsin, USA), 12.5 µl of 10X TaqMan Universal PCR Master Mix (Applied Biosystems), 0.23 µl of 100 µM each primers, 1.25 µl of 5 µM probe and 1 µl of mtDNA extract. At least three wells were run for each sample and reference sample. Non-template control (nuclease free water only to replace the mtDNA extract) was added into each PCR reaction. PCR was carried out under the following cycling conditions: 2 min at 50 ℃, 10 min at 95 ℃, 50 cycles of 15 s at 95 ℃ and 60 s at 60 ℃. Fluorescence intensity data was collected at the annealing stage (60 ℃).

For XL-qRT-PCR, qRT-PCR was performed using GeneAMP XL PCR kit (applied Biosystems) based on the protocol in [62]. The PCR reaction was also performed on the same ABI StepOne Plus™ Real-Time PCR System in MicroAmp optical 96-well reaction plates. The qRT-PCR was conducted using long fragment primers and SYBR Green I nucleic acid gel stain as mentioned above in a 6.3 kbp mitochondrial region. qRT-PCR amplification was performed in 25 µl reactions containing: 4.3 µl of nuclease-free water (Promega, Fitchburg, Wisconsin, USA), 7.5 µl of 3.3 X XL Buffer II, 2 µl of GeneAmp 10 mM dNTP Blend , 1 µl of 10 µM each primer (1st BASE, Singapore), 1.2 µl of 25 mM $Mg(OAc)_2$ Solution, 2.5 µl of 1 mg/ml BSA (New England Biolabs), 4 µl of 0.25 U/µl rTth XL DNA polymerase , 0.5 µl of 10 X SYBR Green I nucleic acid gel stain and 1 µl mtDNA sample or nuclease-free water for Non-template-control. At least three wells were run for each sample and reference sample. Non-template control (water only to replace the mtDNA extract) was added into each PCR reaction. PCR was carried out under the following cycling conditions: 2 min at 94 ℃, followed by 60

cycles of 10 s at 93 ℃ , 10 min at 62 ℃, and 30 s at 68 ℃, ending with a final extension of 30 min at 68 ℃. Fluorescence intensity data was collected at the annealing stage (60 ℃).

mtDNA copy number for each sample in both PCRs, S-qRT-PCR and XL-qRT-PCR was determined based on the mtDNA copy number of the reference sample. The mtDNA copy number was then used for the quantification of mtDNA lesions for the particular samples.

2.13. Blinded lifespan study

Lifespan and healthspan of *C. elegans* were performed under blinded conditions to eliminate the effect of experimental bias [286]. A total initial population of 200 worms was tested for each treatment condition. Using a platinum wire worm pick, Day 3 (post-hatching) age-synchronised nematodes were picked from the culture plate and loaded onto the lifespan plates. Worms were counted and transferred to fresh plates every 2 days till post egg-laying period to prevent contamination by progeny and also to prevent starvation. Worms were scored as alive, dead or lost. Worms that failed to respond to mechanical prodding were scored as dead and removed from the plates. Animals that crawled off the plates and died away from the agar on the sides of the plate were censored from the study.

2.14. Blinded healthspan study

For healthspan study, the same batches of worms from the lifespan studies were scored concurrently for locomotor activity following the scoring framework reported by Herndon [287]. Briefly, all other strain of nematodes were subdivided into three groups: Class “A”, “B” and “C” except the CL2006 animals that were subdivided into 2 classes, class “A” and “C”, due to the nature of their movement where they rotate around the longitudinal axis and move in a circular path.

With the exception of CL2006 animals, animals in class “A” were healthy, highly mobile, showed spontaneous movement, left sinusoidal tracks in the bacterial lawn through which they migrated. Animals in class “B” only moved in respond to prodding, left tracks that were non-sinusoidal, reflecting uncoordinated locomotion. Class “C” animals did not move forward or

backward when prodded but the movement was restricted to the head and/or tail when gently touched.

As for CL2006 animals, class "A" animals were healthy, highly mobile, showed constant movement and rotated around its longitudinal axis. Whereas, class "C" animals did not move the body in response to prodding but only showed head and/or tail movement.

2.15. Relative distance travelled

The relative distance travelled by the nematodes was measured and analysed under blinded to the treatment conditions and samples were randomized. Ten to twenty nematodes were used for each biological repeat for this experiment and the experiment was repeated three times. Briefly, 35 mm petri dishes filled with NGM agar, seeded with 200 µl of OP50-1 at the centre of the plates were used. A marking just at the border of the bacterial lawn was marked to signify the starting point of distance to be travelled of which the worm will be loaded on the marking. Using a platinum worm pick, individual nematodes were transferred onto the marking on the plate and allowed to travel for 15 min. Nematodes were removed and the whole of the 35 mm NGM agar plates was captured in a single photograph using a calibrated Leica MZ10F microscope (Leica, Singapore). Distance travelled by the nematodes was measured using the line tool provided by the Leica Application Suite software (v2.6.0 R1).

2.16. Reactive oxygen species (ROS) measurement in *C. elegans*

General ROS production in whole animal was measured using 2, 7-dichlorofluorescein diacetate (DCFDA) (Sigma-Aldrich, St. Louis, USA) as previously described [62, 288]. 100 worms were transferred into each well of a black 96-well microtiter plate containing 100 µl of M9 buffer. To each well, 100 µl of 100 µM DCFDA dissolved in M9 buffer was added. ROS associated fluorescence levels were read kinetically every 2 minutes for 14 hours using a fluorescence plate reader (SpectraMax Gemini EM, Molecular Devices) at excitation 485 nm and emission 520 nm at room temperature. All samples were normalised to bacterial control in

separate wells on the same plate. At least four samples per condition were used and this experiment was repeated three times.

2.17. Protein carbonyl content (PCC) determination

Protein carbonyl determination was conducted as previously described in [289]. 200 worms were initially transferred from NGM agar plates into micro-centrifuge tubes containing 1 ml of M9 buffer. Samples were centrifuged at 400 g for 2 min at 4 ℃. Supernatants were removed and 1 ml of M9 buffer was added into each tube. Samples were washed three times to remove bacteria and debris. Worm pellets were re-suspended in 100 µl PBS-T lysis buffer (0.1 % Tween-20 in phosphate-buffered saline solution (PBS) containing 1 mM phenylmethylsulfonyl fluoride protease inhibitor (PMSF) and 50 mM of dithiothreitol (DTT)). These sample were then sonicated on ice at 50 % amplitude for 2 min of 20 pulses of 5 s each, within 1 s between pulses.

The lysates were then centrifuged at 15,000 g for 5 min at 4 ℃. The soluble protein concentrations of the lysates were determined using Bradford Protein Assay (Bio-Rad Laboratories, USA). A two-fold serial dilution of 2 mg/ml bovine serum albumin (BSA) with lysis buffer was used to generate a series of standards. The BioRad dye reagent was diluted four times with de-ionized water. 10 µl of samples or standards per well were pipetted into each well of a 96 well plate in triplicate. 200 µl of diluted dye reagent was added into each well and samples were incubated for 20 min at room temperature with gentle shaking at 60 rpm. Protein concentration was measured using a TECAN luminometer at 595 nm.

For each sample, 2 µg of protein (diluted to a final volume of 5 µl) was derivatised according to manufacturer's protocol (OxyBlot Protein Oxidation Detection Kit). To each sample, 5 µl of 12 % sodium dodecyl sulphate (SDS) was added to denature the protein. 10 µl of 20 mM 2, 4-dinitrophenylhydrazine (DNPH) or 1 x derivatisation control solution was then added to the samples or control samples respectively. After 15 min incubation at room temperature to

derivatise the samples, 7.5 µl of neutralisation solution containing 2 M Tris and 30 % glycerol was added to stop the reaction.

The Bio-Dot SF Microfiltration apparatus from BioRad was assembled with filter papers and nitrocellulose membrane according to the instructions from the manufacturer. 25 µl or a total of 2 µg of derivatised samples were loaded into each well of the slot blot apparatus. Vacuum pressure was used to transfer the proteins onto the nitrocellulose membrane assembled in the slot blot apparatus. The membranes were incubated with blocking buffer (1 x PBS solution containing 1 % BSA and 0.05 % Tween-20) for 1 hr at room temperature to prevent non-specific antibody binding. The blocked membrane was then probed with anti-DNPH primary antibody (1:150) diluted with blocking buffer for 1 hr at room temperature with gentle shaking, followed by three washes in 1 x PBS. The membrane was then subjected to secondary detection for 1 hr at room temperature with an anti-rabbit HRP conjugated IgG antibody (1:300) diluted with blocking buffer. Antibody-bound proteins were detected by chemiluminescence using SuperSignal West Dura Eextended duration chemiluminescence substrate mixture (Pierce Biotechnology, Thermo Fisher Scientific Inc., USA). Images were taken using BioRad ChemiDoc XRS system and analysed using Image J. This experiment was repeated five times.

2.18. Adenosine-5'-triphosphate (ATP) measurement

The ATP assay was performed as previously described in [62]. 100 worms were collected in microcentrifuge tubes containing 1 ml M9 buffer. Worms were incubated at room temperature for 30 min to allow the nematodes to digest and clear the bacteria in the gut. The worms were then subjected to low speed centrifugation at 400 g for 2 min at 4 ℃ followed by removal of the supernatant. 1 ml of M9 buffer was then added to the tube. The samples were washed three times to remove bacteria and debris. Tubes containing worm pellet were immediately immersed in liquid nitrogen and stored at -80 ℃ until further analysis.

For each measurement, 50 µl of ice-cold 10% trichloroacetic acid (TAC) was added. The re-suspended worms were immediately sonicated in a water bath sonicator (SONICLEAN,

Thebarton) for 5 min on ice and tubes were allowed to stand on ice for an additional 15 min. Samples were then centrifuged at 15,000 g for 5 min at 4 ℃ to pellet the debris. 45 µl of supernatant from two samples of the same condition were pooled together into a clean microcentrifuge tube.

5 µl of serial dilutions ATP standard and 5 µl of pooled samples were pipetted into the wells of a white 96 well microtiter plate held on ice. 150 µl of freshly prepared arsenite ATP buffer (80 mM $MgSO_4$, 10 mM KH_2PO_4 and 100 mM Na_2HASO_4 in a ratio of 1:1:1, pH 7.4) was added to each well. ATP levels were measured using a TECAN luminometer (Infinite 200, Tecan) pre-programmed to inject 45 µl of freshly prepared 2 mg/ml firefly lantern extract into each well. The luminescence signal was integrated for 10 s. This experiment was repeated three times.

2.19. Oxygen consumption measurement

Oxygen consumption for whole *C. elegans* was assayed using a Clark-type electrode (Hansatech oxygen electrode, Hansatech Instruments) as previously described [62]. Briefly, worms (approximately 1000 worms) were washed off a 94 mm plate into a 15 ml centrifuge tube. Excess M9 buffer was removed leaving 1 ml of M9 buffer in the tube. Worms in 1 ml M9 buffer were placed in the chamber of the Clark-type electrode. The amount of oxygen consumed was monitored polarographically for 2-15 minutes. Worms in the chamber of the Clark-type electrode were transferred to a clean micro-centrifuge tube and allowed to settle for 5 min. 900 µl of M9 buffer without any worms was transferred back to the electrode chamber to measure the oxygen consumption rate of the bacteria in the M9 buffer. The oxygen consumption rate of the worms was corrected against changes in oxygen concentration of the bacterial control. The worms were kept at -80 ℃ until further protein concentration analysis. The protein concentration of the worms was measured using Dc-protein assay kit (Bio-Rad, Hercules, USA). Final oxygen consumption rates were normalised to protein concentration. This experiment was repeated three times.

2.20. Isolation of mitochondria for ETC enzymatic activity

About 10,000 worms were washed off the plate and collected into a microcentrifuge tube with 1 ml of medium containing 250 mM sucrose, 20 mM Hepes, 10 mM KCl, 1.5 mM $MgCl_2$, 1 mM EDTA and 1 mM EGTA, pH 7.4. Worms were then homogenised using a hand-held glass pestle and transferred to a microcentrifuge tube. Homogenised worms were then centrifuged at 800 g for 10 min and the supernatant was transferred to a new microcentrifuge tube. The supernatant was then centrifuged at 14,000 g for 15 min. The supernatant was removed and the pellet was resuspended in the same medium used to wash and homogenise the worms. The resuspended pellet was used immediately for the measurement of ETC enzymatic activity.

2.21. Measurement of complex IV (cytochrome *c* oxidase) activity of ETC

Mitochondria were isolated as described previously[290]. Complex IV activity was measured using a polarographic assay modified from [291] and normalised to mtDNA copy number according to [62]. The assay was started by adding sequentially 65-70 µg of reduced cytochrome *c* in Mir05 buffer, 10 µg of mitochondrial protein and 5 mM azide. A high-resolution respiratory system (Oroboros, Oxygraph-2k) was used.

2.22. Measurement of complex I (NADH dehydrogenase) activity of ETC

Isolation of the mitochondria was carried out as previously described [290]. The enzyme activity of complex I was measured by a decrease in fluorescence of NADH at Ex/Em: 352 nm/464 nm using decylubiquinone as an electron acceptor [292] and normalised to mtDNA copy number according to [62]. Mitochondrial protein (10 µg) was added to a respiratory buffer of pH 7.2 containing 25 mM KH_2PO_4, 2 mM NaN_3, 5 mM $MgCl_2$, 64 mM decylubiquinone, 2 mg/ml albumin and 25 mM NADH. Complex I activity was determined from the difference in NADH oxidation before and after rotenone inhibition.

2.23. Analysis of lipids using high performance liquid chromatography mass spectrometry (LCMS)

Lipid extraction was performed with modification from the Bligh and Dryer double chloroform extraction method [293]. Lipid analysis was performed according to [62]. Briefly, worms were

homogenised in chloroform:methanol (1:2; v/v) and incubated on ice with agitation for 2 h. Following incubation, ice-cold chloroform and ice-cold water were added and the first extract was collected from the lower organic layer. Ice-cold chloroform was added for re-extraction. The lower organic extracts were pooled and dried under a stream of N_2 and stored at -80 ℃. Lipid species were identified and quantified using a high performance liquid chromatography (HPLC) 1200 system coupled with an Applied Biosystem Triple Quadrupole/Ion Trap mass spectrometer (3200 QTrap). Lipids were quantified using spiked internal standards. PC-14:0/14:0, PE-14:0/14:0, CL-15:0(3)/16:1 and C12-SM standards were obtained from Avanti Polar Lipids (Alabaster, AL, USA)

2.24. Statistical analysis

For statistical analysis, GraphPad Prism version 5.02 for Microsoft Windows, GraphPad Software, SanDiego, (USA) was used. Lifespan and healthspan curves were analysed by plotting Kaplan–Meier survival curves and conducting Log-rank tests. All other data were plotted as means±SEM, analysed using ANOVA and Bonferroni's multiple comparisons post-test unless otherwise stated. Differences with $P<0.05$ were considered as statistically significant.

3. Results

3.1. Selection of a good assay

A good assay is critical in determining DNA damage. Many factors can affect the validity of a good assay. Essential criteria for what constitutes a good assay are accuracy, precision, sensitivity and robustness. Accuracy is the extent to which a value obtained from several replicates is found to agree with the reference value or true value if one is available (Figure 3.1). Thus, an accurate assay is free from experimental bias [294]. However, the wide range of basal DNA damage levels reported in the literature using a wide selection of methodologies makes this difficult to achieve as no true reference value exists [168].

Precision is another important factor that has to be considered in validating an assay. Precision is the measurement of deviation around the mean value [294] (Figure 3.1). Precision affects both reproducibility and repeatability. The European Standards Committee for Oxidative DNA Damage (ESCODD) was set up in 1997 to reach an agreement on the normal DNA damage level in human cells [295]. ESCODD has stated that the methods used to measure DNA damage should have low coefficient of variation, ideally less than 5 % [295].

The third criterion for a good assay is sensitivity. To test the sensitivity of the DNA damage assay, I tested the ability of the assay to detect increases in DNA lesions by introducing artificial DNA damage using γ- and UV-radiation. Failure to detect these increases in DNA damage implies insufficient sensitivity of the assay.

Lastly, the robustness of an assay is characterized by its ability to resist changes in assay/sample conditions and to remain unaffected by variations in parameters of the experimental set up. The robustness of an assay also affects repeatability. Robustness allows an assay to work well even if samples have lower purity, primers, fluorescence dyes and tubes/plates quality vary or if pipetting is not perfectly accurate.

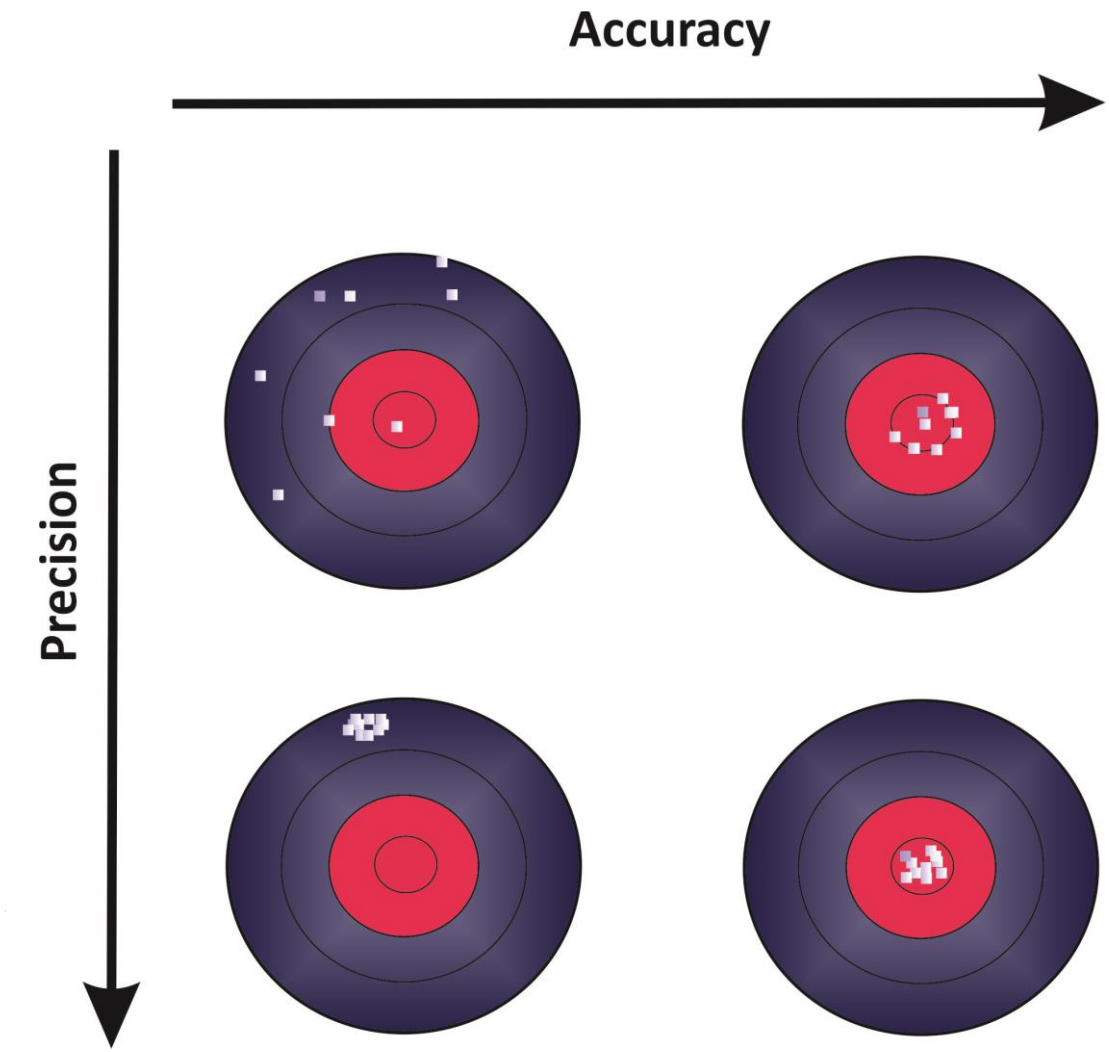

Figure 3.1. Accuracy vs. precision. The diagram shows the difference between precision and accuracy. Accuracy of a measurement or the correctness of the measurement is the amount by which the measurement deviates from the actual value. Whereas, precision is the measurement of deviation around the mean and precision can affect reproducibility of the measurement.

3.2. Comet assay

3.2.1. Principle of comet assay

I first explored a well-established assay for DNA damage in nuclear DNA called the comet assay. DNA damage assessment by comet measurement is a versatile and sensitive microscopic fluorescence method for quantification and analysis of damaged DNA at the level of individual cells. The comet assay (also known as single cell gel electrophoresis) is widely used as a reliable tool for assessing DNA damage and repair in samples ranging from bacteria, *Drosophila* and nematodes to human tissues [283, 296-298]. Hence, I used the comet assay to calibrate the gamma-radiation challenge used (to introduce additional DNA damage) and to compare the sensitivity of the comet assay to the sequence specific DNA damage assay that I utilized in my project (See section 3.3.3).

The comet assay (Figure 3.2) is performed on single cells embedded in a thin agarose gel on a microscope slide. The cell is subjected to gentle lysis with detergent to remove lipids and proteins. The lysed cell is then treated with alkaline solution to unwind and denature the DNA. Following the DNA unwinding, samples are subjected to alkaline electrophoresis, stained with DNA intercalating dye and viewed using a fluorescence microscope. During the electrophoresis, fragmented DNA is drawn towards the anode. Undamaged DNA remains supercoiled, thus the large DNA strands do not leave the cavity of the nucleus when the electric field is applied, resulting in a halo-like structure (Figure 3.3A).

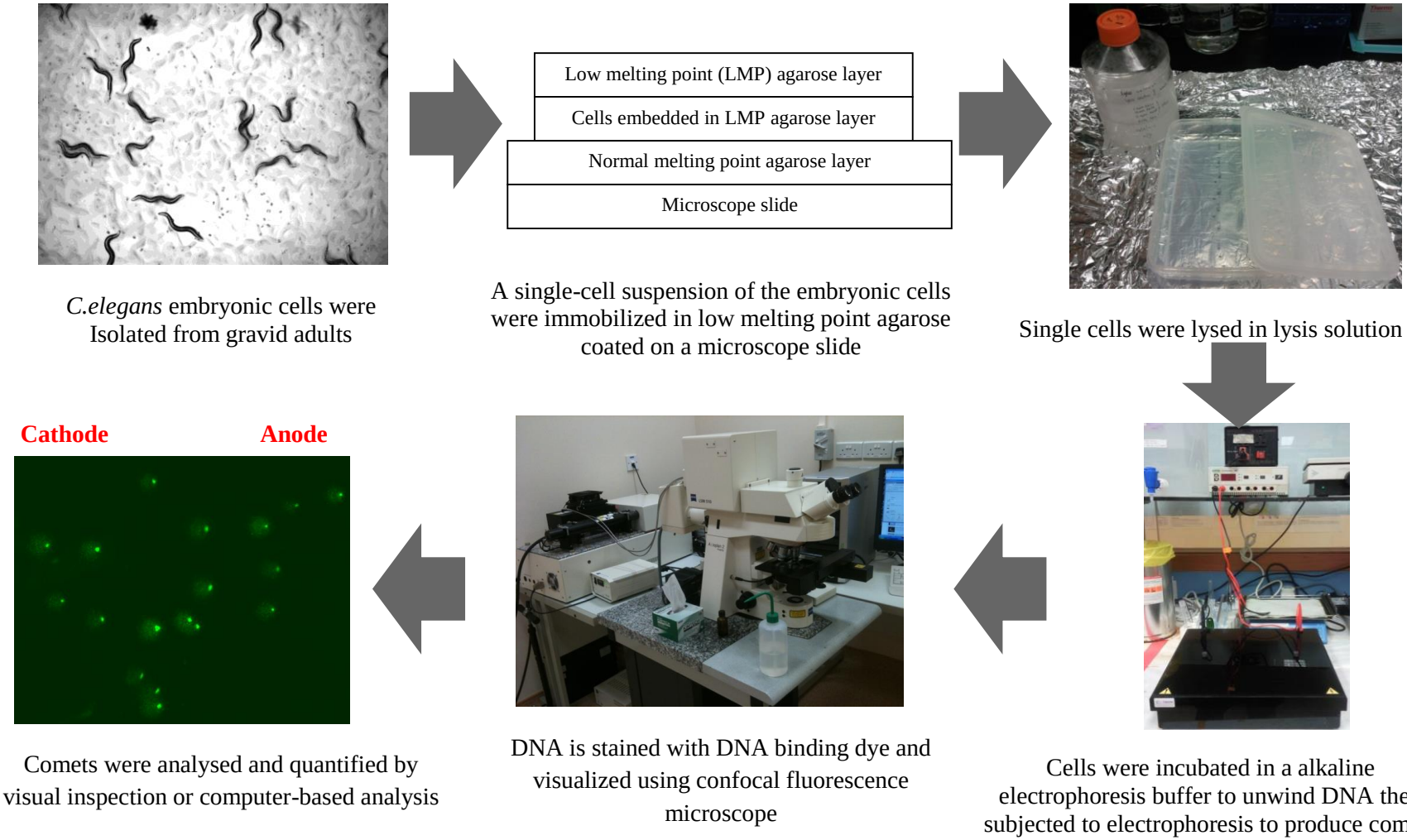

Figure 3.2. Schematic diagram of the comet assay protocol. *C. elegans* embryos were isolated from gravid adults, eggshells were digested by incubation in Chitinase. Dissociated embryonic cells were embedded on agarose-coated slides and subjected to gentle cell lysis with lysis buffer containing detergent and salts at high concentration. The cells on the slides were left in the alkaline electrophoresis buffer to allow unwinding of DNA before electrophoresis. DNA is then visualized by confocal fluorescence microscope after staining with DNA binding Sybr Green dye.

By contrast, in damaged DNA, the DNA organization with matrix proteins in the nucleus is disrupted, causing the DNA to lose its compact structure. When an electric field is applied, damaged DNA therefore expands out from the nucleoid "head" forming a "tail", resulting in a comet-like appearance. The comet "head" contains intact, undamaged (high molecular weight) DNA and the migrated, damaged (low molecular weight) DNA fragments form the comet "tail" [283] (Figure 3.3B). Excessive DNA damage causes large numbers of DNA strand breaks and therefore results in much smaller DNA fragments which will move faster and migrate farther in the comet tail. Therefore, the measurement of DNA damage is based on the amount of DNA in the comet tail relative to the comet head. Features of the comet tail such as the size, shape and distribution of DNA can all be used as qualitative indicators for the DNA damage in the particular sample [299]. In general, the brighter and the longer the comet tail, the greater the DNA damage.

The comet assay can be modified for use to detect various types of DNA damage, depending on the assay conditions. The neutral comet assay was the first to be developed and mainly detects DNA double strand breaks [300]. Later this assay was modified by using alkaline conditions during lysis to allow measurement of both double and single strand breaks [301]. Although the comet assay was primarily developed to detect DNA strand breaks, it can also be modified to detect oxidative DNA damage. This is achieved by introducing damage-specific repair enzymes such as endonuclease III and Fpg following the lysis of cells. These repair enzymes initiate DNA repair by excising damaged bases, thereby introducing strand breaks at the sites of damaged DNA. This approach makes it possible to detect oxidized bases using comet assay [302].

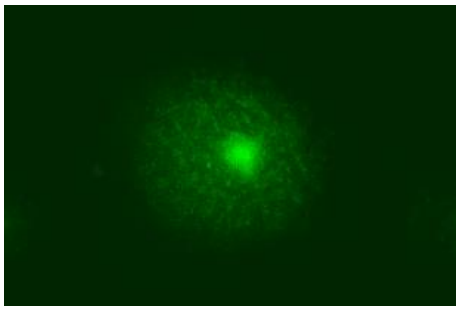

A. undamaged cell: Halo-like appearance

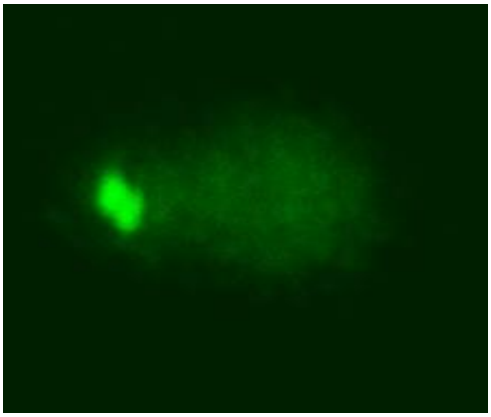

B. Damaged cell: Comet-like appearance

Figure 3.3. Typical comet images of wild type N2 *C. elegans* embryonic cells obtained from (A) untreated control animals (undamaged DNA sample) and (B) *C. elegans* exposed to 40 kRad γ-radiation (damaged DNA sample) from alkaline single-cell gel electrophoresis stained with Sybr Green I dye. (A) In undamaged cells typically, the DNA remains intact within the highly organized structure and is confined to the nucleus when a current is applied, resulting a halo-like structure. (B) When DNA is damaged, the relaxed DNA expands out from the nucleoid and is drawn towards the anode, resulting in a structure that resembles a comet with a head composed of intact undamaged DNA and a tail that consists of damaged /broken fragments of DNA.

In order to quantify the amount of DNA within the comet tail, which correlates to the extent of DNA damage, two approaches can be used; either semi-quantitative visual inspection or computer-based analysis [246, 303]. Typically, in the visual scoring approach, comets are assigned to one of five categories according to subjective comet appearance, with 0 representing undamaged cells (comets with no or barely detectable tails) and 4 representing damaged cells with high tail intensity (almost all DNA in tail). Although this visual scoring approach is fast and simple, allowing significant DNA damage to be quantified without the use of sophisticated image analysis software, there are limitations to using this approach: the comets must be selected without bias (scorers need to be blinded to the experimental conditions), visual scoring does not provide true quantification information of the DNA damage but only produces a score in arbitrary units, and there is high inter-personal variability of DNA damage levels between scorers. Therefore, the results obtained using the visual scoring approach can be difficult to interpret and typically are not comparable between experimental set ups, scorers and laboratories [246, 296].

A better approach, and the one that I used to quantify the DNA damage level, is computer-based analysis. There are a few comet parameters that are commonly used to evaluate the degree of damage including percentage of DNA in tail (measure of relative fluorescence intensity of head and tail), percentage of DNA in head, tail length (total distance of damaged DNA migration), and tail moment (the product of tail length and percentage of DNA in tail, which takes into consideration both the migration of DNA and the amount of DNA in tail) [283]. The percent of DNA in the tail may be a good parameter to quantify DNA damage levels as it has been shown to be linearly related to DNA damage frequency [304]. It has been shown that in some cell types, the percentage of DNA in the tail increases with increasing dose of genotoxins but other parameters such as tail length do not show clear linear correlation with the dosage of the genotoxins [246, 303]. Another parameter, the tail length is only informative when the damage level is very low. It has been reported that when the damage level is high, tail length is not informative as the comet tail's intensity increases with higher damaged DNA but not the

tail length [246, 303]. Lastly, the tail moment has been suggested to be a sensitive parameter but it is not linear with respect to dose increase in DNA damage [246, 303].

3.2.2. Validation of comet assay

The comet assay was first tested using embryonic cells from control *C. elegans*. The method used to quantify the DNA damage in individual embryonic cells is the computer-based analysis approach, determining the percentage of DNA in the tail. Two independent experiments demonstrated that the percentage of DNA in the tail obtained from embryonic cells of control, untreated wild type N2 *C. elegans* was 32.8 % ± 1.6 % and 36.5 % ± 1.5 % (mean ± SEM; Figure 3.4A & B and 3.4C&D, respectively). This result shows that the overall DNA damage in untreated control *C. elegans* embryonic cells, as evaluated by comet assay, appears to be fairly high. Furthermore, this also demonstrated the repeatability of the comet assay. The assay consistently detects similar level of DNA damage in control *C. elegans*, (Figure 3.4B and D, p=0.1, Student's t-test).

I further explored the comet assay by comparing the DNA damage in wild type N2 animals exposed to damaging agents: gamma (γ) radiation.

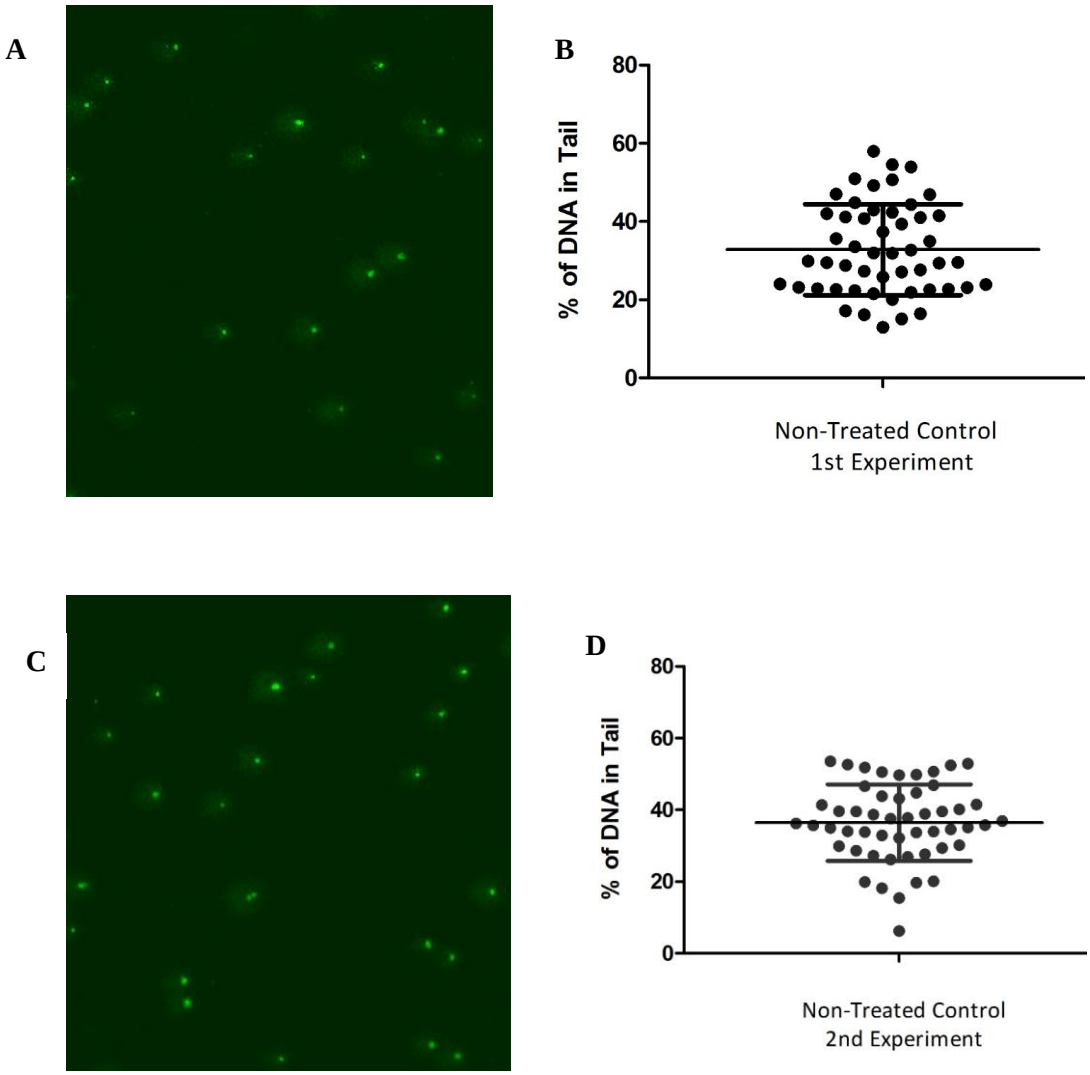

Figure 3.4. Comparison of comet images and analysis of percentage of DNA in tail obtained from embryonic cells of control, untreated *C. elegans* from two separate experimental repeats. Images of comets stained with Sybr green dye obtained from the first experimental repeat (A) and second experimental repeat (C). Percentage of DNA in tail (mean ±SEM) obtained from first (B) and second experimental repeat (D). The percentage of DNA in tail in the first experimental repeat was 32.8 % ± 1.6, n=51. Similarly, the second experimental repeat showed that percentage of DNA in tail was at 36.5 % ± 1.5, n=51. These results are statistically insignificantly different, indicating that the comet assay consistently detects similar level of DNA damage, p=0.1, Student's t-test.

3.2.2.1. Sensitivity test for comet assay

3.2.2.1.1. Gamma (γ) irradiation

I exposed nematodes to γ-radiation as this radiation is known to be a potent inducer of DNA damage [189, 196, 305, 306]. γ-radiation is a type of ionizing radiation that is able to disrupt the electronic structure of molecules. As a result, γ-radiation can break chemical bonds and produce highly reactive ions and free radicals [8, 305]. In biological systems, the significant destructive effect of γ-radiation is mainly due to radiolysis of water [8, 305], the dissociation of water molecules into radicals H• and OH• [8, 307]. γ-radiation possesses enough energy to damage DNA directly, causing a variety of lesions in DNA including DNA single and double strand breaks, DNA protein-crosslink, alkali labile sites, oxidized bases and abasic sites [189].

Using a cobalt-60 γ-radiation source to introduce DNA damage, I Initially explored the effect of various doses of γ-radiation (ranging from 0 to 250 kRad). Our pilot experiment showed that the control animals without any radiation treatment appeared to be healthier and travelled significantly more distances than most γ- irradiated animals (Figure 3.5). Animals exposed to 5 kRad of γ-radiation also appeared healthy and travelled more than animals irradiated with 20, 80 or 250 kRad. Animals exposed to 80 and 250 kRad γ-radiation seemed to travel significantly less with more severe effect at the high dose (Figure 3.5). Furthermore, γ-irradiation also caused sterility in animals. Animals exposed to 80 and 250 kRad generally appeared sick and produced no offspring. This result showed that higher doses of γ-irradiation had strong effects on the motility and sterility of the animals, probably due to higher damage relative to control animals. Therefore, in this project, I investigated DNA lesions induced by γ-irradiation at the relatively lower doses of 20 kRad and 40 kRad with the aim of assessing dose dependent damaging effect of γ-radiation on *C. elegans* using the comet assay. The radiation doses of 20 and 40 kRad used in this project have been selected to be relatively well tolerated by the nematodes with no signs of death detected following their exposure.

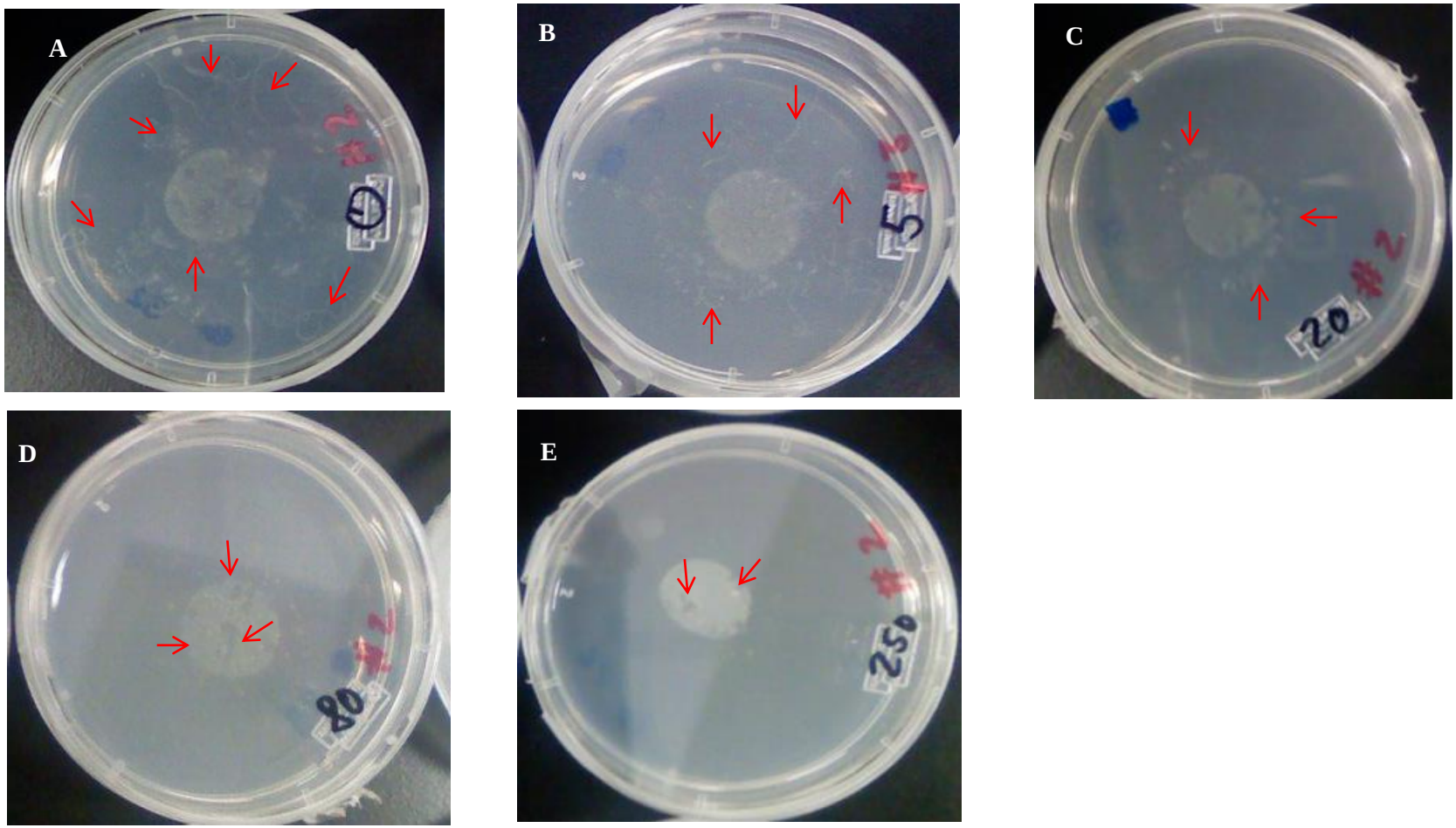

Figure 3.5. Pilot study of various doses of γ-irradiation. Distance travelled by *C. elegans* exposed to 0, 5, 20, 80 and 250 kRad γ-radiation doses using a cobalt-60 γ-radiation source. After γ-irradiation, animals were placed at the center of the NGM agar plate seeded with bacteria and the area explored by the nematodes was observed overnight. Red arrows showed the extent where the nematodes explored from the center of the plate. (A) Untreated control animals (0 kRad) were healthy and active, travelled vigorously to the side of the plate. (B) Animals exposed to 5 kRad γ-radiation remained active but travelled somewhat less than untreated control animals. (C) Animals exposed to 20 kRad γ-radiation travelled even less and only rarely arrived at the edge of the plate. Animals exposed to (D) 80 and (E) 250 kRad γ-radiation appeared sick, moved significantly less than 0, 5 and 20 kRad γ-irradiated animals. These animals only moved slightly around the bacteria spot.

Analysis of the DNA damage induced by γ-radiation (samples were extracted immediately after γ-irradiation) using the comet assay revealed that the DNA damage induced by 20 and 40 kRad γ-irradiation was significantly higher than that of the non-irradiated control animals ($P<0.01$, One-way ANOVA)(Figure 3.6). The percentage of DNA in the comet tail of the non-irradiated control animals in this particular batch of animals was 36 % (Figure 3.6), similar to the percentage of DNA in tail showed in Figure 3.4. The percentage increase following exposure to 20 kRad γ-radiation dose was 4 % higher than non-irradiated control animals (Figure 3.6). At 40 kRad γ-radiation dose, the percentage of DNA in the comet tail was 45 % and this increase was significant ($p<0.001$, Student's t-test) (Figure 3.6) compared to embryonic cells from control animals. Figure 3.6 illustrates a linear relationship between radiation dosage and DNA damage level with a dose response increased in DNA damage (R squared = 1.00) (Figure 3.6).

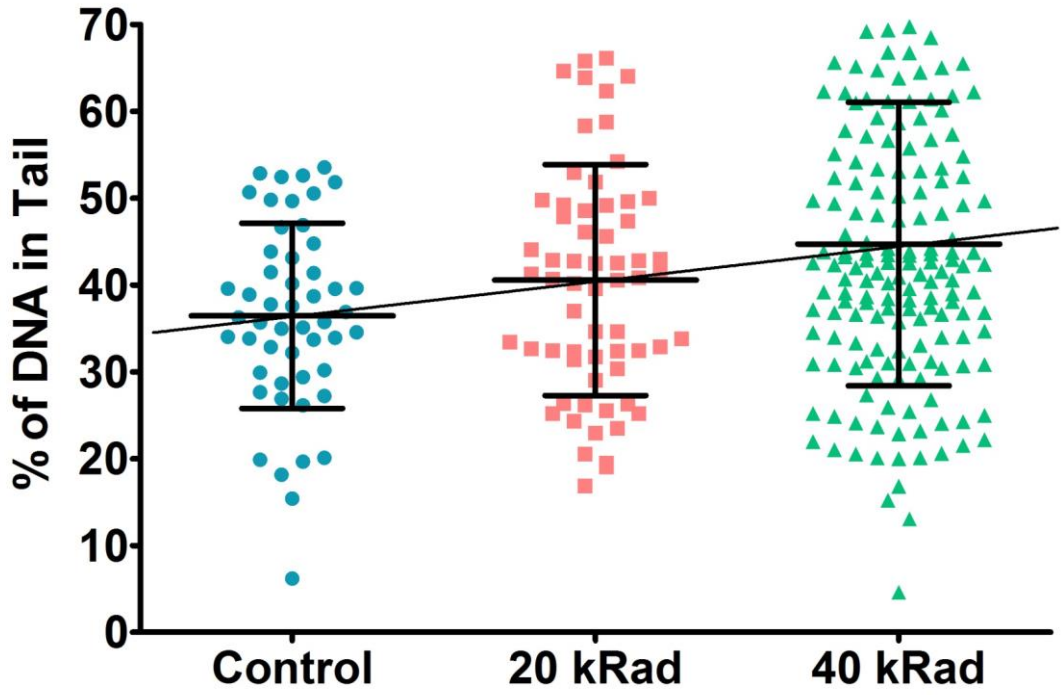

Figure 3.6. The DNA damage of day 4 wild type N2 animals exposed to 0, 20 and 40 kRad γ-irradiation, determined using the comet assay as the percentage of DNA in the tail. Data obtained from one experimental repeat. There were 36, 41 and 45 % of DNA in tail of the comet in control animals, 20 and 40 kRad γ-irradiated animals respectively. There was a linear relationship between radiation dosage and DNA in tail (R squared = 1.00). A minimum of 55 comets analyzed per condition.

3.3. Real Time PCR

After having developed and validated a γ-irradiation protocol suitable to cause robust increases in DNA damage, I then explored several variations of sequence-specific qRT-PCR based DNA damage assays.

3.3.1. Real Time PCR (RT-PCR) concepts

Real Time PCR (RT-PCR) is a technique that enables amplification and simultaneous quantification of newly synthesized DNA molecules during the PCR process. Conventional PCR typically is an end-point detection method that can be used to quantify the amplified PCR products only after the PCR reaction is completed. With large cycle numbers, this is equivalent to only knowing the amount of DNA at the plateau phase of PCR amplification (Figure 3.7). PCR, unless very carefully calibrated, is typically not quantitative. In RT-PCR, the incorporation of DNA binding dyes or probes makes it possible to monitor the amplification of PCR products in real time. Data are therefore collected throughout the PCR process, including the exponential phase and the plateau phase (Figure 3.7). With each PCR cycle, the increase in the fluorescence signal is proportional to the increase in the target amplicon. The threshold cycle (Ct) is the PCR cycle at which the fluorescence signal passes an arbitrary set threshold fluorescence level (Figure 3.7). The threshold (Figure 3.7) fluorescence level is chosen such that the fluorescence intensity is well above background but still within the exponential amplification phase of the PCR reaction. The Ct value of a given sample depends on the starting copy number of target DNA. The higher the initial DNA template copy number, the sooner this fluorescence signal is reached and thus the smaller the Ct value (Figure 3.7). Figure 3.7 shows the amplification plot from one of my RT-PCR runs. A sample with 1,000,000 copies of initial DNA template amplified at Ct 20, whereas for a sample with a starting DNA copy number of 1,000 copies will give a fluorescence signal at Ct 27.

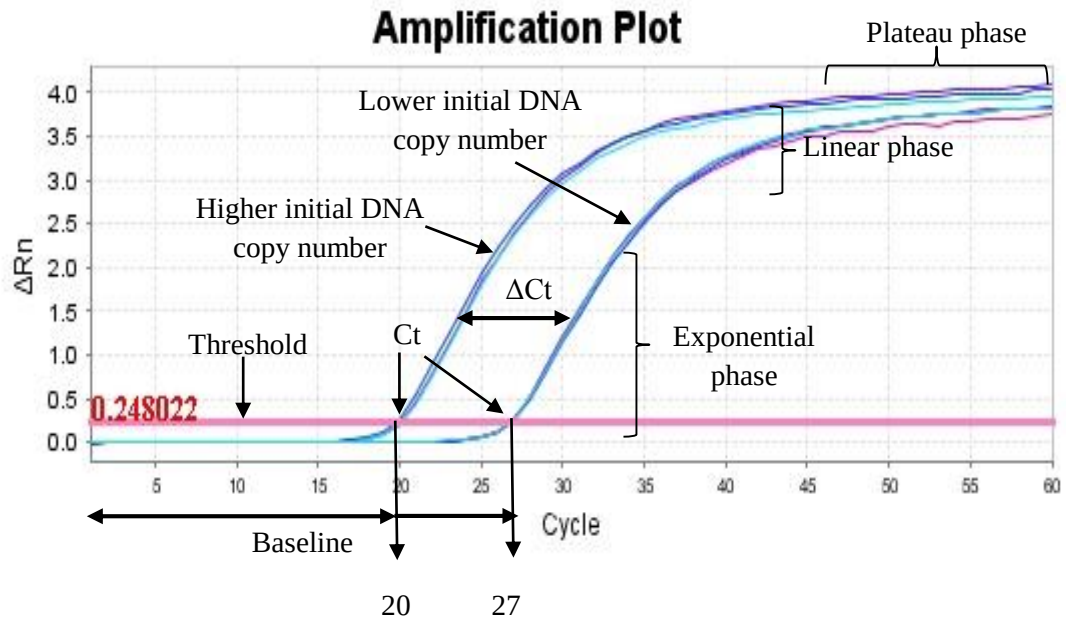

Figure 3.7. Graphical representation of a typical Real Time PCR amplification plot of DNA templates with different initial copy number. In this amplification plot, ΔRn is plotted against PCR cycle number. Rn is the ratio of the fluorescence signal of reporter dye normalized to the passive reference dye. ΔRn is the normalized reporter signal minus baseline and is used for determination of threshold cycle (Ct).

Initially, the increased in fluorescence signal is not visible because it remains below background level (below detectable level by the Real-Time PCR machine), in this case, cycles 1-20 and 1-27 for DNA templates with higher and lower initial DNA copy number, respectively). Eventually, the amplified PCR product accumulates to yield a detectable fluorescence signal. The cycle number at which the fluorescence signal exceeds the defined threshold (an arbitrary level that is set to be above baseline and sufficiently low to be within exponential phase for amplification plot of Rn vs cycle number) is known as Ct. ΔCt corresponds to the difference between Ct of DNA templates with high and low initial copy number.

3.3.2. Real-Time PCR amplification factor

In order to interpret qRT-PCR data quantitatively, we need to understand what the amplification factor, k of a given PCR reaction is. During the exponential amplification phase, the amplification of PCR product can be mathematically described as:

$$X_n = X_0 \cdot k^n \qquad \text{Equation 3.1}$$

Where X_n , the total amount of DNA molecules at cycle number n, depends on the initial number of target DNA molecules present at the beginning of the reaction (X_0) and the amplification factor .

The amplification factor reflects the fractional increase in PCR product between current and previous PCR product quantity in any one cycle. Under ideal conditions, each DNA molecule should replicate once at each replication cycle, resulting in an amplification factor of $k = 2$, thus Equation 3.1 would then become

$$X_n = X_0 \cdot (2)^n$$

This would mean that the number of molecules of the PCR product doubles at each replication cycle during the exponential phase of the reaction. However, different samples, experimental set-ups, reagents and fluorescence dyes can affect PCR performance and PCR reactions typically are not perfect. Because of this the amplification factor is $1 \le k \le 2$. Especially for long fragments, it is inaccurate to assume equal amplification factors of 2 for different PCR targets.

The amplification factor is related to the amplification efficiency, E, where $k = 1 + E$.

From Equation 3.1:

$$X_n = X_0 \cdot (1 + E)^n \qquad \text{Equation 3.2}$$

When $k = 2$, the amplification efficiency is 100 % or $E = 1$, indicating perfect doubling of PCR products in every cycle.

To determine an accurate value of the amplification factor for each template, a standard curve from serial dilutions of the target template is used (Figure 3.8A) (for detailed method, refer to section 2.10). The slope of the standard curve is obtained by constructing a plot of Ct on the logarithmic scale of target template dilutions (Figure 3.8B), yielding *k* for each template used.

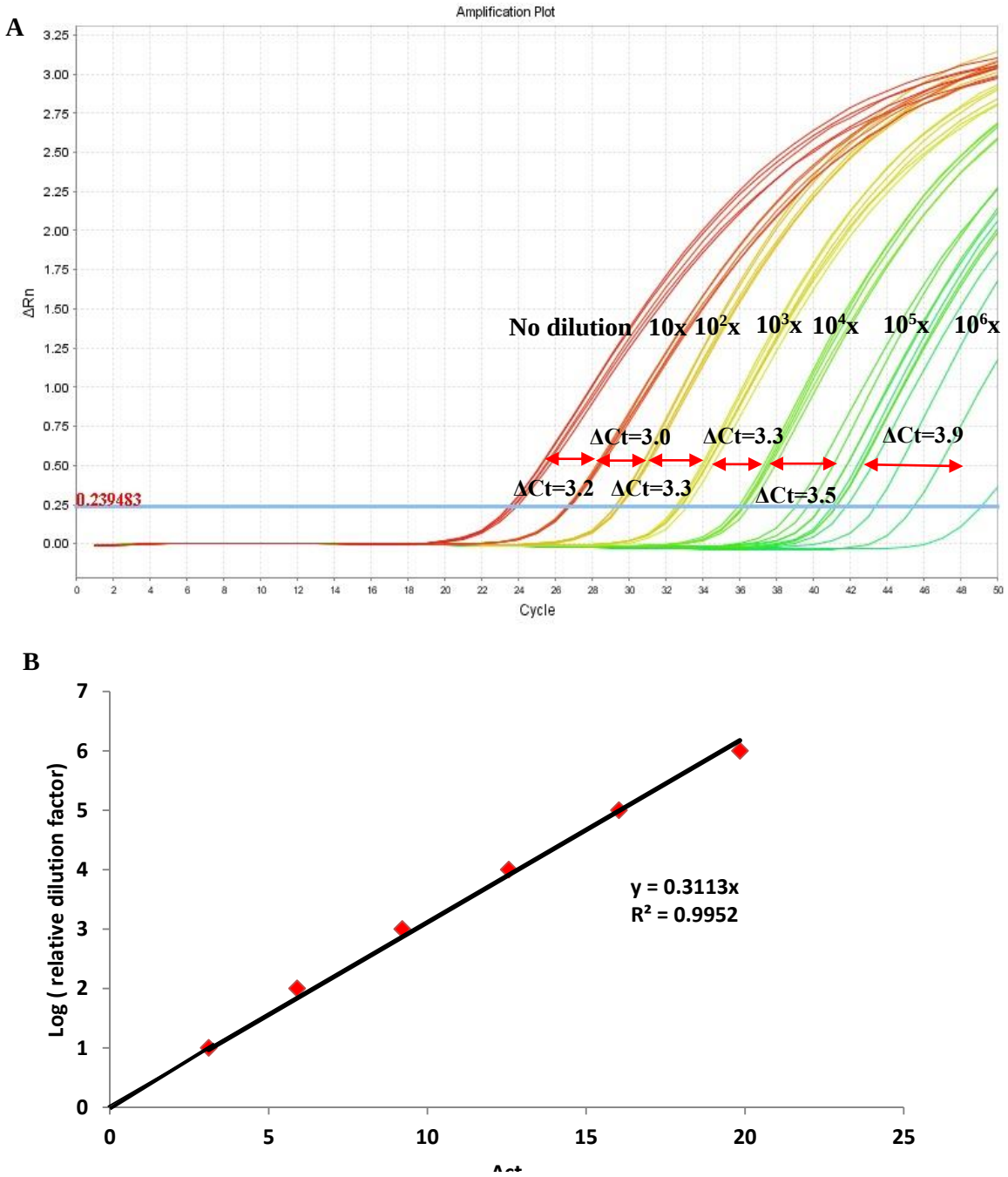

Figure 3.8. (A) Real-Time PCR amplification plot and (B) standard curve of log concentration of DNA versus ΔCt of the DNA sample from day 4 N2 wild type animals using the F1R1 fragment primers. Ten-fold serial dilutions (ranging from no dilution to 10^6-fold dilution) of DNA sample were used to generate a standard curve for determination of amplification factor for the respective primers set used. The data showed high linear correlation with a coefficient (R^2) value of 0.995, n=6 for each dilution factor.

For any serial dilution, 1 / D is the dilution factor between X_{0_i} and $X_{0_{i+1}}$:

$$X_{0_{i+1}} = \frac{1}{D} \cdot X_{0_i} \qquad \text{Equation 3.3}$$

Equation 3.1 then becomes:

$$X_{n_i} = X_{0_i} \cdot k^{n_i} \qquad \text{Equation 3.1A}$$

Similarly, for the next dilution, Equatio n 3.1 becomes:

$$X_{n_{i+1}} = X_{0_{i+1}} \cdot k^{n_{i+1}} \qquad \text{Equation 3.1B}$$

However, at the fluorescence threshold, every real-time PCR amplification reaction must contain the same number of DNA molecules and thus

$$X_{ct_i} = X_{ct_{i+1}}$$

$$\Rightarrow X_{0_i} \cdot k^{Ct_i} = X_{0_{i+1}} \cdot k^{Ct_{i+1}}$$

From Equation 3.3, this can be re-written as:

$$\Rightarrow X_{0_i} \cdot k^{Ct_i} = \frac{1}{D} \cdot X_{0_i} \cdot k^{Ct_{i+1}}$$

$$\Rightarrow k^{Ct_i} = \frac{1}{D} \cdot k^{Ct_{i+1}}$$

$$\Rightarrow D = \frac{k^{Ct_{i+1}}}{k^{Ct_i}}$$

$$\Rightarrow D = k^{Ct_{i+1} - Ct_i}$$

$$\Rightarrow D = k^{\Delta Ct}$$

To evaluate k from the slope of the standard curve, we take the logarithm on both sides,

$$\Rightarrow \log D = \log k^{\Delta Ct}$$

$$\Rightarrow \log D = \Delta Ct \cdot \log k \qquad \text{Equation 3.4}$$

Where k is the amplification factor, $\log D$ is the logarithm of the dilution factor and Δct is the difference in Cts between dilution factors ($Ct_{i+1} - Ct_i$).

In the example, the linear regression equation from Figure 3.8B for short mitochondrial DNA fragment that I used in my qRT-PCR assay is:

$$y = 0.3113\,x$$

Where the slope of the curve of serial dilutions is the log of the amplification factor k, therefore,

$$\log k = 0.3113$$

$$k = 10^{0.3113}$$

$$\Rightarrow k = 2$$

Thus, the amplification factor per cycle for the short mitochondrial DNA fragment for this particular PCR run was found to be 2. While this is amplification factor for this short mtDNA fragment is the often assumed theoretical value of 2, this is not always the case for long fragments (See Table 3.1).

For example, the same method was used to evaluate the amplification factor for other PCR targets (other fragments with different primers set) in my project (Table 3.1).

	Forward and Reverse primers (5'-3')	Amplicon size (bp)	Average amplification factor	SD
Short mtDNA fragment, F1	F:GAGCGTCATTTATTGGGAAGAAGA R:TGTGCTAATCCCATAAATGTAACCTT	71	1.97	0.07
Long mtDNA fragment, L1	F:TCGCTTTTATTACTCTATATGAGCG R:TCAGTTACCAAAACCACCGATT	6300	1.77	0.12
F4 mtDNA fragment, F4	F:GGTATAGTTTTAATCTTTCAGATTTTAACAGGTAC R:CCTGGCCCCATTAAAATGAA	152	1.94	0.02

Table 3.1. Nucleotide sequences of primers, amplicon size and amplification factors for real-time PCR. The average amplification factor for each primer set was determined from the slope of the linear regression of the serial dilutions of the DNA template, which was obtained by constructing a plot of Ct on the logarithmic scale of target template dilutions. For each primers set, a minimum of five RT-PCR reactions was performed and the amplification factor obtained for each primers set was an average of a minimum of 5 amplification factor from the 5 RT-PCR runs.

3.3.3. Principle of qRT-PCR sequence specific DNA damage assay

The amplification of qRT-PCR can be monitored and analyzed using sequence specific fluorescence probes (Taqman probe) or a traditional double strand DNA fluorescence binding dye (SYBR Green dye). The theoretical basis of the qRT-PCR based assays for DNA damage relies on the fact that DNA lesions (including strand breaks, some base modifications, cross links and bulky DNA adducts) can inhibit primer annealing or block DNA polymerase progression [249, 308], but it does not efficiently detect 8-OHdG [309]. Only a DNA template that does not contain any such DNA lesions can amplify perfectly (Figure 3.9). Inhibition of annealing by DNA lesions and blocking of the progression of DNA polymerase can prevent amplification, resulting in an apparent drop in detectable PCR product [249, 308, 310], compared to an equivalent DNA sample with fewer or no such DNA lesions. Therefore, under identical conditions, qRT-PCR amplification of differentially damaged samples but with equal copy number of DNA template will result in different Ct values, since the more damaged sample amplifying later corresponds to a lower apparent copy number. If a particular sample contained on average less DNA lesions (that is the sample contained more amplifiable, undamaged template) (sample A), amplification will be observed in earlier cycles because damaged template do not amplify; whereas, for DNA templates that contained more DNA lesions (sample contained less amplifiable, undamaged template) (sample B), the amplification will be observed in later cycles (Figure 3.10). However, in any real experiment, any difference in the Ct between sample A and B could also be due to the difference in the starting copy number of DNA template. To accurately quantify the amount of relative DNA damage, qRT-PCR therefore has to be carried out either using exactly the same copy number of DNA template or needs to be normalized to the copy number of template added in a particular sample (sample A or B). After normalizing, the difference in the Cts of sample A and B can be interpreted as loss of DNA template amplification of the sample B relative to sample A due to DNA damage and this can be used to quantify the DNA lesion frequency in sample B relative to A.

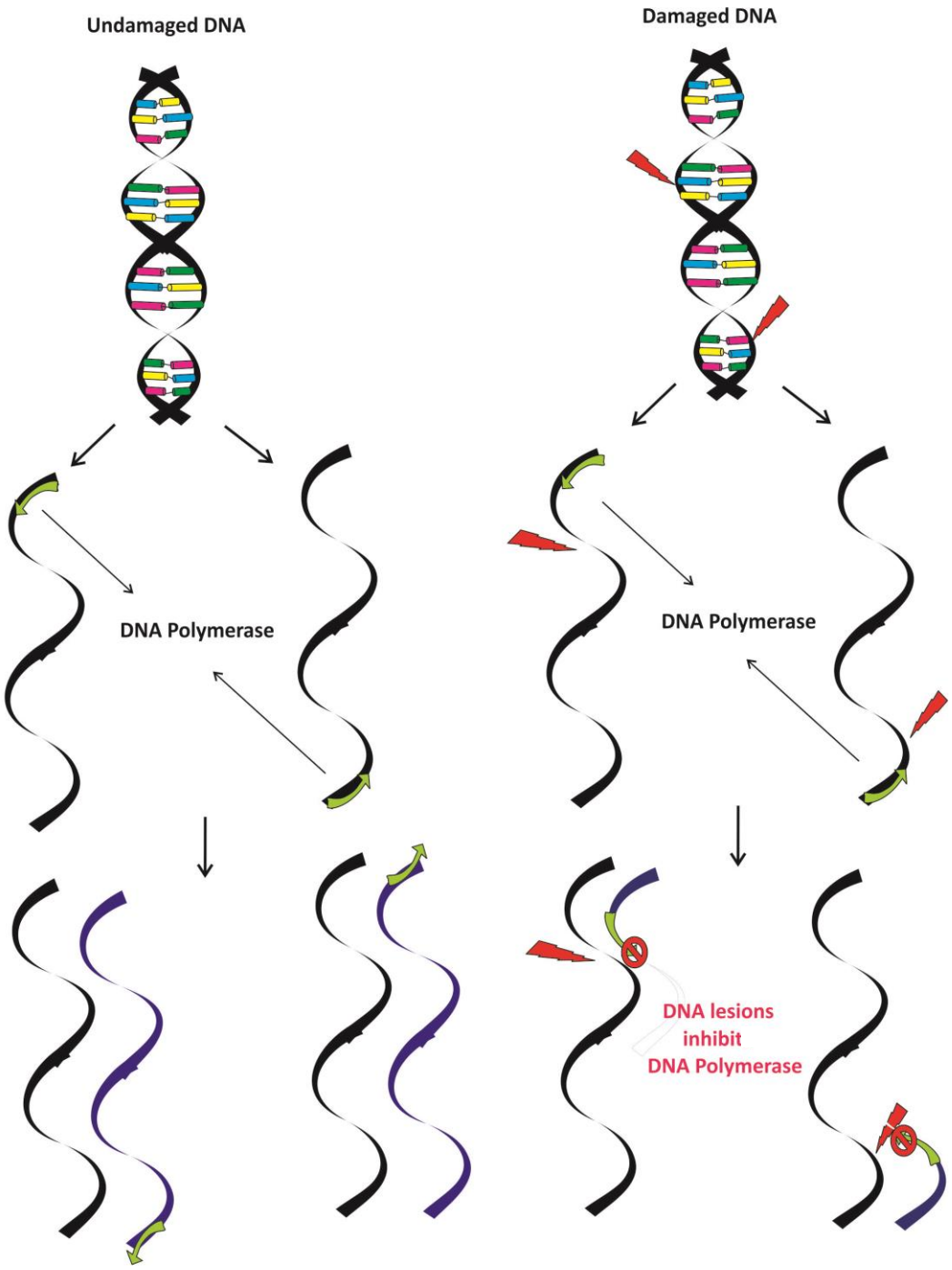

Figure 3.9. Principle of qRT-PCR DNA damage assay. The qRT-PCR DNA damage assay is based on the principle that DNA lesions can inhibit primers annealing and block the progression of DNA polymerase. Only DNA template that does not have DNA lesions can amplify.

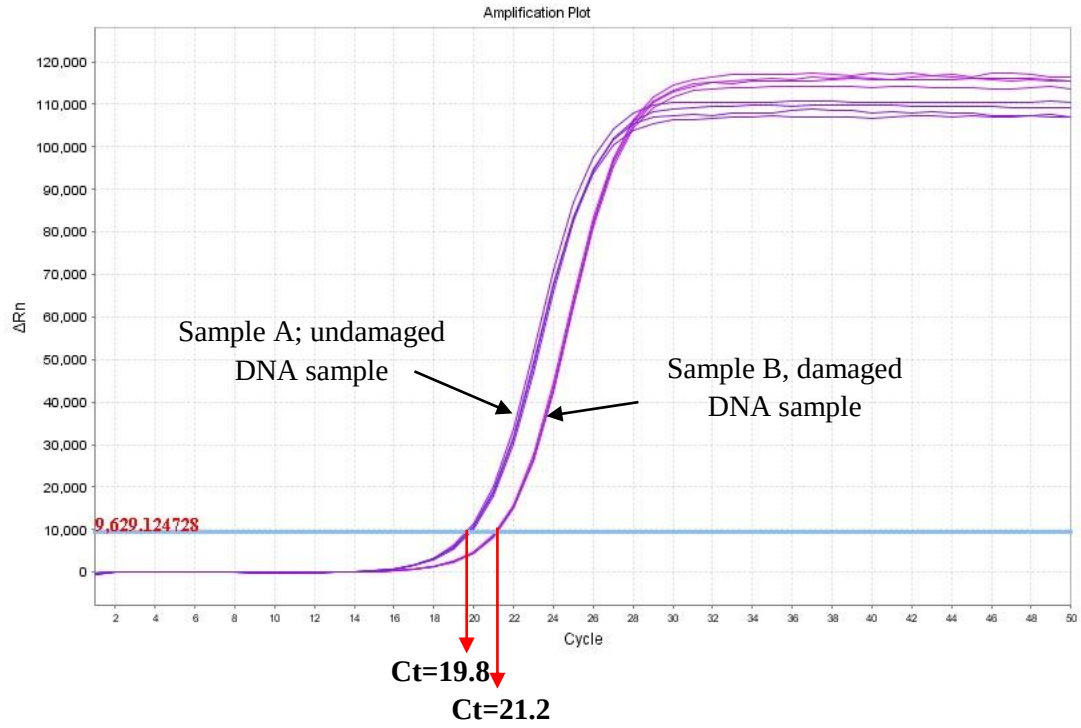

Figure 3.10. Principle of qRT-PCR DNA damage assay. Amplification plot of Real-Time PCR run from day 5 untreated control (sample A; undamaged DNA sample) nematodes and nematodes exposed to 20 kRad γ-irradiation (sample B; damaged DNA sample). Equal copy numbers of DNA templates were added into the respective well. Sample A with less DNA lesions amplified earlier (Ct 19.8) than sample B (Ct 21.2), which was derived from animals that were exposed to 20 kRad of γ-irradiation.

The next step in using this approach for DNA damage determination is to convert the drop in Ct into a quantitative measure of DNA damage (lesions per bp). In order to quantify randomly distributed DNA lesion frequency in a given DNA sample, I used Poisson Equation as probability model.

The probability of observing exactly q DNA lesions in a given DNA template is then given by

$$f(q;\lambda) = \frac{\lambda^q e^{-\lambda}}{q!} \qquad \text{Equation 3.5}$$

Where $\lambda =$ underlying lesion frequency in the total fragment.

Only undamaged templates are assumed to amplify and therefore, to quantify DNA lesion frequency, we need to know the probability of undamaged DNA template (no DNA lesions, that is $\lambda = 0$).

For instance, if we assumed that the DNA copy number in each well of the two samples, sample A and B are the same (Figure 3.10) and that sample A is the sample with no DNA lesions (undamaged DNA sample), we can use this to serve as reference sample to calculate the amount of DNA lesions in sample B (damaged DNA sample).

For sample A, λ is zero ($\lambda = 0$), Equation 3.5 for $q = 0$ then becomes:

$$\mathrm{Pr}_{\mathrm{A}}(\mathrm{q} = 0) = \frac{\lambda^0 \mathrm{e}^{-\lambda}}{0!}$$

$$\mathrm{Pr}_{A}(q = 0) = 1$$

In other words, there is a 100 % probability of having zero lesions in a given template of sample A. This is exactly as expected as A is assumed to be undamaged.

Assume sample B has an unknown number of DNA lesions, $\lambda > 0$, for $q = 0$ Equation 3.5 becomes:

$$\Pr_B(q=0) = \frac{\lambda^0 e^{-\lambda}}{0!}$$

$$\Pr_B(q=0) = e^{-\lambda}$$

In other words, the probability of finding zero lesions in a given template of sample B drops exponentially with the average number of lesions per template (λ) observed. The ratio of undamaged DNA in sample B (note that sample B is the sample with DNA lesions and only template without lesions will amplify, therefore I determined the amount of undamaged DNA in the particular sample) to sample A (undamaged DNA sample) is then exactly $\Pr_B(q=0)$ and can therefore be used to calculate the average DNA lesion per DNA template, λ in B.

Amount of undamaged DNA in sample B, X_B (Damaged DNA sample)	=	Probability of undamaged DNA in sample B, Pr_B	x	Total number of undamaged DNA in sample A, X_A (undamaged reference DNA sample)

Thus, ratio of amount of undamaged DNA in sample B versus sample A is

$$\frac{X_B}{X_A} = \Pr_B(q=0) = e^{-\lambda}$$

$$\frac{X_B}{X_A} = e^{-\lambda}$$

$$\lambda = -\ln\left(\frac{X_B}{X_A}\right)$$

Therefore, average lesion frequency per DNA strand (λ) in sample B is

$$\lambda = -\ln\left(\frac{X_B}{X_A}\right) \qquad \text{Equation 3.6}$$

The average lesion frequency per DNA strand obtained is then divided by the fragment length to express the DNA lesion frequency as DNA lesion per bp.

Finally, if the amplification factor k is known, the ratio of intact DNA template (amount of undamaged DNA) in sample B versus sample A can be obtained directly from the RT-PCR traces. I compared the observed Ct values in both sample A and B and used the ΔCt values to quantify the amount of undamaged DNA in both samples.

Therefore: $\frac{X_{0(B)}}{X_{0(A)}} = k^{Ct(A)-Ct(B)}$

$$\frac{X_{0(B)}}{X_{0(A)}} = k^{\Delta Ct} \qquad \text{Equation 3.7}$$

From the example in Figure 3.10, amplification of long mitochondrial DNA fragment with k=1.77, Ct value for sample A = 19.8; Ct value for sample B= 21.2. Thus, ΔCt = -1.4.

Using Equation 3.7, the ratio of intact DNA templates in sample B versus sample A is

$$\frac{X_{0(B)}}{X_{0(A)}} = 1.77^{-1.4}$$

$$\frac{X_{0(B)}}{X_{0(A)}} = 0.45$$

This means that 55 % of DNA templates in sample B contains at least one lesion.

Therefore, relative to the reference control sample A, 45 % of mtDNA molecules are intact (undamaged) in sample B, while 55 % of mtDNA of the 6.3 kbp fragment in sample B has been damaged.

To determine the DNA lesion frequency per template, we solve Equation 3.6,

$$\lambda = -\ln(0.45)$$

$$\lambda = 0.80$$

On average, the DNA lesion frequency in the 6.3 kbp fragment of mtDNA is 0.80 DNA lesions per template molecule. To express this lesion frequency as lesions per bp, we divide 0.80 lesions per template molecule by the number of base pairs finding that the sample B in Figure 3.10 has 1.27 $x10^{-4}$ lesions per bp.

3.3.4. Practical considerations of qRT-PCR

Technically, the qRT-PCR DNA damage assay measures DNA lesions by comparing the amplification of a sample with that of an undamaged reference sample. However, in practice, there is typically no available confirmed undamaged reference DNA sample. It is therefore impossible to perform absolute quantification directly. Instead, another way of quantifying the drop in apparent copy number due to DNA damage has to be used. I have utilized two different approaches based on PCR for this purpose.

3.3.4.1. Fpg-qRT-PCR DNA damage assay

The first approach is to introduce a damage-specific repair enzyme, such as Fpg enzyme that acts as N-glycosylase and AP-lyase. N-glycosylase selectively releases oxidatively damaged bases from double stranded DNA, generating apurinic sites (AP site). In addition, Fpg also displays AP-lyase activity that cleaves at 3' and 5'of phosphodiester bonds of AP sites resulting in strand breaks that can inhibit PCR amplification [311]. Digestion with Fpg therefore converts 8OHdG and similar lesions into single strand breaks. For quantification of oxidative damage using Fpg, three different samples are prepared: Fpg digest, mock digest and undigested DNA samples. The mock digest, without the addition of the Fpg enzyme, is done under identical treatment conditions as the actual Fpg digest, whereas undigested sample contains exactly the same amount of DNA as the mock digest sample but was incubated at 4 ˚C instead of 37 ˚C. DNA samples subjected to Fpg digest will have more strand breaks resulting in a lower apparent copy number and thus higher threshold cycles compared to mock and undigested DNA samples. This can be seen in Figure 3.11. The mock digest sample serves as the undamaged reference control sample (sample A) for the quantification of the DNA damage in the Fpg digest sample (sample B). Undigested sample serves as an additional control for the Fpg digest to detect non-specific DNA degradation due to the digest reaction. From the amplification plots, the percentage of intact DNA can be determined via the ratio of template after Fpg cleavage (sample B) relative to PCR template present in the mock digest (sample A). The amount of Fpg sensitive DNA lesions can then be quantified as described above (See section 3.3.3) from the

difference in Cts (ΔCt) between Fpg digested and mock digested samples as discussed above using Poisson analysis.

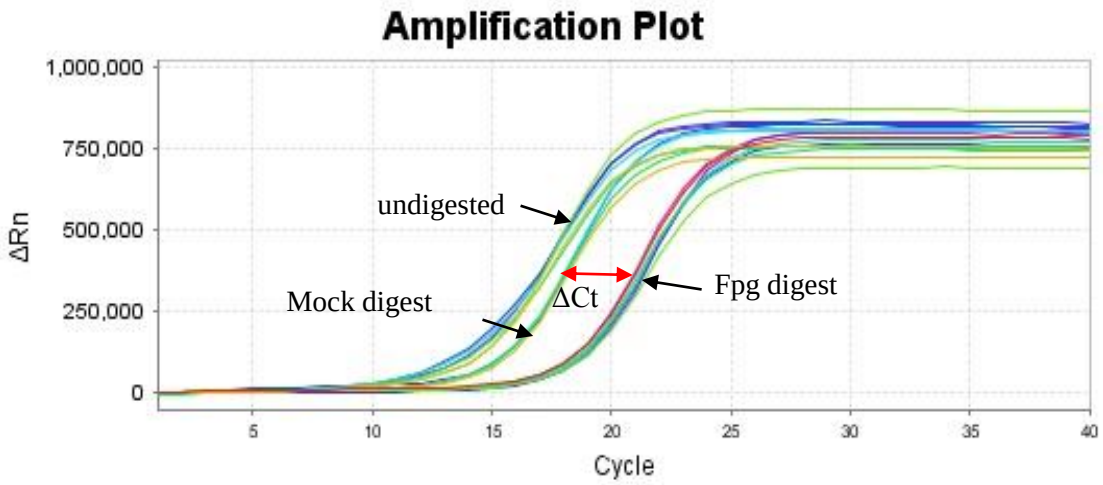

Figure 3.11. Amplification plot of qRT-PCR on mitochondrial extract of day 4 wild type N2 animals that was subjected to Fpg digest. For quantification of oxidative damage using Fpg, three different samples are prepared: Fpg digest, mock digest and undigested DNA samples. To facilitate the quantification of DNA damage, the mock digest sample serves as an undamaged control sample. The ΔCt is the difference in Ct between the Fpg digest and mock digest sample, is used to quantify Fpg sensitive lesions.

Using the data obtained from my experiment for Day 4 N2 nematodes in Figure 3.11, average $\Delta Ct =$ - 4.07, amplification factor was k=1.77, therefore,

$$\frac{X_{0(fpg)}}{X_{0(mock)}} = R = k^{\Delta Ct} = 1.77^{-4.07}$$

R=0.098

This means that relative to mock digested sample, only about 9.8 % of the mtDNA molecules were fully intact (undamaged with zero Fpg sensitive lesions) in the Fpg digested sample, while 90.2 % of mtDNA had been cleaved. Thus, the drop in PCR amplifiable template concentration (relative to mock digest) was 90.2 %

Equating to a DNA lesion frequency, solving Equation 3.6,

$$\lambda = -\ln(0.098)$$

On average, $\lambda = 2.3$ lesions per 6.3 kbp region of mtDNA fragment

Therefore, in a 6.3 Kb fragment of mtDNA of Day 4 (young adult) wild type N2 nematodes that I utilized in this experiment, the DNA lesion frequency was 2.3 DNA lesions per 6.3 kbp or 3.7 x 10^{-4} lesions per bp. Using this Fpg-qRT-PCR method, the number of Fpg sensitive oxidative DNA lesions can be determined for any sample that can be digested using this enzyme.

3.3.4.1.1. Sensitivity test for Fpg-qRT-PCR DNA damage assay

Similar to my test of the comet assay using γ-irradiated animals, the same challenge protocol was used to test the sensitivity of this Fpg-qRT-PCR DNA damage assay.

As assessed by Fpg-qRT-PCR DNA damage assay, animals exposed to γ-irradiation doses of 20 kRad had an average of 3.4 lesions per 10 kbp, while DNA damage in 40 kRad γ-irradiated animals was 3.5 lesions per 10 kbp (Figure 3.12A). Comparing to non-irradiated control animals that had 2.48 lesions per 10 kbp, the assay is unable to detect dose-dependent increase in the DNA damage with increasing γ-irradiation dosage (Figure 3.12A, p=0.49, One-way ANOVA).

This result was disappointing since there is a significant dose-dependent increase in the DNA damage measured using the comet assay (Figure 3.6). I then measured the DNA damage using Fpg-qRT-PCR DNA damage assay in different *C. elegans* strains. I used the *glp-1* (JK1107), which is an egg-laying deficient strain to reduce new mtDNA synthesis by oocytes. The DNA damage in non-irradiated control animals was 3.6 lesions per 10 kbp (Figure 3.12B). The baseline DNA damage in *glp-1* animals was about 40 % more than baseline damage in wild type N2 animals (Figure 3.12A and B), but this difference was not statistically significant (p=0.30,Student's t-test). Furthermore, 20 and 40 kRad γ-irradiation induced mtDNA damage in *glp-1* animals, was measured as 4.2 and 4.6 lesions per 10 kbp, respectively (Figure 3.12B). Overall, analysis of the DNA damage in non-irradiated control, 20 and 40 kRad γ-irradiated animals using One-way ANOVA, again showed that this Fpg-qRT-PCR DNA damage assay was unable to detect significant dose-dependent increase in the DNA damage with higher γ-irradiation dosage (Figure 3.12B, p=0.37), despite the increasing trend.

Failure to detect dose-dependent increase in DNA damage even in different strains showed that the Fpg-qRT-PCR DNA damage assay lacks sensitivity.

In addition, I also detected variations in the DNA damage measured using Fpg-qRT-PCR assay, even though the same sample from the same cohort of animals was used. A robust assay should

remain unaffected by minor variations that may occur over time. A good assay should generate reproducible results when run on replicates of sample both within and between runs [312, 313]. Therefore, robustness and repeatability are important factors that should be considered.

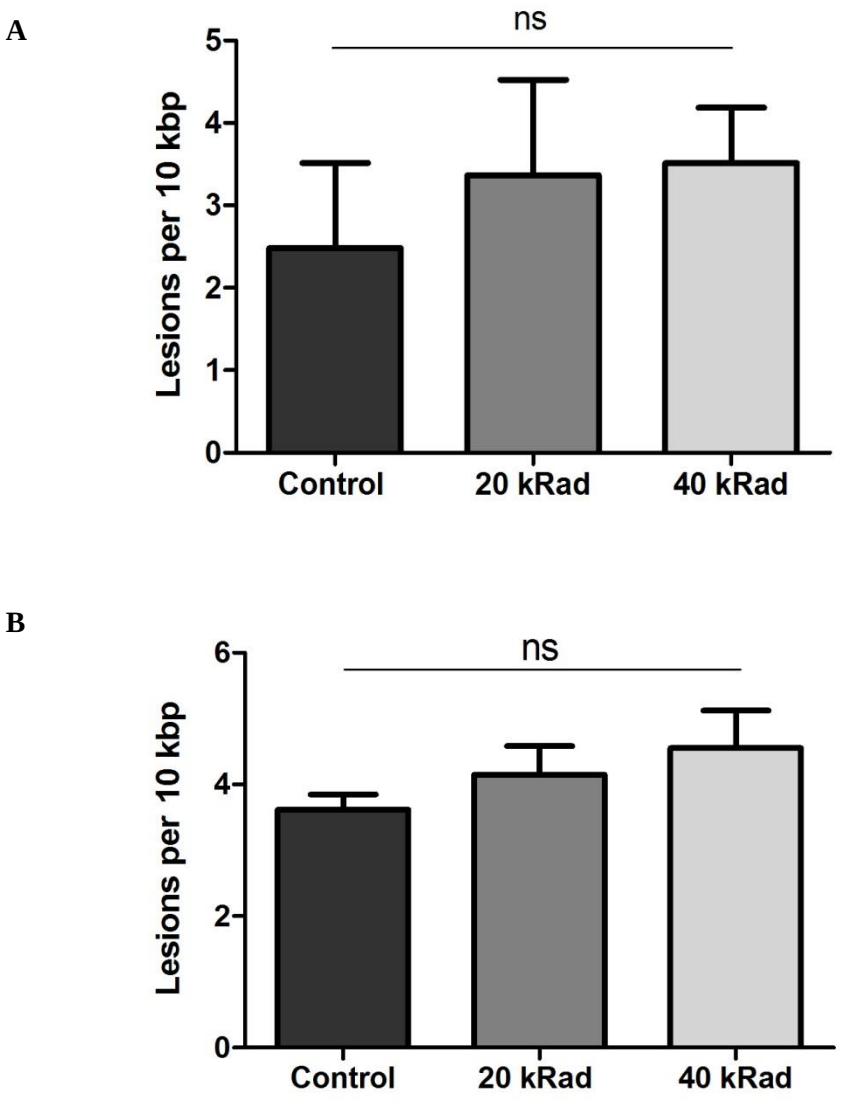

Figure 3.12. The use of a γ-irradiation challenge protocol to test the sensitivity of Fpg-qRT-PCR DNA damage assay. (A) There is no difference in the mtDNA damage in non-irradiated control, 20 and 40 kRad γ-irradiated day 4 wild type N2 animals, p=0.49. (B) mtDNA damage in γ-irradiated day 4 *glp-1* animals also does not show significant dose-dependent trend with increasing dosage of γ-irradiation, p=0.37. The data were analyzed using One-way ANOVA, mean ±SEM. n = 3 independent experiments.

The assay's low sensitivity and high variability led me to address the issue relating to the use of Fpg enzymatic digest. It is common to have variabilities in enzymatic digest, at times, DNA does not appear to be digested, partially digested or unspecific degradation as shown in Figure 3.13. I found that the mock digest and undigested DNA samples (Figure 3.13) sometimes led to inconsistency resulting in variable measurements of DNA lesion frequency. Mock digested samples without the addition of any Fpg enzyme were incubated under the same conditions as the Fpg digested samples. Since there is no addition of any Fpg enzyme, the Ct of the mock digested and undigested DNA should be the same (Figure 3.13A). However, this was not always the case (Figure 3.13) when using *C. elegans* mtDNA extracts. This may be due to the fact that it is hard to obtain pure mtDNA extract without contamination of nuclear DNA, proteins, free metal ions or possible endogenous DNA nucleases. I found that in some repeats, mock digested sample amplified significantly later than undigested samples (Figure 3.13B) while in some cases, they actually amplified earlier than undigested DNA samples (Figure 3.13C). This was the case although the same batch and same amount of Fpg enzyme was used for every repeat of the mock, undigested and digested samples. This variability led to inconsistencies and it is hard to interpret data generated using this assay applied to mitochondrial extract.

Furthermore, in some cases, contamination or impurity in the DNA samples may also inhibit the enzymatic digestion, affecting the level of DNA damage measured [314]. In the repeats, restriction digestion was performed for 4 hours to make sure that restriction reactions go to completion. However, this prolonged incubation time in turn may cause DNA degradation artifacts.

In summary, the Fpg-qRT-PCR DNA damage assay lacks sensitivity, exhibits high variability and is subjected to possible artifacts. Therefore, this assay is not a promising tool for quantitative analysis of DNA damage at least in *C. elegans*.

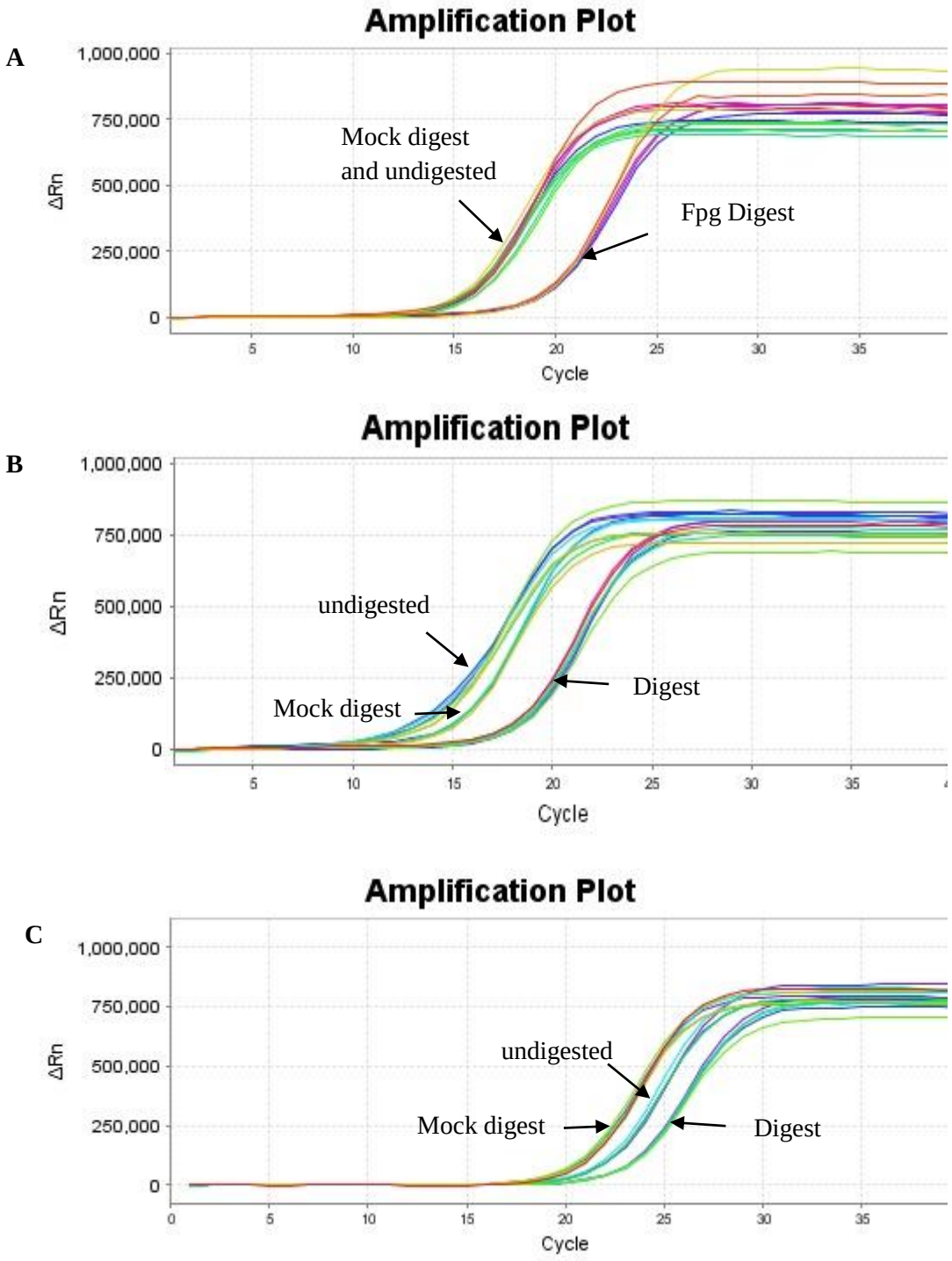

Figure 3.13. Amplification plots from two different RT-PCR runs showing inconsistencies of the mock and undigested sample in the restriction digest reaction. (A) Both mocked and undigested samples were amplified and detected at the same Cts as expected. (B) Mock digested DNA sample amplified later thus higher Ct compared to undigested DNA sample. (C) Mock digested DNA sample amplified earlier thus lower Ct compared to undigested DNA sample.

3.3.4.2. S-XL-qRT-PCR DNA damage assay

While the Fpg digest method is conceptually elegant in that the original, undigested samples can be directly served as reference sample, the problems outlined above led me to explore other approaches. The second approach to perform DNA lesion quantification (given that there is typically no available undamaged reference DNA sample) and to overcome the problems of using Fpg-qRT-PCR to quantify DNA damage is to avoid the digestion step altogether. Determination of the amount of DNA lesions in a sample is also possible by comparing the apparent copy number of a short and long fragment within the same sequence. This involves quantifying the apparent copy number of the same sample using a large

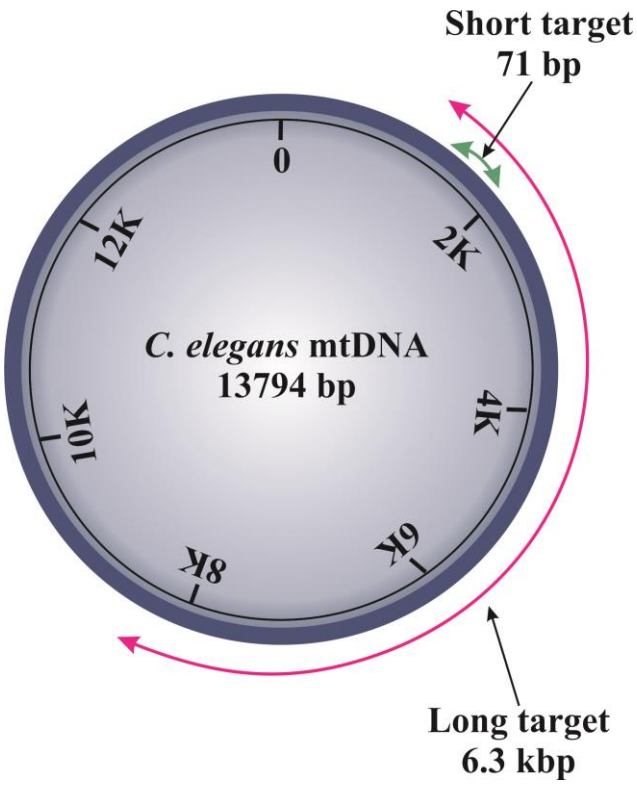

Figure 3.14. Schematic diagram of region amplified by S- and XL-qRT-PCR within *C. elegans* mitochondrial genome. The short amplicon (71 bp) is represented by a green arrow while the long amplicon that amplifies majority of this genome is represented by the red arrow.

amplicon (6.3 kbp) and a small amplicon (71 bp) within the same genome and then comparing the apparent copy numbers (Figure 3.14). The short fragment is too short and is much less affected by DNA damage, therefore can be used as an approximation for the undamaged DNA (this is equivalent to the undamaged sample mentioned above) but the long fragment amplification is significantly affected by DNA damage [309, 315, 316]. The ratio between the apparent copy numbers of the short and long fragment is therefore a measure of DNA damage.

In practice, two independent PCR reactions are used for this purpose: (i) a short-PCR (S-PCR) as quality control and internal normalization to facilitate the quantification of the actual copy number of DNA molecules loaded (without being affected by damage) (ii) an extra-long PCR (XL-PCR) is used for DNA lesion quantification. The amplification of very long genomic targets improves the sensitivity of this assay as the probability of the DNA lesions affecting the PCR within the target sequence increases with increased size of the target. A standard curve method is used to absolutely or relatively quantify the DNA copy number of both the small and large fragments using a known reference sample.

In order to quantify DNA damage, the ratio of intact DNA templates between the small amplicon and large amplicon is calculated. Table 3.2 shows the average Ct values obtained from two independent PCRs of S-PCR and XL-PCR of a reference DNA sample. The input DNA copy number for the known reference sample was determined to be 10,000 copies of DNA per µl or 10,000 copies of DNA per well (as 1 µl of DNA reference sample was added into each well). To quantify DNA lesions for the DNA sample of a cohort of day 4 N2 nematodes in Table 3.2, using the same method as discussed earlier in section 3.3.3, the number of the intact DNA template measured in the unknown sample using S-PCR, $X_{0(S)}$ was 15000 copies. By contrast, the apparent copy number of the long fragment was only 10060 molecules, indicating that there is significant DNA damage in the large fragment, $X_{0(XL)}$.

A

	K factor for small fragment , 71 bp	Average Ct	ΔCt relative to reference sample ($\Delta Ct = Ct(s) - Ct(ref)$)	Initial copy number of intact DNA
Reference sample	1.97	21.2421		
Day 4 N2, small amplicon		20.6436	-0.5984	15000

B

	K factor for large fragment, 6.3 kbp	Average Ct	ΔCt relative to reference sample ($\Delta Ct = Ct(XL) - Ct(ref)$)	Initial copy number of intact DNA
Reference sample	1.77	12.8781		
Day 4 N2, large amplicon		12.8670	-0.0111	10060

Table 3.2. Summary of steps to quantify DNA damage in a sample (day 4 wild type N2 animals). Copy number of intact DNA was determined from the ΔCt of the CT value of particular sample from S- and XL-PCR relative to Ct of a reference sample. The copy number was then used to quantify DNA damage in the particular sample.

Since the same DNA sample was used in both S-PCR and XL-PCR, the actual DNA copy number of S- and XL-PCR reaction should be the same, 15000 molecules in this case. However, for the long fragment (Table 3.2), the apparent copy number was lower with only 10060 molecules. This is the number of large fragments that were undamaged and could still be amplified. Compared to the actual DNA copy number of 15000 molecules for both S- and XL-PCR, the fraction of DNA that could not amplified (that is the percentage of DNA that contains at least one PCR inhibitor lesion in the 6300 bp fragment), X_D is

$$X_D = X_{0(S)} - X_{0(XL)}$$

$$X_D = 15000 - 10060$$

$$X_D = 4940$$

This means that there were 4940 copies or 32.9 % of DNA that contain at least one PCR inhibitory lesion in the 6.3 kbp fragment. To quantify the DNA lesions frequency, the probability of undamaged (intact) DNA molecules needs to be calculated.

Therefore, probability of intact DNA molecules

$$= 1\text{-}0.329$$

$$= 0.671$$

As before, DNA lesion frequency per template can be quantified using Equation 3.6:

$$\lambda = -\ln(0.671)$$

$$\lambda = 0.40$$

Therefore, in the 6.3 kbp fragment of mtDNA of Day 4 (young adult) wild type N2 nematodes, the DNA lesion frequency was 0.40 DNA lesions per 6.3 kbp or 6.3 x 10^{-5} lesions per bp. Using this S-XL-qRT-PCR method, the number of such DNA lesions can be determined for other samples, provided that absolute copy number determination can be performed accurately or known reference samples are available.

However, this approach also has limitations. In particular, it is problematic to study specific types of DNA damage and the inability of the assay to distinguish between different types of DNA damage is a potential limitation [316-318]. However, it might be argued that the measurement of multiple types of DNA damage avoids misleading conclusions that might be drawn from the measurement of a single product [239], because a single product does not necessary reflect the overall DNA damage or biological relevance in the samples. However, a clear limitation of this approach is that this assay can only detect DNA lesions that significantly inhibit the progression of DNA polymerase, in particular, it does not efficiently detect 8-OHdG [309].

3.3.4.2.1. Sensitivity test for S-XL-qRT-PCR DNA damage assay

3.3.4.2.1.1. Gamma radiation

After identifying the problem with the Fpg-qRT-PCR assay, I explored the same challenge protocol in the S-XL-qRT-PCR assay with the aim to test the sensitivity of the assay by comparing the DNA damage in samples exposed to varying amount of damaging agents such as gamma (γ) radiation and ultraviolet (UV) radiation. In contrast to the Fpg-qRT-PCR assay, the S-XL -qRT-PCR mtDNA assay was able to detect significantly elevated oxidative mtDNA damage in animals challenged with increasing doses of γ-radiation (20 and 40 kRad) ($P<0.05$, Figure 3.15). Following γ-irradiation at doses of 20, the mean mtDNA damage in young *glp-1* animals increased (Figure 3.15) to 0.8 lesions per 10 kbp, an approximately 31 % increase in mtDNA damage relative to untreated control young *glp-1* animals (0.6 lesions per 10 kbp). γ-irradiation-induced mtDNA damage in animals exposed to 40 kRad dose was even higher (1.2 lesions per 10 kbp, an approximately 98 % increase compared to untreated control animals).

The comparison of data in Figure 3.15 (mtDNA damage frequency using S-XL-qRT-PCR assay) to nuclear DNA lesions obtained using the comet assay (Figure 3.6) shows that exposure to γ-radiation indeed resulted in a consistent dose-dependent increase in mtDNA damage, which further validates the sequence specific S-XL-qRT-PCR assay (Figure 3.15). Analysis of the results from both comet assay and S-XL-qRT-PCR assay showed high correlation (Figure 3.16) in dose-dependent increase of DNA damage as measured by the comet assay and S-XL-qRT-PCR assay. These dose dependent increases were best fitted by a linear regression line with R-squared value of 0.96. This suggests that the extent of DNA damage caused by increasing doses of γ-irradiation measured using both comet assay and S-XL-qRT-PCR assay may be correlated in which the increased in the percentage of DNA damage will be the same for both assays. Unlike Fpg-qRT-PCR assay, my S-XL-qRT-PCR assay was sensitive.

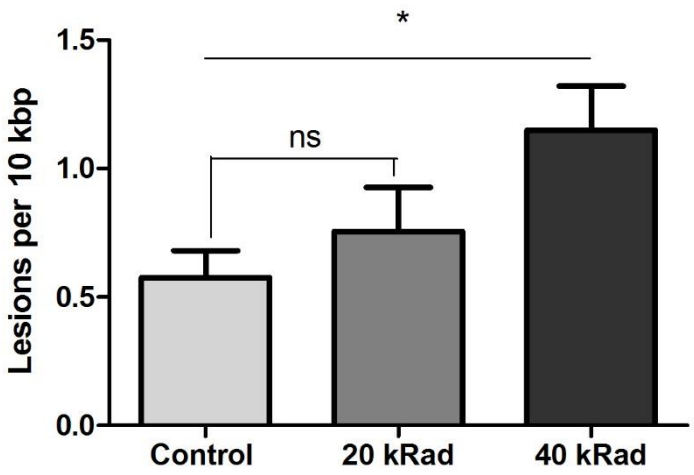

Figure 3.15. γ-irradiation dose-dependence induction of DNA damage in Day 4 young *glp-1 C. elegans*. γ-irradiation dose values given to the nematodes ranging from 0 to 40 kRad. Increasing doses of radiation resulted in a statistically significant enhancement in the extent of DNA damage with 31 % and 98 % increased of DNA lesions at 20 and 40 kRad respectively, relative to untreated control animals. (p=0.02, One-way ANOVA), n= minimum 12 independent experiments.

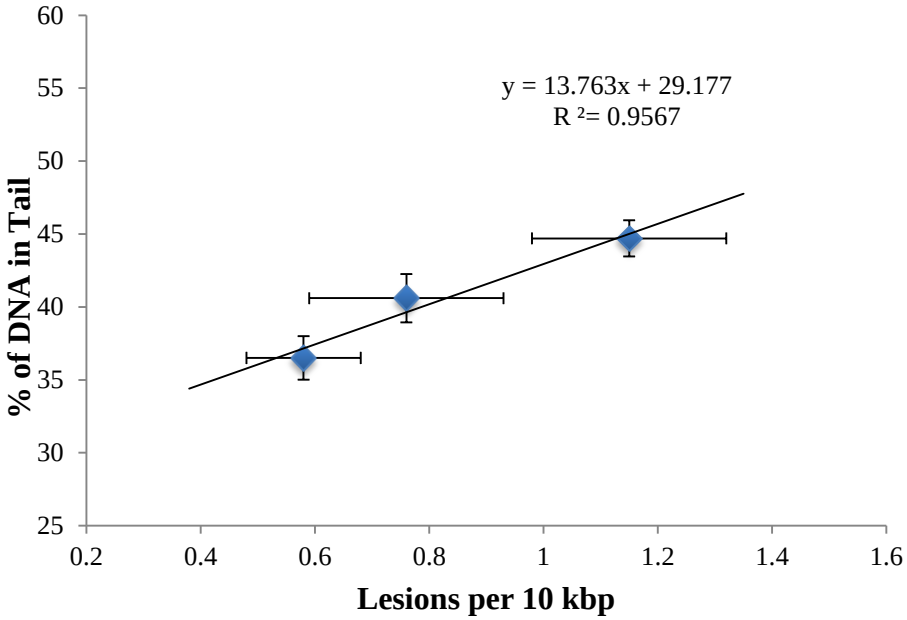

Figure 3.16. Analysis of the results from both comet assay and S-XL-qRT-PCR assay showed high correlation. Both comet assay and S-XL-qRT-PCR DNA damage assay are able to detect γ-irradiation dose-dependent increases in DNA damage. Each point is a mean of minimum 55 comets (for data plotted on Y-axis) or minimum of 12 independent experiments (for data plotted on X-axis).

3.3.4.2.1.2. UV radiation

I then tried another challenge protocol by exposing the nematodes to 400 J/m^2 of ultraviolet C (UVC) radiation. As mentioned in the introduction, there are three main types of UV rays, classified according to their wavelengths. UVA can cause DNA damage through an indirect mechanism by generating highly reactive radicals, thus causing DNA damage such as DNA base modifications, DNA strands breaks, abasic sites and DNA-proteins crosslinks [196]. Unlike UVA, direct UVB and UVC can directly damage DNA resulting in the formation of two types of DNA lesions, the cyclobutane pyrimidine dimers (CPDs) and 6-4 photoproducts (6-4 PPs) [196, 306, 319]. The high energy short wavelength UVC also results in the formation of double-strand breaks at the site of CPDs containing DNA [306, 320, 321]. Further, double-strand breaks can be formed as a consequence of attempted repair of UV-induced DNA damage [322], likely to be detected by S-XL-qRT-PCR assay, unlike 8-OHdG from lysis of water.

Interestingly, I observed statistically significant higher mtDNA damage in UVC-irradiated animals than the mtDNA damage detected in 20 and 40 kRad γ-irradiated animals ($p<0.0001$, One-way ANOVA, Figure 3.15). There were about 120 % more UVC-induced mtDNA lesions than γ-induced mtDNA lesions in young *glp-1* animals. As seen in Figure 3.17, relative to untreated control animals with only 0.6 lesions per 10 kbp, there was a significant increased in mtDNA damage ($P<0.0001$) with 2.5 lesions per 10 kbp or approximately 336 % more DNA lesions detected in UVC-irradiated animals.

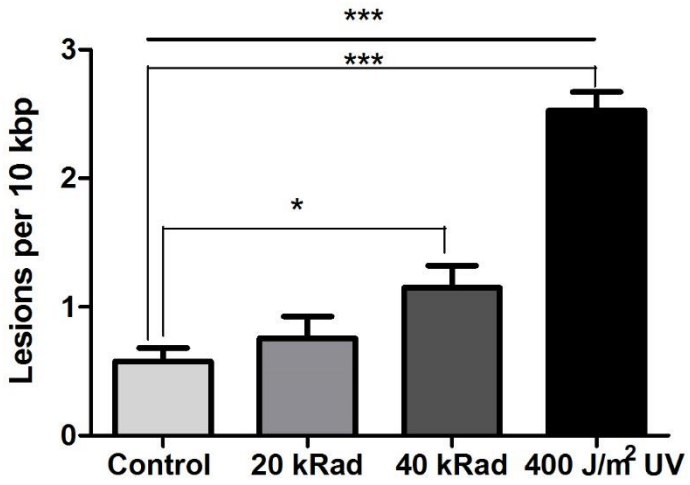

Figure 3.17. Effect of γ- and UV-irradiation on the mtDNA of day 4 young JK1107 nematodes. There is a significant increase in the damaged DNA in animals exposed to γ- and UV-irradiation ($P<0.0001$). (Mean ± SEM, one-way ANOVA, n= 23 independent experiments.

In addition to DNA damage assay validation, I also optimized DNA extraction, storage condition and type of fluorescence dyes used. (For detailed explanations, see Appendix A1, A2 and A3).

In conclusion, I have developed a Real Time PCR based protocol, S-XL- qRT-PCR DNA damage assay that is highly sensitive. This DNA damage assay is highly robust and reproducible, which enables precise quantification of baseline DNA damage in *C.elegans*. It is therefore a sensitive, robust and high repeatability assay for quantitative analysis of DNA damage for a wide range of applications in *C.elegans*.

4. Applications of the Sequence-Specific S-XL-qRT-PCR DNA Damage Assay

4.1. Association of mtDNA damage to growth, development and health of the irradiated animals

In order to address the biological significance of the oxidative mtDNA damage induced by γ-radiation and UV-radiation during the challenge experiments (Figure 3.15-3.17); I investigated their association to lifespan, healthspan and the fitness of the nematodes.

I conducted lifespan studies in which the samples were randomized and the observer was blinded to the treatment conditions. Randomization of samples and blinding when scoring survival minimizes observer bias [289]. Surprisingly, despite the fact that the animals had significantly higher mtDNA damage, I observed that young *C. elegans* exposed to 40 kRad of γ-radiation showed no significant lifespan shortening relative to untreated control animals (Figure 4.1A). Lifespan curve comparison, the mean and maximum (defined as the average lifespan of the top 10 % of the longest surviving animals) lifespan of the γ-irradiated nematodes were all not significantly different, as compared to non-irradiated control animals (Figure 4.1A, B and C, $p=0.97$, $p=0.88$ and $p=0.57$, respectively). The mean and maximum lifespan of γ-irradiated animals for both conditions were 13 and 23 days, respectively (Figure 4.1B and C).

In contrast to γ-irradiated animals, I observed that the lifespan of the animals treated with 400 J/m^2 UV-radiation was significantly shortened compared to control animals (Figure 4.1A, $p<0.05$). Mean lifespan of UV-irradiated animals was significantly shorter than control animals showing a 10.2 % reduction in lifespan (Figure 4.1B, $p<0.05$, Student's t-test). Treatment of animals with 400 J/m^2 UV-radiation also significantly reduced the nematodes' maximum lifespan by 30.3 %, reducing it from 23.2 days to only 16.2 days (Figure 4.1C, $p<0.0001$, Student's t-test).

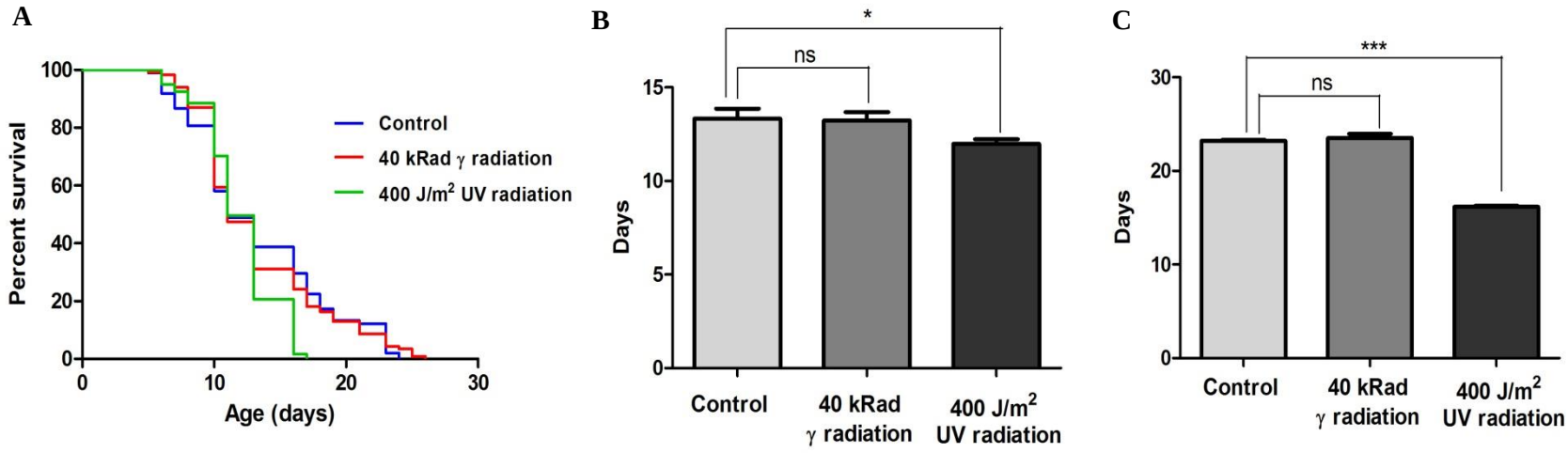

Figure 4.1. Survival of Day 4 *glp-1* nematodes exposed to 40 kRad γ-radiation, 400 J/m^2 UV- radiation and control nematodes (n=200 worms per condition). (A) Survival curves from each condition were compared to that of the non-irradiated control animals and analyzed using Log-rank (Mantel-Cox) test. The survival of animals exposed to 40 kRad γ-radiation was not significantly different from non-irradiated control animals, while exposure to UV-radiation significantly shortened the lifespan of the nematodes, ($p<0.05$). (B) Mean lifespan of UV-irradiated animals was significantly shortened relative to control animals, ($p<0.05$,Student's t-test). (C) γ-radiation had no significant effect on the survival of nematodes but the survival of UV-irradiated animals was significantly shortened as compared to non-irradiated control animals, ($p<0.0001$).

In order to judge the impact of radiation on indicators of overall health status of the muscular and nervous system, I further conducted blinded healthspan studies. I determined healthspan by measuring the animal motility as an indicator of health. Healthspan is an index of physiological capacity, meaning the period of time during which the animals are able to maintain good health [289]. The motility of the nematodes was scored daily into three classes of movement A, B and C [42, 45]. Class A animals are highly mobile animals that move constantly in response to prodding, moving away from the touch stimulus leaving sinusoidal tracks in the bacterial lawn through which they migrate. Class B animals move only in response to touch stimuli leaving non-sinusoidal tracks, reflecting uncoordinated locomotion. Lastly, animals in class C only move their head or tail in response to prodding.

Healthspan curves and locomotor distribution (in percent of total animals alive on the respective day) were plotted to compare the animals' relative health. Generally, animals from γ-, UV-irradiated and non-irradiated control all showed relatively rapid age-dependent decline in terms of locomotor activity (Figure 4.2A and B). A-type movement was predominant at young and early middle age whereas B- and C-type movement became prevalent in the late-middle aged and old-aged nematodes, respectively.

Interestingly, the health status of γ-irradiated and non-irradiated control animals was similar throughout life (Figure 4.2A and B) despite the difference in the mtDNA damage in these animals (Figure 3.15-3.17). The mean healthspan of the γ-irradiated nematodes was similar to non-irradiated control animals (Figure 4.3A) at 13.8 days for both conditions. Surprisingly, I observed that the duration for which the healthiest 10 % of animals from each group were able to maintain good health were 23.0 and 23.8 days, respectively (Figure 4.3B). This difference was statistically significant ($p<0.01$, Student's t-test), meaning that the maximum healthspan of the γ-irradiated animals was significantly improved relative to non-irradiated control animals.

As expected from the high level of damage to mtDNA and shorter lifespan, UV-irradiated animals displayed a significantly lower average locomotor activity compared to the non-

irradiated control animals (Figure 4.2A, $p<0.0001$, log-rank test). At early ages (from day 5 to day 8), there were no differences in the locomotor activity of the γ-, UV-irradiated and control animals. However, the detrimental effect started to take effect from day 10 where only 36 % of the UV-irradiated animals remained active (A-type movement) while 81 % of control animals still remained healthy (A-type movement) (Figure 4.2B). On the whole, UV-irradiated animals were the first treatment group that failed to maintain their class A health status. None of the UV-irradiated animals maintained class A health status beyond day 16 whereas about 38 % of non-irradiated control and 32 % of γ-irradiated animals were able to maintain class A health state at day 16 (Figure 4.2B). In addition, the average number of days that the UV-irradiated animals were able to maintain class A health status was only 11.3 days, which was significantly shorter compared to both γ-irradiated and non-irradiated animals (13.8 days for both conditions) of class A health state (Figure 4.3A, $p<0.0001$, Student's t-test). Comparing the top 10 % motility phenotype of the UV-irradiated animals, I observed that the number of days that the UV-irradiated animals were able to retain good health was significantly shorter (by 30 %) relative to non-irradiated control animals (Figure 4.3B, $p<0.0001$, Student's t-test).

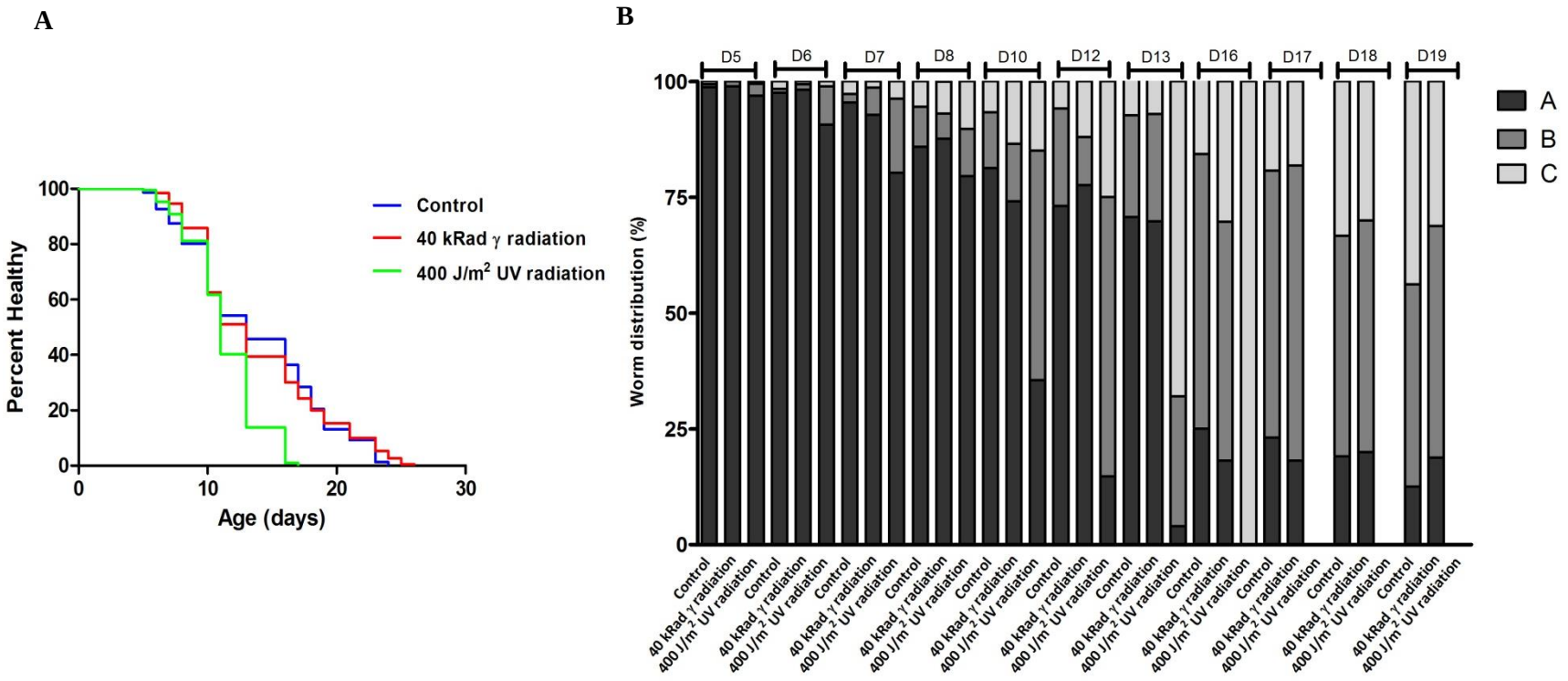

Figure 4.2. . Locomotor activity of γ-, UV-irradiated and non-irradiated Day 4 *glp-1* control nematodes, n=200 worms per condition. A. Healthspan curve from a single experiment. Animals exposed to UV-irradiation were less active and healthy compared to non-irradiated control animals. The difference was statistically significant with $p<0.0001$, analyzed using Log-rank (Mantel-Cox) test. B. Distribution of worms in percentage of total worms alive on the respective day. UV-irradiated animals showed lower locomotor activity relative to non-irradiated control animals.

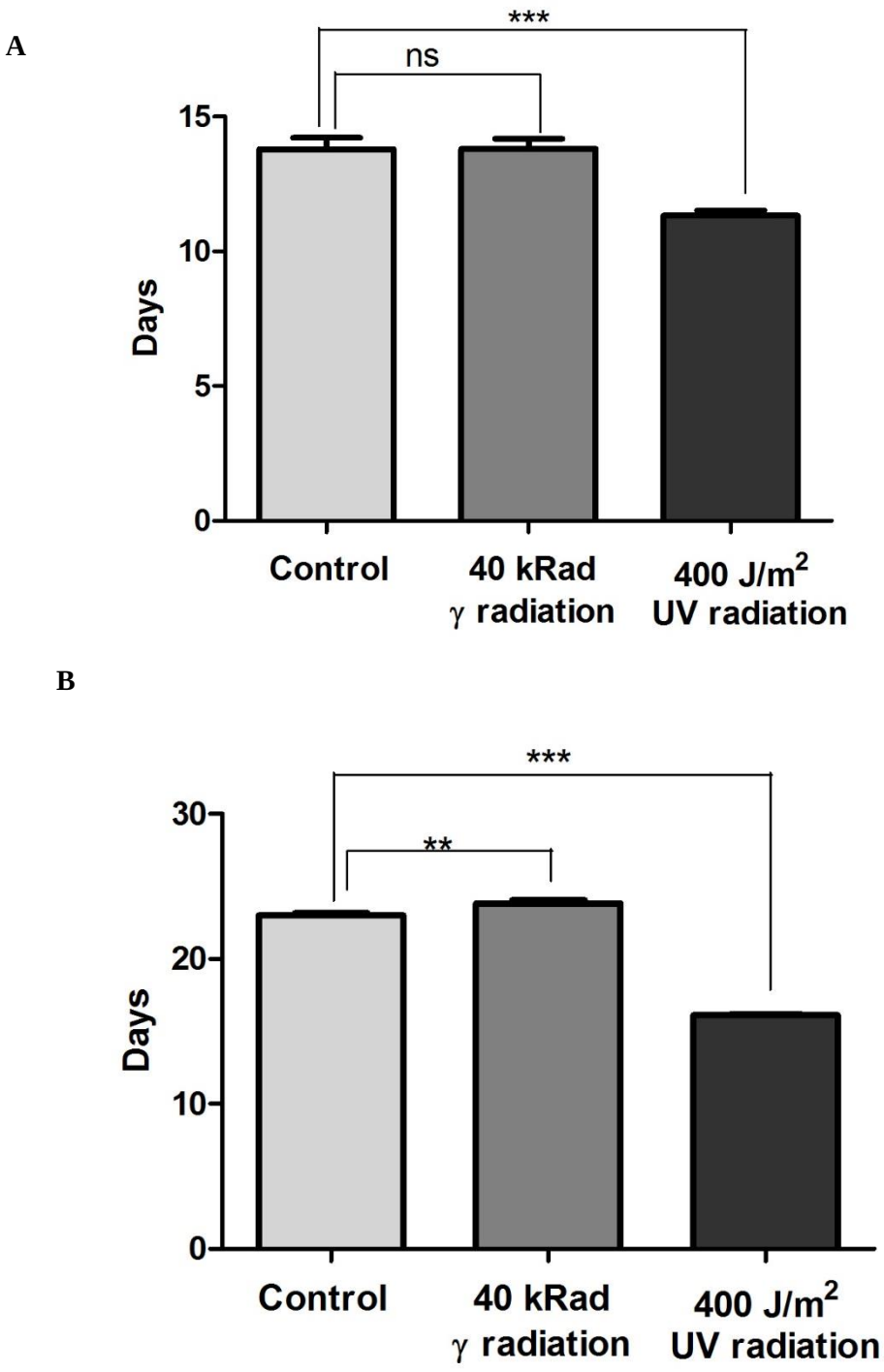

Figure 4.3. Mean and maximum healthspan of the γ-, UV-irradiated and non-irradiated control animals. A. Mean healthspan was significantly shortened in animals exposed to UV-radiation relative to control animals, $p< 0.0001$, Student's t-test. B. UV-irradiation also significantly shortened the maximum healthspan of the nematodes, $p<0.0001$, Student's t-test. Surprisingly, maximum healthspan of the γ-irradiated animals was significantly extended, $p<0.05$, Student's t-test. n= 3 independent replicates.

I also investigated the fitness in terms of ability of the animals to move in a given duration, following γ- and UV-irradiation by measuring the average distance travelled by young nematodes within a 15 minutes period after transferring the animals to a fresh plate with bacterial lawn. All animals tested were class "A". Distance travelled is an indicator of fitness of animals' ability to explore the environment for new resources as well as escape hazardous environments. Surprisingly, given the lack of lifespan and healthspan effect of γ-irradiation, the typical distance travelled by both γ- and UV-irradiated nematodes was markedly reduced relative to non-irradiated control animals (Figure 4.4, $p<0.0001$ for both conditions, Student's t-test). γ-irradiated animals travelled at an average distance of 2400 μm per minute while UV-irradiated animals travelled about 2800 μm per minute (Figure 4.4, $p=0.64$, Student's t-test). By comparison, non-irradiated control animals travelled about 6200 μm per minute. This means that γ-irradiated nematodes travelled approximately 61 % less than the control animals ($p<0.0001$, Student's t-test). UV-irradiated animals despite being much less healthy, unexpectedly, travelled only approximately 56 % less than control animals (Figure 4.4). The difference between distance travelled by the UV-irradiated and non-irradiated animals was statistically significant ($p<0.0001$, Student's t-test).

Despite a significantly higher mtDNA damage in γ- and UV-irradiated animals, I observed no lifespan or healthspan shortening effects in γ-irradiated animals. This is surprising as I observed a clear fitness impairment in γ-irradiated animals. On the other hand, UV-irradiated animals with extremely high mtDNA damage relative to non-irradiated and γ-irradiated animals had significantly shorter lifespan and healthspan as well as fitness impairment. The reason for these differences is unclear and it would be interesting to address this. One explanation for this is that the γ-irradiated animals might have used some of their metabolic energy to survive while UV-irradiated animals with significantly higher DNA damage as measured using my S-XL-qRT-PCR assay might have less metabolic energy declined due to the declined in mitochondrial function. Consequently, UV-irradiated animals are unable to compensate for the DNA damage

and also DNA lesions caused by UV-irradiation are more lethal than DNA lesions caused by γ-irradiation. Therefore, further work is necessary to investigate these changes.

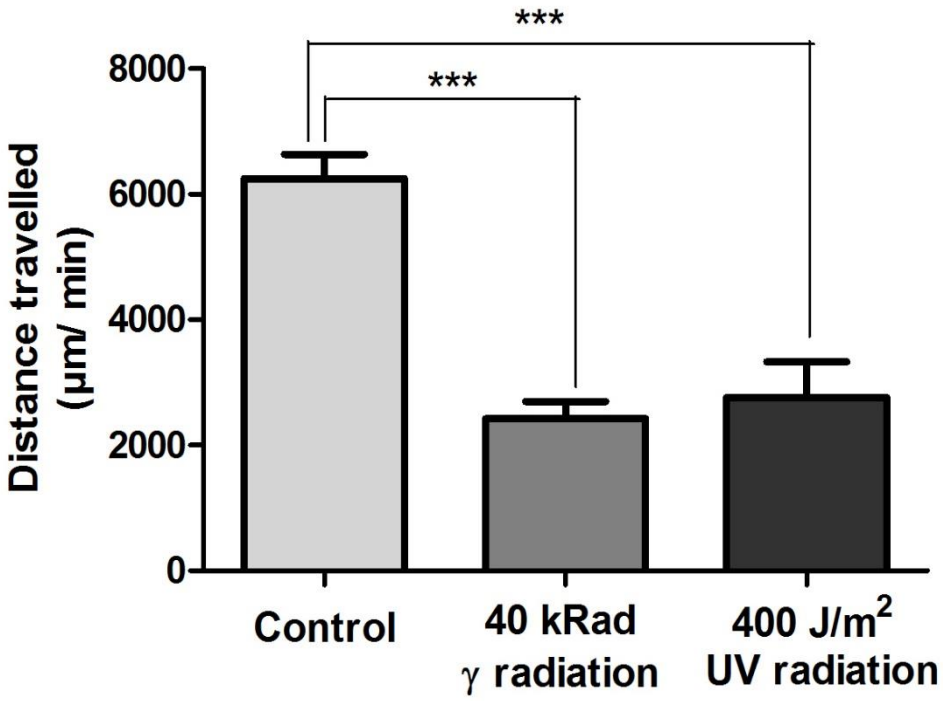

Figure 4.4. Average distance travelled by γ- , UV-irradiated and non-irradiated day 4 *glp-1* nematodes. Both γ- and UV-irradiated animals travelled significantly less than non-irradiated control animals, $p<0.0001$ for both conditions, Student's t-test. n=10 animals per condition.

4.2. mtDNA Age-dependent changes

I then applied the S-XL-qRT-PCR DNA damage assay to an ageing cohort with the aim to investigate age-dependent mtDNA damage *in vivo*. I was able to detect a trend towards higher mtDNA damage in older animals (Figure 4.5A). Although there was a 50 % increase in mtDNA damage with a maximum (at Day 14) of 0.9 lesions per 10 kbp compared to young animals (Day 4) with 0.6 lesions per 10 kbp, the increase was not statistically significant ($p=0.19$, Student's t-test) (Figure 4.5A). MtDNA damage in old animals was low, compared to mtDNA damage in 40 kRad γ-irradiated and 400 J/m^2 UV-irradiated animals that have 1.2 and 2.5 lesions per 10 kbp, respectively (Figure 3.17).

In addition, I also measured the distance travelled by the animals. I found that old animals travelled significantly less than young animals at 3400 μm per minute compared to 6200 μm per minute in young animals (Figure 4.5B, $p<0.0001$, Student's t-test), despite the non-significant difference in the mtDNA damage. This phenomenon experienced by old animals might be similar to the γ-irradiated animals where the animals conserve their energy, in this case, at old age for survival. This also suggested that there might be a certain threshold of mtDNA damage up to which the animals use their metabolic energy to survive. Metabolic energy compensating might not work with mtDNA damage beyond a certain threshold.

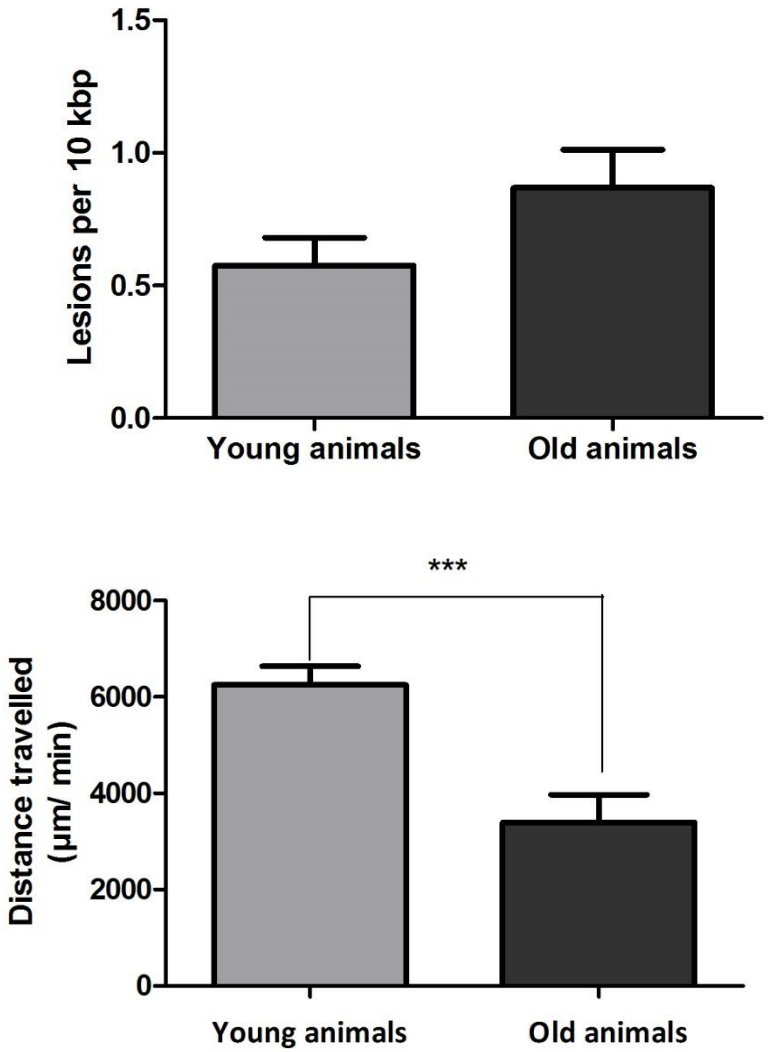

Figure 4.5. mtDNA damage and distance travelled measured in young and old nematodes. (A) Using S-XL-qRT-PCR DNA damage assay to detect the mtDNA lesions in young and old nematodes**.** mtDNA lesions in mtDNA samples of young animals (Day 4) and old animals (Day 14). As judged by S-XL-qRT-PCR DNA assay for mtDNA damage, there was a trend towards more mtDNA lesions in old nematodes (P = 0.19, Student's t-test), n=23 independent experiments. (B) Old animals travelled significantly less than young animals ($p<0.0001$, Student's t-test), n=10 animals per condition.

4.3. mtDNA damage in different mutant strains

Having established that my assay is able to detect and quantify levels of mtDNA damage even below the threshold for significant lifespan effects, I then applied it to investigate mtDNA damage in different mutant strains of *C. elegans*. Strains were selected because they showed differences in lifespan or had modifications in ROS defences with the aim to study the association of mtDNA damage and lifespan.

I first applied my assay to the *glp-1* (germ line deficient-JK1107) strain, a temperature sensitive mutant that is sterile at 25.5 ℃ but fertile at 15 ℃. The *glp-1* gene is required for germ cells mitotic division. Maintenance of young adult *glp-1* nematodes at restrictive temperature of 25.5 ℃ inhibits germ lines proliferation and blocks cell division [323]. Therefore, at 25.5 ℃, these mutant nematodes have post-mitotic somatic cells but few germ cells, which reduces the possibility of DNA from germ line cells affecting measurements of global DNA damage. At 25.5 ℃, *glp-1* nematodes have shorter lifespan (with a mean lifespan of 12.3 days) [286] compare to wild type N2 animals at 20 ℃ that have a mean lifespan of 21 days [289]. Using my S-XL-qRT-PCR DNA damage assay, I found that there is no difference between the mtDNA damage in *glp-1* mutant that were cultured at higher temperature and wild type N2 animals at 20 °C (Figure 4.6, p=0.08, Student's t-test). MtDNA damage was measured in *glp-1* mutant (the commonly used strain) animals for the first time, which suggests that *glp-1* animals have similar DNA damage to wild type N2 animals although these *glp-1* animals were cultivated at higher temperature and have shorter lifespan.

I next investigated the mtDNA damage in *mev-1* (a methyl viologen (paraquat)-sensitive -TK22) mutant strain. The *mev-1* mutation results from an amino acid substitution in cytochrome *b* subunit in complex II, which results in decreased complex II activity [324] and elevated ROS production [325, 326]. The *mev-1* mutant is hypersensitive to both oxygen and methyl viologen with half the wild type *C.elegans*' cytosolic SOD activity [327]. This mutant strain suffers from high oxidative stress [325, 326], and has shorter lifespan relative to wild type N2 animals [326, 328]. Surprisingly, there was no elevation in mtDNA damage in *mev-1* mutant relative to wild type N2 animals with 0.8 and 0.9 lesions per 10 kbp, respectively (Figure 4.6, p=0.67, Student's

t-test). In this case, the *mev-1* mutant animals have higher protein damage [326] but no difference in the mtDNA damage compared to wild type N2 animals, suggesting that oxidative damage is highly specific to the type of molecules and probably to the type of tissues. This illustrates the need for specific markers as clearly protein carbonyl content does not predict mtDNA damage and *vice versa*.

Furthermore, *mev-1* mutant animals have shorter lifespan but no elevation in mtDNA damage. This demonstrates that, lifespan shortening in mitochondrial mutant nematodes is not necessarily mediated by mtDNA damage.

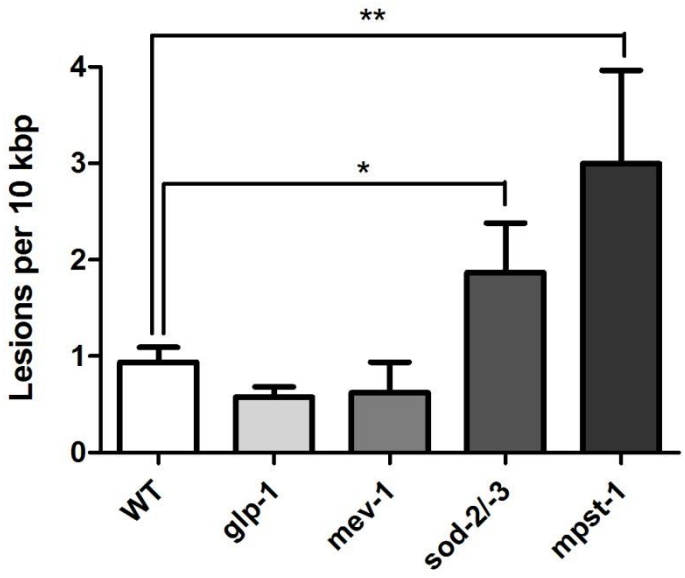

Figure 4.6. mtDNA damage of different young (Day 4) *C.elegans* mutant strains relative to young (Day 4) wild type N2 animals. Relative to wild type N2 *C. elegans*, *glp-1* and *mev-1* mutant *C. elegans* strains had no significant difference in mtDNA damage as measured by S-XL-qRT-PCR assay and expressed as lesions per 10 kbp of mtDNA (P=0.08 and 0.67, respectively, Student's t-test). Compared to wild type N2 animals, *sod-2/sod-3* double mutant animals had significantly higher mtDNA lesions (P=0.04, Student's t-test). *mpst-1* animals that lack the H_2S synthesizing enzyme, had three-fold higher mtDNA damage relative to wild type N2 animals (P<0.01, Student's t-test), n=minimum 3 independent experiments.

Another mutant strain that I tested is the *sod-2/sod-3* (GA 480) double knockout mutant strain, lacking both mitochondrial forms of superoxide dismutase (SOD). SOD is an antioxidant enzyme that detoxifies superoxide by catalyzing the dismutation of superoxide into oxygen and hydrogen peroxide. *C. elegans* has five SOD genes, of which only *sod-2* and *sod-3* are localized to mitochondria [62, 63]. Surprisingly, *sod-2/sod-3* mutant animals do not exhibit lifespan shortening effect despite an increase in sensitivity to oxidative stress due to impairment in antioxidant defence [88, 329]. It has also been shown that deletion of *sod-2/sod-3* genes does not elevate oxidative damage to protein [88]. Surprisingly, consistent with other studies, our lab has also found that *sod-2/sod-3* mutant animals have significantly lower ROS production and consequently, no elevation in oxidative mtDNA damage using the Fpg-qRT-PCR as compared to wild type N2 animals [62]. However, using the more sensitive S-XL-qRT-PCR DNA damage assay, I observed a significant increase in mtDNA damage in *sod-2/sod-3* mutant animals relative to wild type N2 animals (Figure 4.6, $p=0.04$, Student's t-test). The mtDNA damage in *sod-2/sod-3* mutant animals represents a two-fold increase in mtDNA damage in comparison to wild type N2 animals. The significantly higher mtDNA damage in *sod-2/sod-3* mutant animals suggests that depleting the antioxidant defence in mitochondria causes a mild increase in oxidative damage. However, this mild increase does not shorten the lifespan of the *sod-2/sod-3* mutant animals, again suggesting that mtDNA damage is not a determinant of lifespan in mitochondrial mutants.

Lastly, I applied this S-XL-qRT-PCR DNA damage assay to *mpst-1* (ok2040) mutant animals. The *Mpst-1* gene codes for one of the three enzymes (namely: cystathionine γ lyase (CSE), cystathionine β synthetase, and 3-mercaptopyruvate transferase (MPST or 3-MST)) that synthesize hydrogen sulphide (H_2S) naturally in *C. elegans*. H_2S has been shown to increase *C.elegans* lifespan and healthspan by acting as antioxidant or modulator of ROS production [330, 331]. Loss of *mpst-1* gene in *C.elegans* reduces endogenous H_2S production, significantly decreasing their lifespan and healthspan with significant elevation of ROS production [331]. I then used my S-XL-qRT-PCR DNA damage assay to investigate the mtDNA damage and found

that consistent with expectation in this case, mtDNA damage was significantly elevated in *mpst-1* mutant animals (Figure 4.6, $p<0.01$, Student's t-test). The damaged mtDNA in *mpst-1* mutant animals was 3.2 fold higher than wild type N2 animals. In contrast to the mitochondrial mutants, these data for the *mpst-1* mutant animals are in agreement with mFRTA where high ROS production at certain baseline threshold, elevates oxidative damage sufficiently to shorten lifespan in *C. elegans*.

Impairment of antioxidant defence or increase hypersensitivity to oxygen may not necessarily shorten the lifespan or elevate oxidative damage. Even when damage is elevated through radiation or genetic interventions, lifespan is not necessary shortened, at least in *C.elegans*. The data above shows that the effect of oxidative damage is probably molecule-, cell- or tissue-type specific and mtDNA may not be a determinant of lifespan in *C. elegans*. Measurement of a single biomarker cannot be interpreted as an indicator of global oxidative stress.

4.4. Therapeutic approaches against mtDNA damage and ageing/age-related diseases

The S-XL-qRT-PCR DNA damage assay was applied successfully to different genetic strains of *C. elegans*. I next investigated the changes in mtDNA damage due to pharmacological interventions in ageing and age-related diseases.

I tested a mitochondria-targeted antioxidant, MitoQ (see section 1.10.1.) in a transgenic *C. elegans, Aβ 1-42* (CL2006) model of Alzheimer disease (AD). Aβ has been previously found to target the mitochondria, elevating ROS production thus causing mitochondrial dysfunction [232, 233]. It is believed that Aβ accumulation is closely associated with oxidative stress and plays an important role in AD pathogenesis [90, 225-227]. This transgenic AD model constitutively expresses high-levels of human Aβ under a muscle specific promoter [17], and thus relates Aβ-expression and cellular toxicity to an easily visible progressive-paralytic phenotype thus greatly facilitates pharmacological evaluation of intervention strategies [11, 12].

Given the mitochondrial localization of Aβ, I first hypothesized that mtDNA damage might play a significant role in modulating the *C. elegans*' lifespan. I therefore expected that mtDNA damage should be higher in Aβ-expressing transgenic nematodes relative to wild type N2 nematodes.

In order to examine the ability of this mitochondria-targeted antioxidant to modulate mitochondrial oxidative damage burden, I tested the potential of the mitochondria-targeted antioxidant, MitoQ in a transgenic *C. elegans* model of AD. I hypothesized that if MitoQ does modulate oxidative damage in Aβ-expressing transgenic nematodes, then administration of MitoQ should extend the lifespan and reduce mtDNA damage in these animals.

4.4.1. Determining the effective dose of MitoQ in Aβ-expressing nematodes

My first goal was to determine the effective dose of the MitoQ to be used for this study. I started by conducting a blinded dose-response lifespan study at MitoQ concentrations of 0.1 μM, 1 μM and 5 μM with the aim to identify the lowest MitoQ concentration resulting in optimal lifespan effects. As mentioned in the introduction (see section 1.10.1.), MitoQ is produced by covalently attaching an ubiquinone moiety to the lipophilic decyltriphenylphosphonium (dTPP) cation through a 10-carbon aliphatic carbon chain [271]. Studies have shown that the lipophilic cation, dTPP promotes mitochondrial depolarisation at high concentration [272, 332]. Therefore, a dTPP-only control at the same concentrations as MitoQ was used in order to control for nonspecific effect of dTPP on the survival of *C. elegans.* In addition to the dTPP controls, a negative control experiment in the absence of both MitoQ and dTPP was carried out.

The dose-response lifespan study showed that Aβ-expressing transgenic animals treated with 1 and 5 μM MitoQ displayed significant lifespan extension effects relative to untreated control *Aβ 1-42* mutants. No lifespan prolonging effect was seen in 0.1 μM MitoQ treated animals (Table 4.1, Figure 4.7A-C). The mean lifespans for animals treated with 1 and 5 μM MitoQ were 15.0 and 15.2 days, respectively compared to untreated control animals with a mean lifespan of 13.2 days (Table 4.1, Figure 4.7A-C).

Dose	Mean Lifespan (SEM) (Days)	p-value
Control	13.2 ± 0.4; n=145	
0.1 µM MitoQ	13.8 ± 0.4; n=148	ns
0.1 µM dTPP	15.2 ± 0.4; n=155	**
1 µM MitoQ	15.0 ± 0.4; n=161	**
1 µM dTPP	14.7 ± 0.4; n=158	ns
5 µM MitoQ	15.2 ± 0.5; n=148	**
5 µM dTPP	13.7 ± 0.4; n=148	ns

Table 4.1. Mean lifespan of transgenic Aβ-expressing *C. elegans* from pilot dose-response survival study, Lifespan study A. Lifespan study was performed under blinded conditions. At each concentration, mean lifespan for MitoQ and dTPP vs. untreated control animals was analysed using ANOVA with Bonferroni's post-test, mean ±SEM. Only 1 and 5 µM MitoQ treatment significantly affected the mean lifespan of the transgenic animals.

(ns: not significant,*: P<0.05, **: P<0.01)

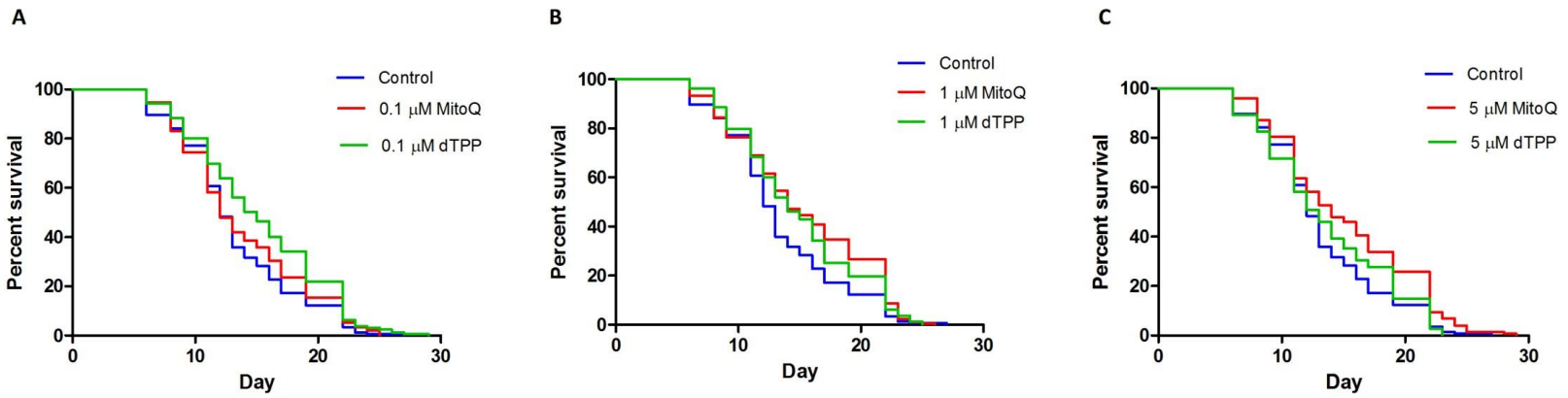

Figure 4.7. Dose-response survival study (Lifespan study A) of Aβ-expressing transgenic *C. elegans* treated with different concentrations of MitoQ or dTPP (n=200 worms per condition). Survival curves from each condition were compared to that of the untreated control, analyzed using Log-rank (Mantel-Cox) test. (A) Administration of 0.1 μM MitoQ had no significant lifespan extension benefit to the transgenic animals but 0.1 μM dTPP treatment significantly extended survival of the nematodes ($p<0.01$). (B) Nematodes treated with either 1 μM MitoQ or dTPP showed significant lifespan extension ($p<0.01$ and $p<0.05$ respectively) although lifespan extension in 1 μM dTPP treated nematodes was less significant. (C) High concentration of MitoQ (5 μM) also showed significant lifespan extension benefit but its respective control, 5 μM dTPP did not increase the survival of the transgenic *C. elegans*.

In addition to MitoQ, 1 and 5 μM dTPP showed no significant lifespan extension or reduction on the survival of the transgenic Aβ-expressing mutant *C. elegans* (Table 4.1, Figure 4.7B and C). The mean lifespans of 1 and 5 μM dTPP treated animals were 14.7 and 13.7 days, respectively, but the differences were not statistically significant relative to untreated control animals (Table 4.1, Figure 4.7B and C). Surprisingly, in this initial study, there appeared to be a significant lifespan benefit on animals treated with 0.1 μM dTPP, with treated nematodes showing a significantly longer mean lifespan of 15.2 days compared to untreated control animals (Table 4.1, Figure 4.7A). However, this observation did not reproduce in subsequent studies.

The results from this initial pilot lifespan study indicated that administration of 1 and 5 μM MitoQ showed the most lifespan extension effects with both concentrations having similar lifespan benefits ($p=0.63$, Log-rank(Mantel-Cox)-test). This suggested that higher concentrations of MitoQ (5 μM and above) had no additional lifespan benefit on the transgenic Aβ-expressing *C. elegans*. I therefore chose to explore 1 μM MitoQ as it was the lowest concentration that displayed optimal lifespan extension effect.

To further confirm the effective dose of MitoQ to be used for this study, I then conducted two further lifespan studies. Similar to the pilot survival study, only administration of 1 μM MitoQ showed a consistent lifespan extension effect ($P<0.01$ for both 2nd and 3rd lifespan studies, Figure 4.8A and B, 4.9A).

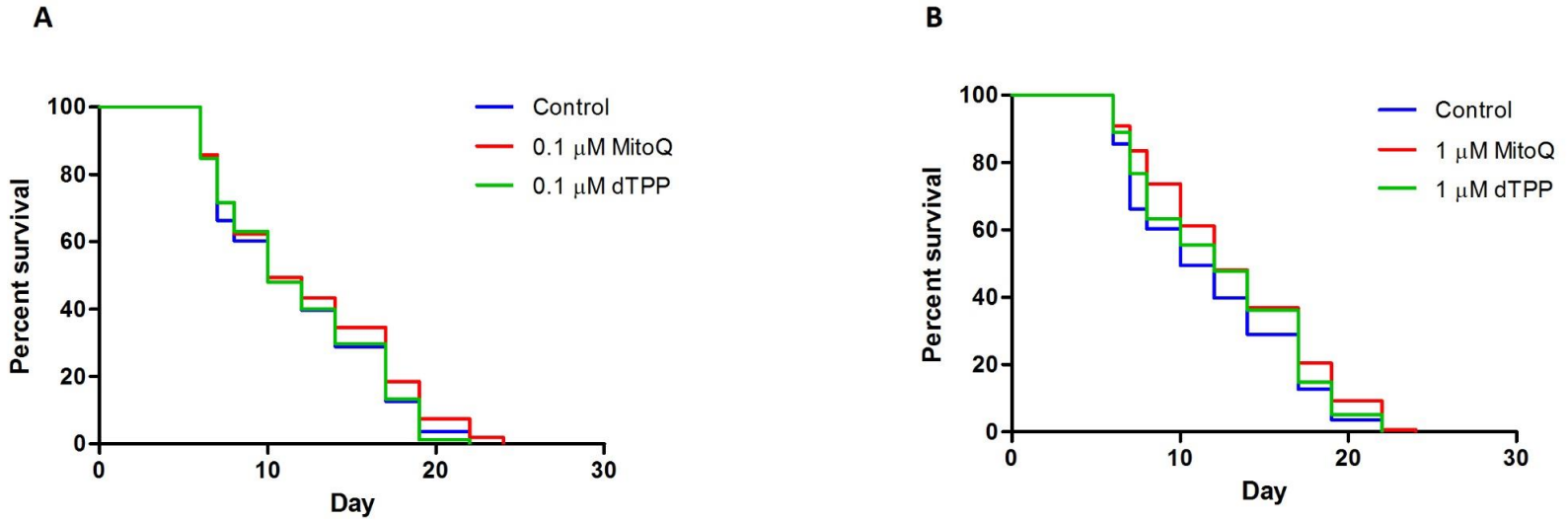

Figure 4.8. Second dose-response survival study (Lifespan study B) of Aβ-expressing transgenic *C. elegans* treated with 0.1 and 1 μM MitoQ or dTPP (n=200 worms per condition). Survival curves from each condition were compared to that of the untreated control, analyzed using Log-rank (Mantel-Cox) test. (A) Administration of 0.1 μM MitoQ or dTPP did not increase the survival of the transgenic animals. (B) Treatment with 1 μM MitoQ significantly increased the survival ($p<0.01$) of nematodes while administration of 1 μM dTPP did not increase the nematodes' survival.

4.4.2. MitoQ decreases the mortality associated with Aβ-induced toxicity in transgenic *C. elegans*

Combined data from three experiments showed that 1 μM MitoQ prolonged mean lifespan of the transgenic nematodes on average by about 14 % (Figure 4.9A and B) compared to untreated-control animals and this effect was statistically significant ($p<0.0001$). The maximum lifespan was also significantly extended in the MitoQ-treated nematodes compared to both dTPP-treated and untreated control animals (Figure 4.9A and C, $p<0.0001$). In fact, the MitoQ-treated animals had a 9 % increase in the maximum lifespan. The observation that MitoQ but not dTPP, extended the lifespan of the Aβ-expressing transgenic nematodes supports the notion that the lifespan extension effect in MitoQ treated animals was dependent on the antioxidant ubiquinone moiety, supporting an antioxidant mode of action.

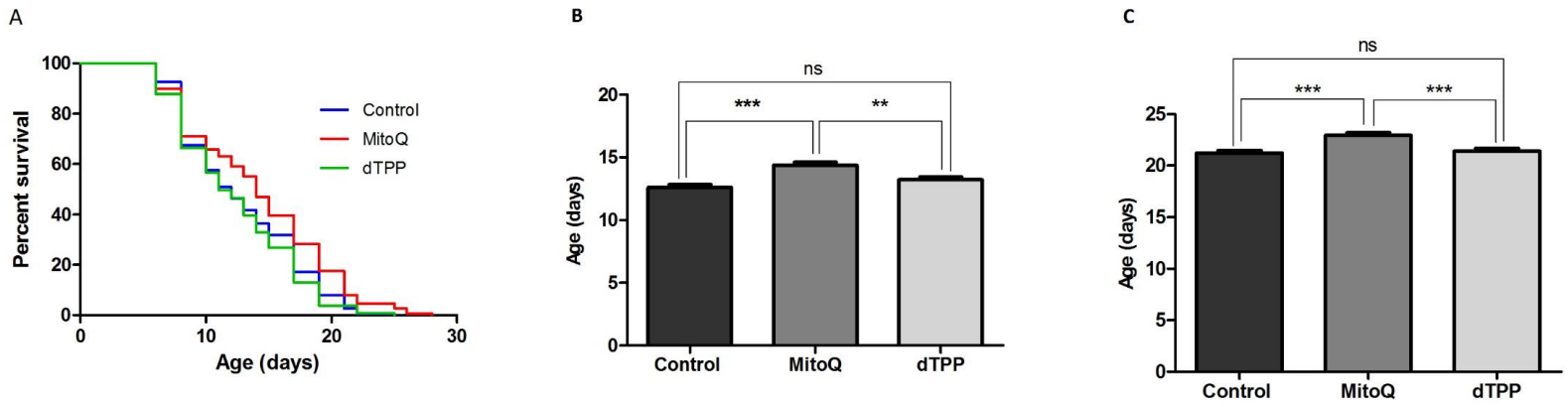

Figure 4.9. Lifespan study C, 3rd lifespan study of Aβ- expressing transgenic animals treated with 1 µM MitoQ, dTPP or vehicle (n=200 worms per condition). (A) Administration of 1 µM MitoQ extended the nematodes' survival, log-rank test showed a significant difference between MitoQ and untreated control ($p<0.01$). (B) Combined data of mean lifespan from three independent experiments, analyzed using Bonferroni's post-test, mean ±SEM. MitoQ significantly prolonged the mean lifespan of transgenic nematodes by about 14 % relative to untreated control animals ($p<0.0001$); while dTPP did not extend the mean lifespan of the transgenic animals. (C) Maximum lifespan average from three independent experiments, analyzed using Bonferroni's post-test, mean ±SEM. A significant maximum lifespan prolonging of 9 % was observed in animals administered with MitoQ ($p<0.0001$) relative to untreated control animals, while dTPP did not extend the maximum lifespan of transgenic animals.

4.4.3. MitoQ delays Aβ-induced paralysis in transgenic *C. elegans*

Pharmacological interventions for promoting healthspan have recently gained much interest due to the fact that lifespan modulation alone is of limited interest and is not a reliable indicator of overall health status. Healthspan is an index of physiological capacity which is the period of time that the animals are able to maintain good health [289]. In addition to survival study, I conducted a blinded healthspan study measuring motility as an indicator of health.

In the healthspan study of the Aβ-overexpressing transgenic animals, only two classes of locomotion were scored: non-paralyzed and paralyzed. This is because this strain of animals also carries the *rol-6* gene which causes the animals to rotate around their longitudinal axis, having uncoordinated movement instead of the coordinated sinusoidal movement. Non-paralyzed animals were healthy, highly mobile, showed constant movement and rotated around their longitudinal axis, whereas paralyzed animals only moved their head or tail in response to prodding.

As expected, health status of the nematodes in all groups declined as they aged. Figure 4.10A shows the healthspan curve from a single experiment of nematodes treated with 1 µM MitoQ or dTPP alongside with untreated control. Administration of MitoQ significantly delayed the onset of paralysis ($p<0.0001$, Figure 4.10A) and the animals remained healthy for a longer period of time. On Day 6, 82 % of untreated-control animals were non-paralysed, while, 95 % of MitoQ-treated and 93 % of dTPP-treated animals were non-paralysed. At day 10, 77 %, 70 % and 50 % of MitoQ-treated, dTPP-treated and untreated-animals, respectively, remained healthy (non-paralysed). The significant healthspan advantage even in dTPP-treated animals illustrates that dTPP also delayed paralysis in the animals, although to a lesser degree than MitoQ. The mechanism of this protection remained unclear at this point (see section 4.4.9. for explanation).

Overall, MitoQ treated animals were healthier ($p<0.0001$, Figure 4.10B). Combined data from three independent experiments showed that MitoQ extended the mean healthspan of the

transgenic animals to 15 days or by about 13 % relative to untreated control animals ($p<0.0001$, Figure 4.10B). Comparing the mean healthspan of MitoQ and dTPP-treated animals, MitoQ significantly extended the mean healthspan by about 8 % (Figure 4.10B).

Even at the later stages, when only 10 % of animals remained non-paralyzed (maximum healthspan), MitoQ again improved health, increasing the maximum healthspan relative to untreated control animals (Figure 4.10C). This difference was statistically significant ($p<0.0001$, Figure 4.10C). Overall, 10 % of animals treated with MitoQ remained healthy until day 23 which equates to an extension of maximum healthspan by about 7% relative to untreated control animals ($P<0.0001$). Relative to dTPP-treated animals, administration of MitoQ also significantly extended the animals' maximum healthspan ($p<0.0001$, Figure 4.10C). In addition, comparing to untreated control animals, administration of dTPP improved neither the mean nor the maximum healthspan of the transgenic nematodes (Figure 4.10B and C).

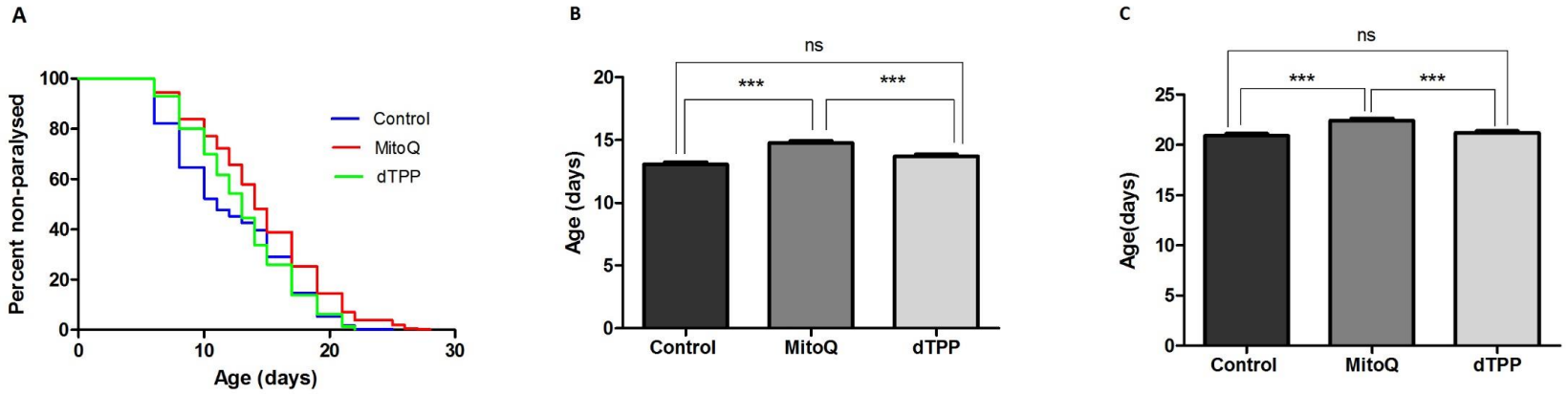

Figure 4.10. Healthspan of the surviving Aβ-expressing transgenic animals treated with MitoQ, dTPP or vehicle (n=200 worms per conditions). (A) Healthspan curve from a single experiment, representative of n=3 independent experiments. Administration of MitoQ significantly improved the healthspan by delaying the onset of paralysis in the transgenic nematodes ($p<0.0001$, Log-rank (Mantel-Cox) test).

Combined data average from 3 independent experiments of mean and maximum healthspan, analyzed using ANOVA with Bonferroni's post-test,mean ±SEM. (B) MitoQ treatment significantly extended the mean healthspan of the transgenic animals, delayed the onset of paralysis by about 13 % compared to untreated control animals ($p<0.0001$). (C) Compared to untreated transgenic animals, administration of MitoQ significantly extended the maximum healthspan of the transgenic animals by about 7 % ($p<0.0001$) while dTPP had no significant maximum healthspan extending effect.

4.4.4. MtDNA damage in pharmacologically treated animals: MitoQ treatment does not affect the mtDNA damage burden

I found that Aβ expression reduces the lifespan of the nematodes and administration of MitoQ extends lifespan and improves healthspan of the transgenic animals. To test the hypothesis that mtDNA damage was involved in the lifespan and healthspan effect, I first examined the mtDNA damage in wild type N2 and Aβ-expressing transgenic animals.

Surprisingly, using my S-XL-qRT-PCR DNA damage assay, I observed that there was no significant difference in the mtDNA damage in untreated Aβ-expressing transgenic animals relative to untreated wild type N2 animals (to avoid confusion, untreated, MitoQ-and dTPP-treated wild type N2 animals will be labelled as WT-control, WT-MitoQ and WT-dTPP, respectively) (Figure 4.11, p=0.07, Student's t-test). This result is unexpected given that Aβ expressions shorten the lifespan of the nematodes and also studies have shown elevation of oxidative damage to mtDNA in AD patients [155, 333, 334] and that MitoQ is an agent that is specifically designed to deliver its antioxidant moiety to mitochondria. I then determined the efficacy of MitoQ to modulate oxidative DNA damage burden in mitochondria in the Aβ-expressing transgenic *C. elegans.* Using the S-XL-qRT-PCR DNA damage assay, I found that, while there appeared to be a slight trend toward lower mtDNA damage in MitoQ treated Aβ-expressing transgenic animals relative to untreated control Aβ-expressing animals (Figure 4.11), there was no statistically significant effect. Animals treated with dTPP also exhibited a non-significant trend to lower mtDNA damage relative to untreated Aβ-expressing control animals (Figure 4.11).

This lack of effect was unexpected as MitoQ is one of the best-characterised mitochondria-targeted antioxidants [272]. However, in this strain, it did not attenuate mtDNA damage burden in Aβ-expressing transgenic animals. This could be due to the extremely low mtDNA damage already in these animals, which is typically 0.4 lesions per 10 kbp according to my assay, or on the order of one lesion (or less) per mtDNA molecule. It is possible that the mtDNA damage level was too low for MitoQ to significantly suppress the damage level further. While the effect

of MitoQ on mtDNA damage might have been below the sensitivity of the assay, it is worth noting that damage levels are so low as to raise the question if any further decline in DNA damage would be functionally or physiologically relevant. Clearly, however, neither lifespan shortening nor extension depended on mtDNA damage in this strain.

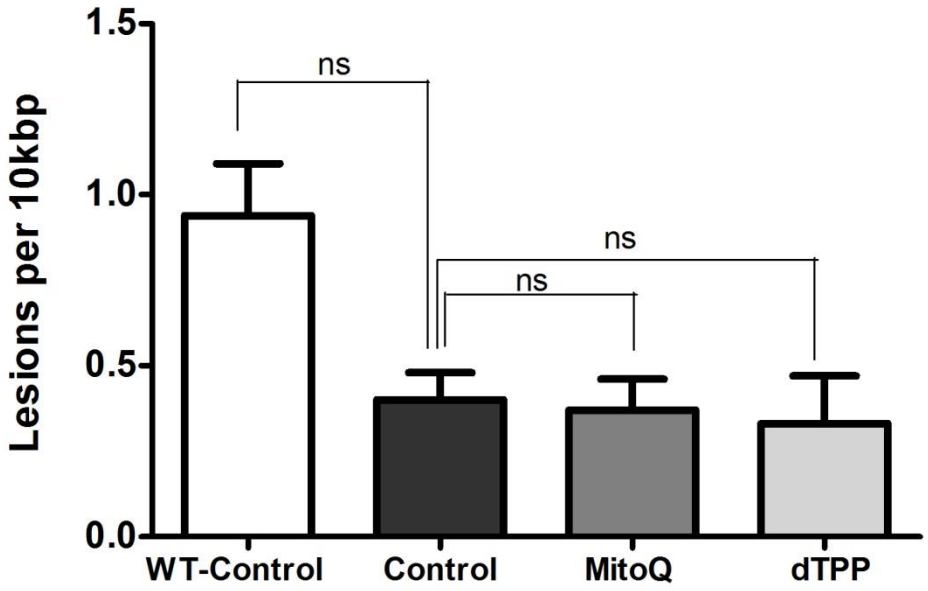

Figure 4.11. mtDNA damage in wild type N2, untreated Aβ-expressing control animals, MitoQ and dTPP-treated Aβ-expressing animals. mtDNA damage quantified using S-XL-qRT-PCR DNA damage assay shows that there is no significant difference in the mtDNA damage in untreated wild type N2 animals relative to untreated control Aβ-expressing control animals (p=0.07, Student's t-test). mtDNA damage in untreated control Aβ-expressing animals was 0.4 lesions per 10 kbp. Administration of MitoQ did not significantly lower the mtDNA damage burden in the nematodes, the DNA lesion frequencies were 0.37 and 0.33 for every 10,000 bp in MitoQ and dTPP treated animals, respectively. Although administration of MitoQ or dTPP appeared to show a trend to slightly lower the mtDNA damage in the nematodes, this difference is not statistically significant (p=0.9, ANOVA, mean±SEM), n = minimum 3 independent experiments.

4.4.5. MitoQ does not affect global oxidative stress

In order to test whether MitoQ was able to modulate other biomarkers of oxidative stress and damage, I employed two different additional biomarkers, ROS production and protein carbonyl content.

I employed the dichlorofluorescein diacetate (DCFDA) method in whole *C. elegans* to explore the efficacy of MitoQ in modulating global ROS level. In cells, DCFDA is cleaved by endogenous esterases into dichlorofluorescin (DCFH) which then reacts with ROS to form the fluorescent dichlorofluorescein [8]. Our laboratory has found that, using this whole nematode DCFDA assay in intact animals, we are able to show a reproducible, mild, age-dependent increase in DCFDA signal in ageing cohorts [62]. Lysing worms or cells, in contrast, will cause the release of transition ions such as iron and these may participate in redox cycling thereby generating more ROS and leading to overestimation of ROS levels. When cells are not disrupted, iron remains sequestered avoiding this particular set of artifacts [240, 335, 336]. However, elevation of DCFDA level, intermediate DCF radical formation and cytochrome *c*, all can cause artefactual DCFDA fluorescence signal [8, 336]. Therefore, DCFDA is an indirect measure of global ROS production rather than a specific measure of ROS generation and should be approached with caution.

Administration of MitoQ resulted in lower apparent ROS level relative to the untreated control animals; however, this was not statistically significant (Figure 4.12). In fact, the ROS level in the dTPP-treated animals was similar to the MitoQ-treated animals (Figure 4.12). Despite several well-known limitations of this assay [240, 335], these data may be taken together to indicate that MitoQ had no significant effect on the global ROS flux relative to untreated control animals.

The presence of oxidized protein can modify key enzymes and structural proteins and has been suggested to be part of the neurodegenerative process in AD [337]. To compare my null result in term of mtDNA to a more general marker of ROS-mediated damage, I utilize the protein

carbonyl content assay, which is a well-established marker of protein oxidation. Consistent with my mtDNA results and the DCFDA results, there was no significant differences in the levels of protein carbonyls in MitoQ, dTPP-treated and untreated control animals (Figure 4.13A and B). This shows that neither MitoQ nor dTPP appeared to be able to modulate global oxidative damage. Despite being a well-characterized mitochondria-targeted antioxidant, MitoQ therefore failed to modify oxidative stress as determined by global mtDNA damage, ROS flux or whole animal protein damage.

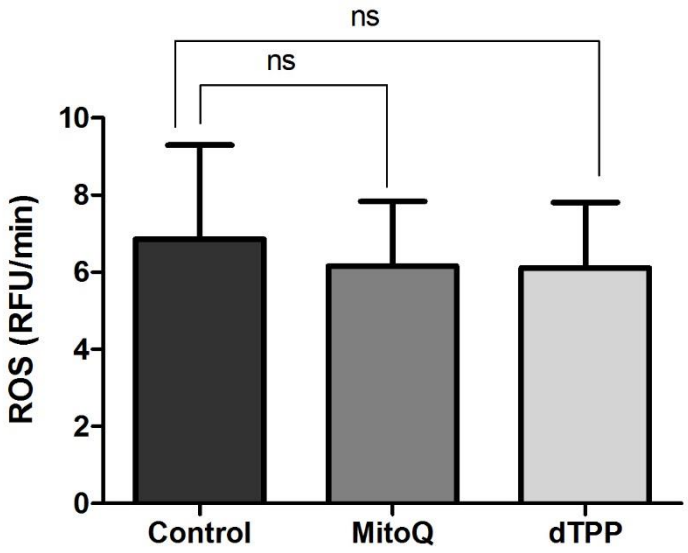

Figure 4.12. Generalized ROS production rate measured using whole-worm DCFDA assay in intact animals administered with MitoQ, dTPP and untreated control animals. MitoQ and dTPP treatment had no significant effect on the global ROS flux compared to untreated control animals ($p>0.5$, ANOVA, mean ±SEM.), n=3 independent experiments.

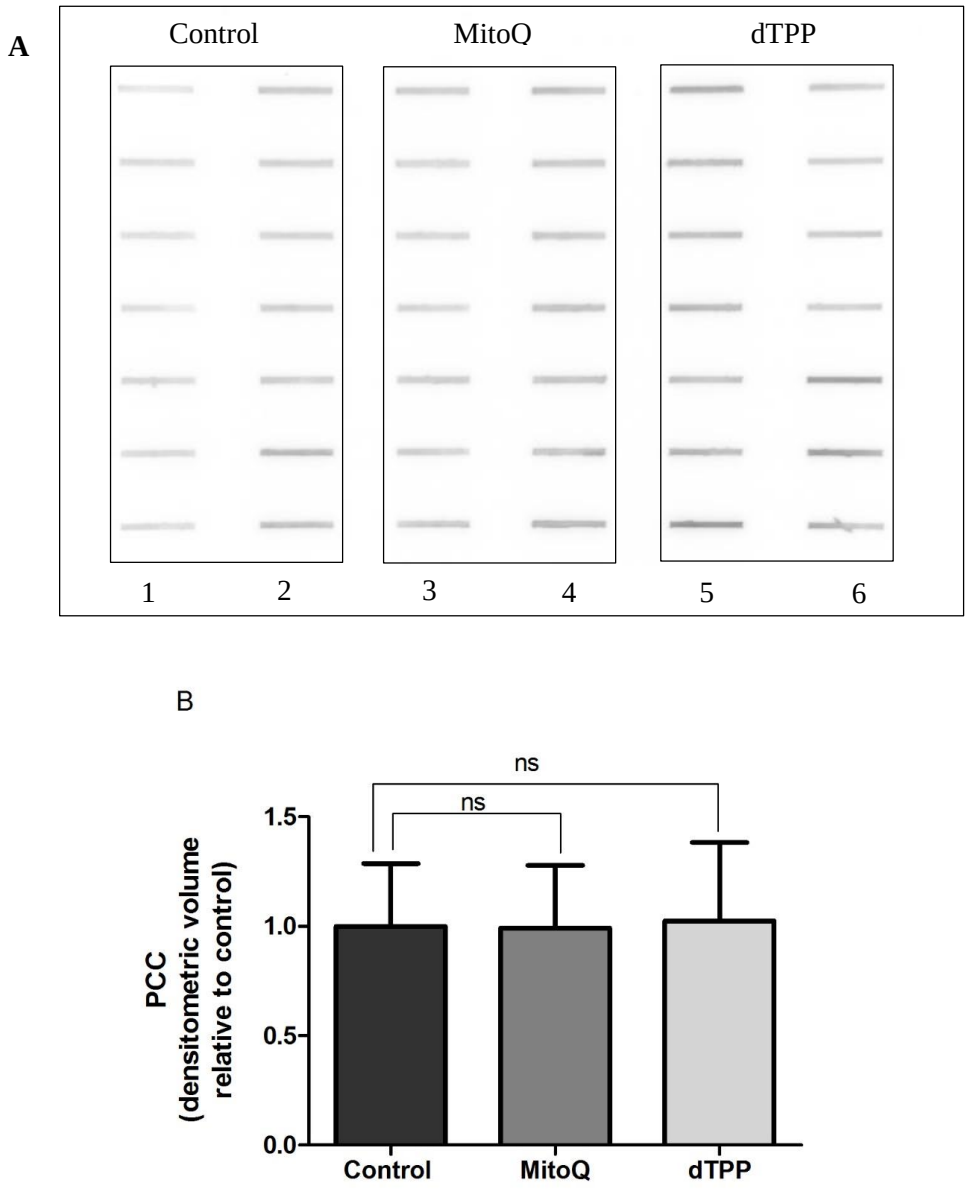

Figure 4.13. Protein carbonyl content in Aβ-expressing transgenic animals treated with MitoQ, dTPP or vehicle. (A) A representative oxyblot image of protein carbonyl content from a single experiment. Lanes 1 and 2 show protein carbonyl content of untreated control transgenic animals. Lanes 3 and 4 show protein carbonyl content of transgenic animals treated with MitoQ while lanes 5 and 6 show protein carbonyl content of transgenic animals treated with dTPP. (B) Relative protein carbonyl content normalised to worm protein from 5 independent experiments, measured by a densitometric analysis of the slot blot intensity. The protein carbonyl contents of the MitoQ and dTPP-treated animals were similar to the untreated control animals ($p>0.5$, ANOVA, mean ±SEM.), n=20 independent replicates.

4.4.6. MitoQ does not alter ATP levels and oxygen consumption rates

The lifespan and healthspan studies showed a clear ability of MitoQ to extend the lifespan and healthspan of the transgenic animals. This was surprising given that neither global oxidative damage nor mtDNA damage differs significantly between untreated control animals and MitoQ or dTPP-treated animals.

In order to explore this discrepancy further and to test the efficacy of MitoQ, in altering the global energy metabolic parameter, I next measured oxygen consumption rate and steady-state ATP content of Aβ-expressing transgenic animals. MitoQ administration did not alter the ATP content of the Aβ-expressing transgenic animals relative to untreated control animals (Figure 4.14). I found that dTPP-treated animals had a trend toward lower ATP content (about 19 % less ATP content than untreated control animals) but the difference was not statistically significant (Figure 4.14).

Aβ has been found to cause mitochondrial dysfunction as determined by impaired oxygen consumption. The determination of oxygen uptake rate is also a measure of mitochondrial function. Compared to untreated control animals, there were no significant changes in the oxygen uptake of MitoQ- and dTPP-treated animals (Figure 4.15). In fact, the oxygen uptake rates of untreated control, MitoQ- and dTPP-treated animals were similar. The untreated control animals consumed 0.36 µmol of oxygen per hour per mg of worm protein whereas oxygen uptake rate for both MitoQ- and dTPP-treated animals were 0.37 µmol per hour per mg of worm protein (Figure 4.15).

Overall, MitoQ treatment did not alter the steady-state ATP content and oxygen consumption rate of the three treatment groups, suggesting that MitoQ was not able to modulate the mitochondrial metabolism thus not able to increase mitochondrial energy supply.

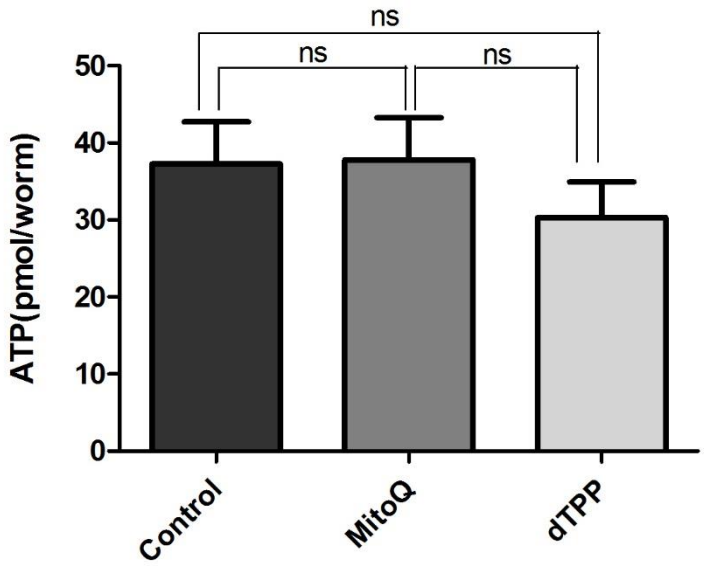

Figure 4.14. MitoQ treatment did not alter steady-state ATP level. There were no significant difference in the steady state ATP levels of Day 6 untreated-control, MitoQ- and dTPP-treated animals ($p>0.5$, ANOVA, mean ±S.E.M.), n=9 independent replicates.

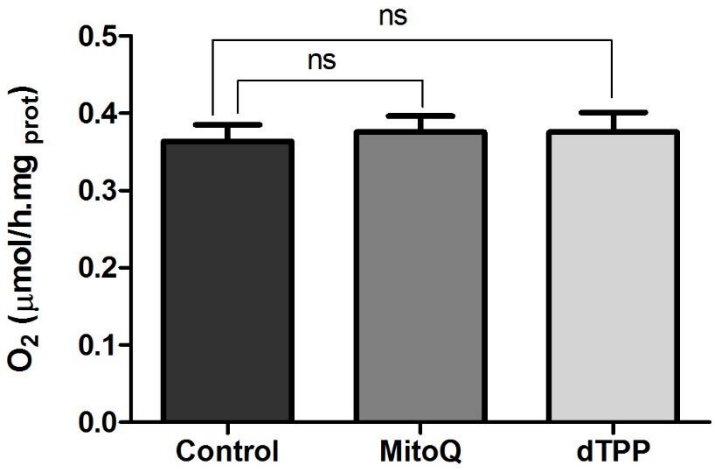

Figure 4.15. Administration of MitoQ did not modulate the oxygen uptake of the Aβ-expressing transgenic animals. Average oxygen consumption normalized to worm protein. Neither MitoQ nor dTPP had any significant effect on the oxygen consumption rate of the transgenic animals compared to untreated-control, ($p>0.5$, ANOVA, mean ±SEM.), n=9

4.4.7. MitoQ protects complex IV of ETC

My experiments up to this point, demonstrated that MitoQ did not modulate mtDNA damage burden, global oxidative stress nor alter global energy metabolism. This is surprising as MitoQ is an antioxidant that was designed to accumulate within mitochondria in order to protect mitochondrial membrane against oxidative damage. However, it did not show any positive effects in protecting mitochondria. I then investigated the efficacy of MitoQ to protect mitochondria and mitochondrial function more locally in the mitochondrial membrane by examining the function of the ETC protein complexes, complex IV and complex I.

Complex IV is a large and terminal trans-membrane protein complex of the ETC. Complex IV receives electrons from cytochrome *c* and transfers the electrons to oxygen, converting oxygen to water [113]. Numerous studies have reported that complex IV activity is reduced in AD tissues [236, 338-340]. Therefore, we used a sensitive polarographic complex IV activity assay that measured complex IV activity in mitochondrial extracts. Complex IV activity was significantly higher in MitoQ-treated animals only ($p<0.01$, Figure 4.16) relative to untreated control animals and dTPP-treated animals. Compared to untreated control animals, there was a 60 % increase in the complex IV activity in the MitoQ-treated animals (Figure 4.16). In contrast, no significant changes of the complex IV activity were detected in dTPP-treated animals relative to untreated control animals (Figure 4.16).

In order to test for any direct artefactual effect of MitoQ on complex IV activity, a spiking assay was conducted using several concentrations of MitoQ. Figure 4.17 shows that spiking with different MitoQ concentrations did not change the complex IV activity detected. This confirms that MitoQ did not directly interfere with the complex IV activity measurement. Therefore, the elevation in complex IV activity detected in MitoQ-treated animals was most likely due to a protective effect of MitoQ on the complex IV of ETC in the mitochondria.

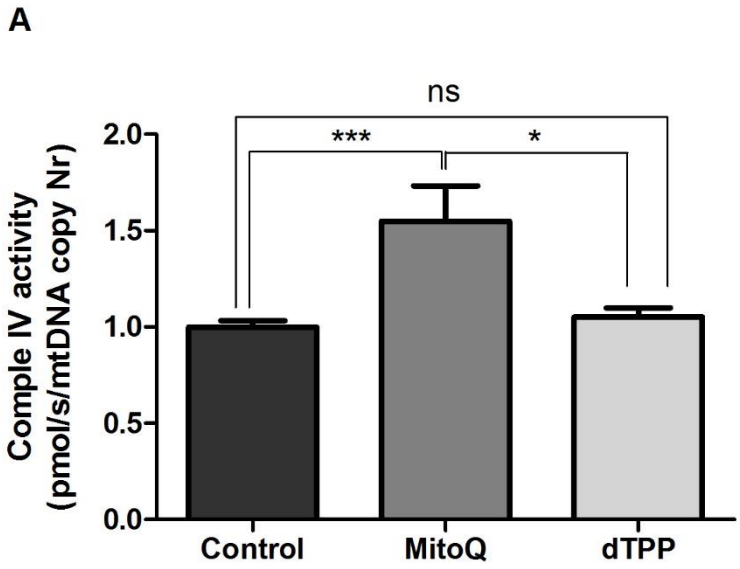

Figure 4.16. Effect of MitoQ and dTPP on complex IV activity. A polarographic complex IV activity assay was conducted and normalised to the mtDNA copy number of the respective mitochondria extract. Administration of MitoQ significantly elevated the complex IV activity in Aβ-expressing transgenic animals ($p<0.01$, ANOVA with Bonferroni's post-test, mean±SEM.) but there were no significant changes of complex IV activity in dTPP-treated animals compared to untreated-control, n=9 independent replicates.

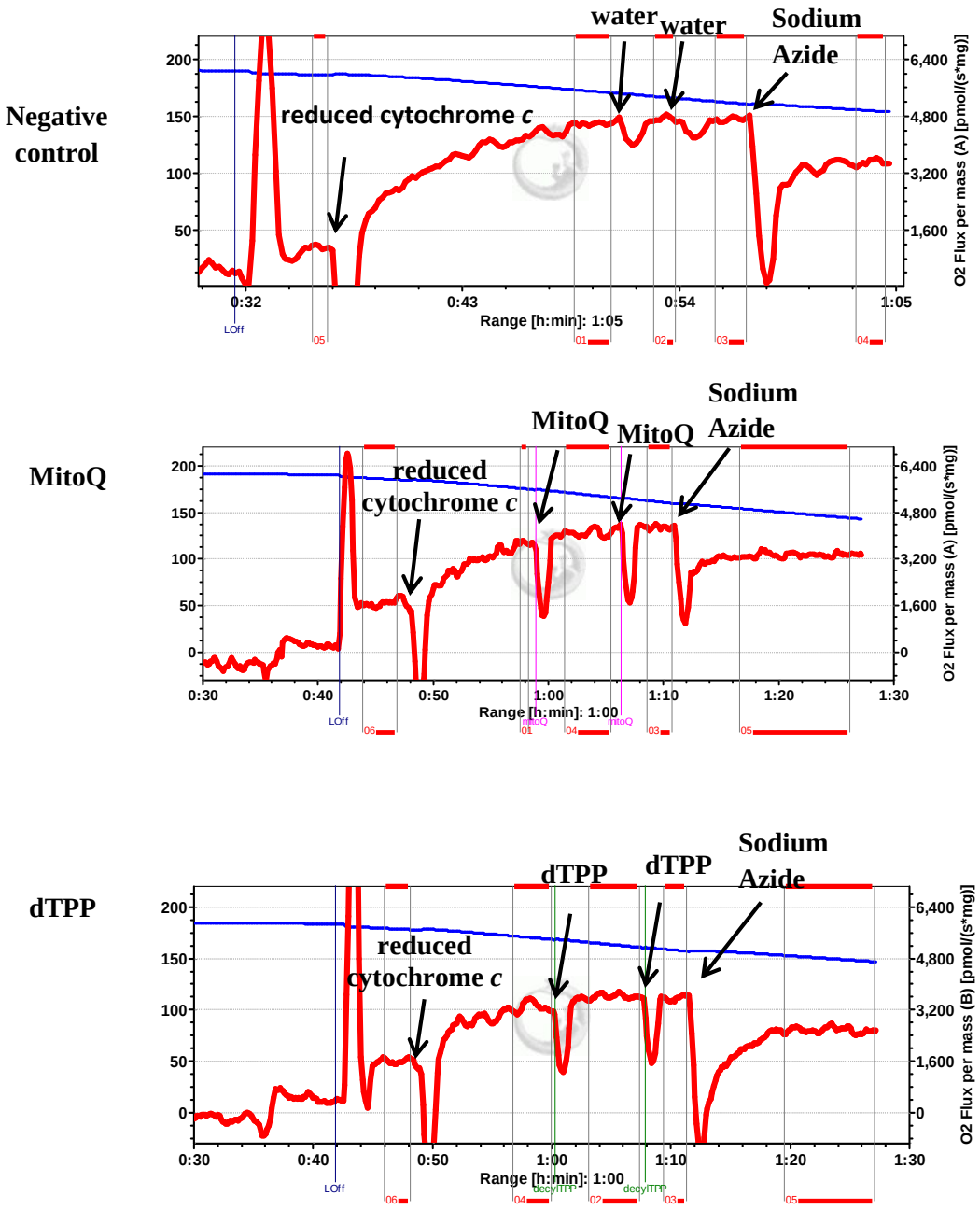

Figure 4.17. Spiking assay: sample of traces of the Oxygraph-2K using water, MitoQ or dTPP. The blue line indicates the oxygen concentration in the sample. The red line indicates its derivative (control (water only), MitoQ or dTPP), the oxygen consumed by the sample. Spiking assay using different MitoQ or dTPP concentrations showed that neither MitoQ nor dTPP had any direct effect on the complex IV activity measurement.

4.4.8. MitoQ also protects complex I of ETC

We further explored the efficacy of MitoQ in modulating another ETC key enzyme complex, complex I. This is because complex I is the first enzyme in the mitochondrial ETC that catalyzes the transfer of electrons from NADH to coenzyme Q10 and is the primary site of superoxide generation in the ETC, releasing superoxide to the mitochondrial matrix [8, 74, 119].

Administration of MitoQ as well as dTPP significantly increased complex I activity in Aβ-expressing transgenic animals relative to the untreated control animals ($p<0.01$, Figure 4.18). There were 42 and 54 % increases in the complex I activity in MitoQ- and dTPP-treated animals respectively ($P<0.05$ and $p<0.01$ respectively, Figure 4.18). In fact, dTPP-treated animals had a trend towards higher (about 9 %) complex I activity compared to MitoQ-treated animals and this is not statistically significant. This implies that the increase in complex I activity in MitoQ- and dTPP-treated animals could be due to a mild uncoupling effect of the dTPP moiety, not due to the antioxidant ubiquinone moiety.

A spiking assay with different MitoQ or dTPP concentrations was also conducted and this verified that neither treatment of MitoQ nor dTPP interfered directly with complex I activity measurement (Figure 4.19).

In summary, only MitoQ but not dTPP was able to elevate the complex IV activity in Aβ-expressing transgenic animals, whereas, both MitoQ and dTPP significantly increased complex I activity in this strain. This suggests that MitoQ treatment either protected ETC enzymes complexes positioned in the mitochondrial membrane or promoted their activity.

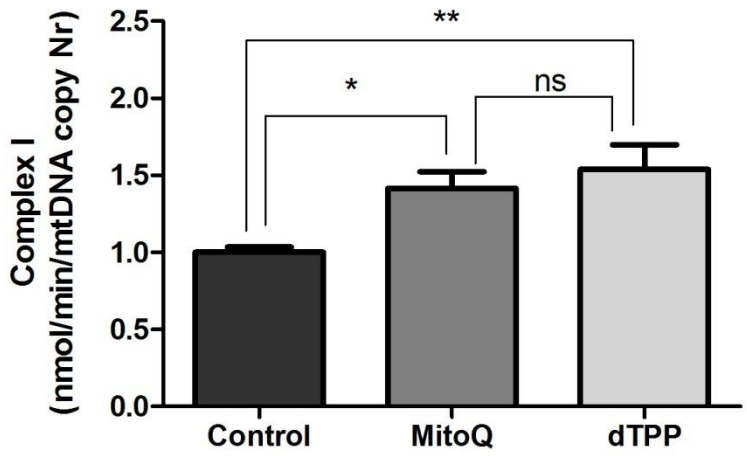

Figure 4.18. Effect of MitoQ and dTPP on complex I activity. Rotenone sensitive complex I activity was measured based on decrease in fluorescence of NADH and normalized to mtDNA copy number of the respective mitochondrial extract. Administration of MitoQ and dTPP significantly elevated ($p<0.01$, ANOVA with Bonferroni's post-test, mean ±SEM) the complex I activity of the Aβ-expressing transgenic animals relative to untreated control animals. n=9 independent replicates.

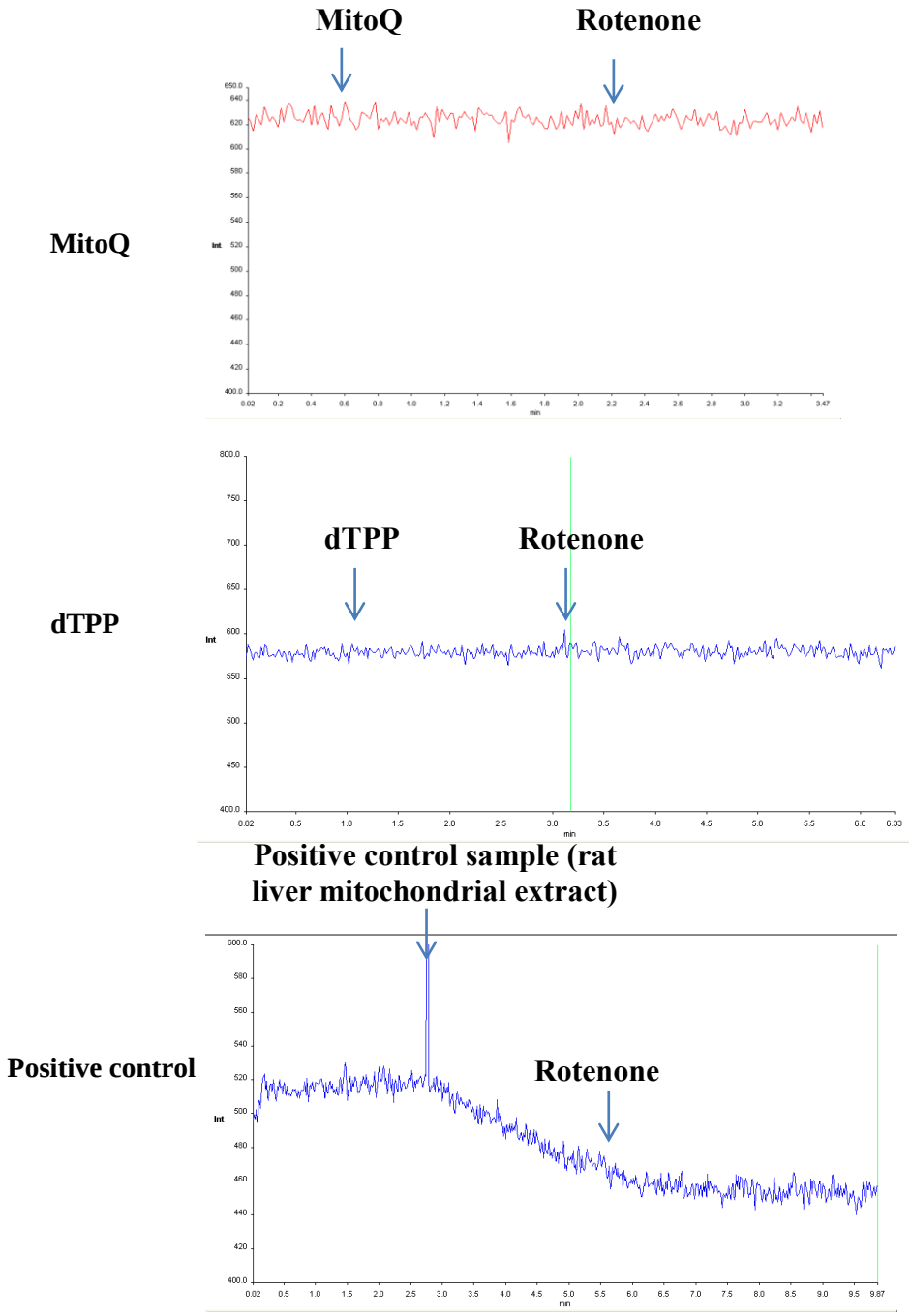

Figure 4.19. Representative traces of fluorescence of NADH at ex/em wavelength 352/464 nm (for MitoQ, dTPP and positive control). Addition of MitoQ or dTPP did not interfere with the readout of complex I activity's assay even after the addition of the complex I inhibitor, Rotenone.

4.4.9. MitoQ increases cardiolipin content of mitochondrial membranes

Changes in enzyme activity of the mitochondrial ETC can be secondary to changes in mitochondrial lipid, particularly to decreases in cardiolipin content in the mitochondria [339]. Cardiolipin is an inner mitochondrial membrane phospholipid [137, 138]. It is one of the lipid components of the ETC that interacts with ETC proteins to regulate a wide range of mitochondrial functions [341]. Cardiolipin is highly vulnerable to peroxidation due to its high polyunsaturated fatty acid content and its location near ROS production sites [137]. Therefore, loss of cardiolipin may be one of the factors that contribute to mitochondrial dysfunction in ageing and neurodegenerative diseases. To investigate MitoQ's potential as a targeted antioxidant and its possible protective effect on mitochondrial lipids (MitoQ was specifically design to prevent lipid peroxidation), we employed a lipidomics method [62] to characterise mitochondrial cardiolipin species and determine the level of each cardiolipin species in untreated-control, MitoQ- and dTPP-treated animals.

In general, MitoQ- and dTPP-treated animals showed a trend towards higher global cardiolipin levels relative to untreated control animals but this trend was not statistically significant (Figure 4.20). We further employed a more detailed lipidomic analysis of individual cardiolipin species to evaluate the effect of MitoQ treatment on changes in mitochondrial lipids. We found that MitoQ treatment tended to increase the amount of cardiolipin in most cardiolipin species that we examined, particularly CL78, CL79 and CL80 (Figure 4.21). Interestingly, within the cardiolipin species, the highly unsaturated forms of cardiolipin (20:4) were significantly increased in MitoQ-treated animals (Figure 4.21), compared to relatively less unsaturated forms of cardiolipin (20:3). Among these unsaturated cardiolipin species, we consistently detected a significant, at least 16 % elevation (CL80:16, CL79:14, CL78:15 ($p<0.05$, $p<0.01$, $p<0.01$ respectively). As highly unsaturated cardiolipin is more vulnerable to oxidative damage due to its polyunsaturated fatty acids structures [339], these data are consistent with the notion that MitoQ administration may protect the mitochondrial membrane, specifically highly unsaturated cardiolipin species from oxidative damage. Moreover, the increase in cardiolipin content is

consistent with the higher ETC activity that we observed in complex IV and I in MitoQ treated animals, suggesting that MitoQ may protect mitochondrial lipids and associated lipid bound ETC complexes.

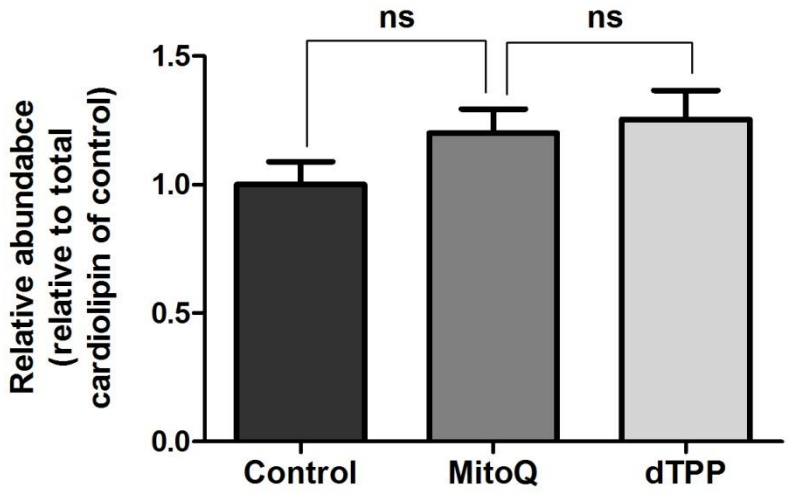

Figure 4.20. Effect of MitoQ administration on the content of the mitochondrial specific lipid cardiolipin. (A) MitoQ and dTPP treatment increased total cardiolipin content of mitochondrial membranes in the Aβ-expressing transgenic animals, but the difference was not statistically significant ($p>0.05$, ANOVA, mean ±S.E.M.), n=7 independent replicates.

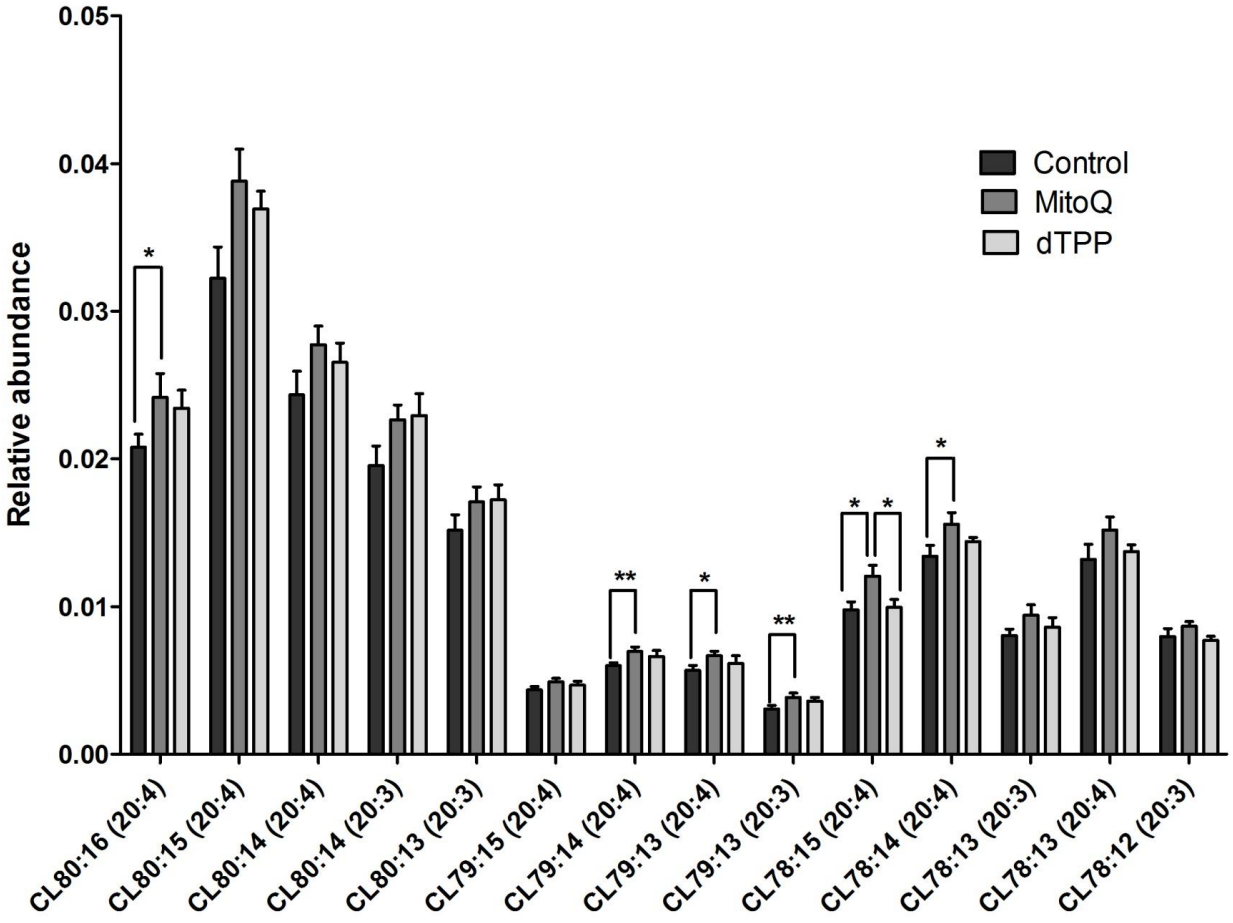

Figure 4.21.A more detailed lipidomics method was used to characterize different cardiolipin species in the nematodes. Higher level of unsaturated cardiolipin (20:4) species were detected in MitoQ-treated animals relative to untreated-control nematodes (comparison: control vs. MitoQ, *.p<0.05, **.p<0.01, ANOVA with Tukey's post-test, mean±SEM.), n=7 independent replicates.

4.4.10. MitoQ does not modulate lifespan and healthspan of wild type N2 nematodes

My experiments up to this point show that MitoQ did not attenuate mtDNA oxidative damage nor reduce DCFDA fluorescence or protein carbonyl levels or modulate steady state ATP levels or oxygen consumption rate. However, I resolved that the protective effect on lifespan and healthspan might be due to the mode of action of MitoQ to ameliorate depletion of the mitochondrial lipid cardiolipin and protection of complex IV and I of the ETC, in particularly the protection to complex IV that is pathologically reduced in AD. MitoQ is predominantly localized to mitochondrial membrane thus protecting the ETC complexes and mitochondrial lipid. I therefore conducted a lifespan experiment in wild type N2 animals, expecting that MitoQ would not have any effect on the lifespan or healthspan of the wild type animals.

Consistent with my hypothesis, no lifespan prolonging effect was seen in wild type N2 animals treated with MitoQ or dTPP compared to untreated control wild type N2 animals (Figure 4.22). Similar to the lifespan study, administration of MitoQ did not improve the healthspan of the wild type N2 animals (Figure 4.23). There are no differences in the motility of the MitoQ, dTPP-treated as well as untreated control animals (Figure 4.23). Hence, MitoQ may be an antioxidant that is only beneficial under stressed or diseased conditions.

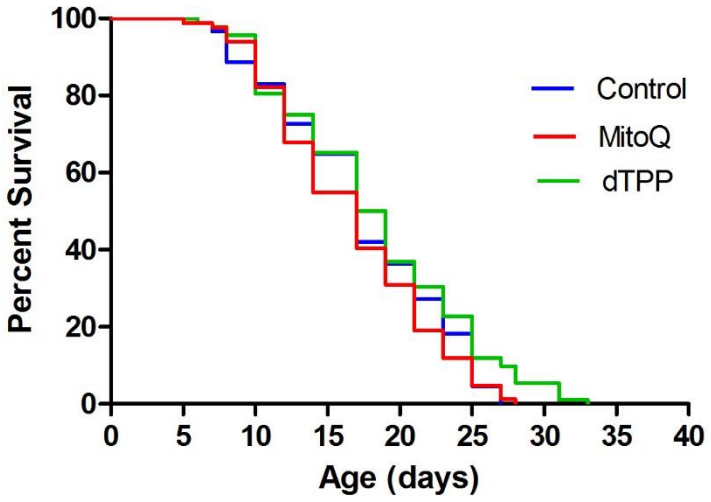

Figure 4.23. Survival curve of wild type N2 *C. elegans* in the presence of 1 µM MitoQ, dTPP or vehicle (n=200 worms per condition). Neither MitoQ nor dTPP treated animals significantly extended the lifespan of the wild type N2 animals

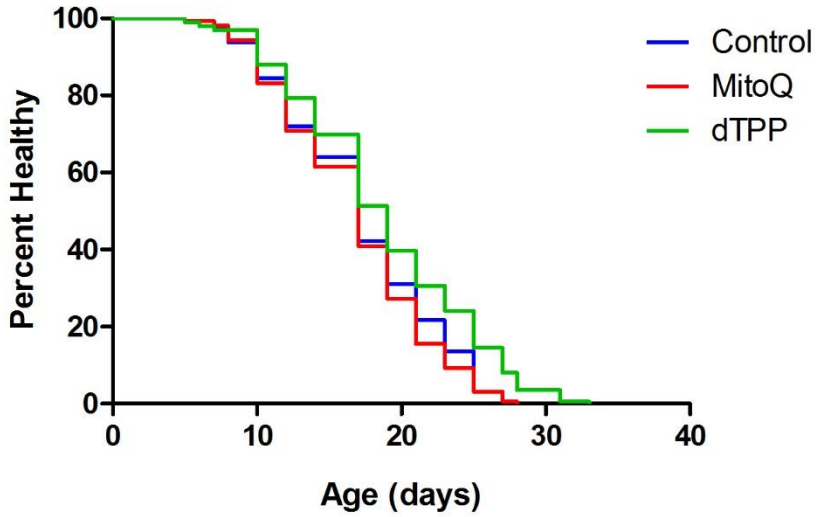

Figure 4.22. Healthspan curve of wild type N2 *C. elegans* administered with MitoQ, dTPP or untreated control wild type animals (n=200 worms per condition). Neither administration of MitoQ nor dTPP had any effect on the health progression of the wild type N2 animals.

5. Discussion

5.1. Consequences of ROS perturbation in *C. elegans*

Damage due to mitochondrial ROS has been suggested to be a main cause of ageing. However, even if this is true, mitochondrial ROS production alone is not sufficient to explain longevity as living systems are protected by antioxidant defense systems. These systems are responsible to safeguard cells from ROS-mediated oxidative damage and steady state damage levels, therefore, are complex functions of ROS production, ROS detoxification and damage repair. These antioxidant systems provide a popular avenue for testing the mFRTA. This is because, if the mFRTA is correct, impaired expression of, for instance, mitochondrial SOD enzymes might be expected to increase oxidative damage and shorten lifespan. I found that mtDNA damage as evaluated by my S-XL-qRT-PCR DNA damage assay was indeed significantly elevated in MnSOD mutant nematodes. However, in contrast to expectation from the FRTA, the lifespan of these nematodes, although devoid of all mitochondrial MnSOD and suffering from elevated oxidative damage, was not shortened [88, 213]. Surprisingly, we further found that impairment of mitochondrial SOD detoxification capacity does not appear to elevate total ROS, at least as measured by DCFDA fluorescence dye, but instead dramatically decreases the generalized ROS production [62]. This surprising result can likely be explained as part of a broad set of compensation strategies found in *C. elegans* that sacrifice mitochondrial energy for reduced ROS production, especially during situations where ROS detoxification is impaired. In the case of the SOD mutants, the reduction of ROS production was probably due to repression of flux through the ETC by direct mitochondrial ETC inhibition [62]. In support of this hypothesis, deletion of mitochondrial MnSOD resulting in phenotypes with reduced energy production, such as reduction in the number of progeny that survive and smaller size [88, 213].

This example illustrates two important insights that I encountered several times during my work on this project. First, the phenotypes of the SOD mutant strains reveal features of a complex regulatory system where unexpected effects and even counter-intuitive effects in response to perturbation are typical features. Such complexity can be observed relatively common in the

free radical feedback systems that control lifespan. Secondly, given this degree of complexity, the SOD mutants are another example for the need for carefully validated biomarkers of damage, ROS production and metabolism. Given that on ROS homodynamic systems are complex, it is difficult or impossible to guess what the consequences of a given perturbation might be in terms of damage, unless damage is actually measured and measured well.

5.1.1. Complexity in antioxidant perturbations in *C. elegans*

I already discussed the unexpected results in terms of ROS production and metabolism when mitochondrial SODs are knocked out. Unexpected consequences also occur not only with knockout nematodes but also with overexpression of the same mitochondrial SODs, in *C. elegans*. As expected by FRTA, overexpression of mitochondrial *sod-2* does increase the lifespan (by about 25 %) without however, reducing oxidative damage accumulation, at least in *C. elegans* as assessed by protein carbonyl accumulation [342]. Similar complexity also became apparent when we repressed another antioxidant enzymes , mitochondrial *prdx-3* [342]. In nematodes, this intervention, again, neither shortens nematodes' lifespan nor elevates oxidative damage to proteins. Instead, loss of *prdx-3*, similar to the case of SOD knock out, reduces total energy availability, manifesting in reducing motility and brood size. However, in this case, we showed that the compensatory mechanism involves mitochondrial uncoupling instead of mitochondrial ETC inhibition [343].

5.1.2. Complexity in mutation that alters mitochondrial function in *C.elegans*

I have also found similar complexity in regulatory mechanism in nematodes harbouring a mutation of the ETC, *mev-1*. M*ev-1* encodes a subunit of the enzyme succinate dehydrogenase cytochrome *b*, which is part of the mitochondrial ETC complex II. Nematodes with *mev-1* mutation, lack functional complex II and produce excess ROS [324, 328]. These *mev-1* mutants are known to suffer from high oxidative stress and short lifespan [324, 328]. Instead *mev-1* mutants have specifically been reported to suffer from high accumulation of protein damage at old age [326]. I investigated mtDNA damage in this strain, expecting it to be high as well. Surprisingly, I instead found low mtDNA damage (in the level of less than one lesion per

mitochondrial molecule) as measured using my S-XL-qRT-PCR DNA damage assay. In fact, mtDNA damage in this *mev-1* mutant is even lower than mtDNA damage in wild type N2 animals as discussed in section 4.3. This is surprising as *mev-1* lies in the mitochondrial inner membrane in succinate dehydrogenase cytochrome *b* of complex II facing the mitochondrial matrix [344]. While mtDNA is housed in the mitochondrial matrix, it is anticipated that *mev-1* mutation may increase the ROS production at the mitochondrial matrix, thus mtDNA that is located in matrix would be expected to be damaged. However, for unknown reasons, this apparently is not the case.

Another example of this complexity due to regulatory mechanisms in nematodes are short-lived *mpst-1* (3-mercaptopyruvate sulfurtransferase (3- MST) orthologues) mutants. These mutants do not have the ability to produce endogenous H_2S, suffer from elevated ROS and short lifespan. These animals also have high mtDNA damage but there was no elevation in protein carbonylation [331]. Interestingly, ROS production is elevated in this *mpst-1* mutant as determined using both DCFDA and MitoSOX dye. Again, I observed surprising results in *C. elegans* when I attempted to confirm one mutant with another in a short-lived strain. It is unclear why damage levels are inconsistent between different macromolecules, while lifespan is shortened in some cases.

5.1.3. Complexity in non-genetic perturbations: γ-irradiation response in *C. elegans*

As shown above, perturbation of antioxidant system and endogenous ROS in *C. elegans* results in complex processes that are often difficult to interpret. In order to more directly test the relevance of mtDNA in the context of lifespan determination, I used γ- irradiation to artificially introduce additional damage to mtDNA directly in *C. elegans*. Strikingly, I found that lifespan of nematodes exposed even to 40 kRad γ-radiation was not shortened, despite a significant increase in the mtDNA damage. This lack of lifespan shortening in C. *elegans* after 40 kRad γ-irradiation was surprising because lifespan has previously reported to be significantly shortened in *C. elegans* even exposed to γ-irradiation as low as 5 kRad [345]. For example, Ye *et al.*

reported that 5 and 20 kRad γ-irradiation were both able to shorten the mean lifespan of *C. elegans* by 41 and 69 %, respectively [345]. A likely explanation for these discrepancies is that Ye *et al.* exposed nematodes to γ-radiation during first larvae stage while in my experiment, nematodes were only treated with γ-radiation after they had reached adulthood. During the larvae stage, *C. elegans* somatic blast cells undergo cell divisions, while no cell divisions take place during adult stage [346]. Damaged DNA is passed on to the new cells during the larvae stage cell division which impacts the survivorship of the nematodes. Furthermore, dividing cells are generally more susceptible to DNA damage and more likely to undergo apoptosis. Unfortunately, no data on oxidative biomarkers were reported in the nematodes exposed to γ-radiation at larvae stage. This is another example where nematodes are able to survive for a long period of time (normal lifespan) despite having high oxidative mtDNA damage. However, similar to the case of the antioxidant system perturbations discussed above, these animals again exhibit a low energy phenotype. They do not have normal healthspan and move significantly less.

5.2. The need for good biomarkers?

As discussed above, given these complexities in terms of lifespan, healthspan and damage response, it is difficult to understand the consequences of genetic, physical and pharmacological perturbations and mechanism of ageing in the absence of carefully validated markers of oxidative damage. Therefore, good biomarkers with stable oxidation products that reflect oxidation status at specific site at macromolecules are needed. Previously, no such marker was available for mtDNA in nematodes.

Using a previous marker, we had found that mtDNA damage was not significantly elevated in the MnSOD mutant nematodes [62]. However, as mentioned earlier in section 3.3.4., the basic Fpg-qRT-PCR DNA damage assay lacks sensitivity, exhibits high variability and is subjected to possible artifacts. Therefore, I developed a new S-XL-qRT-PCR DNA damage assay in order to overcome the limitations of the Fpg-qRT-PCR DNA damage assay. Using this new assay, I was able to detect statistically significant increases in damage to mtDNA in the SOD mutants.

These animals now therefore pose a stronger challenge to mFRTA, at least in *C. elegans*, because the damage level to mtDNA is higher but lifespan is normal.

We should be aware that we cannot make the assumption that oxidative damage in one set of macromolecules is necessarily correlated closely to elevated damage in other macromolecules. For example, in the case of both the *mev-1* and *mpst-1* mutant nematodes, not all macromolecules showed high oxidative damage. Unexpected results were also observed in the aforementioned study, where overexpression of *sod-1* increases the level of H_2O_2 [347]. However, overexpression of *sod-1* increases the levels of protein oxidation but does not alter the levels of lipid oxidation. This is an example illustrating that animals suffer from high oxidative damage in one macromolecules do not necessary also suffer from high damage in another macromolecule and *vice versa*. Our data are consistent with this view in the case of *mpst-1* mutant nematodes, where we initially expected that high ROS level in *mpst-1* mutant nematodes would equally elevate damage to all macromolecules. However, this is not the case. We have observed that the *mpst-1* mutant has increased mtDNA damage but normal level of protein damage. Good biomarkers are clearly required to determine if oxidative damage to a given target is actually elevated.

Many studies attempted to test the mFRTA either by modulating antioxidant defenses or pharmacological interventions, however, often only lifespan studies are reported and data on oxidative damage accumulation is usually missing [88, 275, 328, 348-350]. For example, original study of the SOD mutants, the authors concluded that the superoxide radical is not a major determinant of ageing [88]. However, this conclusion was uncertain without any data on oxidative damage. This is because in the absence of oxidative damage data, the underlying mechanisms that determined the lifespan, whether these data challenge the mFRTA was unclear.

In the context of pharmacological interventions, reliable oxidative biomarkers are also needed in order to answer the questions concerning interventions that can attenuate oxidative stress. For example, I found that mitoQ, a mitochondrially-targeted antioxidant not only prolongs the lifespan of transgenic Aβ overexpressing nematodes but also improves their healthspan.

However, we cannot assume that the observed beneficial effects on lifespan and healthspan in response to exposure to MitoQ are due to a global antioxidant effects without confirmation of this expectation through the use of appropriate biomarkers. Attempting to do so, I found that MitoQ did not in fact decrease ROS levels as measured by DCFDA fluorescence dye, and did not reduce protein carbonyl levels or modulate levels of oxidative damage in mtDNA in the transgenic Aβ overexpressing nematodes despite its clear efficacy in ameliorating the phenotype of early death. This is surprising as MitoQ is an antioxidant that is specifically designed to selectively absorb and accumulate within mitochondria, making it reasonable to expect that MitoQ might exert its effects through modulation of oxidative stress. However, I found that administration of MitoQ instead specifically increases or protects mitochondrial lipids (cardiolipin) and associated lipid bound ETC complexes (Complex I and IV), suggesting that MitoQ may be effective specifically in protecting the mitochondrial inner membrane. Based on the results, I expected that MitoQ might improve mitochondrial general metabolic energy availability. However, when I measured ATP content and oxygen consumption rate, I found that administration of MitoQ did not in fact affect the global energy availability, despite an improvement in mitochondrial ETC activities.

These data illustrate that not all antioxidants reduce oxidative damage to all macromolecules, even when they show efficacy in treatment conditions associated with elevated oxidative damage. Relationships between lifespan and oxidative damage accumulation should be carefully examined. Oxidative and metabolic biomarkers are important tools to investigate antioxidant activity of compounds in order to study how and where the interventions work. Furthermore, an ideal oxidative biomarker should be molecule, cell and tissue-specific to overcome some of the complexity of free radical metabolism and stress response system in the context of the process of ageing. It may be not surprising that I also found that MitoQ does not affect lifespan in wild type N2 animals.

5.3. Mitochondrial DNA is not a determinant of ageing in *C. elegans*

With the establishment of appropriate biomarkers, it is possible to test prediction of the mFRTA directly. Mitochondria are often believed to be the major site of ROS production as well as a major target of oxidative damage.

5.3.1. mFRTA: Mitochondrial DNA damage and ageing

If the accumulation of oxidative damage as a consequence of inadequate detoxification of ROS by antioxidants controls ageing rate, modulating the expression of antioxidant enzymes should increase or decrease the lifespan. Similarly, according to mFRTA, long-lived mutants should show low levels of oxidative damage, such as low level of mtDNA damage, lipid peroxidation and protein carbonylation. MtDNA damage in particular, is of interest because among different types of ROS-mediated molecular damage, damaged to mtDNA can lead to irreversible loss or alteration of mitochondrial coding sequences, thus changing its genetic information.

Using my S-XL-qRT-PCR assay, I found that there is some age-associated mtDNA damage pattern in *C. elegans* with a trend toward more mtDNA lesions in old nematodes. This is somewhat consistent with the expectations of mFRTA and studies in humans that also show mtDNA damage accumulation with age, at least when determined using a HPLC method [207, 351]. Using a HPLC-ECD method, the most commonly measured DNA lesion, 8-OHdG is shown to accumulate with age in human heart [207]. However, it is still unclear whether this accumulation of mtDNA damage is related to ageing given the small change in the level of mtDNA damage, so it is difficult to know what the important functional consequences are.

Normal lifespan in MnSOD mutant nematodes might be attributable to reduced general ROS production and decreased energy metabolism, delaying development and reproduction [62, 88, 213], which is the phenotypic characteristics of long-lived animals. This lack of effect on lifespan can be explained by mechanisms that alter mitochondrial function in these SOD mutants. As suggested by Van Raamsdonk *et al.*, none of the *sod* genes are responsible for lifespan effect in these *sod* deleted mutants and genetic manipulations that affect mitochondrial

functions and lifespan in a number of mutants in *C. elegans* show phenotypes of long-lived mutants [63]. This indicates that deletion of MnSOD in *C. elegans* does not decrease the survival of the nematodes possibly due to alteration of mitochondrial function where generalized ROS production as measured by DCFDA fluorescence dye was reduced, although the mtDNA damage is clearly higher but lifespan was unchanged. However, while the level of damaged mtDNA in the MnSOD mutant is significantly higher than in wild type nematodes, the absolute level remains low (1.9 lesions per mtDNA molecule, see section 4.3, Table 5.1) and this absolute level might be too low to suppress functional mitochondria and too low to affect lifespan.

S/N	Type of *C. elegans*	Level of damaged mtDNA (Lesions per 10 kbp)	P-value (mtDNA damage Vs control)	Lifespan	References
1	Wild type N2	0.9	NA	Normal	#[213]
2	MnSOD knockout	1.9	*	Normal	#[213]
3	*mev-1* knockout	0.6	ns	Decreased (21.1%)	#[213]
4	*mpst-1* knockout	3.0	**	Decreased (15.4 %)	#[331]
5	*glp-1*	0.6	NA	Normal	
6	γ-irradiated	1.2	**	Normal	
7	UV-irradiated	2.5	***	Decreased (10.5%)	

# denotes lifespan data obtained from journal papers.

Table 5.1. Levels of mtDNA damage and lifespan. 2 to 4: mtDNA damage and lifespan of mutants were compared wild type N2 nematodes. 6-7: mtDNA damage and lifespan for mutants were compared to *glp-1* nematodes.

While data in MnSOD and *mev-1* mutants imply that small variations in mtDNA damage may not be a determinant of ageing rate, the levels of damaged mtDNA in these mutants are well below three lesions per mtDNA molecule (Table 5.1). In fact, the level of mtDNA damage in *mev-1* mutant is even lower than wild type N2 nematodes (Table 5.1). One interpretation of the data therefore is that for the mtDNA damage to significantly affect and thus shorten the lifespan of the nematodes, the level of mtDNA damage has to be higher than some threshold. As previously mentioned, I found that short-lived mpst-*1* mutant nematodes suffer from higher (more than three lesions per mtDNA molecule) mtDNA damage compared to wild type *C. elegans* and these animals are short-lived [331]. However, while some have reported association of mitochondrial function and mtDNA damage [352, 353], there are also suggestions that H_2S production by mitochondrial 3-MST controls mitochondrial function directly, e.g. by serving as electron donor to enhance mitochondrial electron transport [353]. It is thus still unclear whether the shortening of the *mpst-1* mutants' lifespan is due to the elevation of the mtDNA damage or dysfunctioned mitochondria by some other mechanisms.

To investigate the idea that mtDNA damage may affect lifespan only above certain thresholds, I compared the levels of mtDNA damage in nematodes exposed to γ- and UV-irradiation. I found that exposure to γ-radiation elevates damaged mtDNA but lifespan is not shortened, possibly because the level of mtDNA damage is still below the threshold level that is sufficient to decrease lifespan. However, interestingly, γ-irradiated nematodes move significantly less than non-irradiated nematodes. The decrease in the distance travelled in γ-irradiated nematodes may suggest that these animals, similar to the SOD and PRDX mutants, may sacrifice energy for survival.

Also, using my S-XL-qRT-PCR DNA damage assay, I found that 400 J/m^2 UV-irradiation increases mtDNA damage to a significantly higher degree, reaching about three lesions per mtDNA molecule. Using a similar approach, Leung *et al.* have also shown that mtDNA damage is elevated in larvae of UV-irradiated *C. elegans* [354]. These UV-irradiated larvae also consume less oxygen while maintaining a normal level of steady state ATP [354]. Thus,

consistent with my idea, the lifespan shortening effect in UV-irradiated animals could also be due to failing mitochondria. While the γ- and UV irradiation experiments were initially designed only to test the damage detection method, the lack of lifespan result in γ-irradiated animals is surprising. Therefore it would be interesting to titrate the mtDNA damage over a wider range, so as to identify more clearly whether a threshold of mtDNA damage that affects lifespan exists.

Mitochondria do clearly fail in ageing nematodes and whether these dysfunctional mitochondria are a cause of ageing, remains to be studied. Also, one would expect that the shortest-lived animal, for instance, C. *elegans* has higher damage than other longer-lived species. However, this not the case as the total DNA damage levels are comparable between humans, mice and *C. elegans* [355-357].

In some cases where *C. elegans* were used as a model, the mFRTA seems to be supported by the notion that lifespan was reduced in the animals (*mpst-1* mutant nematodes or UV-irradiated nematodes) with high mtDNA damage. However, we should be aware that these are mutants of antioxidant perturbations or oxidative damage perturbations. The lifespan effects do not reflect the actual natural ageing process, but may in fact be pathology due to excessive high oxidative damage to mtDNA or other molecules.

Previously, it has been reported that protein carbonyl contents in long-lived mutants such as *daf-2* and *age-1* mutant nematodes were low [326, 358]. The authors concluded that oxidative damage is the major determinant of ageing in *C. elegans* by determining the oxidative damage to protein only. This is an area that needs to be addressed to determine the consistency of the levels of oxidative damage to other macromolecules. I have yet to apply my new assay to these mutants.

5.4. *C. elegans* as a model system for studying human ageing/ diseases

5.4.1. Relevance of the *C. elegans* system to mammals systems

Despite its evolutionary distance from mammals, *C. elegans* has become a prominent model organism for studying aging. *C. elegans* shares 60-80 % homologues of genes identified in humans [259]. Several age-related changes associated with ageing are similar in worms, flies and humans [359]. For example, as nematodes age, they gradually slow in their movement and display uncoordinated movement activity [257]. This reduction in physical activity is consistent with flies, mice and humans where old age is associated with poorer movement skill [360-362]. In *C. elegans*, these age-related changes in the patterns of movement are due to deterioration in muscle cells [287]. We and others have also shown that mitochondrial function, oxygen consumption and metabolic rate in nematodes decline with ageing, which also happens in other animals, including human beings.

Another area in ageing where nematodes are increasingly used, are age-dependent diseases. An example to study human age-related diseases is the study of Alzheimer disease, where transgenic animals were engineered to overexpress human Aβ. I showed that in *C. elegans*, transgenic Aβ overexpressing nematodes have deficiency in mitochondrial ETC complex IV activity. This finding is in line with several studies conducted in humans' brain and transgenic AD mouse model, where complex IV activity is also significantly reduced in AD tissues [236, 338-340].

However, *C. elegans* is obviously not appropriate in all regards as a model for human biology. For example, I exposed *C. elegans* to 40 kRad γ-radiation and measured the mtDNA damage and physical changes caused by this γ-radiation dose. 40 kRad γ-radiation is 100 times higher than the 0.4 kRad radiation dose that is expected to cause a 50 % death rate in humans [363]. This dosage is needed to observe significant effect in nematodes because fully developed adult *C. elegans* consist of non-dividing somatic cells with no cellular replication [364]. This non-proliferative property of adult *C. elegans* somatic cells is important when considering radiation responses. Irradiation of nematodes during post-egg laying period involves only somatic cells

that can tolerate higher levels of damaged DNA and therefore much more resistance to radiation damage [365].

Like mammals, *C. elegans* possesses all the typical antioxidant genes such as SOD and PRDX. However, one difficulty in using *C. elegans* as a model to study mammalian ageing are the significant differences in the response of nematodes to perturbations between *C. elegans* and mammals.

Numerous studies have been done to characterize the effect of impaired SOD on lifespan and oxidative stress resistance in different model systems. As previously discussed in sections 5.1. and 5.1.1., mitochondrial MnSOD knockout mutants nematodes suffer from increased mtDNA damage but the lifespan of the nematodes is not altered [88, 213]. Unlike nematodes, mice lacking mitochondrial SOD die at very early ages and also suffer from high accumulation of lipid peroxidation products and reduced mitochondrial ETC function [366, 367]. Overall, deletion of mitochondrial SOD in both *C. elegans* and mice models results in dramatically different consequences in terms of lifespan and healthspan.

Similarly, deletion of mitochondrial PRDX, *prdx-3* in *C. elegans*, neither shortens lifespan nor elevates oxidative protein damage. Instead, loss of *prdx-3* reduces total energy available by reducing motility and brood size. We believe this to be due to mitochondrial uncoupling as a compensatory changes in response to lack of *prdx-3* [343]. Unlike the effect of repression of PRDX in mitochondria in nematodes, knocking out of mitochondrial PRDX in mice does increase ROS generation and elevates DNA and protein oxidative damage [368]. However, at present it is unclear whether mice lacking mitochondrial PRDX suffer from early death or elevated mtDNA damage. This is another example that shows differences between mice and nematodes. Overall, antioxidant enzymes are conserved throughout all the biological kingdom, but the regulatory mechanisms and damage responses in *C. elegans* are different from mammalian systems. In the case of SOD, *C. elegans* contains more homologues of SOD than mice with an additional mitochondrial SOD, *sod-3* that exists in *C. elegans*. It seems that, at

least in *C.elegans*, mitochondrial ETC inhibition and mitochondrial uncoupling are the response for the repression of SOD and PRDX, respectively.

Finally, as discussed above, using my DNA damage assay, I found no elevation of mtDNA damage in *mev-1* mutant nematodes, despite the fact that the animals are short-lived. Similar to *mev-1 C. elegans*, mouse embryonic fibroblast cells with equivalent mutation suffer from high cell death and accumulate high oxidized protein [324, 369]. By contrast to my DNA damage results, studies in young mouse fibroblast cells showed two-fold higher accumulation of 8-OHdG, a DNA damage marker, in the *mev-1* cells than control cells [324, 369].

It is obvious from these results that in many ways *C. elegans* are not like mice. It seems that some of the compensatory mechanisms are private to the nematodes.

5.5 Conclusions

It is becoming increasingly apparent that mitochondria are involved in ageing. As the major producer and target of ROS, oxidative damage accumulation in mitochondria has been implicated to be the major cause of ageing. However, it is still unknown as to what type of oxidative damage, if any, is a determinant of ageing rate.

Many studies have attempted to test the mFRTA by perturbing oxidative damage through various genetic, pharmacology and physical interventions. Changes in lifespan have often been reported together with only sparse data on oxidative damage. It is usually assumed that perturbation of antioxidants system will affect oxidative damage and that this, in turn, will affect lifespan; however, this is clearly an oversimplified view and consequently results are conflicting. I found features of a complex regulatory system in *C. elegans*. There is complexity in terms of lifespan and damage response and several compensatory mechanisms that alter mitochondrial activity have evolved to maintain ROS homeostasis in nematodes.

My data also show that it is possible for the nematodes to be long-lived with high oxidative damage (eg. MnSOD mutant and γ-irradiated nematodes) or short-lived with low mtDNA damage (eg. *mev-1* mutant nematodes). While, in some cases, I indeed found nematodes to be

short-lived with high oxidative damage, for example, in the case of short-lived UV-irradiated nematodes and *mpst-1* mutant nematodes with high levels of damaged mtDNA. This may not be a causal relationship and may not be due to accelerated ageing. Furthermore, one should not expect high oxidative damage in all macromolecules of a given short-lived nematode. For example, damage to protein and to mtDNA were inconsistent in antioxidant perturbation in both *mpst-1* and *mev-1* mutant nematodes. Short-lived *mpst-1* mutant animals suffer from high mtDNA damage but, surprisingly, do not suffer from elevated oxidative damage to protein. Given these complexity, results of perturbation are often difficult to interpret. Therefore, well validated markers of oxidative damage are needed in order to test the relevance of oxidative damage to macromolecules, particularly, mtDNA to the survival of nematodes.

I found evidence that a level of mtDNA damage below a certain threshold does not affect the nematodes survival. However, when mtDNA damage is sufficient to cause variations in lifespan, this appears as pathological and this lifespan shortening may not be a determinant of ageing either. Finally, pharmacological intervention using MitoQ improves the lifespan and healthspan of the transgenic Aβ-expressing nematodes but does not ameliorate damaged mtDNA and protein. MitoQ also does not affect lifespan of wild type N2 nematodes.

Comparing this to mice, I found that regulatory mechanisms in *C. elegans* are quite different from mice. In nematodes, antioxidant perturbations results in compensatory mechanisms involving mitochondrial uncoupling or mitochondrial ETC inhibitions and resulting in significant metabolic suppression. In mice, perturbations of antioxidants appear to elevate oxidative damage and shorten lifespan. It is therefore unsurprising that reported data in nematodes and mice often appear inconsistent.

6. References

[1] WHO Ageing and Life Course. *Interesting facts about ageing*. http://www.who.int/ageing/about/facts/en/

[2] Bloom, D. E.; Canning, D.; Fink, G. Implications of population ageing for economic growth. *Oxford Review of Economic Policy* **26:**583-612; 2011.

[3] Harper, S. Mature Societies: Planning for Our Future Selves. *Daedalus* **135:**20-31; 2006.

[4] Kaneda, C. H. T. 2012 world population data sheet. In: Bureau, P. R., ed.; 2012.

[5] Nations, U. World Population Ageing: 1950-2050. *Chapter I: Demographic determinants of population ageing*; 2002.

[6] Latest data: Births and deaths. In: Statistics, D. o., ed. Singapore: Department of Statistics; 2012.

[7] Preston, S. H. The changing relation between mortality and level of economic development. *Population Studies* **29:**231-248; 1975.

[8] Halliwell, B.; Gutteridge, J. *Free radicals in biology and medicine.* 5th Edition.Oxford, UK: Oxford UP; 2015. In Press.

[9] Price, D. L.; Sisodia, S. S.; Borchelt, D. R. Alzheimer disease--when and why? *Nature genetics* **19:**314-316; 1998.

[10] Barnes, D. E.; Yaffe, K. The projected effect of risk factor reduction on Alzheimer's disease prevalence. *Lancet neurology* **10:**819-828; 2011.

[11] Stanton, M. The High Concentration of U.S. Health Care Expenditures. In: Eisel, F., ed. *Research in Action*. Rockville: Agency for Healthcare Research and Quality; 2005.

[12] WHO Global health and ageing. In: Aging, N. I. o., ed. United states of America; 2011: 32. http://www.who.int/ageing/publications/global_health.pdf

[13] Meek, P. D.; McKeithan, K.; Schumock, G. T. Economic considerations in Alzheimer's disease. *Pharmacotherapy* **18:**68-73; discussion 79-82; 1998.

[14] Lindsley, C. W. Alzheimer's disease: development of disease-modifying treatments is the challenge for our generation. *ACS chemical neuroscience* **3:**804-805; 2012.

[15] Our Demographic Challenges and What These Mean to Us. Singapore: National Population and Talent Division, Prime Minister's Office, Government of Singapore; 2012.

[16] Harman, D. The aging process. *Proceedings of the National Academy of Sciences of the United States of America* **78:**7124-7128; 1981.

[17] Strehler, B. L. *Time, cells, and aging* New York Academic Press; 1977.

[18] Vina, J.; Borras, C.; Miquel, J. Theories of ageing. *IUBMB life* **59:**249-254; 2007.

[19] Cummings, S. R. The biology of aging. *Journal of musculoskeletal & neuronal interactions* **7:**340-341; 2007.

[20] Weinert, B. T.; Timiras, P. S. Invited review: Theories of aging. *Journal of applied physiology* **95:**1706-1716; 2003.

[21] Medvedev, Z. A. An attempt at a rational classification of theories of ageing. *Biological reviews of the Cambridge Philosophical Society* **65:**375-398; 1990.

[22] Tosato, M.; Zamboni, V.; Ferrini, A.; Cesari, M. The aging process and potential interventions to extend life expectancy. *Clinical interventions in aging* **2:**401-412; 2007.

[23] Rattan, S. I. Theories of biological aging: genes, proteins, and free radicals. *Free radical research* **40:**1230-1238; 2006.

[24] Trindade, L. S.; Aigaki, T.; Peixoto, A. A.; Balduino, A.; Manica da Cruz, I. B.; Heddle, J. G. A novel classification system for evolutionary aging theories. *Frontiers in genetics* **4:**25; 2013.

[25] Kirkwood, T. B. Evolution of ageing. *Mech Ageing Dev* **123:**737-745; 2002.

[26] Gavrilov, L. A.; Gavrilova, N. S. Evolutionary theories of aging and longevity. *TheScientificWorldJournal* **2:**339-356; 2002.

[27] Kirkwood, T. B.; Austad, S. N. Why do we age? *Nature* **408:**233-238; 2000.

[28] Quinlan, R. J. Extrinsic Mortality Effects on Reproductive Strategies in a Caribbean Community. *Human Nature* **21:**124-139; 2010.

[29] Ljubuncic, P.; Reznick, A. Z. The evolutionary theories of aging revisited--a mini-review. *Gerontology* **55:**205-216; 2009.

[30] Austad, S. N. Retarded Senescence in an Insular Population of Virginia Opossums (Didelphis-Virginiana). *J Zool* **229:**695-708; 1993.

[31] Medawar, P. *The Uniqueness of the Individual.* New York:: Basic Books Inc; 1952.

[32] Le Bourg, E. A mini-review of the evolutionary theories of aging. *Demographic Research* **4:**1-28; 2001.

[33] Turker, M. Premature Aging. In: JE, B., ed. *Encyclopedia of gerontology*: Academic Press; 1996: 341-354.

[34] Haldane, J. *New Paths in Genetics.* London: Allen&Unwin; 1941.

[35] Pollex, R. L.; Hegele, R. A. Hutchinson-Gilford progeria syndrome. *Clinical genetics* **66:**375-381; 2004.

[36] Harper, B. Huntington disease. *Journal of the Royal Society of Medicine* **98:**550; 2005.

[37] Warby, S. C.; Visscher, H.; Collins, J. A.; Doty, C. N.; Carter, C.; Butland, S. L.; Hayden, A. R.; Kanazawa, I.; Ross, C. J.; Hayden, M. R. HTT haplotypes contribute to differences in Huntington disease prevalence between Europe and East Asia. *European journal of human genetics : EJHG* **19:**561-566; 2011.

[38] Williams, G. Pleiotropy, Natural Selection, and the Evolution of Senescence. *Evolution; international journal of organic evolution***:**398-411; 1957.

[39] Bryant, M. J.; Reznick, D. Comparative studies of senescence in natural populations of guppies. *The American naturalist* **163:**55-68; 2004.

[40] Reznick, D. N.; Bryant, M. J.; Roff, D.; Ghalambor, C. K.; Ghalambor, D. E. Effect of extrinsic mortality on the evolution of senescence in guppies. *Nature* **431:**1095-1099; 2004.

[41] Kirkwood, T. B. Evolution of ageing. *Nature* **270:**301-304; 1977.

[42] Kirkwood, T. B.; Holliday, R. The evolution of ageing and longevity. *Proceedings of the Royal Society of London. Series B, Containing papers of a Biological character. Royal Society* **205:**531-546; 1979.

[43] Kirkwood, T. B. Human senescence. *BioEssays : news and reviews in molecular, cellular and developmental biology* **18:**1009-1016; 1996.

[44] Sgr; ograve; M., C. A Delayed Wave of Death from Reproduction in Drosophila. *Science* **286:**2521-2524; 1999.

[45] Arantes-Oliveira, N.; Apfeld, J.; Dillin, A.; Kenyon, C. Regulation of life-span by germ-line stem cells in Caenorhabditis elegans. *Science* **295:**502-505; 2002.

[46] Rattan, S. I. The science of healthy aging: genes, milieu, and chance. *Annals of the New York Academy of Sciences* **1114:**1-10; 2007.

[47] Hulbert, A. J.; Pamplona, R.; Buffenstein, R.; Buttemer, W. A. Life and death: metabolic rate, membrane composition, and life span of animals. *Physiological reviews* **87:**1175-1213; 2007.

[48] Rubner, M. Das Problem det Lebensdaur und seiner beziehunger zum Wachstum und Ernarnhung (The Problem of Longevity and Its Relation to Growth and Nutrition). *Munich: Oldenberg*; 1908.

[49] Pearl, R. *The rate of living: Being an account of some experimental studies on the biology of life duration.* New York: A.A. Knopf 1928.

[50] Loeb, J.; Northrop, J. H. On the influence of food and temperature upon the duration of life. *Journal of Biological Chemistry* **32:**103-121; 1917.

[51] Goranson, N. C.; Ebersole, J. P.; Brault, S. Resolving an adaptive conundrum: reproduction in Caenorhabditis elegans is not sperm-limited when food is scarce. *Evol Ecol Res* **7:**325-333; 2005.

[52] Garigan, D.; Hsu, A. L.; Fraser, A. G.; Kamath, R. S.; Ahringer, J.; Kenyon, C. Genetic analysis of tissue aging in Caenorhabditis elegans: a role for heat-shock factor and bacterial proliferation. *Genetics* **161:**1101-1112; 2002.

[53] Gems, D.; Riddle, D. L. Genetic, behavioral and environmental determinants of male longevity in Caenorhabditis elegans. *Genetics* **154:**1597-1610; 2000.

[54] Speakman, J. R. Body size, energy metabolism and lifespan. *Journal of Experimental Biology* **208:**1717-1730; 2005.

[55] Muller, F. L.; Lustgarten, M. S.; Jang, Y.; Richardson, A.; Van Remmen, H. Trends in oxidative aging theories. *Free radical biology & medicine* **43:**477-503; 2007.

[56] Garsin, D. A.; Villanueva, J. M.; Begun, J.; Kim, D. H.; Sifri, C. D.; Calderwood, S. B.; Ruvkun, G.; Ausubel, F. M. Long-lived C. elegans daf-2 mutants are resistant to bacterial pathogens. *Science* **300:**1921; 2003.

[57] Harman, D. Aging: a theory based on free radical and radiation chemistry. *Journal of gerontology* **11:**298-300; 1956.

[58] Van Raamsdonk, J. M.; Hekimi, S. Reactive Oxygen Species and Aging in Caenorhabditis elegans: Causal or Casual Relationship? *Antioxidants & redox signaling* **13:**1911-1953; 2010.

[59] Balaban, R. S.; Nemoto, S.; Finkel, T. Mitochondria, oxidants, and aging. *Cell* **120:**483-495; 2005.

[60] Harman, D. Free radical theory of aging. *Mutation research* **275:**257-266; 1992.

[61] Commoner, B.; Townsend, J.; Pake, G. E. Free Radicals in Biological Materials. *Nature* **174:**689-691; 1954.

[62] Gruber, J.; Ng, L. F.; Fong, S.; Wong, Y. T.; Koh, S. A.; Chen, C. B.; Shui, G.; Cheong, W. F.; Schaffer, S.; Wenk, M. R.; Halliwell, B. Mitochondrial changes in ageing Caenorhabditis elegans--what do we learn from superoxide dismutase knockouts? *PloS one* **6:**e19444; 2011.

[63] Van Raamsdonk, J. M.; Hekimi, S. Deletion of the mitochondrial superoxide dismutase sod-2 extends lifespan in Caenorhabditis elegans. *PLoS genetics* **5:**e1000361; 2009.

[64] Dai, D. F.; Chen, T.; Wanagat, J.; Laflamme, M.; Marcinek, D. J.; Emond, M. J.; Ngo, C. P.; Prolla, T. A.; Rabinovitch, P. S. Age-dependent cardiomyopathy in mitochondrial mutator mice is attenuated by overexpression of catalase targeted to mitochondria. *Aging cell* **9:**536-544; 2010.

[65] Fleming, J. E.; Reveillaud, I.; Niedzwiecki, A. Role of Oxidative Stress in Drosophila Aging. *Mutation research* **275:**267-279; 1992.

[66] Mccord, J. M.; Fridovic.I. Superoxide Dismutase-an Enzymic Function for Erythrocuprein. *Federation proceedings* **28:**346-&; 1969.

[67] Miquel, J.; Economos, A. C.; Fleming, J.; Johnson, J. E., Jr. Mitochondrial role in cell aging. *Experimental gerontology* **15:**575-591; 1980.

[68] Sanz, A.; Stefanatos, R. K. The mitochondrial free radical theory of aging: a critical view. *Current aging science* **1:**10-21; 2008.

[69] Harman, D. The biologic clock: the mitochondria? *Journal of the American Geriatrics Society* **20:**145-147; 1972.

[70] Linnane, A. W.; Marzuki, S.; Ozawa, T.; Tanaka, M. Mitochondrial DNA mutations as an important contributor to ageing and degenerative diseases. *Lancet* **1:**642-645; 1989.

[71] Chance, B.; Sies, H.; Boveris, A. Hydroperoxide metabolism in mammalian organs. *Physiological reviews* **59:**527-605; 1979.

[72] Gruber, J.; Schaffer, S.; Halliwell, B. The mitochondrial free radical theory of ageing--where do we stand? *Frontiers in bioscience : a journal and virtual library* **13:**6554-6579; 2008.

[73] Bratic, A.; Larsson, N. G. The role of mitochondria in aging. *The Journal of clinical investigation* **123:**951-957; 2013.

[74] Turrens, J. F. Mitochondrial formation of reactive oxygen species. *Journal of Physiology* **552:**335-344; 2003.

[75] Fraga, C. G.; Shigenaga, M. K.; Park, J. W.; Degan, P.; Ames, B. N. Oxidative damage to DNA during aging: 8-Hydroxy-2'-deoxyguanosine in rat organ DNA and urine. *Proceedings of the National Academy of Sciences of the United States of America* **87:**4533-4537; 1990.

[76] Stadtman, E. R. Protein oxidation and aging. *Science* **257:**1220-1224; 1992.

[77] J. Marnett, L.; Hurd, H. K.; Hollstein, M. C.; Levin, D. E.; Esterbauer, H.; Ames, B. N. Naturally occurring carbonyl compounds are mutagens Salmonella tester strain TA104. *Mutation Research/Fundamental and Molecular Mechanisms of Mutagenesis* **148:**25-34; 1985.

[78] Corral-Debrinski, M.; Horton, T.; Lott, M. T.; Shoffner, J. M.; Beal, M. F.; Wallace, D. C. Mitochondrial DNA deletions in human brain: Regional variability and increase with advanced age. *Nature genetics* **2:**324-329; 1992.

[79] Kenyon, C. The plasticity of aging: insights from long-lived mutants. *Cell* **120:**449-460; 2005.

[80] de Magalhaes, J. P.; Church, G. M. Cells discover fire: employing reactive oxygen species in development and consequences for aging. *Experimental gerontology* **41:**1-10; 2006.

[81] Tatar, M.; Kopelman, A.; Epstein, D.; Tu, M. P.; Yin, C. M.; Garofalo, R. S. A mutant Drosophila insulin receptor homolog that extends life-span and impairs neuroendocrine function. *Science* **292:**107-110; 2001.

[82] Boylston, W. H.; DeFord, J. H.; Papaconstantinou, J. Identification of longevity-associated genes in long-lived Snell and Ames dwarf mice. *Age* **28:**125-144; 2006.

[83] Holzenberger, M.; Dupont, J.; Ducos, B.; Leneuve, P.; Geloen, A.; Even, P. C.; Cervera, P.; Le Bouc, Y. IGF-1 receptor regulates lifespan and resistance to oxidative stress in mice. *Nature* **421:**182-187; 2003.

[84] Tower, J. Transgenic methods for increasing Drosophila life span. *Mech Ageing Dev* **118:**1-14; 2000.

[85] Orr, W. C.; Sohal, R. S. Extension of life-span by overexpression of superoxide dismutase and catalase in Drosophila melanogaster. *Science* **263:**1128-1130; 1994.

[86] Arking, R.; Burde, V.; Graves, K.; Hari, R.; Feldman, E.; Zeevi, A.; Soliman, S.; Saraiya, A.; Buck, S.; Vettraino, J.; Sathrasala, K.; Wehr, N.; Levine, R. L. Forward and reverse selection for longevity in Drosophila is characterized by alteration of antioxidant gene expression and oxidative damage patterns. *Experimental gerontology* **35:**167-185; 2000.

[87] Larsen, P. L. Aging and resistance to oxidative damage in Caenorhabditis elegans. *Proceedings of the National Academy of Sciences of the United States of America* **90:**8905-8909; 1993.

[88] Doonan, R.; McElwee, J. J.; Matthijssens, F.; Walker, G. A.; Houthoofd, K.; Back, P.; Matscheski, A.; Vanfleteren, J. R.; Gems, D. Against the oxidative damage theory of aging:

superoxide dismutases protect against oxidative stress but have little or no effect on life span in Caenorhabditis elegans. *Genes & development* **22:**3236-3241; 2008.

[89] Rodriguez, K. A.; Wywial, E.; Perez, V. I.; Lambert, A. J.; Edrey, Y. H.; Lewis, K. N.; Grimes, K.; Lindsey, M. L.; Brand, M. D.; Buffenstein, R. Walking the Oxidative Stress Tightrope: A Perspective from the Naked Mole-Rat, the Longest-Living Rodent. *Current pharmaceutical design* **17:**2290-2307; 2011.

[90] Halliwell, B. Oxidative stress and neurodegeneration: where are we now? *Journal of neurochemistry* **97:**1634-1658; 2006.

[91] Valko, M.; Rhodes, C. J.; Moncol, J.; Izakovic, M.; Mazur, M. Free radicals, metals and antioxidants in oxidative stress-induced cancer. *Chemico-biological interactions* **160:**1-40; 2006.

[92] Valko, M.; Leibfritz, D.; Moncol, J.; Cronin, M. T.; Mazur, M.; Telser, J. Free radicals and antioxidants in normal physiological functions and human disease. *The international journal of biochemistry & cell biology* **39:**44-84; 2007.

[93] Morrell, C. N. Reactive oxygen species: finding the right balance. *Circulation research* **103:**571-572; 2008.

[94] Maulik, S. K.; Kumar, S. Oxidative stress and cardiac hypertrophy: a review. *Toxicology mechanisms and methods* **22:**359-366; 2012.

[95] Tsihlis, N. D.; Oustwani, C. S.; Vavra, A. K.; Jiang, Q.; Keefer, L. K.; Kibbe, M. R. Nitric oxide inhibits vascular smooth muscle cell proliferation and neointimal hyperplasia by increasing the ubiquitination and degradation of UbcH10. *Cell biochemistry and biophysics* **60:**89-97; 2011.

[96] Lenaz, G. The mitochondrial production of reactive oxygen species: mechanisms and implications in human pathology. *IUBMB life* **52:**159-164; 2001.

[97] Genova, M. L.; Pich, M. M.; Bernacchia, A.; Bianchi, C.; Biondi, A.; Bovina, C.; Falasca, A. I.; Formiggini, G.; Castelli, G. P.; Lenaz, G. The Mitochondrial Production of Reactive Oxygen Species in Relation to Aging and Pathology. *Annals of the New York Academy of Sciences* **1011:**86-100; 2004.

[98] Donald Voet, J. G. V., Charlotte W. Pratt. *Fundamentals of biochemistry* New York John Wiley; 2002.

[99] Green, D. R. Apoptotic pathways: the roads to ruin. *Cell* **94:**695-698; 1998.

[100] Oh-hama, T. Evolutionary consideration on 5-aminolevulinate synthase in nature. *Origins of life and evolution of the biosphere : the journal of the International Society for the Study of the Origin of Life* **27:**405-412; 1997.

[101] Hajnoczky, G.; Csordas, G.; Das, S.; Garcia-Perez, C.; Saotome, M.; Sinha Roy, S.; Yi, M. Mitochondrial calcium signalling and cell death: approaches for assessing the role of mitochondrial Ca2+ uptake in apoptosis. *Cell calcium* **40:**553-560; 2006.

[102] Rossier, M. F. T channels and steroid biosynthesis: in search of a link with mitochondria. *Cell calcium* **40:**155-164; 2006.

[103] Ryan, M. T.; Hoogenraad, N. J. Mitochondrial-nuclear communications. *Annual review of biochemistry* **76:**701-722; 2007.

[104] Clementi, E.; Nisoli, E. Nitric oxide and mitochondrial biogenesis: a key to long-term regulation of cellular metabolism. *Comparative biochemistry and physiology. Part A, Molecular & integrative physiology* **142:**102-110; 2005.

[105] Krauss, S. Mitochondria: Structure and Role in Respiration. *eLS*: John Wiley & Sons, Ltd; 2001.

[106] van der Bliek, A. M.; Shen, Q.; Kawajiri, S. Mechanisms of mitochondrial fission and fusion. *Cold Spring Harbor perspectives in biology* **5**; 2013.

[107] Kanazawa, T.; Zappaterra, M. D.; Hasegawa, A.; Wright, A. P.; Newman-Smith, E. D.; Buttle, K. F.; McDonald, K.; Mannella, C. A.; van der Bliek, A. M. The C. elegans Opa1 homologue EAT-3 is essential for resistance to free radicals. *PLoS genetics* **4:**e1000022; 2008.

[108] Ranieri, M.; Brajkovic, S.; Riboldi, G.; Ronchi, D.; Rizzo, F.; Bresolin, N.; Corti, S.; Comi, G. P. Mitochondrial fusion proteins and human diseases. *Neurology research international* **2013:**293893; 2013.

[109] Wang, X.; Su, B.; Siedlak, S. L.; Moreira, P. I.; Fujioka, H.; Wang, Y.; Casadesus, G.; Zhu, X. Amyloid-beta overproduction causes abnormal mitochondrial dynamics via differential modulation of mitochondrial fission/fusion proteins. *Proceedings of the National Academy of Sciences of the United States of America* **105:**19318-19323; 2008.

[110] Wang, X.; Su, B.; Lee, H. G.; Li, X.; Perry, G.; Smith, M. A.; Zhu, X. Impaired balance of mitochondrial fission and fusion in Alzheimer's disease. *The Journal of neuroscience : the official journal of the Society for Neuroscience* **29:**9090-9103; 2009.

[111] Levine, T. B.; Levine, A. B. Mitochondria. *Metabolic Syndrome and Cardiovascular Disease*: Blackwell Publishing Ltd.; 2012: 3-39.

[112] Wallace, D. C. Diseases of the mitochondrial DNA. *Annual review of biochemistry* **61:**1175-1212; 1992.

[113] Musatov, A.; Robinson, N. C. Susceptibility of mitochondrial electron-transport complexes to oxidative damage. Focus on cytochrome c oxidase. *Free radical research* **46:**1313-1326; 2012.

[114] Rolo, A. P.; Teodoro, J. S.; Palmeira, C. M. Role of oxidative stress in the pathogenesis of nonalcoholic steatohepatitis. *Free radical biology & medicine* **52:**59-69; 2012.

[115] Jastroch, M.; Divakaruni, A. S.; Mookerjee, S.; Treberg, J. R.; Brand, M. D. Mitochondrial proton and electron leaks. *Essays in biochemistry* **47:**53-67; 2010.

[116] Pamplona, R. Mitochondrial DNA damage and animal longevity: insights from comparative studies. *Journal of aging research* **2011:**807108; 2011.

[117] Sanz, A.; Pamplona, R.; Barja, G. Is the mitochondrial free radical theory of aging intact? *Antioxidants & redox signaling* **8:**582-599; 2006.

[118] St-Pierre, J.; Buckingham, J. A.; Roebuck, S. J.; Brand, M. D. Topology of superoxide production from different sites in the mitochondrial electron transport chain. *The Journal of biological chemistry* **277:**44784-44790; 2002.

[119] Xu, X.; Arriaga, E. A. Qualitative determination of superoxide release at both sides of the mitochondrial inner membrane by capillary electrophoretic analysis of the oxidation products of triphenylphosphonium hydroethidine. *Free radical biology & medicine* **46:**905-913; 2009.

[120] Halliwell, B. Biochemistry of oxidative stress. *Biochemical Society transactions* **35:**1147-1150; 2007.

[121] Zhang, D. X.; Gutterman, D. D. Mitochondrial reactive oxygen species-mediated signaling in endothelial cells. *American journal of physiology. Heart and circulatory physiology* **292:**H2023-2031; 2007.

[122] Muller, F. L.; Liu, Y.; Van Remmen, H. Complex III releases superoxide to both sides of the inner mitochondrial membrane. *The Journal of biological chemistry* **279:**49064-49073; 2004.

[123] Muller, F. The nature and mechanism of superoxide production by the electron transport chain: Its relevance to aging. *Journal of the American Aging Association* **23:**227-253; 2000.

[124] Lenaz, G. Role of mitochondria in oxidative stress and ageing. *Bba-Bioenergetics* **1366:**53-67; 1998.

[125] Rich, P. R.; Bonner, W. D. The sites of superoxide anion generation in higher plant mitochondria. *Archives of biochemistry and biophysics* **188:**206-213; 1978.

[126] Huang. Research progress in the radioprotective effect of superoxide dismutase. *Drug Discoveries & Therapeutics*; 2012.

[127] Figueira, T. R.; Barros, M. H.; Camargo, A. A.; Castilho, R. F.; Ferreira, J. C.; Kowaltowski, A. J.; Sluse, F. E.; Souza-Pinto, N. C.; Vercesi, A. E. Mitochondria as a source of reactive oxygen and nitrogen species: from molecular mechanisms to human health. *Antioxidants & redox signaling* **18:**2029-2074; 2013.

[128] Brand, M. D.; Affourtit, C.; Esteves, T. C.; Green, K.; Lambert, A. J.; Miwa, S.; Pakay, J. L.; Parker, N. Mitochondrial superoxide: production, biological effects, and activation of uncoupling proteins. *Free radical biology & medicine* **37:**755-767; 2004.

[129] Li, Y.; Huang, T. T.; Carlson, E. J.; Melov, S.; Ursell, P. C.; Olson, J. L.; Noble, L. J.; Yoshimura, M. P.; Berger, C.; Chan, P. H.; Wallace, D. C.; Epstein, C. J. Dilated cardiomyopathy and neonatal lethality in mutant mice lacking manganese superoxide dismutase. *Nature genetics* **11:**376-381; 1995.

[130] Kirby, K.; Hu, J.; Hilliker, A. J.; Phillips, J. P. RNA interference-mediated silencing of Sod2 in Drosophila leads to early adult-onset mortality and elevated endogenous oxidative stress. *Proceedings of the National Academy of Sciences of the United States of America* **99:**16162-16167; 2002.

[131] Brown, G. C.; Borutaite, V. There is no evidence that mitochondria are the main source of reactive oxygen species in mammalian cells. *Mitochondrion* **12:**1-4; 2012.

[132] Gross, E.; Sevier, C. S.; Heldman, N.; Vitu, E.; Bentzur, M.; Kaiser, C. A.; Thorpe, C.; Fass, D. Generating disulfides enzymatically: reaction products and electron acceptors of the endoplasmic reticulum thiol oxidase Ero1p. *Proceedings of the National Academy of Sciences of the United States of America* **103:**299-304; 2006.

[133] Kukreja, R. C.; Kontos, H. A.; Hess, M. L.; Ellis, E. F. PGH synthase and lipoxygenase generate superoxide in the presence of NADH or NADPH. *Circulation research* **59:**612-619; 1986.

[134] Boveris, A.; Oshino, N.; Chance, B. The cellular production of hydrogen peroxide. *The Biochemical journal* **128:**617-630; 1972.

[135] O'Donnell, V. B.; Azzi, A. High rates of extracellular superoxide generation by cultured human fibroblasts: involvement of a lipid-metabolizing enzyme. *The Biochemical journal* **318 (Pt 3):**805-812; 1996.

[136] McNally, J. S.; Davis, M. E.; Giddens, D. P.; Saha, A.; Hwang, J.; Dikalov, S.; Jo, H.; Harrison, D. G. Role of xanthine oxidoreductase and NAD(P)H oxidase in endothelial superoxide production in response to oscillatory shear stress. *American journal of physiology. Heart and circulatory physiology* **285:**H2290-2297; 2003.

[137] Shi, Y. Emerging roles of cardiolipin remodeling in mitochondrial dysfunction associated with diabetes, obesity, and cardiovascular diseases. *Journal of Biomedical Research* **24:**6-15; 2010.

[138] Schlame, M.; Rua, D.; Greenberg, M. L. The biosynthesis and functional role of cardiolipin. *Progress in lipid research* **39:**257-288; 2000.

[139] Rhoads, D. M.; Umbach, A. L.; Subbaiah, C. C.; Siedow, J. N. Mitochondrial reactive oxygen species. Contribution to oxidative stress and interorganellar signaling. *Plant physiology* **141:**357-366; 2006.

[140] Nigam, S.; Schewe, T. Phospholipase A2s and lipid peroxidation. *Biochimica et Biophysica Acta (BBA) - Molecular and Cell Biology of Lipids* **1488:**167-181; 2000.

[141] Catala, A. Lipid peroxidation of membrane phospholipids generates hydroxy-alkenals and oxidized phospholipids active in physiological and/or pathological conditions. *Chemistry and physics of lipids* **157:**1-11; 2009.

[142] Echtay, K. S.; Brand, M. D. 4-hydroxy-2-nonenal and uncoupling proteins: an approach for regulation of mitochondrial ROS production. *Redox report : communications in free radical research* **12:**26-29; 2007.

[143] Butterfield, D. A.; Castegna, A.; Lauderback, C. M.; Drake, J. Evidence that amyloid beta-peptide-induced lipid peroxidation and its sequelae in Alzheimer's disease brain contribute to neuronal death. *Neurobiology of aging* **23:**655-664; 2002.

[144] Szeto, H. H. Mitochondria-targeted peptide antioxidants: novel neuroprotective agents. *The AAPS journal* **8:**E521-531; 2006.

[145] Vasquez-Vivar, J. Mitochondrial Aconitase Is a Source of Hydroxyl Radical. AN ELECTRON SPIN RESONANCE INVESTIGATION. *Journal of Biological Chemistry* **275:**14064-14069; 2000.

[146] Cantu, D.; Schaack, J.; Patel, M. Oxidative inactivation of mitochondrial aconitase results in iron and H2O2-mediated neurotoxicity in rat primary mesencephalic cultures. *PloS one* **4:**e7095; 2009.

[147] Smith, C. D.; Carney, J. M.; Starke-Reed, P. E.; Oliver, C. N.; Stadtman, E. R.; Floyd, R. A.; Markesbery, W. R. Excess brain protein oxidation and enzyme dysfunction in normal

aging and in Alzheimer disease. *Proceedings of the National Academy of Sciences of the United States of America* **88:**10540-10543; 1991.

[148] Mecocci, P.; Fano, G.; Fulle, S.; MacGarvey, U.; Shinobu, L.; Polidori, M. C.; Cherubini, A.; Vecchiet, J.; Senin, U.; Beal, M. F. Age-dependent increases in oxidative damage to DNA, lipids, and proteins in human skeletal muscle. *Free radical biology & medicine* **26:**303-308; 1999.

[149] Martinez, M.; Hernandez, A. I.; Martinez, N.; Ferrandiz, M. L. Age-related increase in oxidized proteins in mouse synaptic mitochondria. *Brain research* **731:**246-248; 1996.

[150] Yasuda, K.; Ishii, T.; Suda, H.; Akatsuka, A.; Hartman, P. S.; Goto, S.; Miyazawa, M.; Ishii, N. Age-related changes of mitochondrial structure and function in Caenorhabditis elegans. *Mech Ageing Dev* **127:**763-770; 2006.

[151] Gensler, H. L.; Bernstein, H. DNA damage as the primary cause of aging. *Quarterly Review of Biology* **56:**279-303; 1981.

[152] Alexeyev, M. F.; LeDoux, S. P.; 'Wilson, G. L. Mitochondrial DNA and aging. *Clinical science* **107:**355-364; 2004.

[153] Loft, S.; Poulsen, H. E. Cancer risk and oxidative DNA damage in man. *Journal of molecular medicine* **74:**297-312; 1996.

[154] Birch-Machin, M. A. The role of mitochondria in ageing and carcinogenesis. *Clinical and experimental dermatology* **31:**548-552; 2006.

[155] Wang, J.; Xiong, S.; Xie, C.; Markesbery, W. R.; Lovell, M. A. Increased oxidative damage in nuclear and mitochondrial DNA in Alzheimer's disease. *Journal of neurochemistry* **93:**953-962; 2005.

[156] Cline, S. D. Mitochondrial DNA damage and its consequences for mitochondrial gene expression. *Biochimica et biophysica acta* **1819:**979-991; 2012.

[157] Nass, M. M. K.; Nass, S. Intramitochondrial Fibers with DNA Characteristics .1. Fixation and Electron Staining Reactions. *Journal of Cell Biology* **19:**593-&; 1963.

[158] Tsang, W. Y.; Lemire, B. D. The role of mitochondria in the life of the nematode, Caenorhabditis elegans. *Biochimica et Biophysica Acta (BBA) - Molecular Basis of Disease* **1638:**91-105; 2003.

[159] Wiesner, R. J.; Zsurka, G.; Kunz, W. S. Mitochondrial DNA damage and the aging process: facts and imaginations. *Free radical research* **40:**1284-1294; 2006.

[160] Lemire, B. Mitochondrial genetics. *WormBook : the online review of C. elegans biology***:**1-10; 2005.

[161] Tsang, W. Y.; Lemire, B. D. Mitochondrial genome content is regulated during nematode development. *Biochemical and biophysical research communications* **291:**8-16; 2002.

[162] Moraes, C. T. What regulates mitochondrial DNA copy number in animal cells? *Trends in Genetics* **17:**199-205; 2001.

[163] Dickinson, A.; Yeung, K. Y.; Donoghue, J.; Baker, M. J.; Kelly, R. D.; McKenzie, M.; Johns, T. G.; St John, J. C. The regulation of mitochondrial DNA copy number in glioblastoma cells. *Cell death and differentiation* **20:**1644-1653; 2013.

[164] Mishina, Y.; Duguid, E. M.; He, C. Direct reversal of DNA alkylation damage. *Chem Rev* **106:**215-232; 2006.

[165] Bordin, D. L.; Lima, M.; Lenz, G.; Saffi, J.; Meira, L. B.; Mésange, P.; Soares, D. G.; Larsen, A. K.; Escargueil, A. E.; Henriques, J. A. P. DNA alkylation damage and autophagy induction. *Mutation Research/Reviews in Mutation Research*; 2013.

[166] Shapiro, R. Damage to DNA Caused by Hydrolysis. In: Seeberg, E.; Kleppe, K., eds. *Chromosome Damage and Repair*: Springer US; 1982: 3-18.

[167] Gates, K. S. An Overview of Chemical Processes That Damage Cellular DNA: Spontaneous Hydrolysis, Alkylation, and Reactions with Radicals. *Chem Res Toxicol* **22:**1747-1760; 2009.

[168] Alexeyev, M.; Shokolenko, I.; Wilson, G.; LeDoux, S. The maintenance of mitochondrial DNA integrity--critical analysis and update. *Cold Spring Harbor perspectives in biology* **5:**a012641; 2013.

[169] Liehr, J. G. Is estradiol a genotoxic mutagenic carcinogen? *Endocrine reviews* **21:**40-54; 2000.

[170] De Bont, R.; van Larebeke, N. Endogenous DNA damage in humans: a review of quantitative data. *Mutagenesis* **19:**169-185; 2004.

[171] Balansky, R.; Izzotti, A.; Scatolini, L.; DAgostini, F.; DeFlora, S. Induction by carcinogens and chemoprevention by N-acetylcysteine of adducts to mitochondrial DNA in rat organs. *Cancer research* **56:**1642-1647; 1996.

[172] el-Khamisy, S. F.; Caldecott, K. W. DNA single-strand break repair and spinocerebellar ataxia with axonal neuropathy-1. *Neuroscience* **145:**1260-1266; 2007.

[173] McKinnon, P. J.; Caldecott, K. W. DNA strand break repair and human genetic disease. *Annual review of genomics and human genetics* **8:**37-55; 2007.

[174] Mills, K. D.; Ferguson, D. O.; Alt, F. W. The role of DNA breaks in genomic instability and tumorigenesis. *Immunological reviews* **194:**77-95; 2003.

[175] Goodsell, D. S. The Molecular Perspective: Ultraviolet Light and Pyrimidine Dimers. *The oncologist* **6:**298-299; 2001.

[176] Mouret, S.; Baudouin, C.; Charveron, M.; Favier, A.; Cadet, J.; Douki, T. Cyclobutane pyrimidine dimers are predominant DNA lesions in whole human skin exposed to UVA radiation. *Proceedings of the National Academy of Sciences of the United States of America* **103:**13765-13770; 2006.

[177] Cooke, M. S.; Evans, M. D.; Dizdaroglu, M.; Lunec, J. Oxidative DNA damage: mechanisms, mutation, and disease. *FASEB journal : official publication of the Federation of American Societies for Experimental Biology* **17:**1195-1214; 2003.

[178] Hutchinson, F. Chemical Changes Induced in DNA by Ionizing Radiation. **32:**115-154; 1985.

[179] Kanvah, S.; Joseph, J.; Schuster, G. B.; Barnett, R. N.; Cleveland, C. L.; Landman, U. Oxidation of DNA: Damage to Nucleobases. *Accounts Chem Res* **43:**280-287; 2010.

[180] Shaw, A. A.; Cadet, J. Formation of cyclopyrimidines via the direct effects of gamma radiation of pyrimidine nucleosides. *International journal of radiation biology* **54:**987-997; 1988.

[181] Jaruga, P.; Dizdaroglu, M. 8,5'-Cyclopurine-2'-deoxynucleosides in DNA: mechanisms of formation, measurement, repair and biological effects. *DNA repair* **7:**1413-1425; 2008.

[182] Mao, P.; Reddy, P. H. Aging and amyloid beta-induced oxidative DNA damage and mitochondrial dysfunction in Alzheimer's disease: implications for early intervention and therapeutics. *Biochimica et biophysica acta* **1812:**1359-1370; 2011.

[183] Santos, R. X.; Correia, S. C.; Zhu, X.; Smith, M. A.; Moreira, P. I.; Castellani, R. J.; Nunomura, A.; Perry, G. Mitochondrial DNA oxidative damage and repair in aging and Alzheimer's disease. *Antioxidants & redox signaling* **18:**2444-2457; 2013.

[184] Alam, Z. I.; Jenner, A.; Daniel, S. E.; Lees, A. J.; Cairns, N.; Marsden, C. D.; Jenner, P.; Halliwell, B. Oxidative DNA damage in the parkinsonian brain: an apparent selective increase in 8-hydroxyguanine levels in substantia nigra. *Journal of neurochemistry* **69:**1196-1203; 1997.

[185] Cadet, J.; Delatour, T.; Douki, T.; Gasparutto, D.; Pouget, J. P.; Ravanat, J. L.; Sauvaigo, S. Hydroxyl radicals and DNA base damage. *Mutat Res-Fund Mol M* **424:**9-21; 1999.

[186] Dizdaroglu, M. Oxidative Damage to DNA in Mammalian Chromatin. *Mutation research* **275:**331-342; 1992.

[187] Borek, C. Antioxidants and radiation therapy. *The Journal of nutrition* **134:**3207S-3209S; 2004.

[188] Sudprasert, W.; Navasumrit, P.; Ruchirawat, M. Effects of low-dose gamma radiation on DNA damage, chromosomal aberration and expression of repair genes in human blood cells. *International journal of hygiene and environmental health* **209:**503-511; 2006.

[189] Henner, W. D.; Grunberg, S. M.; Haseltine, W. A. Sites and structure of gamma radiation-induced DNA strand breaks. *The Journal of biological chemistry* **257:**11750-11754; 1982.

[190] Min, J.; Lee, C. W.; Gu, M. B. Gamma-radiation dose-rate effects on DNA damage and toxicity in bacterial cells. *Radiation and environmental biophysics* **42:**189-192; 2003.

[191] Birch-Machin, M. A.; Swalwell, H. How mitochondria record the effects of UV exposure and oxidative stress using human skin as a model tissue. *Mutagenesis* **25:**101-107; 2010.

[192] Farhadinejad, Z.; Ehsani, M.; Ahmadi-Joneidi, I.; Shayegani, A.; Mohseni, H. Effects of UVC radiation on thermal, electrical and morphological behavior of silicone rubber insulators. *IEEE Transactions on Dielectrics and Electrical Insulation* **19:**1740-1749; 2012.

[193] Britt, A. B. Repair of DNA-Damage Induced by Ultraviolet-Radiation. *Plant physiology* **108:**891-896; 1995.

[194] Mitchell, D. L.; Nairn, R. S. The Biology of the (6-4) Photoproduct. *Photochemistry and photobiology* **49:**805-819; 1989.

[195] Studer, A.; Cubillos, V. M.; Lamare, M. D.; Poulin, R.; Burritt, D. J. Effects of ultraviolet radiation on an intertidal trematode parasite: An assessment of damage and protection. *International Journal for Parasitology* **42:**453-461; 2012.

[196] Kielbassa, C.; Roza, L.; Epe, B. Wavelength dependence of oxidative DNA damage induced by UV and visible light. *Carcinogenesis* **18:**811-816; 1997.

[197] Blum, J.; Fridovich, I. Superoxide, hydrogen peroxide, and oxygen toxicity in two free-living nematode species. *Archives of biochemistry and biophysics* **222:**35-43; 1983.

[198] Dinis-Oliveira, R. J.; Duarte, J. A.; Sanchez-Navarro, A.; Remiao, F.; Bastos, M. L.; Carvalho, F. Paraquat poisonings: mechanisms of lung toxicity, clinical features, and treatment. *Critical reviews in toxicology* **38:**13-71; 2008.

[199] Thakur, A. Juglone: A therapeutic phytochemical from Juglans regia L. *Journal of Medicinal Plant Research* **5:**5324-5330; 2011.

[200] Aithal, B. K.; Kumar, M. R.; Rao, B. N.; Udupa, N.; Rao, B. S. Juglone, a naphthoquinone from walnut, exerts cytotoxic and genotoxic effects against cultured melanoma tumor cells. *Cell biology international* **33:**1039-1049; 2009.

[201] Babula, P.; Adam, V.; Kizek, R.; Sladký, Z.; Havel, L. Naphthoquinones as allelochemical triggers of programmed cell death. *Environmental and Experimental Botany* **65:**330-337; 2009.

[202] Von Zglinicki, T.; Bürkle, A.; Kirkwood, T. B. L. Stress, DNA damage and ageing - An integrative approach. *Experimental gerontology* **36:**1049-1062; 2001.

[203] Brand, F. N.; Kiely, D. K.; Kannel, W. B.; Myers, R. H. Family patterns of coronary heart disease mortality: the Framingham Longevity Study. *Journal of clinical epidemiology* **45:**169-174; 1992.

[204] Shigenaga, M. K.; Hagen, T. M.; Ames, B. N. Oxidative damage and mitochondrial decay in aging. *Proceedings of the National Academy of Sciences of the United States of America* **91:**10771-10778; 1994.

[205] Mecocci, P.; MacGarvey, U.; Beal, M. F. Oxidative damage to mitochondrial DNA is increased in Alzheimer's disease. *Annals of neurology* **36:**747-751; 1994.

[206] Lee, C. M.; Lopez, M. E.; Weindruch, R.; Aiken, J. M. Association of age-related mitochondrial abnormalities with skeletal muscle fiber atrophy. *Free radical biology & medicine* **25:**964-972; 1998.

[207] Hayakawa, M.; Sugiyama, S.; Hattori, K.; Takasawa, M.; Ozawa, T. Age-associated damage in mitochondrial DNA in human hearts. *Molecular and cellular biochemistry* **119:**95-103; 1993.

[208] Hamilton, M. L.; Van Remmen, H.; Drake, J. A.; Yang, H.; Guo, Z. M.; Kewitt, K.; Walter, C. A.; Richardson, A. Does oxidative damage to DNA increase with age? *Proceedings of the National Academy of Sciences of the United States of America* **98:**10469-10474; 2001.

[209] Chaubey, R. C.; Bhilwade, H. N.; Rajagopalan, R.; Bannur, S. V. Gamma ray induced DNA damage in human and mouse leucocytes measured by SCGE-Pro: a software developed for automated image analysis and data processing for Comet assay. *Mutation research* **490:**187-197; 2001.

[210] Dhawan, A.; Bajpayee, M.; Parmar, D. Chapter 7. Detection of DNA Damage in Drosophila and Mouse.151-170; 2009.

[211] Schriner, S. E.; Linford, N. J.; Martin, G. M.; Treuting, P.; Ogburn, C. E.; Emond, M.; Coskun, P. E.; Ladiges, W.; Wolf, N.; Van Remmen, H.; Wallace, D. C.; Rabinovitch, P. S. Extension of murine life span by overexpression of catalase targeted to mitochondria. *Science* **308:**1909-1911; 2005.

[212] Campisi, J.; Vijg, J. Does damage to DNA and other macromolecules play a role in aging? If so, how? *The journals of gerontology. Series A, Biological sciences and medical sciences* **64:**175-178; 2009.

[213] Honda, Y.; Tanaka, M.; Honda, S. Modulation of longevity and diapause by redox regulation mechanisms under the insulin-like signaling control in Caenorhabditis elegans. *Experimental gerontology* **43:**520-529; 2008.

[214] Yang, W.; Li, J.; Hekimi, S. A Measurable increase in oxidative damage due to reduction in superoxide detoxification fails to shorten the life span of long-lived mitochondrial mutants of Caenorhabditis elegans. *Genetics* **177:**2063-2074; 2007.

[215] Petriv, O. I.; Rachubinski, R. A. Lack of peroxisomal catalase causes a progeric phenotype in Caenorhabditis elegans. *The Journal of biological chemistry* **279:**19996-20001; 2004.

[216] Ankarcrona, M.; Mangialasche, F.; Winblad, B. Rethinking Alzheimer's disease therapy: are mitochondria the key? *Journal of Alzheimer's disease : JAD* **20 Suppl 2:**S579-590; 2010.

[217] Pinto, M.; Pickrell, A. M.; Fukui, H.; Moraes, C. T. Mitochondrial DNA damage in a mouse model of Alzheimer's disease decreases amyloid beta plaque formation. *Neurobiology of aging* **34:**2399-2407; 2013.

[218] Bender, A.; Krishnan, K. J.; Morris, C. M.; Taylor, G. A.; Reeve, A. K.; Perry, R. H.; Jaros, E.; Hersheson, J. S.; Betts, J.; Klopstock, T.; Taylor, R. W.; Turnbull, D. M. High levels of mitochondrial DNA deletions in substantia nigra neurons in aging and Parkinson disease. *Nature genetics* **38:**515-517; 2006.

[219] Lowell, B. B.; Shulman, G. I. Mitochondrial dysfunction and type 2 diabetes. *Science* **307:**384-387; 2005.

[220] Lin, C.-S.; Wang, L.-S. Mitochondrial DNA instability in human cancers. *Formosan Journal of Surgery* **46:**71-75; 2013.

[221] Ayala-Pena, S. Role of oxidative DNA damage in mitochondrial dysfunction and Huntington's disease pathogenesis. *Free radical biology & medicine* **62:**102-110; 2013.

[222] Price, D. L.; Tanzi, R. E.; Borchelt, D. R.; Sisodia, S. S. Alzheimer's disease: genetic studies and transgenic models. *Annual review of genetics* **32:**461-493; 1998.

[223] Lee, M. K.; Borchelt, D. R.; Wong, P. C.; Sisodia, S. S.; Price, D. L. Transgenic models of neurodegenerative diseases. *Current opinion in neurobiology* **6:**651-660; 1996.

[224] Sisodia, S. S.; Price, D. L. Role of the beta-amyloid protein in Alzheimer's disease. *FASEB journal : official publication of the Federation of American Societies for Experimental Biology* **9:**366-370; 1995.

[225] Smith, M. A.; Rottkamp, C. A.; Nunomura, A.; Raina, A. K.; Perry, G. Oxidative stress in Alzheimer's disease. *Biochimica et biophysica acta* **1502:**139-144; 2000.

[226] Yan, M. H.; Wang, X.; Zhu, X. Mitochondrial defects and oxidative stress in Alzheimer disease and Parkinson disease. *Free radical biology & medicine*; 2012.

[227] Mattson, M. P.; Mattson, E. P. Amyloid peptide enhances nail rusting: novel insight into mechanisms of aging and Alzheimer's disease. *Ageing research reviews* **1:**327-330; 2002.

[228] Butterfield, D. A.; Hensley, K.; Harris, M.; Mattson, M.; Carney, J. beta-Amyloid peptide free radical fragments initiate synaptosomal lipoperoxidation in a sequence-specific fashion: implications to Alzheimer's disease. *Biochemical and biophysical research communications* **200:**710-715; 1994.

[229] Subbarao, K. V.; Richardson, J. S.; Ang, L. C. Autopsy samples of Alzheimer's cortex show increased peroxidation in vitro. *Journal of neurochemistry* **55:**342-345; 1990.

[230] Smith, M. A.; Sayre, L. M.; Monnier, V. M.; Perry, G. Radical AGEing in Alzheimer's disease. *Trends in neurosciences* **18:**172-176; 1995.

[231] Smith, M. A.; Richey Harris, P. L.; Sayre, L. M.; Beckman, J. S.; Perry, G. Widespread peroxynitrite-mediated damage in Alzheimer's disease. *The Journal of neuroscience : the official journal of the Society for Neuroscience* **17:**2653-2657; 1997.

[232] Chen, J. X.; Yan, S. S. Role of mitochondrial amyloid-beta in Alzheimer's disease. *Journal of Alzheimer's disease : JAD* **20 Suppl 2:**S569-578; 2010.

[233] Manczak, M.; Anekonda, T. S.; Henson, E.; Park, B. S.; Quinn, J.; Reddy, P. H. Mitochondria are a direct site of A beta accumulation in Alzheimer's disease neurons: implications for free radical generation and oxidative damage in disease progression. *Human molecular genetics* **15:**1437-1449; 2006.

[234] Casley, C. S.; Canevari, L.; Land, J. M.; Clark, J. B.; Sharpe, M. A. Beta-amyloid inhibits integrated mitochondrial respiration and key enzyme activities. *Journal of neurochemistry* **80:**91-100; 2002.

[235] Crouch, P. J.; Barnham, K. J.; Duce, J. A.; Blake, R. E.; Masters, C. L.; Trounce, I. A. Copper-dependent inhibition of cytochrome c oxidase by Abeta(1-42) requires reduced methionine at residue 35 of the Abeta peptide. *Journal of neurochemistry* **99:**226-236; 2006.

[236] Kish, S. J.; Bergeron, C.; Rajput, A.; Dozic, S.; Mastrogiacomo, F.; Chang, L. J.; Wilson, J. M.; DiStefano, L. M.; Nobrega, J. N. Brain cytochrome oxidase in Alzheimer's disease. *Journal of neurochemistry* **59:**776-779; 1992.

[237] Maruszak, A.; Zekanowski, C. Mitochondrial dysfunction and Alzheimer's disease. *Progress in neuro-psychopharmacology & biological psychiatry* **35:**320-330; 2011.

[238] Indo, H. P.; Davidson, M.; Yen, H. C.; Suenaga, S.; Tomita, K.; Nishii, T.; Higuchi, M.; Koga, Y.; Ozawa, T.; Majima, H. J. Evidence of ROS generation by mitochondria in cells with impaired electron transport chain and mitochondrial DNA damage. *Mitochondrion* **7:**106-118; 2007.

[239] Dizdaroglu, M.; Jaruga, P.; Birincioglu, M.; Rodriguez, H. Free radical-induced damage to DNA: mechanisms and measurement. *Free radical biology & medicine* **32:**1102-1115; 2002.

[240] Halliwell, B.; Whiteman, M. Measuring reactive species and oxidative damage in vivo and in cell culture: how should you do it and what do the results mean? *British journal of pharmacology* **142:**231-255; 2004.

[241] Laws, G. M.; Skopek, T. R.; Reddy, M. V.; Storer, R. D.; Glaab, W. E. Detection of DNA adducts using a quantitative long PCR technique and the fluorogenic 5 ' nuclease assay (TaqMan (R)). *Mutat Res-Fund Mol M* **484:**3-18; 2001.

[242] Collins, A. R.; Dusinska, M.; Gedik, C. M.; Stetina, R. Oxidative damage to DNA: Do we have a reliable biomarker? *Environmental health perspectives* **104:**465-469; 1996.

[243] Cadet, J.; D'Ham, C.; Douki, T.; Pouget, J. P.; Ravanat, J. L.; Sauvaigo, S. Facts and artifacts in the measurement of oxidative base damage to DNA. *Free radical research* **29:**541-550; 1998.

[244] Reddy, M. V. Methods for testing compounds for DNA adduct formation. *Regulatory toxicology and pharmacology : RTP* **32:**256-263; 2000.

[245] Ayala-Torres, S.; Chen, Y.; Svoboda, T.; Rosenblatt, J.; Van Houten, B. Analysis of gene-specific DNA damage and repair using quantitative polymerase chain reaction. *Methods* **22:**135-147; 2000.

[246] Collins, A. R.; Oscoz, A. A.; Brunborg, G.; Gaivao, I.; Giovannelli, L.; Kruszewski, M.; Smith, C. C.; Stetina, R. The comet assay: topical issues. *Mutagenesis* **23:**143-151; 2008.

[247] Pfeifer, G. P.; Drouin, R.; Holmquist, G. P. Detection of DNA-Adducts at the DNA-Sequence Level by Ligation-Mediated Pcr. *Mutation research* **288:**39-46; 1993.

[248] Lu, T.; Pan, Y.; Kao, S. Y.; Li, C.; Kohane, I.; Chan, J.; Yankner, B. A. Gene regulation and DNA damage in the ageing human brain. *Nature* **429:**883-891; 2004.

[249] Kalinowski, D. P.; Illenye, S.; Vanhouten, B. Analysis of DNA Damage and Repair in Murine Leukemia-L1210 Cells Using a Quantitative Polymerase Chain-Reaction Assay. *Nucleic acids research* **20:**3485-3494; 1992.

[250] Grimaldi, K. A.; Mcadam, S. R.; Souhami, R. L.; Hartley, J. A. DNA-Damage by Anticancer Agents Resolved at the Nucleotide Level of a Single-Copy Gene - Evidence for a Novel Binding-Site for Cisplatin in Cells. *Nucleic acids research* **22:**2311-2317; 1994.

[251] Santos, J. H.; Mandavilli, B. S.; Van Houten, B. Measuring oxidative mtDNA damage and repair using quantitative PCR. *Methods Mol Biol* **197:**159-176; 2002.

[252] Austad, S. N. Animal models of aging (worms to birds). *Generations* **24:**25-30; 2000.

[253] Lavery, W. L. How relevant are animal models to human ageing? *Journal of the Royal Society of Medicine* **93:**296-298; 2000.

[254] Gallagher, M.; Rapp, P. R. The use of animal models to study the effects of aging on cognition. *Annu Rev Psychol* **48:**339-370; 1997.

[255] Martin, G. M.; Austad, S. N.; Johnson, T. E. Genetic analysis of ageing: Role of oxidative damage and environmental stresses. *Nature genetics* **13:**25-34; 1996.

[256] Partridge, L.; Gems, D. Mechanisms of ageing: public or private? *Nature reviews. Genetics* **3:**165-175; 2002.

[257] Olsen, A.; Vantipalli, M. C.; Lithgow, G. J. Using Caenorhabditis elegans as a model for aging and age-related diseases. *Annals of the New York Academy of Sciences* **1067:**120-128; 2006.

[258] Riddle, D. L. *C. elegans II.* Plainview, N.Y.: Cold Spring Harbor Laboratory Press; 1997.

[259] Kaletta, T.; Hengartner, M. O. Finding function in novel targets: C. elegans as a model organism. *Nature reviews. Drug discovery* **5:**387-398; 2006.

[260] Friedman, D. B.; Johnson, T. E. A mutation in the age-1 gene in Caenorhabditis elegans lengthens life and reduces hermaphrodite fertility. *Genetics* **118:**75-86; 1988.

[261] Link, C. D. Expression of human beta-amyloid peptide in transgenic Caenorhabditis elegans. *Proceedings of the National Academy of Sciences of the United States of America* **92:**9368-9372; 1995.

[262] Lakso, M.; Vartiainen, S.; Moilanen, A. M.; Sirvi ö, J.; Thomas, J. H.; Nass, R.; Blakely, R. D.; Wong, G. Dopaminergic neuronal loss and motor deficits in Caenorhabditis elegans overexpressing human α-synuclein. *Journal of neurochemistry* **86:**165-172; 2003.

[263] Faber, P. W.; Voisine, C.; King, D. C.; Bates, E. A.; Hart, A. C. Glutamine/proline-rich PQE-1 proteins protect Caenorhabditis elegans neurons from huntingtin polyglutamine neurotoxicity. *Proceedings of the National Academy of Sciences of the United States of America* **99:**17131-17136; 2002.

[264] Atamna, H.; Kumar, R. Protective role of methylene blue in Alzheimer's disease via mitochondria and cytochrome c oxidase. *Journal of Alzheimer's disease : JAD* **20 Suppl 2:**S439-452; 2010.

[265] Hornsten, A.; Lieberthal, J.; Fadia, S.; Malins, R.; Ha, L.; Xu, X.; Daigle, I.; Markowitz, M.; O'Connor, G.; Plasterk, R.; Li, C. APL-1, a Caenorhabditis elegans protein related to the human beta-amyloid precursor protein, is essential for viability. *Proceedings of the National Academy of Sciences of the United States of America* **104:**1971-1976; 2007.

[266] Wentzell, J.; Kretzschmar, D. Alzheimer's disease and tauopathy studies in flies and worms. *Neurobiology of disease* **40:**21-28; 2010.

[267] Murphy, M. P.; Smith, R. A. Drug delivery to mitochondria: the key to mitochondrial medicine. *Adv Drug Deliv Rev* **41:**235-250; 2000.

[268] Bjelakovic, G.; Nikolova, D.; Ll, G.; Simonetti, R. G.; Gluud, C. Antioxidant supplements for prevention of mortality in healthy participants and patients with various diseases. *Cochrane Db Syst Rev*; 2008.

[269] Cochemé, H. M.; Murphy, M. P. Can antioxidants be effective therapeutics? *Current opinion in investigational drugs* **11:**426-431; 2010.

[270] James, A. M.; Cocheme, H. M.; Smith, R. A.; Murphy, M. P. Interactions of mitochondria-targeted and untargeted ubiquinones with the mitochondrial respiratory chain and reactive oxygen species. Implications for the use of exogenous ubiquinones as therapies and experimental tools. *The Journal of biological chemistry* **280:**21295-21312; 2005.

[271] Kelso, G. F.; Porteous, C. M.; Coulter, C. V.; Hughes, G.; Porteous, W. K.; Ledgerwood, E. C.; Smith, R. A.; Murphy, M. P. Selective targeting of a redox-active ubiquinone to mitochondria within cells: antioxidant and antiapoptotic properties. *The Journal of biological chemistry* **276:**4588-4596; 2001.

[272] McManus, M. J.; Murphy, M. P.; Franklin, J. L. The mitochondria-targeted antioxidant MitoQ prevents loss of spatial memory retention and early neuropathology in a transgenic mouse model of Alzheimer's disease. *The Journal of neuroscience : the official journal of the Society for Neuroscience* **31:**15703-15715; 2011.

[273] Murphy, M. P. Selective targeting of bioactive compounds to mitochondria. *Trends in biotechnology* **15:**326-330; 1997.

[274] Smith, R. A.; Porteous, C. M.; Coulter, C. V.; Murphy, M. P. Selective targeting of an antioxidant to mitochondria. *European journal of biochemistry / FEBS* **263:**709-716; 1999.

[275] Magwere, T.; West, M.; Riyahi, K.; Murphy, M. P.; Smith, R. A.; Partridge, L. The effects of exogenous antioxidants on lifespan and oxidative stress resistance in Drosophila melanogaster. *Mech Ageing Dev* **127:**356-370; 2006.

[276] Smith, R. A.; Hartley, R. C.; Cocheme, H. M.; Murphy, M. P. Mitochondrial pharmacology. *Trends in pharmacological sciences* **33:**341-352; 2012.

[277] Mitchell, T.; Rotaru, D.; Saba, H.; Smith, R. A.; Murphy, M. P.; MacMillan-Crow, L. A. The mitochondria-targeted antioxidant mitoquinone protects against cold storage injury of renal tubular cells and rat kidneys. *The Journal of pharmacology and experimental therapeutics* **336:**682-692; 2011.

[278] T, S. *Maintenance of C. elegans.* Worm Book; 2006.

[279] Lewis, J. A.; Fleming, J. T. Chapter 1 Basic Culture Methods. **48:**3-29; 1995.

[280] Strange, K.; Christensen, M.; Morrison, R. Primary culture of Caenorhabditis elegans developing embryo cells for electrophysiological, cell biological and molecular studies. *Nature protocols* **2:**1003-1012; 2007.

[281] Bianchi, L., Driscoll, M. *Culture of embryonic C. elegans cells for electrophysiological and pharmacological analyses.* Wormbook; 2006.

[282] Sobkowiak, R.; Lesicki, A. Genotoxicity of nicotine in cell culture of Caenorhabditis elegans evaluated by the comet assay. *Drug and chemical toxicology* **32:**252-257; 2009.

[283] Olive, P. L.; Banath, J. P. The comet assay: a method to measure DNA damage in individual cells. *Nature protocols* **1:**23-29; 2006.

[284] Golden, T. R.; Beckman, K. B.; Lee, A. H.; Dudek, N.; Hubbard, A.; Samper, E.; Melov, S. Dramatic age-related changes in nuclear and genome copy number in the nematode Caenorhabditis elegans. *Aging cell* **6:**179-188; 2007.

[285] Melov, S.; Lithgow, G. J.; Fischer, D. R.; Tedesco, P. M.; Johnson, T. E. Increased frequency of deletions in the mitochondrial genome with age of Caenorhabditis elegans. *Nucleic acids research* **23:**1419-1425; 1995.

[286] Gruber, J.; Ng, L. F.; Poovathingal, S. K.; Halliwell, B. Deceptively simple but simply deceptive--Caenorhabditis elegans lifespan studies: considerations for aging and antioxidant effects. *FEBS letters* **583:**3377-3387; 2009.

[287] Herndon, L. A.; Schmeissner, P. J.; Dudaronek, J. M.; Brown, P. A.; Listner, K. M.; Sakano, Y.; Paupard, M. C.; Hall, D. H.; Driscoll, M. Stochastic and genetic factors influence tissue-specific decline in ageing C. elegans. *Nature* **419:**808-814; 2002.

[288] Pun, P. B.; Gruber, J.; Tang, S. Y.; Schaffer, S.; Ong, R. L.; Fong, S.; Ng, L. F.; Cheah, I.; Halliwell, B. Ageing in nematodes: do antioxidants extend lifespan in Caenorhabditis elegans? *Biogerontology* **11:**17-30; 2010.

[289] Schaffer, S.; Gruber, J.; Ng, L. F.; Fong, S.; Wong, Y. T.; Tang, S. Y.; Halliwell, B. The effect of dichloroacetate on health- and lifespan in C. elegans. *Biogerontology* **12:**195-209; 2011.

[290] Goo, C. K.; Lim, H. Y.; Ho, Q. S.; Too, H. P.; Clement, M. V.; Wong, K. P. PTEN/Akt signaling controls mitochondrial respiratory capacity through 4E-BP1. *PloS one* **7:**e45806; 2012.

[291] Varela, A. T.; Gomes, A. P.; Simoes, A. M.; Teodoro, J. S.; Duarte, F. V.; Rolo, A. P.; Palmeira, C. M. Indirubin-3'-oxime impairs mitochondrial oxidative phosphorylation and prevents mitochondrial permeability transition induction. *Toxicology and applied pharmacology* **233:**179-185; 2008.

[292] Birch-Machin, M. A.; Briggs, H. L.; Saborido, A. A.; Bindoff, L. A.; Turnbull, D. M. An evaluation of the measurement of the activities of complexes I-IV in the respiratory chain of human skeletal muscle mitochondria. *Biochemical medicine and metabolic biology* **51:**35-42; 1994.

[293] Bligh, E. G.; Dyer, W. J. A rapid method of total lipid extraction and purification. *Canadian journal of biochemistry and physiology* **37:**911-917; 1959.

[294] Bank, H. L.; Schmehl, M. K. Parameters for evaluation of viability assays: accuracy, precision, specificity, sensitivity, and standardization. *Cryobiology* **26:**203-211; 1989.

[295] Comparison of different methods of measuring 8-oxoguanine as a marker of oxidative DNA damage. ESCODD (European Standards Committee on Oxidative DNA Damage). *Free radical research* **32:**333-341; 2000.

[296] Dhawan, A.; Bajpayee, M.; Parmar, D. Comet assay: a reliable tool for the assessment of DNA damage in different models. *Cell biology and toxicology* **25:**5-32; 2009.

[297] Nandhakumar, S.; Parasuraman, S.; Shanmugam, M. M.; Rao, K. R.; Chand, P.; Bhat, B. V. Evaluation of DNA damage using single-cell gel electrophoresis (Comet Assay). *Journal of pharmacology & pharmacotherapeutics* **2:**107-111; 2011.

[298] Gedik, C. M.; Ewen, S. W.; Collins, A. R. Single-cell gel electrophoresis applied to the analysis of UV-C damage and its repair in human cells. *International journal of radiation biology* **62:**313-320; 1992.

[299] Fairbairn, D. W.; Olive, P. L.; Oneill, K. L. The Comet Assay - a Comprehensive Review. *Mutat Res-Rev Genet* **339:**37-59; 1995.

[300] Ostling, O.; Johanson, K. J. Microelectrophoretic study of radiation-induced DNA damages in individual mammalian cells. *Biochemical and biophysical research communications* **123:**291-298; 1984.

[301] Singh, N. P.; McCoy, M. T.; Tice, R. R.; Schneider, E. L. A simple technique for quantitation of low levels of DNA damage in individual cells. *Experimental cell research* **175:**184-191; 1988.

[302] Domijan, A. M.; Zeljezic, D.; Kopjar, N.; Peraica, M. Standard and Fpg-modified comet assay in kidney cells of ochratoxin A- and fumonisin B(1)-treated rats. *Toxicology* **222:**53-59; 2006.

[303] Collins, A. R. The comet assay for DNA damage and repair: principles, applications, and limitations. *Molecular biotechnology* **26:**249-261; 2004.

[304] McKelvey-Martin, V. J.; Green, M. H.; Schmezer, P.; Pool-Zobel, B. L.; De Meo, M. P.; Collins, A. The single cell gel electrophoresis assay (comet assay): a European review. *Mutation research* **288:**47-63; 1993.

[305] Lahtz, C.; Bates, S. E.; Jiang, Y.; Li, A. X.; Wu, X.; Hahn, M. A.; Pfeifer, G. P. Gamma irradiation does not induce detectable changes in DNA methylation directly following exposure of human cells. *PloS one* **7:**e44858; 2012.

[306] Rastogi, R. P.; Richa; Kumar, A.; Tyagi, M. B.; Sinha, R. P. Molecular mechanisms of ultraviolet radiation-induced DNA damage and repair. *Journal of nucleic acids* **2010:**592980; 2010.

[307] Le Caër, S. Water Radiolysis: Influence of Oxide Surfaces on H2 Production under Ionizing Radiation. *Water* **3:**235-253; 2011.

[308] Govan, H. L., 3rd; Valles-Ayoub, Y.; Braun, J. Fine-mapping of DNA damage and repair in specific genomic segments. *Nucleic acids research* **18:**3823-3830; 1990.

[309] Santos, J. H.; Meyer, J. N.; Mandavilli, B. S.; Van Houten, B. Quantitative PCR-based measurement of nuclear and mitochondrial DNA damage and repair in mammalian cells. *Methods Mol Biol* **314:**183-199; 2006.

[310] Sikorsky, J. A.; Primerano, D. A.; Fenger, T. W.; Denvir, J. DNA damage reduces Taq DNA polymerase fidelity and PCR amplification efficiency. *Biochemical and biophysical research communications* **355:**431-437; 2007.

[311] Tchou, J.; Bodepudi, V.; Shibutani, S.; Antoshechkin, I.; Miller, J.; Grollman, A. P.; Johnson, F. Substrate specificity of Fpg protein. Recognition and cleavage of oxidatively damaged DNA. *The Journal of biological chemistry* **269:**15318-15324; 1994.

[312] Caraguel, C.; Stryhn, H.; Gagne, N.; Dohoo, I.; Hammell, L. Traditional descriptive analysis and novel visual representation of diagnostic repeatability and reproducibility:

application to an infectious salmon anaemia virus RT-PCR assay. *Preventive veterinary medicine* **92:**9-19; 2009.

[313] Caraguel, C.; Stryhn, H.; Gagne, N.; Dohoo, I.; Hammell, L. A modelling approach to predict the variation of repeatability and reproducibility of a RT-PCR assay for infectious salmon anaemia virus across infection prevalences and infection stages. *Preventive veterinary medicine* **103:**63-73; 2012.

[314] Phillips, D. H.; Farmer, P. B.; Beland, F. A.; Nath, R. G.; Poirier, M. C.; Reddy, M. V.; Turteltaub, K. W. Methods of DNA adduct determination and their application to testing compounds for genotoxicity. *Environmental and molecular mutagenesis* **35:**222-233; 2000.

[315] Neher, D. A.; Sturzenbaum, S. R. Extra-long PCR, an identifier of DNA adducts in single nematodes (Caenorhabditis elegans). *Comparative biochemistry and physiology. Toxicology & pharmacology : CBP* **144:**279-285; 2006.

[316] Meyer, J. N. QPCR: a tool for analysis of mitochondrial and nuclear DNA damage in ecotoxicology. *Ecotoxicology* **19:**804-811; 2010.

[317] Riesco, M. F.; Robles, V. Quantification of DNA damage by q-PCR in cryopreserved zebrafish Primordial Germ Cells. *Journal of Applied Ichthyology* **28:**925-929; 2012.

[318] Hunter, S. E.; Jung, D.; Di Giulio, R. T.; Meyer, J. N. The QPCR assay for analysis of mitochondrial DNA damage, repair, and relative copy number. *Methods* **51:**444-451; 2010.

[319] Clancy, S. DNA damage & repair: mechanisms for maintaining DNA integrity. *Nature Education* **1**; 2008.

[320] Rolfsmeier, M. L.; Laughery, M. F.; Haseltine, C. A. Repair of DNA double-strand breaks following UV damage in three Sulfolobus solfataricus strains. *Journal of bacteriology* **192:**4954-4962; 2010.

[321] Bogdanov, K. V.; Chukhlovin, A. B.; Zaritskey, A. Y.; Frolova, O. I.; Afanasiev, B. V. Ultraviolet irradiation induces multiple DNA double-strand breaks and apoptosis in normal granulocytes and chronic myeloid leukaemia blasts. *British journal of haematology* **98:**869-872; 1997.

[322] Bradley, M. O. Double-strand breaks in DNA caused by repair of damage due to ultraviolet light. *Journal of Supramolecular and Cellular Biochemistry* **16:**337-343; 1981.

[323] Austin, J.; Kimble, J. glp-1 required in the germ line for regulation of the decision between mitosis and meiosis in C. elegans. *Cell* **51:**589-599; 1987.

[324] Ishii, T.; Miyazawa, M.; Hartman, P. S.; Ishii, N. Mitochondrial superoxide anion (O(2)(-)) inducible "mev-1" animal models for aging research. *BMB reports* **44:**298-305; 2011.

[325] Yasuda, K.; Hartman, P. S.; Ishii, T.; Suda, H.; Akatsuka, A.; Shoyama, T.; Miyazawa, M.; Ishii, N. Interrelationships between mitochondrial fusion, energy metabolism and oxidative stress during development in Caenorhabditis elegans. *Biochemical and biophysical research communications* **404:**751-755; 2011.

[326] Adachi, H.; Fujiwara, Y.; Ishii, N. Effects of oxygen on protein carbonyl and aging in Caenorhabditis elegans mutants with long (age-1) and short (mev-1) life spans. *The journals of gerontology. Series A, Biological sciences and medical sciences* **53:**B240-244; 1998.

[327] Hunter, T.; Bannister, W. H.; Hunter, G. J. Cloning, expression, and characterization of two manganese superoxide dismutases from Caenorhabditis elegans. *The Journal of biological chemistry* **272:**28652-28659; 1997.

[328] Ishii, N.; Takahashi, K.; Tomita, S.; Keino, T.; Honda, S.; Yoshino, K.; Suzuki, K. A methyl viologen-sensitive mutant of the nematode Caenorhabditis elegans. *Mutation research* **237:**165-171; 1990.

[329] Gems, D.; Doonan, R. Antioxidant defense and aging in C. elegans: is the oxidative damage theory of aging wrong? *Cell Cycle* **8:**1681-1687; 2009.

[330] Miller, D. L.; Roth, M. B. Hydrogen sulfide increases thermotolerance and lifespan in Caenorhabditis elegans. *Proceedings of the National Academy of Sciences of the United States of America* **104:**20618-20622; 2007.

[331] Qabazard, B.; Li, L.; Gruber, J.; Peh, M. T.; Ng, L. F.; Dinesh Kumar, S.; Rose, P.; Tan, C. H.; Dymock, B. W.; Wei, F.; Swain, S. C.; Halliwell, B.; Sturzenbaum, S. R.; Moore, P. K. Hydrogen Sulfide Is an Endogenous Regulator of Aging in Caenorhabditis elegans. *Antioxidants & redox signaling*; 2013.

[332] Marthandan, S.; Murphy, M. P.; Billett, E.; Barnett, Y. An investigation of the effects of MitoQ on human peripheral mononuclear cells. *Free radical research* **45:**351-358; 2011.

[333] Lyras, L.; Cairns, N. J.; Jenner, A.; Jenner, P.; Halliwell, B. An assessment of oxidative damage to proteins, lipids, and DNA in brain from patients with Alzheimer's disease. *Journal of neurochemistry* **68:**2061-2069; 1997.

[334] Coppede, F.; Migliore, L. DNA damage and repair in Alzheimer's disease. *Current Alzheimer research* **6:**36-47; 2009.

[335] Fong, S., Gruber, J., & Halliwell, B. Measuring reactive oxygen species in C. elegans using DCFDA—a word of caution. *The Worm Breeder's Gazette*; 2010.

[336] Kalyanaraman, B.; Darley-Usmar, V.; Davies, K. J.; Dennery, P. A.; Forman, H. J.; Grisham, M. B.; Mann, G. E.; Moore, K.; Roberts, L. J., 2nd; Ischiropoulos, H. Measuring reactive oxygen and nitrogen species with fluorescent probes: challenges and limitations. *Free radical biology & medicine* **52:**1-6; 2012.

[337] Aksenov, M. Y.; Aksenova, M. V.; Butterfield, D. A.; Geddes, J. W.; Markesbery, W. R. Protein oxidation in the brain in Alzheimer's disease. *Neuroscience* **103:**373-383; 2001.

[338] Pickrell, A. M.; Fukui, H.; Moraes, C. T. The role of cytochrome c oxidase deficiency in ROS and amyloid plaque formation. *Journal of bioenergetics and biomembranes* **41:**453-456; 2009.

[339] Mutisya, E. M.; Bowling, A. C.; Beal, M. F. Cortical cytochrome oxidase activity is reduced in Alzheimer's disease. *Journal of neurochemistry* **63:**2179-2184; 1994.

[340] Fukui, H.; Diaz, F.; Garcia, S.; Moraes, C. T. Cytochrome c oxidase deficiency in neurons decreases both oxidative stress and amyloid formation in a mouse model of Alzheimer's disease. *Proceedings of the National Academy of Sciences of the United States of America* **104:**14163-14168; 2007.

[341] Kim, J.; Minkler, P. E.; Salomon, R. G.; Anderson, V. E.; Hoppel, C. L. Cardiolipin: characterization of distinct oxidized molecular species. *Journal of lipid research* **52:**125-135; 2011.

[342] Andreyev, A. Y.; Kushnareva, Y. E.; Starkov, A. A. Mitochondrial metabolism of reactive oxygen species. *Biochemistry. Biokhimiia* **70:**200-214; 2005.

[343] Ranjan, M.; Gruber, J.; Ng, L. F.; Halliwell, B. Repression of the mitochondrial peroxiredoxin antioxidant system does not shorten life span but causes reduced fitness in Caenorhabditis elegans. *Free Radical Biology and Medicine* **63:**381-389; 2013.

[344] Levine, R. L.; Stadtman, E. R. Oxidative modification of proteins during aging. *Experimental gerontology* **36:**1495-1502; 2001.

[345] Ye, K.; Ji, C. B.; Lu, X. W.; Ni, Y. H.; Gao, C. L.; Chen, X. H.; Zhao, Y. P.; Gu, G. X.; Guo, X. R. Resveratrol attenuates radiation damage in Caenorhabditis elegans by preventing oxidative stress. *Journal of radiation research* **51:**473-479; 2010.

[346] Boxem, M. Cyclin-dependent kinases in C. elegans. *Cell division* **1:**6; 2006.

[347] Cabreiro, F.; Ackerman, D.; Doonan, R.; Araiz, C.; Back, P.; Papp, D.; Braeckman, B. P.; Gems, D. Increased life span from overexpression of superoxide dismutase in Caenorhabditis elegans is not caused by decreased oxidative damage. *Free radical biology & medicine* **51:**1575-1582; 2011.

[348] Lebovitz, R. M.; Zhang, H.; Vogel, H.; Cartwright, J., Jr.; Dionne, L.; Lu, N.; Huang, S.; Matzuk, M. M. Neurodegeneration, myocardial injury, and perinatal death in mitochondrial superoxide dismutase-deficient mice. *Proceedings of the National Academy of Sciences of the United States of America* **93:**9782-9787; 1996.

[349] Huang, T. T.; Carlson, E. J.; Kozy, H. M.; Mantha, S.; Goodman, S. I.; Ursell, P. C.; Epstein, C. J. Genetic modification of prenatal lethality and dilated cardiomyopathy in Mn superoxide dismutase mutant mice. *Free radical biology & medicine* **31:**1101-1110; 2001.

[350] Olahova, M.; Taylor, S. R.; Khazaipoul, S.; Wang, J.; Morgan, B. A.; Matsumoto, K.; Blackwell, T. K.; Veal, E. A. A redox-sensitive peroxiredoxin that is important for longevity has tissue- and stress-specific roles in stress resistance. *Proceedings of the National Academy of Sciences of the United States of America* **105:**19839-19844; 2008.

[351] Mecocci, P.; MacGarvey, U.; Kaufman, A. E.; Koontz, D.; Shoffner, J. M.; Wallace, D. C.; Beal, M. F. Oxidative damage to mitochondrial DNA shows marked age-dependent increases in human brain. *Annals of neurology* **34:**609-616; 1993.

[352] Cui, H.; Kong, Y.; Zhang, H. Oxidative stress, mitochondrial dysfunction, and aging. *Journal of signal transduction* **2012:**646354; 2012.

[353] Modis, K.; Coletta, C.; Erdelyi, K.; Papapetropoulos, A.; Szabo, C. Intramitochondrial hydrogen sulfide production by 3-mercaptopyruvate sulfurtransferase maintains mitochondrial electron flow and supports cellular bioenergetics. *FASEB journal : official publication of the Federation of American Societies for Experimental Biology* **27:**601-611; 2013.

[354] Leung, M. C.; Rooney, J. P.; Ryde, I. T.; Bernal, A. J.; Bess, A. S.; Crocker, T. L.; Ji, A. Q.; Meyer, J. N. Effects of early life exposure to ultraviolet C radiation on mitochondrial DNA content, transcription, ATP production, and oxygen consumption in developing Caenorhabditis elegans. *BMC pharmacology & toxicology* **14:**9; 2013.

[355] Rothfuss, O.; Gasser, T.; Patenge, N. Analysis of differential DNA damage in the mitochondrial genome employing a semi-long run real-time PCR approach. *Nucleic acids research* **38:**e24; 2010.

[356] Ballinger, S. W. Mitochondrial Integrity and Function in Atherogenesis. *Circulation* **106:**544-549; 2002.

[357] Bess, A. S.; Crocker, T. L.; Ryde, I. T.; Meyer, J. N. Mitochondrial dynamics and autophagy aid in removal of persistent mitochondrial DNA damage in Caenorhabditis elegans. *Nucleic acids research* **40:**7916-7931; 2012.

[358] Yasuda, K.; Adachi, H.; Fujiwara, Y.; Ishii, N. Protein carbonyl accumulation in aging dauer formation-defective (daf) mutants of Caenorhabditis elegans. *The journals of gerontology. Series A, Biological sciences and medical sciences* **54:**B47-51; discussion B52-43; 1999.

[359] O'Kane, C. J. Modelling human diseases in Drosophila and Caenorhabditis. *Seminars in cell & developmental biology* **14:**3-10; 2003.

[360] Raw, R. K.; Kountouriotis, G. K.; Mon-Williams, M.; Wilkie, R. M. Movement control in older adults: Does old age mean middle of the road? *Journal of Experimental Psychology: Human Perception and Performance* **38:**735-745; 2012.

[361] Le Bourg, E.; Lints, F. A. Hypergravity and aging in Drosophila melanogaster. 5. Patterns of movement. *Gerontology* **38:**65-70; 1992.

[362] Araghi-Niknam, M.; Lane, L.; Watson, R. R. Modification of Physical Movement in Old C57BL/6 Mice by DHEA and Melatonin Supplementation. *Experimental biology and medicine* **221:**193-197; 1999.

[363] Mole, R. H. The LD50 for uniform low LET irradiation of man. *British Journal of Radiology* **57:**355-369; 1984.

[364] Flemming, A. J.; Shen, Z. Z.; Cunha, A.; Emmons, S. W.; Leroi, A. M. Somatic polyploidization and cellular proliferation drive body size evolution in nematodes. *Proceedings of the National Academy of Sciences of the United States of America* **97:**5285-5290; 2000.

[365] Bailly, A.; Gartner, A. Caenorhabditis elegans Radiation Responses. In: DeWeese, T. L.; Laiho, M., eds. *Molecular Determinants of Radiation Response*: Springer New York; 2011: 101-123.

[366] Li, Y. B.; Huang, T. T.; Carlson, E. J.; Melov, S.; Ursell, P. C.; Olson, T. L.; Noble, L. J.; Yoshimura, M. P.; Berger, C.; Chan, P. H.; Wallace, D. C.; Epstein, C. J. Dilated Cardiomyopathy and Neonatal Lethality in Mutant Mice Lacking Manganese Superoxide-Dismutase. *Nature genetics* **11:**376-381; 1995.

[367] Kokoszka, J. E.; Coskun, P.; Esposito, L. A.; Wallace, D. C. Increased mitochondrial oxidative stress in the Sod2 (+/-) mouse results in the age-related decline of mitochondrial function culminating in increased apoptosis. *Proceedings of the National Academy of Sciences of the United States of America* **98:**2278-2283; 2001.

[368] Li, L.; Shoji, W.; Takano, H.; Nishimura, N.; Aoki, Y.; Takahashi, R.; Goto, S.; Kaifu, T.; Takai, T.; Obinata, M. Increased susceptibility of MER5 (peroxiredoxin III) knockout mice to LPS-induced oxidative stress. *Biochemical and biophysical research communications* **355:**715-721; 2007.

[369] Ishii, T.; Yasuda, K.; Akatsuka, A.; Hino, O.; Hartman, P. S.; Ishii, N. A mutation in the SDHC gene of complex II increases oxidative stress, resulting in apoptosis and tumorigenesis. *Cancer research* **65:**203-209; 2005.

[370] Anchordoquy, T. J.; Molina, M. C. Preservation of DNA. *Cell Preservation Technology* **5:**180-188; 2007.

7. Appendix

7.A.1. DNA extraction

The development and validation of good assays is important to measure and report the true level of DNA damage.

Careful DNA extraction for DNA damage assays is essential. A good DNA extraction technique should optimize DNA yield while minimizing DNA degradation and artifacts. Special care should be taken to avoid nicking, shearing or introducing additional oxidative DNA damage during the DNA extraction and purification process. DNA extraction protocols should also result in reproducible yield and generate DNA samples that can be stored without DNA degradation. In order to obtain a DNA extraction method that met these criteria, I tested DNA samples obtained from total genomic DNA and compared these to nuclear/mitochondrial DNA obtained by organelle separation. The mitochondrial and nuclear fractions were obtained from differential centrifugation (a method that allows the isolation of nuclei and mitochondria from homogenates) of worm lysate. Mitochondrial and nuclear fractions were then cleaned up using the Prepman Ultra sample preparation reagent, whereas the total genomic DNA was cleaned up using a spin column-based nucleic acid purification method according to the manufacturer's protocol.

I tested the quality of DNA from these different extraction methods early in the method development using the Fpg-qRT-PCR approach, which I based on the method demonstrated by Lu *et al.* [248]. I found that the mtDNA damage in DNA samples obtained from mitochondrial fractions were not significantly different from mtDNA damage in total genomic DNA, with 2.5 ± 1.7 and 1.1 ± 0.3 lesions per 10 kbp respectively (Figure 7.1A). Similarly, nuclear DNA damage in DNA samples extracted from nuclear fractionswas not significantly different from nuclear DNA damage measured in total genomic DNA with 1.0 ± 0.3 and 1.2 ± 0.3 lesions per 10 kbp respectively (Figure 7.1B). Furthermore, statistical analysis showed that there was no significant different in the DNA damage between mitochondrial and nuclear DNA (Figure 7.1C). Taking these data together, Figure 7.1 shows that there is no significant difference in the

DNA damage levels obtained from different DNA extraction methods at least for baseline damage.

The extraction of total genomic DNA requires a relatively large quantity of worms due to the small size of *C. elegans* and loss of sample using the spin column-based DNA purification method. Therefore, all subsequent assay optimization for the DNA damage assay was performed using mtDNA or nuclear DNA extract obtained using differential centrifugation method as described in section 2.9.

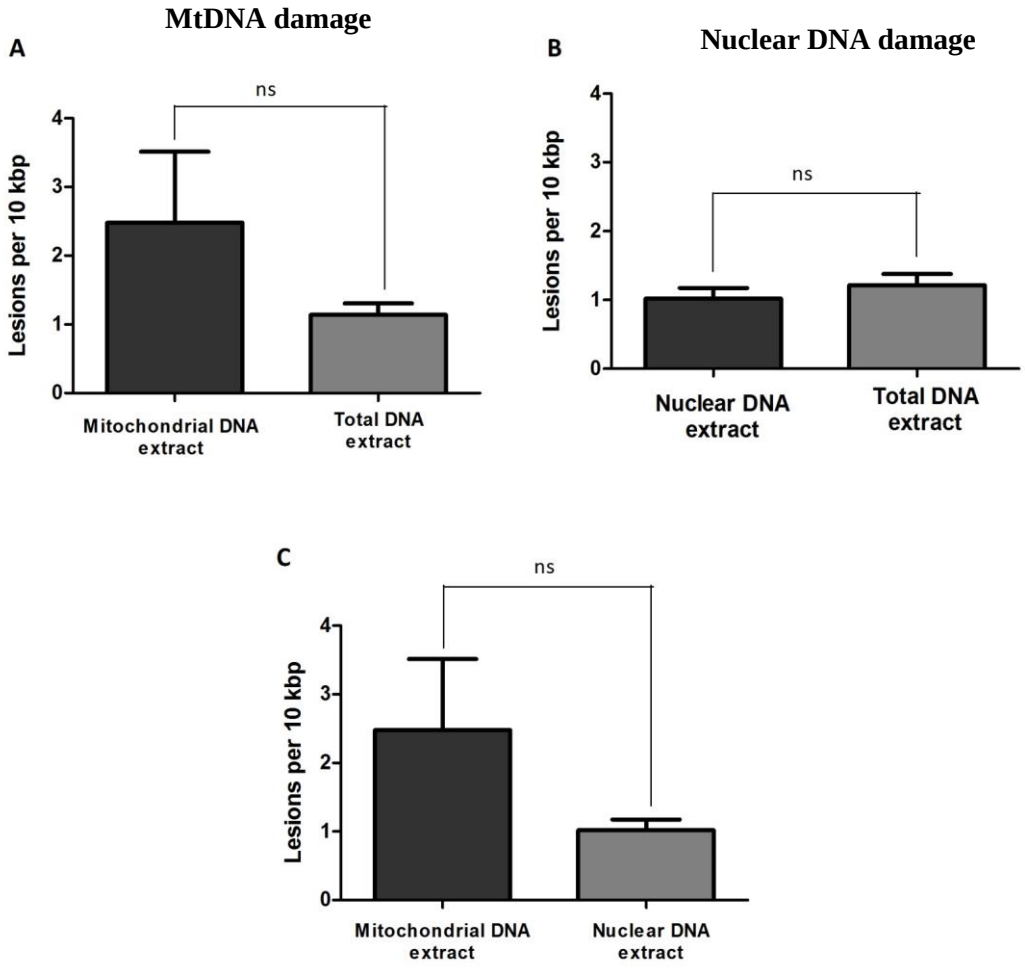

Figure 7.1. DNA damage level of different DNA extracts of Day 4 wild type N2 animals determined using Fpg-qRT-PCR approach. (A) DNA damage in mitochondrial DNA and total DNA extracts determined using mitochondria primers set. There was no statistically significant difference in the DNA damage per base pairs in mtDNA obtained using differential centrifugation and total genomic DNA, (p=0.3, Student's t-test). (B) DNA damage level of nuclear DNA and total DNA extracts determined using nuclear primers set. There was no statistically significant difference in the DNA damage using the nuclear DNA obtained by differential centrifugation, (p=0.4, Student's t-test). (C) The DNA damage in the mtDNA extract was not statistically significant higher than DNA damage level in nuclear DNA extract.

Using the comet assay, I had earlier shown that there was a significant dose-dependence increase in nuclear DNA damage in γ-irradiated animals (Figure 3.6). At this stage, all the different DNA extraction methods appeared to be similar. I therefore, used the Fpg-qRT-PCR approach to further assess which DNA extraction protocols were able to detect elevation of DNA damage with increasing γ-radiation dosage. However, using the Fpg-qRT-PCR DNA damage assay, DNA damage in the mitochondrial fraction, nuclear fraction and total genomic DNA amplified using mitochondrial or nuclear primers set, did not show a statistically significant dose-response increased of γ-irradiated DNA damage (Figure 7.2A). Although the samples from mitochondria, nuclear fraction and total genomic DNA amplified using nuclear primers set, showed increasing trends, these were not statistically significant (Figure 7.2A, C and D).

Furthermore, the large variations in oxidative DNA damage values demonstrated that this Fpg-qRT-PCR approach lacks robustness and the fact that this assay cannot detect the dose-dependence increase in the level DNA damage in γ-irradiated animals, irrespective of the DNA extraction methods used, indicates that this Fpg-qRT-PCR assay lacks sensitivity; therefore, I decided to explore the alternative short versus long fragments of S-XL-qRT-PCR DNA damage assay which I will discuss later in section 3.3.4.2.

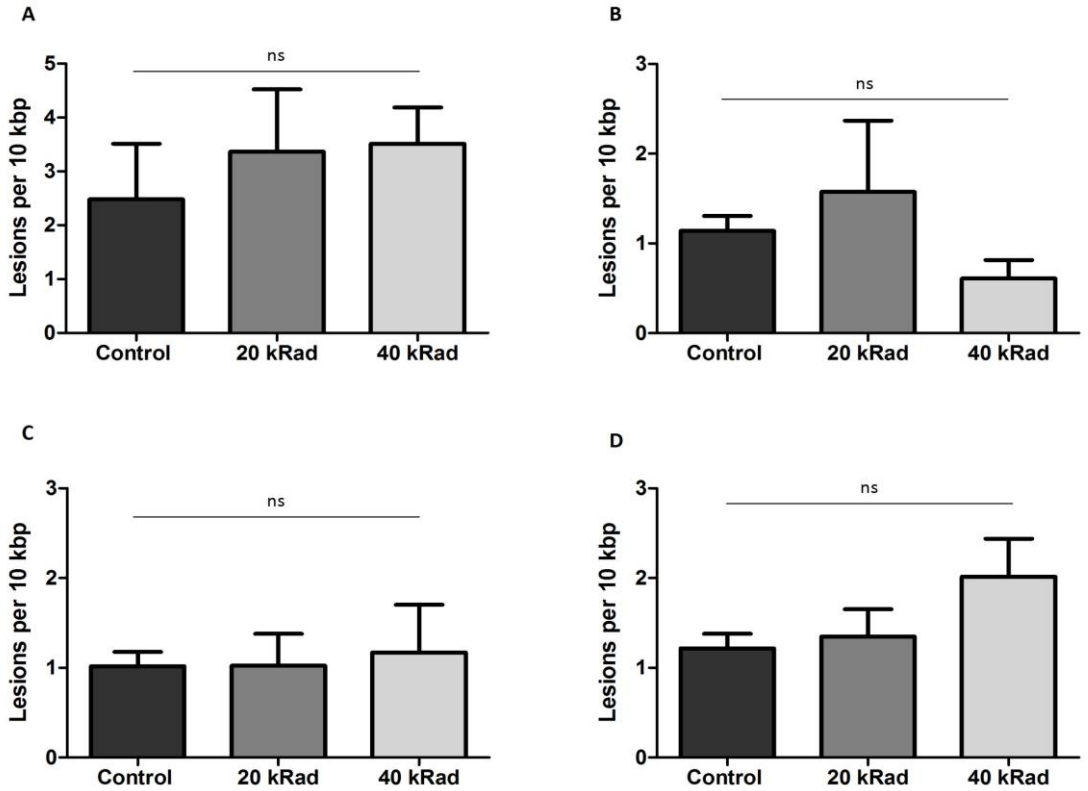

Figure 7.2 .DNA damage level of Day 4 wild type nematodes exposed to 0, 20 and 40 kRad γ-radiation, determined using Fpg-qRT-PCR approach in different DNA extracts. (A) Mitochondrial DNA extract. There were slightly more (not significant) DNA lesions detected in the mitochondrial DNA fraction of 20 and 40 kRad γ-irradiated animals relative to untreated control animals. The increase was not statistically significant. (B) qRT-PCR of total genomic DNA using mitochondria primers set. DNA lesions frequency in the animals exposed to the higher dosage of γ-irradiation (40 kRad) appeared lower than control and 20 kRad γ-irradiated animals. There was no dose-dependent increased in the level of mt DNA damage determined using the total genomic DNA. (C) Nuclear DNA extracts. (D) qRT-PCR of total genomic DNA using nuclear primers set. There were no significant dose-dependent increased in the level of nuclear DNA damage determined using nuclear DNA obtained from differential centrifugation and total genomic DNA. The observed trends were not statistically significant. All the data were analyzed using ANOVA, mean ±sem. n =3 independent experiments.

7.A.2. Determination of Real-Time chemistry (intercalation dye Vs fluorogenic probe) for S-XL-qRT-PCR assay

To overcome the limitations in Fpg-qRT-PCR methodology (see section 3.3.4), I optimized the sequence specific S-XL-qRT-PCR DNA damage assay.

In my S-XL-qRT-PCR method, the amplifications of the short and large fragments were initially monitored and analyzed using the same PCR amplification temperature profile by the intercalation of the fluorescence dye, SYBR Green I to double-stranded DNA. The amount of fluorescence emitted is proportional to the amount of double-stranded PCR product generated, thus, PCR products can be detected as these products accumulate during PCR amplification (Figure 7.3A). Using the same sample and copy number, the samples were detected using SYBR Green I dye and amplified using long and short amplicon primers set (XL and S respectively). Samples amplified using XL primers were detected earlier than sample amplified using S primers (Figure 7.3A). This demonstrates the detection limit of long and short fragment. However, the primary disadvantage of SYBR Green I dye is that the dye binds all double-stranded DNAs, including non-specific reaction products. I further analyzed the samples using gel electrophoresis and found that some non-specific amplification in PCR reactions using both XL and S primers set (Figure 7.3B). However, the gel photo showed that the true signal (actual band intensity) for the long amplicons is higher than the signal from non-specific bands. In contrast, the actual band intensity for the short amplicons is comparable to the band intensity for the amplification of non-specific fragments suggesting significant artifacts. This demonstrated that short fragment is much more sensitive towards non-specific amplification and SYBR green I dye may not be ideal to detect short amplicon. Therefore, I chose to instead detect short fragments using Taqman probes. The Taqman system utilizes a fluorogenic-labeled probe that contains a reporter molecule attached to a nucleotide probe. This fluorogenic probe is specific to the target gene and has a reporter dye and quencher dye attached to it. When the probe is intact, the quencher dye signal blocks the fluorescence signal emitted by reporter dye. In contrast, during PCR primer extension, DNA polymerase cleaved the probes thus separating

the reporter dye from the quencher dye. This results in the increase in the fluorescence signal of the reporter dye which is proportional to the molecule of amplified template.

To improve PCR specificity of my S-XL-qRT-PCR damage assay for all subsequent experiments, the amplification of short PCR products was monitored using the Taqman system while the amplification of long PCR product was monitored using SYBR Green I dye. The product specificity of the long PCR fragment that uses SYBR Green I dye was tested by routinely checking for non-specific product formation by dissociation curves [317].

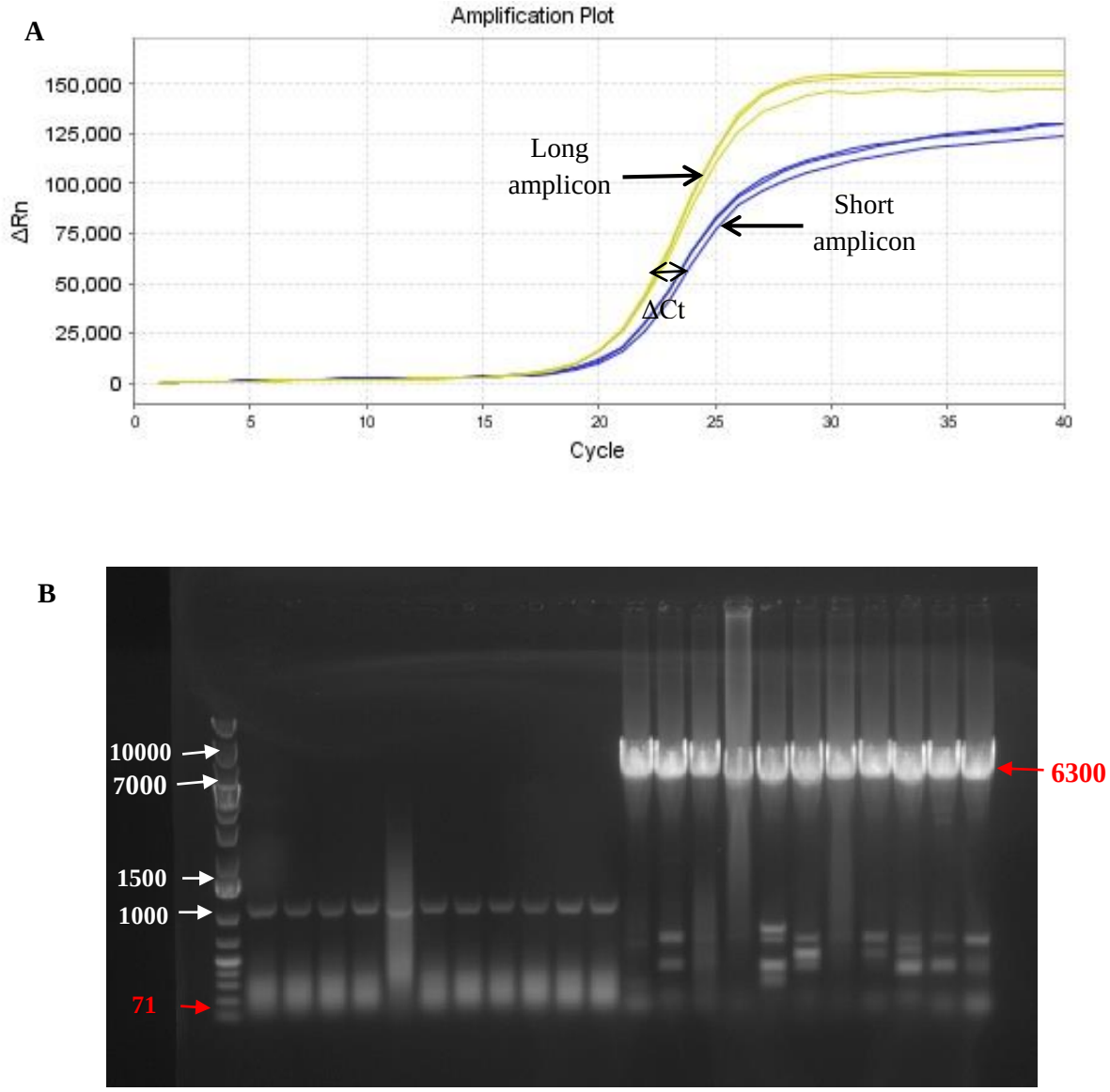

Figure 7.3. A. qRT-PCR amplification plots of short and long PCR fragments detected using intercalation dye (SYBR Green I dye). Mitochondrial extract of day 4 young JK1107 was used and RT-PCR was amplified using mitochondria primers sets, F1 (short amplicon) and L1 (large amplicon). The yellow amplification plots represent the sample amplified using long amplicon primers set while the blue amplification plots represent sample amplified using short amplicon primers set. ΔCt shows the difference in the detection limit of long and short amplicon although the same copy number was used. **B.** PCR products of short and long PCR fragments detected using intercalation dye (SYBR Green I dye) evaluated using agarose gel electrophoresis. PCR products electrophoresed in agarose gel shows non-specific amplification using SYBR Green I dye.

7. A.3. Sample storage conditions

After identifying the problem with the Fpg-qRT-PCR assay, I then explored the sample storage conditions using the S-XL-qRT-PCR DNA damage assay. I found that DNA degradation occasionally happened when samples were stored for extended periods of time. The effects of different storage conditions are important as the quality of starting material and method of DNA sample storage conditions prior to PCR analysis can affect PCR amplification efficiency.

The extraction of a single sample requires 2 hours and there are at least three different samples to be extracted for each experimental repeat. Therefore, it is not feasible to routinely run the qRT-PCR on the same day as extraction. Moreover, a good storage protocol enables the comparison of samples, for example, samples from animals at different ages, time points or cohorts. DNA samples were resuspended and stored in TE buffer (alkaline conditions) to inhibit DNA depyrimination, deamination, depurination and hydrolytic cleavage during DNA storage thus preserving the DNA integrity [370].

In our laboratory, DNA samples are most commonly stored at 4 ℃, -20 ℃, or -80 ℃. The four DNA storage conditions that I have tested are stored aliquoted DNA sample at 4 ℃, -20 ℃, -80 ℃ or stored DNA at -80 ℃ with or without multiple freeze-thaws. Using the S-XL-qRT-PCR method, the amount of DNA was determined. Comparing the intact DNA in both S- and XL-qRT-PCR, artefactual degradation and damage due to different storage conditions can then be quantified.

Using this approach, DNA damage for DNA samples stored at -80 ˚C, 4 ℃, -20 ℃ or multiple freeze thaw at -80 ℃ were 0.49, 0.57, 3.90 and 3.36 lesions per 10 kbp respectively (Table 7.1). It should be noted that the sample used for this experiment is not an undamaged control sample; thus, a certain background level of DNA lesions is expected. In appropriately stored DNA samples (DNA samples stored at -80 ˚C), the DNA damage level quantified was the lowest (Table 7.1) with no change in DNA damage comparing the DNA damage among the DNA samples from the same batch of animals but stored at 4 ℃ and measured immediately after

DNA extraction. Therefore, this DNA lesions frequency is the DNA lesions that represent the actual damage existing in the sample, not the level of DNA damage due to additional damage caused by storing the samples under different conditions.

Furthermore, short term (up to 3 days) storage of DNA pellets at 4 ˚C did not impact the PCR analysis. The DNA damage for samples stored at 4 ˚C was closer to DNA damage level for DNA samples stored at -80 ˚C (Table 7.1). The DNA samples stored at -20 ˚C and -80 ˚C with multiple freeze-thaws had the highest artifacts, resulted in higher DNA damage relative to DNA sample stored at -80 ˚C (Table 7.1).

These results clearly demonstrated that repeated freeze thaw of DNA samples should be avoided as this will lead to loss of intact undamaged DNA and artifacts that will result in increased DNA lesions frequency as determined by this approach. Furthermore, DNA samples stored at 4 and -80 ℃ do not cause any measurable artifacts. Quantification using S-XL-qRT-PCR also showed that long term storage in -20 ˚C may also decrease the amount of intact, undamaged DNA. DNA pellets used in this project were either analyzed within 3 days and stored at 4 ˚C to reduce the impact of freeze-thaw, or if long term storage was required, DNA pellets were aliquoted and stored at -80 ˚C without freeze-thaw.

Storage conditions	**DNA lesions (per 10 kbp)**	**Fold change in additional DNA lesions produced relative to DNA sample stored at -80 ℃**
4 ℃	0.57	0.2
- 20 ℃	3.90	7.0
- 80 ℃	0.49	-
Stored at – 80 ℃ with multiple freeze thaw	3.36	5.9

Table 7.1. **Different DNA storage conditions affect PCR amplification.** mtDNA damage in day 4 *glp-1* animals assessed using S-XL-qRT-PCR approach. DNA samples stored for a week at 4 ℃ and -80 ℃ degraded less than DNA samples kept at -20 ℃ and multiple freeze thaws at -80 ℃. Higher DNA lesions frequencies were detected in samples stored at -20 ℃ and with multiple freeze-thaw at -80 ℃.